UNIVERSITY OF LIVERPOOL

Iridium-catalysed cleavage and formation of unstrained aliphatic carbon-carbon bonds

Thesis submitted in accordance with the requirements of the University of Liverpool for the degree of **Doctor of Philosophy** by:

Marta Fernández Giménez

October 2017

Deixem de témer allò que s'ha après a entendre

(Marie Curie)

Als meus pares

(To my parents)

Abstract

This thesis discusses the study of the cleavage and the formation of unstrained aliphatic carbon-carbon bonds mediated by homogeneous iridium catalysts. The main project of this thesis consists in mechanistic studies of Ir-catalysed selective, reductive cleavage of unstrained C-C single bonds in dinitriles. Whereas the second project focuses on the development of a novel methodology for the catalytic C-C bond formation *via* a Michael-type hydroalkylation reaction envisioned as a result of our mechanistic studies.

Chapter 1 contains a review of transition-metal catalysed cleavage of C-C single bonds and a discussion of the existing strategies to facilitate the cleavage of these highly stable bonds and the relevant progress in this field. Particularly, this review is focused on reported examples of catalytic reductive cleavage of unstrained C-C single bonds. This overview highlights the lack of mechanistic understanding of this transformation which encouraged us to initiate our research.

Chapter 2 discusses the mechanistic studies of Ir-catalysed selective, reductive cleavage of unstrained carbon-carbon single bonds in dinitriles. Our experimental and computational results allowed to propose that this process occurs *via* C-H activation followed by retro-Michael type reaction involving alkene deinsertion. Our investigations also provide understanding about the driving force of the process that enables this thermodynamically unfavourable transformation. Moreover, the results of the mechanistic studies evidence that the C-C bond cleavage is a reversible process.

These findings allowed us to develop a new catalytic method for the formation of C-C bonds catalysed by the same iridium catalyst employed for the cleavage process. Thus, Chapter 3 provides a discussion of our research on the iridium-catalysed Michael-type hydroalkylation of cyclic α,β-unsaturated ketones with alkyl aryl nitriles. This method provides a facile access to 3-substituted cyclohexanones containing a quaternary carbon atom. To exemplify the synthetic utility of these new compounds, we then conducted preliminary studies on the catalytic dehydrogenation of 3-substituted cyclohexanones to *meta*-substituted phenols that are difficult to obtain *via* common synthetic routes.

Publications

Iridium-catalysed reversible cleavage of unstrained aliphatic C-C bonds in 1,5-dinitriles: insight into the catalytic cycle

Marta Fernández-Giménez, Konstantin V. Luzyanin, Neil G. Berry, Nathan Halcovitch, and Alexey G. Sergeev.

Manuscript in preparation.

Acknowledgements

After these four years of learning, challenges, effort and chemistry, I have words to thank a lot of people who accompanied me in this long journey.

First, I would like to thank my supervisor, Dr Alexey Sergeev, for giving me the opportunity to come to Liverpool to join his research group, for all the chemistry that I learnt during these years and for his constant availability to help me with anything I needed.

Secondly, I would like to thank Dr Konstantin Luzyanin for collaborating in our project and for his help with NMR. He was a constant support since we started the collaboration until the very last day of my PhD.

During these years I met loads of nice people in the chemistry department. I am grateful to my lab mates, Martin and Claudia for the daily coffees and the music. Also, to Robyn for the time I spent with her in the lab. Aldo who always had time for a chat and a break with the Barça's mug. Also, I would like to thank Matt who I can consider a friend, for his support and for "all the pints, all the latins".

I would like also to thank one of the most important persons for me in Liverpool, my friend and my flatmate Lorena. You have been my family in Liverpool since the very beginning and I could not imagine this experience without her. Thanks for the trips, the parties, the laughs and el cariño.

Moving to Liverpool was one of the best decisions I could have ever made and this was thank to my family. To my parents, Jordi and Teresa, for their constant support, for being always by my side with every step and for reminding me that I can achieve any personal goal. Also, I would like to thank my sister for being always there despite the distance.

Als meus pares, Teresa i Jordi, pel seu suport constant i per estar sempre del meu costat en cada pas que faig. Per recordar-me que puc aconseguir qualsevol cosa que em proposi com la amazona que sóc. Gràcies per la educació que m'heu donat i per permetre'm ser qui sóc avui. També, a la meva germana Esther per estar sempre de la meva part tot i la distància.

Table of Contents

Abstract IV

Publications V

Acknowledgements VI

Abbreviations XIV

1. Cleavage of C-C single bonds catalysed by transition metals 1

1.1. Introduction 1

1.2. Strategies for the cleavage of C-C bonds 4

1.3. Cleavage of unstrained C-C bonds 8

1.3.1. Oxidative addition of unstrained C-C bonds 9

1.3.2. β-alkyl elimination of unstrained molecules 13

1.4. Reductive cleavage of C-C single bonds 18

1.4.1. Reductive cleavage of Csp-Csp^2 and Csp-Csp^3 single bonds 19

1.4.2. Reductive cleavage of Csp^2-Csp^3 single bonds 21

1.4.3. Reductive cleavage of Csp^3-Csp^3 single bonds 22

1.5. Summary and objectives 28

1.6. References 30

2. Ir-catalysed selective reductive cleavage of unstrained aliphatic C-C bonds: Insight into the catalytic cycle 35

2.1. Introduction 35

2.2. Ir-catalysed reductive cleavage of unstrained aliphatic C-C bonds of dinitriles: first evidences towards the insight into the catalytic cycle 37

2.3. Screening of the catalytic system 44

2.4. Effect of directing groups in the reductive C-C bond cleavage 52

2.4.1. Syntheses of substrates 57

2.4.2. Ir-catalysed reductive C-C bond cleavage of synthesised substrates 60

2.5. C-H activation versus C-C activation: distinguishing two possible mechanistic pathways 65

2.6. Deuterium labelling studies 71

2.7. Detection and isolation of catalyst resting state complex 37 74

2.8. Reductive C-C bond cleavage of dinitrile 2 catalysed by complex 37 81

2.9. Computational studies 83

2.10. Proposed mechanism of Ir-catalysed reductive cleavage of unstrained C-C bond of dinitriles 94

2.11. Progress towards the development of a more general reductive C-C bond cleavage of dinitriles: sequential C-C cleavage and alkene hydrogenation reaction 102

2.11.1. Ir-catalysed hydrogenolysis of C-C single bonds of dinitriles with H_2 103

2.11.2. Ir-catalysed transfer hydrogenolysis of unstrained aliphatic C-C bonds of dinitriles 104

2.12. Conclusions 106

2.13. Experimental section 108

2.13.1. General Experimental Information 108

2.13.2. Syntheses of Iridium complexes 110

2.13.2.1. Synthesis of $Ir(P^iPr_3)_2H_5$ (1) 110

2.13.2.2. Synthesis of ^{iPr}PCPIrHCl 111

2.13.2.3. Synthesis of ^{Ad}PCPIrHCl 112

2.13.3. Syntheses of substrates 113

2.13.4. Iridium-catalysed reductive cleavage of unstrained aliphatic C-C bonds with $Ir(P^iPr_3)_2H_5$ 131

2.13.5. Screening of the catalytic system for reductive cleavage of unstrained aliphatic C-C bonds in dinitriles 131

2.13.5.1. Catalytic reductive cleavage of unstrained aliphatic C-C bonds with [Ir(cod)Cl]$_2$ and phosphine, phenanthroline or NHC ligands 131

2.13.5.2. Catalytic reductive cleavage of unstrained aliphatic C-C bonds with iridium pincer ligands (^{R}PCPIrHCl) 132

2.13.5.3. Control experiments of catalytic reductive cleavage of unstrained aliphatic C-C bonds of dinitrile 2 with P^{i}Pr$_3$ 132

2.13.5.4. Control experiments of catalytic reductive cleavage of unstrained aliphatic C-C bonds of dinitrile with benzoyl peroxide or AIBN..... 133

2.13.6. Study on the effect of directing groups in the reductive C-C bond cleavage 133

2.13.7. Ir-catalysed reductive cleavage of C-C single bond of unstrained dinitriles in the presence of diphenylacetonitrile or acrylonitrile 140

2.13.8. Iridium-catalysed hydrogenation and polymerization of acrylonitrile 141

2.13.9. Ir(P^{i}Pr$_3$)$_2$H$_5$-catalysed hydroalkylation of acrylonitrile with diphenylacetonitrile 142

2.13.9.1. Ir(P^{i}Pr$_3$)$_2$H$_5$-catalysed hydroalkylation of acrylonitrile with diphenylacetonitrile: scaled-up experiment for the isolation of trinitrile 6 143

2.13.10. Stoichiometric experiment with dimethylated substrate 22 and Ir(P^{i}Pr$_3$)$_2$H$_5$ complex 144

2.13.11. Deuterium labelling studies 145

2.13.11.1. Deuterium labelling experiments with 2,2-dideuterium-4,4-diphenylpentanedinitrile (2-d$_2$) 145

2.13.11.2. Deuterium labelling experiments with 2-deuterium-2,2-diphenylacetonitrile (3-d) 148

2.13.12. General procedure for NMR monitoring of iridium-catalysed reactions 149

2.13.12.1. NMR monitoring experiment of Ir(P^{i}Pr$_3$)$_2$H$_5$-catalysed cleavage of C-C bond of dinitrile 2 149

2.13.12.2. NMR monitoring of the reaction of diphenylacetonitrile and $Ir(P^iPr_3)_2H_5$ 151

2.13.12.3. NMR monitoring of the reaction of acrylonitrile with complex 37.. 152

2.13.12.4. NMR monitoring experiment of the reaction of acrylonitrile and P^iPr_3 with complex 37 153

2.13.12.5. NMR monitoring of the reaction of 2,2-diphenylpentanedinitrile with $Ir(P^iPr_3)_2H_5$ (1 equiv) 154

2.13.13. Independent synthesis and isolation of intermediate complexes 156

2.13.13.1. Synthesis of complex 37 156

2.13.13.2. Stoichiometric reaction of 2,2-diphenylpentanedinitrile with $Ir(P^iPr_3)_2H_5$ 157

2.13.13.3. NMR monitoring of the reaction mixture of complex 37 with hydrochloric acid 158

2.13.14. Iridium-catalyzed C-C hydrogenolysis of 2,2-diphenylpentanedinitrile in the presence of hydrogen 159

2.13.14.1. Iridium-catalysed hydrogenation of diphenylacetonitrile 160

2.13.15. Iridium-catalyzed transfer hydrogenation of 2,2-diphenylpentanedinitrile with cyclohexanol 161

2.13.16. Crystallographic experimental details 162

2.13.16.1. Crystallographic data and structure refinement for complex 32 162

2.13.16.1.1. Crystal structure of complex 32 163

2.13.16.1.2. Table of selected bond length and angles for complex 32 163

2.13.16.2. Crystallographic data and structure refinement for complex 33 164

2.13.16.2.1. Crystal structure of complex 33 165

2.13.16.2.2. Table of selected bond length and angles for complex 33 165

2.13.16.3. Crystallographic data and structure refinement for complex 37 166

2.13.16.3.1. Crystal structure of complex 37 167

2.13.16.3.2. Table of selected bond length and angles for complex 37 167
2.13.16.4. Crystallographic data and structure refinement for complex 51..... 168
2.13.16.4.1. Crystal structure of complex 51 169
2.13.16.4.2. Table of selected bond length and angles for complex 51 169
2.13.17. DFT calculations 170
2.13.17.1. Optimised geometries of complexes relevant to proposed mechanistic pathways 1A, 2A, 1B, 2B and intermolecular mechanism 171
2.14. References 175

3. Ir-catalysed Michael-type hydroalkylation of alkyl aryl nitriles to cyclic α,β-unsaturated ketones 183
3.1. Introduction 183
3.2. Development of Ir-catalysed Michael addition of aryl nitriles to 2-cyclohexen-1-one 192
3.2.1. Optimization of reaction conditions with $Ir(P^iPr_3)_2H_5$ catalyst 193
3.2.2. Proposed catalytic cycle 196
3.2.3. Screening of catalysts 198
3.2.4. Scope of cyclic α,β-unsaturated ketones 204
3.2.5. Scope of Michael donors 207
3.2.5.1. Synthesis of aryl nitrile substrates 208
3.2.5.2. Screening of Michael donors 209
3.3. Towards the dehydrogenation of substituted cyclohexanones to meta-substituted phenols 213
3.3.1. Introduction 213
3.3.2. Screening of reaction conditions for the dehydrogenation of substituted cyclohexanones to meta-substituted phenols..... 216

3.4. Conclusions 222
3.5. Future work 223
3.6. Experimental section 225
3.6.1. General procedure for Ir-catalyzed hydroalkylation of alkyl aryl nitriles with 2-cyclohexen-1-one 225
3.6.2. Scope of substrates 225
3.6.2.1. Scope of nucleophiles 225
3.6.2.2. Scope of cyclic α,β-unsaturated ketones 234
3.6.3. Syntheses of substrates 234
3.6.4. Screening of catalysts 237
3.6.4.1. General procedure 237
3.6.4.2. Control experiments for Ir-catalysed Michael addition of alkyl aryl nitriles with 2-cyclohexen-1-one 60a 239
3.6.4.2.1. Control experiments with 2-cyclohexen-1-one 60a and ^{t}BuONa .. 239
3.6.4.3. General procedure for BIMBOL-catalyzed Michael addition of diphenylacetonitrile 3 to 2-cyclohexen-1-one 55a 240
3.6.4.3.1. Synthesis of (±)-3,3'-Bis(diphenylhydroxymethyl)-2,2'-dihydroxy[1,1']-binaphtalenyl ((±)-BIMBOL) 241
3.6.4.3.2. Synthesis of lithium phenoxide 243
3.6.5. Dehydrogenation of 2-(3-oxocyclohexyl)-2,2-diphenylacetonitrile to the corresponding meta-substituted phenols 244
3.6.5.1. General procedure for Pd-catalyzed aerobic oxidative dehydrogenation of cyclohexanone 61a to meta-substituted phenol 66 (Stahl´s conditions) 244
3.6.5.1.1. Optimisation of reaction conditions (Stahl´s conditions) 246
3.6.5.1.2. Screening of oxidants 247
3.6.5.2. Screening of alternative methods for dehydrogenation of cyclohexanone 56a 247

3.6.5.2.1. Pd/C-catalyzed dehydrogenation of cyclohexanone 61a to phenol 66 247

3.6.5.2.2. $Pd(AcO)_2$-catalyzed dehydrogenation of cyclohexanone 61a to phenol 66 248

3.6.5.2.3. I_2-catalyzed dehydrogenation of cyclohexanone 61a to phenol 66 249

3.6.5.2.4. Dehydrogenation of cyclohexanone 61a to phenol 67 with DDQ . 249

3.7. References 250

4. Conclusions 257

Abbreviations

Å	Angstrom
δ	chemical shift
acac	acetylacetonate
Ad	adamantyl
BINAP	2,2'-*bis*(diphenylphosphino)-1,1´-binaphtyl
bp	boiling point
br. s	broad singlet
calcd	calculated
C-C	carbon-carbon
C-H	carbon-hydrogen
CI	chemical ionisation
cm^{-1}	$centimeter^{-1}$
CN	cetane number
cod	1,5-cyclooctadiene
coe	cyclooctene
cy	cyclohexyl
CyJohnPhos	2-(dicyclohexylphosphino)biphenyl
d	doublet
DBU	1,8-diazobicyclo[5,4,0]undec-7-ene
DCE	1,2-dichloroethane
DCM	dichloromethane
dd	doublet of doublets
DDQ	2,3-dichloro-5,6-dicyano-1,4-benzoquinone
DFT	Density Functional Theory
DG	directing group
DME	1,2-dimethoxyethane
DMF	dimethylformamide

DMSO	dimethylsulfoxide
dppf	bisdiphenylphosphinoferrocene
dr	diastereomeric ratio
EI	electron ionization
equiv	equivalents
ESI	electrospray ionisation
et al.	et alias
EtOAc	ethyl acetate
EWG	electron-withdrawing group
FTIR	Fourier transform infra-red
GC	gas chromatography
GC-MS	gas chromatography- mass spectrometry
h	hours
HRMS	high resolution mass spectrometry
Hz	hertz
IAd·HBF_4	1,3-Bis(1-adamantyl)imidazolium tetrafluoroborate
IBu·HBF_4	1,3-Di-*tert*-butylimidazolium tetrafluoroborate
IPr·HCl	1,3-Bis(2,4,6-trimethylphenyl)imidazolium chloride
*i*PrOH	isopropanol
IPropyl·HBF_4	1,3-Diisopropylimidazolium tetrafluoroborate
IR	infrared
J	coupling constant
JohnPhos	2-(di-*tert*-butylphosphino)biphenyl
m	multiplet
MHz	MegaHerzt
min	minutes
mm	millimetre
MS	mass spectrometry
NHC	N-heterocyclic carbene

NMR	Nuclear magnetic resonance
NOESY	Nuclear Overhauser Effect Spectroscopy
^{R}PCP	2,6-*bis*[Di(R)phosphinomethyl]phenyl
phen	phenanthroline
ppm	parts per million
py	pyridine
q	quartet
rt	room temperature
s	singlet
SIAd·HBF_4	1,3-Bis(1-adamantyl)imidazolinium tetrafluoroborate
SIMes·HCl	1,3-Bis(2,4,6-trimethylphenyl)imidazolinium chloride
t	triplet
T	temperature
TBAA	tetrabutylammoniumacetate
TBAB	tetrabutylammoniumbromide
*t*Bu	*tert*-butyl
TEP	Tolman electronic parameter
TFA	trifluoroacetate
THF	tetrahydrofuran
TS	transition state
w/w	weight/weight

Chapter 1

Cleavage of C-C single bonds catalysed by transition metals

1.1. Introduction

The cleavage of carbon-carbon single bonds catalysed by transition metals is of great interest as it can be employed to produce chemical feedstock and fuels from natural sources such as petroleum and biomass.[1] In particular, the cleavage of C-C single bonds is an important transformation involved in many large scale industrial processes, such as hydrocracking of heavy oil fractions implicated in petroleum refinery processes for the production of diesel. It is also a key transformation for plastic recycling, converting polymers into short chain hydrocarbons.[2,3] Over the last few decades, transition metal catalysed cleavage of C-C bonds has received special attention in organic synthesis as it allows to design useful methods for the synthesis of highly functionalised molecules by skeletal modifications of readily available starting materials in atom economical manner.[4]

The transition metal-catalysed cleavage of C-C single bonds, however, is generally difficult due to the high stability of these bonds. The inert nature of C-C single bonds is explained by thermodynamic and kinetic barriers that make the cleavage of this type of bonds a real challenge. The thermodynamic factor arises from the large bond energies of C-C σ-bonds which make them significantly stable. The cleavage products are typically less stable than the reagents and therefore, the cleavage is often an unfavourable reaction. In addition, the thermodynamic stability of expected intermediates is also a problem. The bond energies of C-C σ-bond (85-90 kcal/mol) are often larger than the energy of two formed C-M bonds (20-30 kcal/mol) therefore the insertion of the metal into C-C single bonds is a thermodynamically disfavoured process (Scheme 1.1).[5]

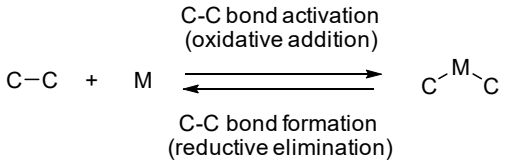

Scheme 1.1: Insertion of a metal into a C-C bond (oxidative addition) and its microscopic reversible process (reductive elimination)

The kinetic factor comes from the constrained directionality of C-C σ-bonds which is restricted along the bond axis. The interaction between the C-C bond orbital and the metal orbital requires a considerable distortion for an effective interaction demanding a high activation energy (Scheme 1.2). In addition, the C-C bond is sterically hindered by the substituents on both atoms which complicates the approach of the metal.

a) Interaction of LUMO of the metal centre with sigma bonding C-C orbital

b) Interaction of HOMO of the metal centre with sigma antibonding C-C orbital

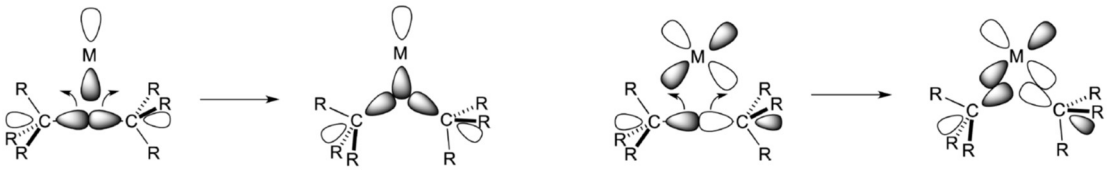

Scheme 1.2: Orbital interactions of a metal with a C-C single bond, adapted from reference 4

In addition, the C-C bonding orbital has low energy and the C-C anti-bonding orbital has high energy, which makes their interactions with the LUMO and HOMO orbitals of the metal energetically difficult. Another complication is that many functional groups have bonding orbitals energetically closer to the LUMO orbital of the metal compared to C-C σ-bonds and therefore, the metal centre interacts preferentially with these other functional groups. Consequently, many functionalities are often activated by the metal centre preferentially which triggers alternative reaction pathways and leaves C-C bonds intact.[6] For example, cleavage of the more abundant C-H bonds can occur faster than the C-C cleavage. This is explained by kinetic reasons, in which the interaction of the metal orbitals with the C-H orbitals is more

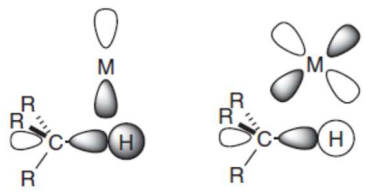

Figure 1.1: Orbital interactions between C-H and metal center adapted from reference 6

favourable than with C-C bonds. Despite the high directionality along the axis of the σ-orbital connecting a carbon and a hydrogen atom, the spherical nature of the 1s orbital of the hydrogen atom facilitates the interaction with the metal orbital from any direction without distortion (Figure 1.1).[6] Moreover, the preferential C-H activation by metal catalysts is also explained by thermodynamic factors as C-H bonds are stronger than the C-C single bonds. For instance, the bond dissociation energy (BDE) of a C-H bond in ethane is 101 kcal/mol whereas the BDE of C-C bond in the same molecule is 90 kcal/mol.[7] The cleavage of a strong bond leads to the formation of a strong bond and consequently, the activation of a C-H bond is more favourable.[8] Thus, C-H bonds are inherently more reactive than C-C bonds and in order to boost the reactivity of C-C bonds and enable their functionalisations, specific strategies should be developed.

Despite the inertness of C-C bonds, the development of their cleavage involving transition metals has made significant progress over the last few decades. Various methods have been devised for the catalytic C-C cleavage which can be achieved *via* two main pathways: oxidative addition and β-carbon elimination (Scheme 1.3). Oxidative addition involves direct insertion of the metal into the C-C bond increasing the oxidation state of the metal centre by two (Scheme 1.3A). This reaction is the inverse process of reductive elimination forming a C-C bond. As the metal centre undergoes formal increase of partial positive charge, oxidative addition typically occurs faster with electron-rich metal centres. A second important elementary reaction is β-carbon elimination which consists of the deinsertion of an olefin from a metal-alkyl bond (Scheme 1.3B). This transformation is the microscopic reverse reaction of migratory insertion. Any type of β-elimination requires a free coordination site to accommodate the incoming ligand and the metal-alkyl molecule must adopt a syn-coplanar conformation for this reaction to proceed.[9] In addition, there are other less common types of mechanisms for the cleavage of C-C single bonds such as retro-allylation (Scheme 1.3C) and σ-bond metathesis (Scheme 1.3D). Retro-allylation involves the scission of the bond between the β- and the γ-carbons to form an allyl metal species via a six-membered transition state. The retro-allylation can be considered a specific case of β-carbon elimination, but occurs typically more facilely due to the six-membered transition state which is less-strained than the four-membered transition state of common β-carbon eliminations. Finally, the σ-bond

metathesis consists in the simultaneous scission of C-C and M-R bonds and formation of new C-R and M-C bonds without variation of the oxidation state of the metal centre, resulting in a ligand exchange via a four-centred transition state.

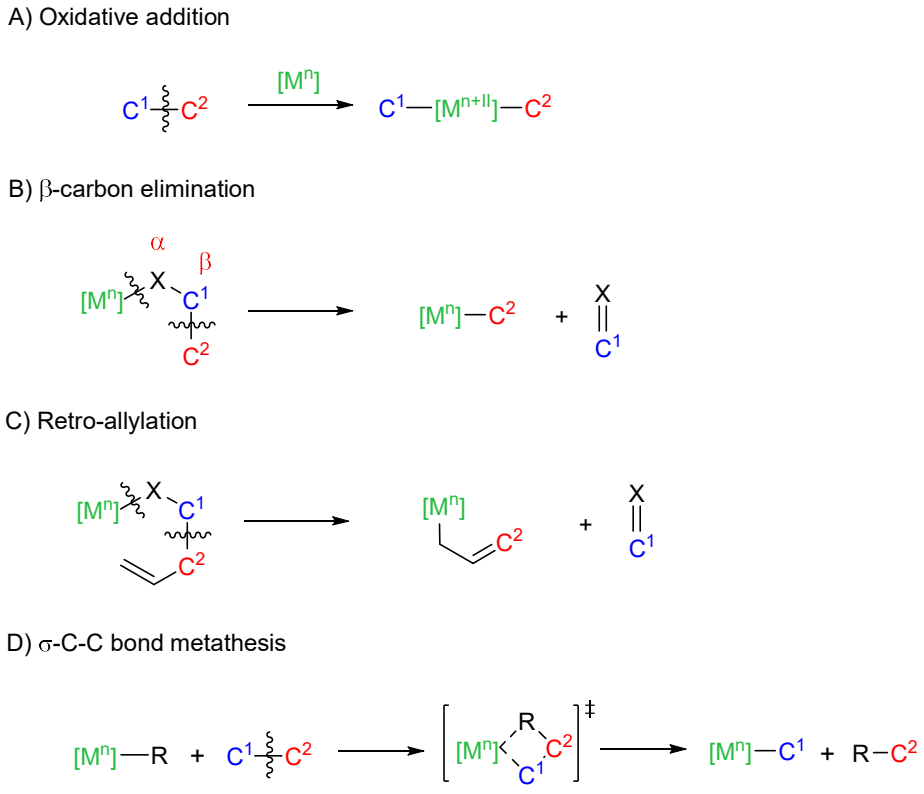

Scheme 1.3: Pathways of C-C bond cleavage, A) oxidative addition, B) β-carbon elimination, C) σ-bond metathesis and D) retro-allylation

To enable the unfavourable C-C bond cleavage, these elementary reactions have been used in several strategies that assist the scission both thermodynamically and kinetically. Among these strategies, release of ring-strain, chelation assistance and aromatisation processes are used to induce the breaking of C-C bonds.[6]

1.2. Strategies for the cleavage of C-C bonds

In order to facilitate the cleavage of C-C bonds, two basic approaches can be considered to lower the activation barrier of this transformation. The first one consists of increasing

the energy state of the starting materials and the second one lowers the energy state of the products of C-C bond cleavage. The first strategy involves the use of highly reactive starting materials such as 3- and 4-membered ring compounds. The relief of ring strain in these molecules constitutes a driving force for the C-C bond cleavage through the formation of a more stable ring expanded cyclometallated intermediate.

The C-C bond cleavage of strained molecules has been achieved via the elementary pathways described in the preceding section. An early example of strained C-C bond cleavage was reported by Tipper on the reaction of cyclopropane with $PtCl_2$ (Scheme 1.4).[10] The platinum centre inserts into the C-C bond of cyclopropane *via* oxidative addition to form an adduct intermediate which was subsequently shown to react with pyridine to form the final platinacyclobutane complex depicted in Scheme 1.4.

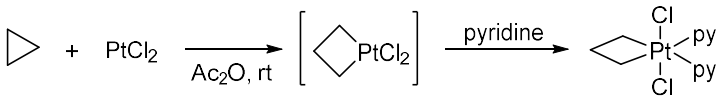

Scheme 1.4: An early example of cleavage of strained C-C bonds via oxidative addition

This early example showed the feasibility of oxidative addition of strained C-C bonds to the metal centre. Activation of strained C-C bonds in cyclopropanes has been then successfully applied for the design of many useful catalytic transformations. An example of the synthetic application of C-C bonds cleavage in cyclopropane involves rhodium catalysed oxidative addition in the presence of H_2 at 130 ºC (Scheme 1.5).[11] The branched alkane product is proposed to be afforded after the insertion of the metal centre into the less-sterically hindered C-C bond of the cyclopropyl ring followed by β-hydrogen elimination. The hydrogenation of the formed alkene afforded the final product.

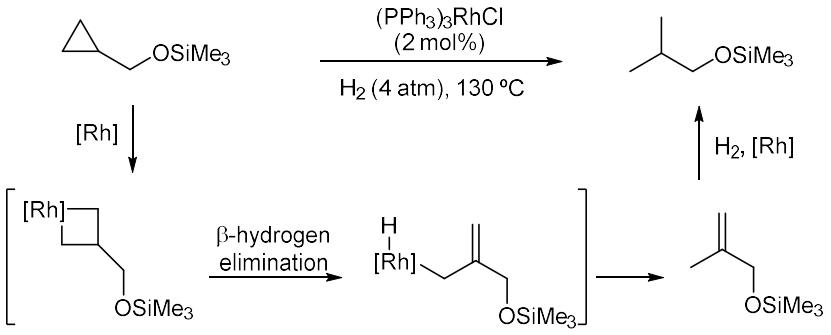

Scheme 1.5: Cleavage of C-C bond of a cyclopropane derivative via oxidative addition

Insertion of metals onto strained C-C bonds was also described for 4-membered ring compounds and provided a basis for a range of synthetic applications. An example of C-C functionalisation in cyclobutanones is shown in Scheme 1.6. Here the initial C-C cleavage is driven by the relief of ring-strain via formation of 5-membered rhodium metallacycle, which reacts with hydrogen to afford the final alcohol in a regio- and stereoselective manner.[12]

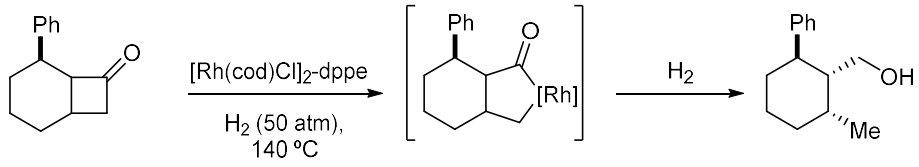

Scheme 1.6: Ring-opening of cyclobutanone via oxidative addition

Another example of functionalization of C-C bonds in cyclobutanes includes the oxidative addition into the cyclobutyl ring of biphenylene assisted by ring-strain relief (Scheme 1.7).[13] Transition metals, such as nickel, rhodium or palladium, participate in a series of catalytic insertion reactions with CO,[14] dihydrogen[15] or alkenes[16] to afford corresponding functionalised products.

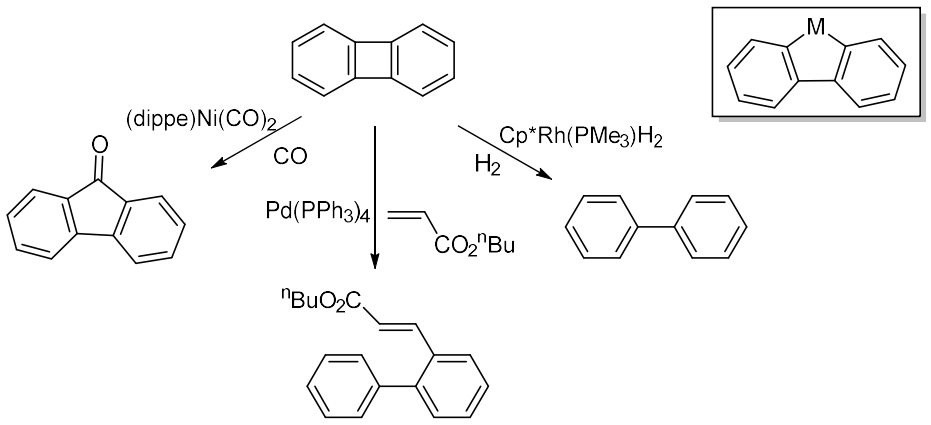

Scheme 1.7: Transition-metal-catalysed C-C cleavage of biphenylene assisted by ring-strain relief

Besides oxidative addition, the ring-opening of 4-membered rings can proceed via β-carbon elimination. A recent example of this process was reported by Flood and co-workers for the cleavage of a platinum-(methylcyclobutyl) complex that yields 2-methylpenta-1,4-diene (Scheme 1.8).[17] This process occurs through β-carbon elimination which is facilitated by the dissociation of the phosphine ligand. The release of PMe_3

creates a free vacant site that enables the coordination of the olefin moiety and permits the subsequent β-hydrogen elimination to afford the final products.

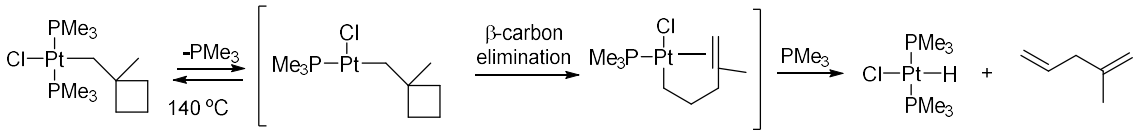

Scheme 1.8: Cleavage of a cyclobutane via β-carbon elimination

All these examples indicate that C-C cleavage can be facilitated through relief of ring-strain in strained cyclic compouds. However, the cleavage of non-strained molecules requires special driving forces to form thermodynamically more stable C-C cleaved complexes that decrease the energy state of these intermediates. One of these strategies consists of stabilization *via* aromatization of the formed complexes. Thus, non-aromatic starting materials are transformed into aromatic complexes during the C-C breaking step. For example, Crabtree *et al.* developed this strategy to break the *endo*-methyl groups of 1,1-dimethylcyclopentane using a cationic iridium complex and *tert*-butylethylene as a hydrogen acceptor (Scheme 1.9).[18]

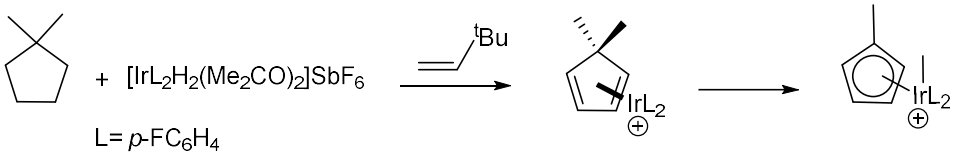

Scheme 1.9: C-C cleavage of a cyclopentane via aromatisation strategy

A second strategy to facilitate the cleavage of non-strained C-C bonds is the chelation assistance strategy. This approach uses a directing group (DG) which coordinates to the metal centre and places it next to the bond to be cleaved facilitating the metal insertion (Scheme 1.10).

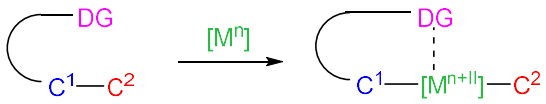

Scheme 1.10: Chelation-assisted C-C oxidative addition (DG = directing group)

A representative example of this strategy is the activation of the C-C bond next to the carbonyl group in 8-quinolinyl alkyl ketones directed by the nitrogen atom (Scheme

1.11).[19] The 8-quinolinyl butyl ketone reacts with ethylene to give 8-quinolinyl ethyl ketone through oxidative addition to the C_{butyl}-C(C=O) using a rhodium catalyst.[20] By employing the 8-quinolinyl directing group, the activation energy for the C-C bond cleavage is lowered, since a stable 5-membered rhodacycle intermediate is formed. This acylrhodium butyl complex undergoes β-hydrogen elimination to generate an acylrhodium hydride and release 1-butene. Further reaction of acylrhodium hydride complex with ethylene leads to 8-quinolinyl ethyl ketone as a final compound.

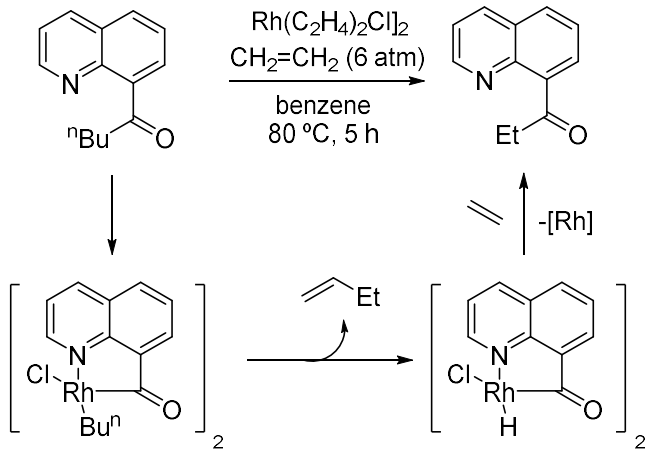

Scheme 1.11: Chelation-assisted cleavage of C-C bond of 8-quinolinyl butyl ketone

1.3. Cleavage of unstrained C-C bonds

The cleavage of unstrained C-C bonds commonly employs the chelation-assistance strategy, as introduced in the preceding section. The C-C cleavage typically proceeds through complex multi-step pathways that can be rationalised by considering the elementary steps described in Section 1.1. The scission of unstrained C-C bonds commonly involves oxidative addition or β-alkyl elimination assisted by a directing group (Scheme 1.12).

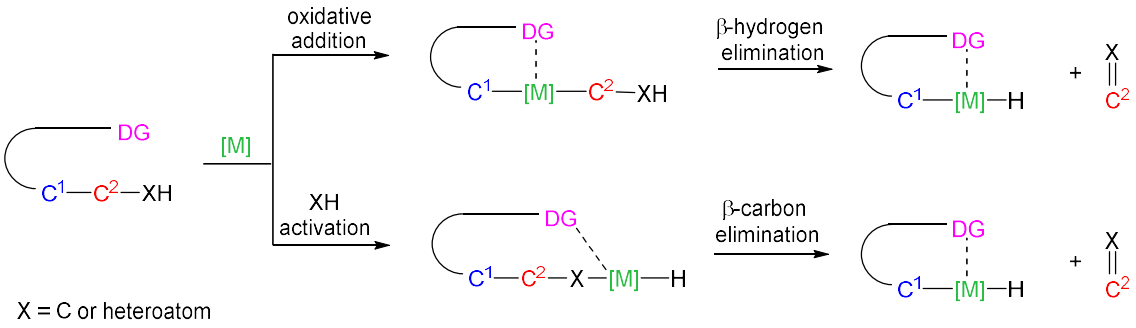

Scheme 1.12: Possible pathways for the directed cleavage of non-strained C-C bonds through 1) C-C activation (oxidative addition) or 2) β-carbon elimination

1.3.1. Oxidative addition of unstrained C-C bonds

The chelation-assisted oxidative addition has proved to be an effective method to cleave unstrained C-C bonds. This approach has been described for activation of substrates bearing appropriate directing groups such as pincer-type moieties or nitrogen-containing groups. A remarkable example was reported by Milstein and co-workers for the reaction between a bulky pincer-type diphosphine ligand and $[RhCl(CH_2{=}CH_2)_2]_2$ complex (Scheme 1.13).[21]

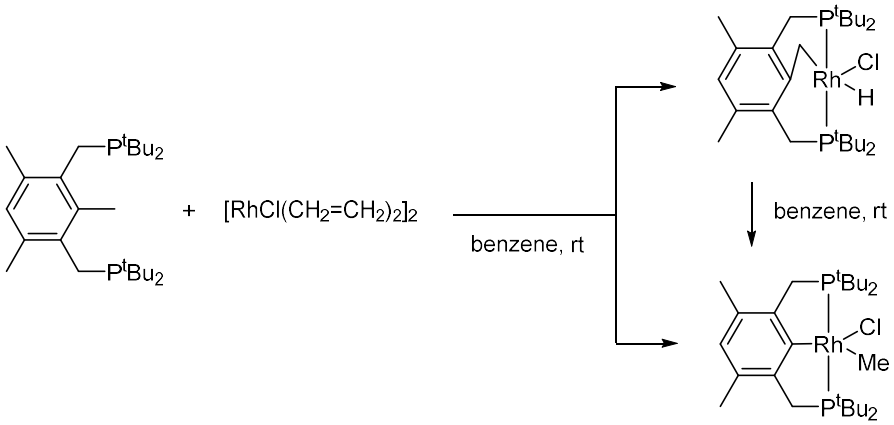

Scheme 1.13: C-C and C-H oxidative additions directed by phosphine groups of the pincer-type ligand

The chelating phosphine ligand directs the site-selective metal insertion into the C_{aryl}-C_{Me} bond at room temperature. The high stability of the C-C activation product under the reaction conditions serves as a driving force of this process, making it thermodynamically

favourable. In this example, the C-C bond cleavage was demonstrated to be thermodynamically and kinetically preferred over the competing C-H activation step. Both C-C and C-H activations are shown to be two independent concurrent processes. The C-H activation product undergoes a facile C-H reductive elimination at room temperature, followed by C-C oxidative addition which irreversibly leads to the clean formation of the C-C activation product.

The cleavage of non-strained C-C bonds through oxidative addition has also been assisted by nitrogen-containing directing groups, such as oxazoline. Murai *et al.* described the ruthenium-catalysed decarbonylative C-C cleavage of an alkyl phenyl ketone bearing an oxazoline moiety under CO atmosphere (Scheme 1.14).[22] The authors describe that the CO pressure is essential to maintain the catalyst in an active form. The Csp^2-Csp^2 bond activation is promoted by the insertion of the ruthenium complex into this bond which is assisted by the nitrogen atom of the oxazoline group. This step forms a 5-membered metallacycle which is proposed to undergo β-hydrogen elimination to generate a ruthenium hydride complex, that after release of phenyl ketene gives the decarboxylated aryl oxazoline as a final product.

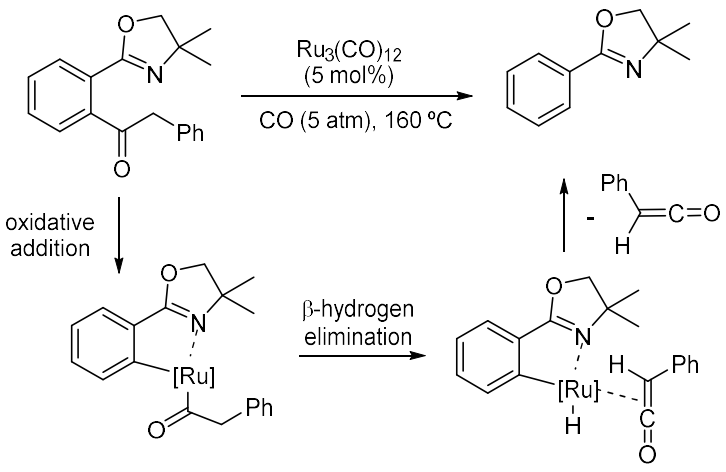

Scheme 1.14: Oxidative addition of aryl-carbonyl bond directed by an oxazoline moiety

The chelation strategy also extends to the cleavage of C-CN bonds facilitated by the coordination abilities of the nitrile nitrogen. For example, the C-CN bond of 2-naphthonitrile was cleaved by silylmetal complexes to produce arylsilanes in the presence of a rhodium catalyst (Scheme 1.15).[23] The decyanative silylation reaction proceeds *via*

oxidative addition of silylmetal complexes to the C_{aryl}-C(CN) bond to furnish metal isocyanide complexes. Finally, the reaction of the rhodium isocyanide complex with disilane affords the final aryl silane product.

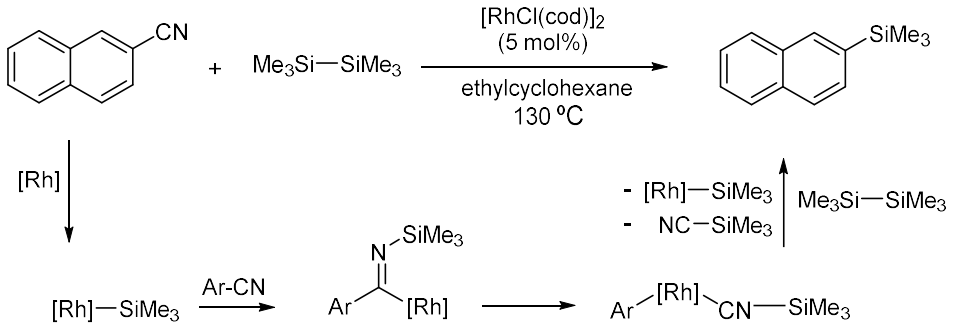

Scheme 1.15: Oxidative addition of a C-CN bond assisted by silylmetal complexes

Despite the usefulness of chelation assistance strategy, it is often complicated to remove a directing group from the product formed which diminishes the synthetic utility of the process. To overcome this issue, the cleavage of unstrained C-C bonds has also been developed with detaching directing groups. In this respect, a remarkable cooperative catalysis between 2-amino-3-picoline and a rhodium catalyst promotes the scission of an unstrained Csp^2-Csp^3 bond of ketones (Scheme 1.16).[24]

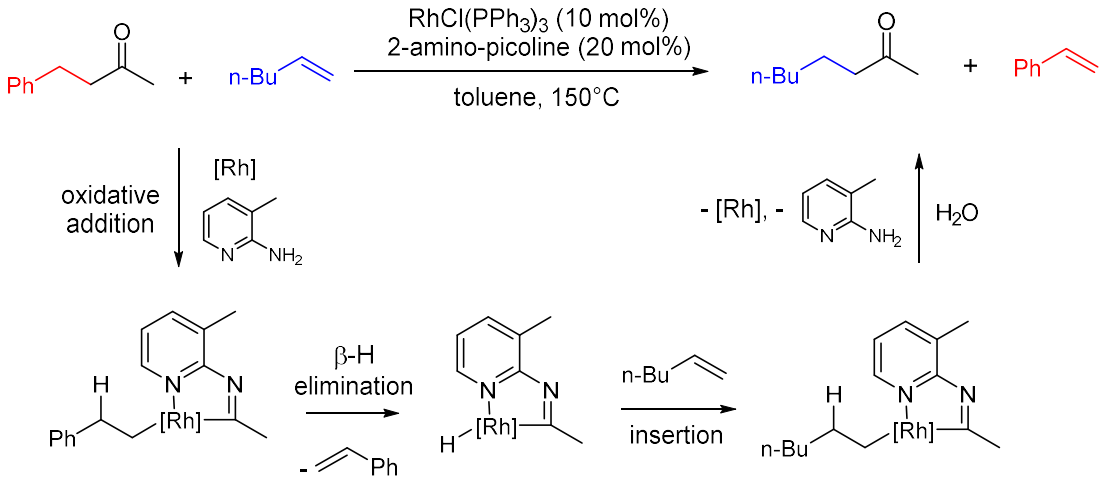

Scheme 1.16: Rh-catalysed C-C bond activation of unstrained ketones

The reaction of 4-phenyl-2-butanone and 1-hexene in the presence of a rhodium catalyst and 2-amino-3-picoline led to the formation of a 2-octanone and styrene. Initially, the removable pyridine-based directing group is installed by condensation with the ketone to

form a transient ketamine. Subsequently, oxidative addition of the C-C bond forms a five-membered rhodacycle intermediate which undergoes β-hydrogen elimination to give styrene and a hydride rhodacyle. The rhodacyle undergoes insertion of 1-hexene into the Rh-H bond and the resulting n-hexyl rhodium complex yields C-C coupling products after reductive elimination and hydrolysis of the pyridine directing group.

A related example of chelation-assisted oxidative addition with temporary directing groups was reported for the C-C cleavage of unstrained alcohols (Scheme 1.17).[25] The transformation of phenyl *sec*-alcohols into *tert*-butyl ketones was described to occur through the breaking of a C-C bond using a rhodium catalyst and 2-amino-3-picoline. Initially, a *sec*-alcohol is converted to the ketone **A** via transfer hydrogenation with *tert*-butylethylene. Similar to the previous example, the 2-amino-3-picoline couples to this ketone to form imine intermediate **B**, which coordinates to the rhodium centre facilitating the activation of the Csp^2-Csp^3 bond and the subsequent release of styrene. Then, insertion of the *tert*-butylethylene, reductive elimination and removal of the temporary directing group give the ketone product.

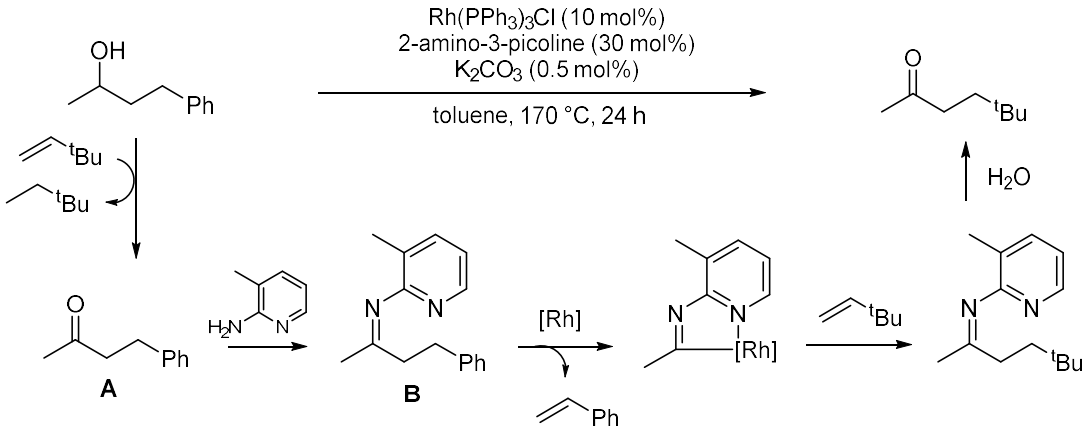

Scheme 1.17: Rh-catalysed C-C activation of *sec*-alcohols assisted by 2-amino-3-picoline

1.3.2. β-alkyl elimination of unstrained molecules

Similar to oxidative addition, the cleavage of unstrained C-C bonds *via* β-alkyl elimination has been facilitated by the use of the chelation-assistance strategy. The β-alkyl elimination is often found for the catalytic cleavage of tertiary alcohols.[26] For example, Miura described a catalytic *ortho*-phenylation of tertiary benzylic alcohols through the scission of Csp^2-Csp^3 bonds using a palladium complex (Scheme 1.18).[27] A series of α,α-disubstituted arylmethanols undergo arylative C-C bond cleavage with bromobenzene to give biaryl compounds in the presence of a palladium catalyst and Cs_2CO_3 at 150 ºC. The *ortho*-phenylation reaction might proceed *via* the coupling of the starting alcohol with bromobenzene after β-carbon elimination. Initially, bromobenzene undergoes oxidative addition onto palladium followed by transmetalation with the hydroxyl group. Then, β-carbon elimination cleaves the C-C bond releasing acetone and producing a diarylpalladium intermediate which reductively eliminates the biaryl product.

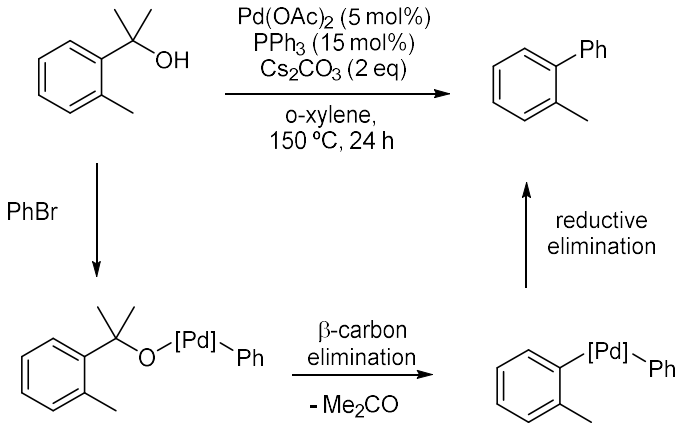

Scheme 1.18: Pd-catalysed arylative Csp^2-Csp^3 bond cleavage of arylmethanols

Recent investigations showed that the use of pyridine-directing group enabled cyanation of arene rings through β-alkyl elimination in arylmethanols. The scission of Csp^2-Csp^3 bonds of secondary and tertiary arylmethanols have been accomplished by a cobalt catalyst with $AgSbF_6$ at 120 ºC (Scheme 1.19).[28] Firstly, a 5-membered Co species is generated after β-alkyl elimination of the alcohol moiety. The cyclic cobalt complex reacts with NCTS (N-cyano-N-phenyl-p-toluenesulfonamide) to form the final product through the formation of a new C-CN bond.

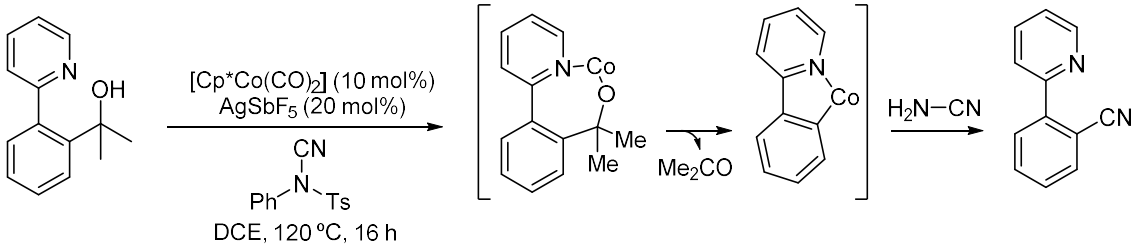

Scheme 1.19: Co-catalysed Csp^2-Csp^3 cleavage of arylmethanols with subsequent cyanation

Another example of the cleavage of unstrained C-C bonds in tertiary alcohols was reported by Uemura *et al*. A tertiary propargylic alcohol reacts with ethyl acrylate to give enyne compounds in the presence of a palladium complex, pyridine and MS3Å under an oxygen atmosphere (Scheme 1.20).[29] The Csp-Csp^3 bond of a propargylic alcohol was broken *via* β-carbon elimination directed by the hydroxyl group to form an alkynyl palladium complex. Subsequently, the final compound is formed through the insertion of ethyl acrylate into the C-Pd bond and subsequent β-hydrogen elimination. Thus, this method shows the utility of the cleavage of *tert*-propargylic alcohols as a convenient method for the production of ethylene.

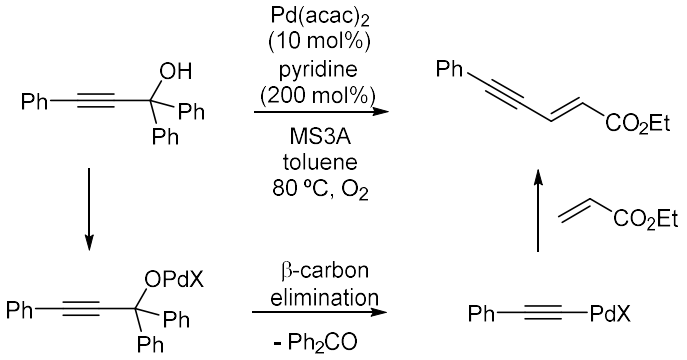

Scheme 1.20: Pd-catalysed alkynylation of allyl alcohols *via* β-carbon elimination

As illustrated by these examples, the β-carbon elimination often occurs in catalytic reactions involving the cleavage of unstrained Csp-Csp^3 and Csp^2-Csp^3 bonds. Compared to these type of bonds, the cleavage of unstrained Csp^3-Csp^3 bonds via β-carbon elimination is less favourable. This fact is explained by considering thermodynamic and kinetic factors. The activation of Csp-Csp^3 and Csp^2-Csp^3 bonds is thermodynamically more favourable than Csp^3-Csp^3 bond activation due to the fact that M-Csp and M-Csp^2 bonds are stronger than M-Csp^3 in alkyl metal complexes.[30] Moreover, the π-bonds

attached to sp- and sp^2-hybridised carbon atoms can coordinate to the metal facilitating the cleavage.

Generally, β-carbon elimination of unstrained Csp^3-Csp^3 bonds to give an olefin is an endothermic process that can only be feasible under special conditions that promote shift of the equilibrium to the products. Early examples of this process involved stoichiometric β-carbon elimination of early transition and rare earth metal alkyl complexes.[31–33] A seminal example is the thermal decomposition of a lutetium-isobutyl complex forming a lutetium-methyl complex and propene *via* β-alkyl elimination (Scheme 1.21).[34] Interestingly, the driving force of the process is the formation of Lu-allyl complexes from the reaction of the formed olefin and the resulting lutetium complex which enables the unfavourable cleavage.

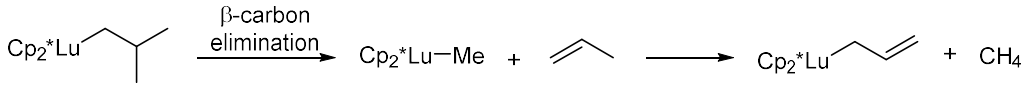

Scheme 1.21: Lutetium complex undergoing β-methyl elimination

More recently, some examples of catalytic cleavage of Csp^3-Csp^3 bonds of certain alcohols through β-alkyl elimination have been reported employing different driving forces to enable the process. In this regard, the deallylation of unstrained tertiary homoallylic alcohols have been described using a ruthenium catalyst, CO and allyl acetate to give acetophenone and propene (Scheme 1.22).[35] The cleavage of the Csp^3-Csp^3 bond proceeds through a six-membered transition state preceding the β-allyl elimination. This reaction is facilitated by the formation of a stable η^3-allyl ruthenium complex that acts as a driving force, as supported by the fact that the similar alcohol bearing no homoallylic functionality did not give any C-C cleavage product. The presence of CO and allyl acetate was crucial for this reactivity. Carbon monoxide operates as an effective π-acid which may coordinate to ruthenium centre and promote the reductive elimination of propene from the η^3-allyl ruthenium intermediate. Although the role of allyl acetate is unclear, it is believed that is required for the formation and stabilisation of catalytically active species.

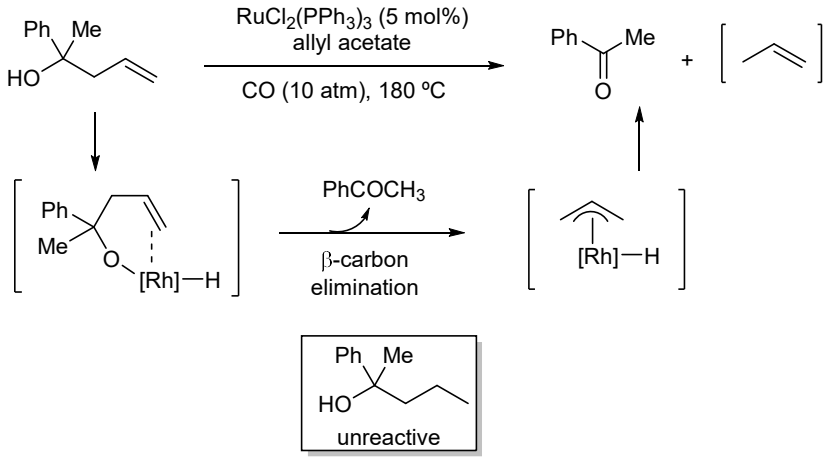

Scheme 1.22: β-allyl elimination of tertiary homoallylic alcohols catalysed by a ruthenium

Following on from this research, an analogous β-carbon elimination of secondary homoallyl alcohols was developed by Kang and co-workers. A palladium complex catalysed the sequential selective C-C bond cleavage of a variety of secondary homoallyl alcohols and esterification with acids as nucleophiles (Scheme 1.23).[36] Alcohols reacted with aromatic acids in the presence of a palladium catalyst and Ag_2CO_3 in *o*-dichlorobenzene (ODCB) at 100 ºC to give allyl benzoates. The authors proposed that this transformation is initiated by the deprotonation of the homoallyl alcohol by Ag_2CO_3 which acts as a base. Then, the deprotonated alcohol coordinates to palladium to form a palladium complex intermediate, which undergoes β-carbon elimination to give benzaldehyde and a π-allyl palladium species. The driving force of this reaction might be the formation of this stable allyl palladium complex. Subsequently, the allyl moiety reacts with the acid to yield the final allylic ester product.

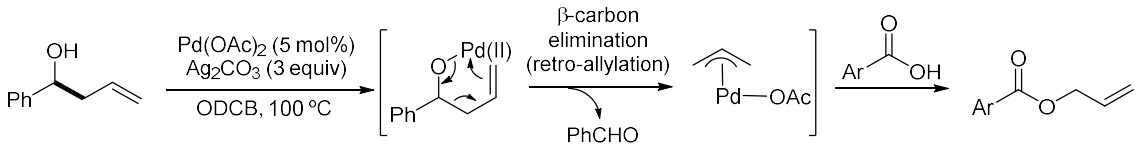

Scheme 1.23: Pd-catalysed cleavage of homoallyl alcohols via β-C elimination followed by esterification of aryl acids

Similarly, catalytic cleavage of Csp^3-Csp^3 bonds through β-carbon elimination has been described for primary alcohols. For example, β-carbon elimination was proposed to be an intermediate step in the synthesis of 1*H*-pyrazoles from allylic hydrazones catalysed by a

palladium complex using atmospheric oxygen (Scheme 1.24).[37] Initially, hydrazones, which are generated *in situ* from allylic ketones and hydrazines, undergo an aminohydroxylative reaction to give the corresponding primary alcohol in the presence of oxygen. This alcohol intermediate is proposed to undergo β-carbon elimination which is assisted by the hydroxyl group. Subsequently, β-hydrogen elimination gives the aromatised 1*H*-pyrazole product whose formation might be the driving force of the C-C cleavage step.

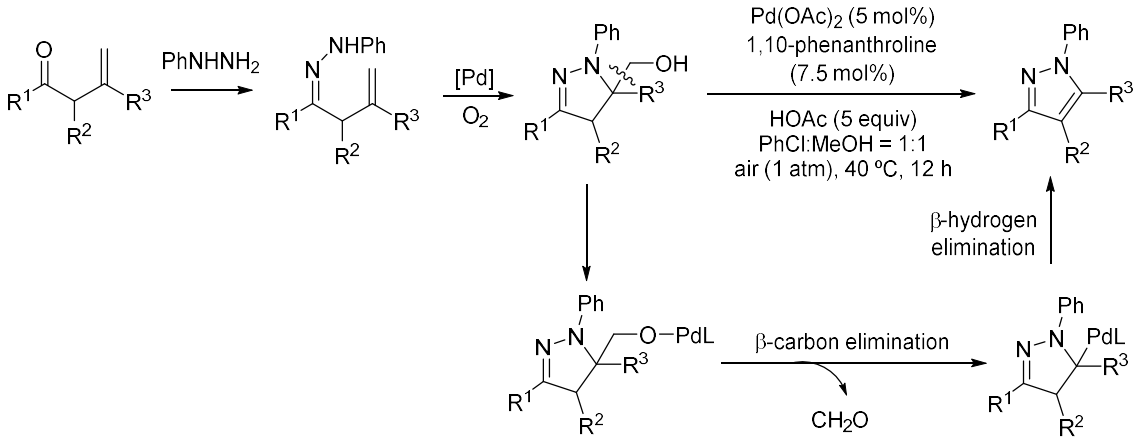

Scheme 1.24: Cleavage of Csp^3-Csp^3 bonds of primary alcohols *via* β-carbon elimination

These discussed methods constitute some of the scarcely reported reactions of catalytic cleavage of unstrained C-C single bonds through oxidative addition or β-carbon elimination. The scope of these methods is limited to certain substrates that contain nitrogen directing groups or tertiary alcohol moieties.[38,39] These examples illustrate that the cleavage of this type of bonds can be facilitated by the use of special driving forces to displace the equilibrium of the reaction, such as the formation of stable transition metal intermediates. Alternatively, other possible driving force to facilitate the unfavourable process can be the consumption of the cleaved products to drive the thermodynamic equilibrium. In this regard, the cleavage of non-strained C-C bonds has been developed under reducing conditions which enables the endothermic process.

1.4. Reductive cleavage of C-C single bonds

The reductive cleavage of C-C single bonds consists in the scission of a C-C bond to form two new C-H bonds employing a hydrogen source (Scheme 1.25). Various reducing agents have been employed for this process such as alkylaluminum,[40] metal hydrides[41] and hydrosilanes.[23] However, H_2 is more commonly used since this is the cheapest and cleanest reducing agent.

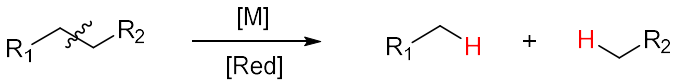

Scheme 1.25: Reductive cleavage of C-C bonds

The catalytic hydrogenolysis of aliphatic C-C bonds is a key process for converting fossil fuel and polyalkene plastic into fuel and value-added chemicals. Catalytic hydrogenolysis is a relevant transformation for converting the polynuclear aromatic impurities of diesel fuel into linear alkanes improving diesel quality (Scheme 1.26).

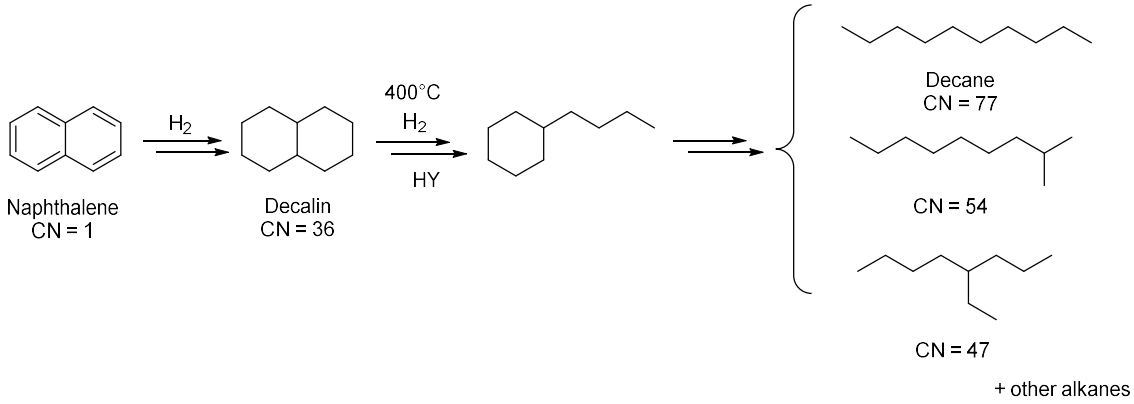

Scheme 1.26: Application of reductive C-C bond cleavage for upgrading diesel fuel through conversion of aromatic impurities into alkanes

This quality is measured by the cetane number (CN) which is higher for linear and low-branched hydrocarbons.[42] Initially, the aromatic impurities are hydrogenated to saturated naphthenic compounds and subsequently, the C-C bonds of these cycloalkanes are cleaved. Heterogeneous HY and Pt/HY zeolite catalysts effectively mediate the one-ring opening and ring-contraction of saturated naphthenic diesel impurities, such as decalin,

at a range of temperatures between 260 and 400 °C.[43] Unfortunately, the high temperatures required leads to a complex mixture of high-branched hydrocarbons with cetane numbers similar to those of saturated cyclic hydrocarbons.[44,45] Under these high temperatures, desirable linear and low-branched alkanes are difficult to obtain.

Another important application of the reductive cleavage of C-C bonds is the chemical recycling of polyalkene polymers into gasoline or lower alkanes, which is an excellent means to utilise plastic waste unsuitable for mechanical recycling.[46] One way to address this problem was proposed by Basset who reported the transformation of polyethylene and polypropylene to lower alkanes by silica-supported zirconium hydride catalysts at low temperature (150 ºC) and hydrogen pressure (0.4 atm).[47] During the course of the reaction, polyethylene is cleaved into oligomers (C_{10}-C_{17}) and into lower alkanes (C_1-C_9) at early times. Further heating leads to light alkanes, where methane and ethane are the major products. Although mild conditions were used, this catalytic process is unselective as indicated by the wide spectrum of products obtained.

Despite these important applications, the reductive cleavage of C-C bonds has been poorly investigated and only few examples have been reported to date. Only few examples of reductive cleavage of non-strained C-C bonds are known and among them, catalytic reductions of Csp-Csp^2 or Csp-Csp^3 and Csp^2-Csp^3 σ bonds are more common than that of Csp^3-Csp^3 bonds. In the next section, known examples of reductive cleavage of this type of C-C single bonds are discussed.

1.4.1. Reductive cleavage of Csp-Csp^2 and Csp-Csp^3 single bonds

The reductive cleavage has been shown an effective method for the scission of Csp-Csp^2 or Csp-Csp^3. Specifically, reductive elimination has been applied for the conversion of C-CN bonds into C-H bonds which offers a facile strategy for the removal of a widely employed directing group such as cyano group. For example, reduction of aryl nitriles into arenes with trimethylaluminum and hydrogen gas in the presence of nickel catalyst was reported by Maiti (Scheme 1.27).[48] Aryl cyanides containing hydroxyl, amide, keto or fluoro groups as well as heterocyclic cyanide compounds underwent hydrogenolysis in good yields (51-93%). The role of $AlMe_3$ was found to be crucial for the reductive

cleavage. It was proposed that $AlMe_3$ acts as a Lewis acid that activates the inert C-CN bond and facilitates the oxidative addition to the nickel centre. In addition, $AlMe_3$ can help to remove the HCN formed during the reaction. In addition, Maiti and co-workers also reported the nickel-catalysed reductive cleavage of C-CN bonds of aryl nitriles using tetramethyldisiloxane as the hydride source.[49]

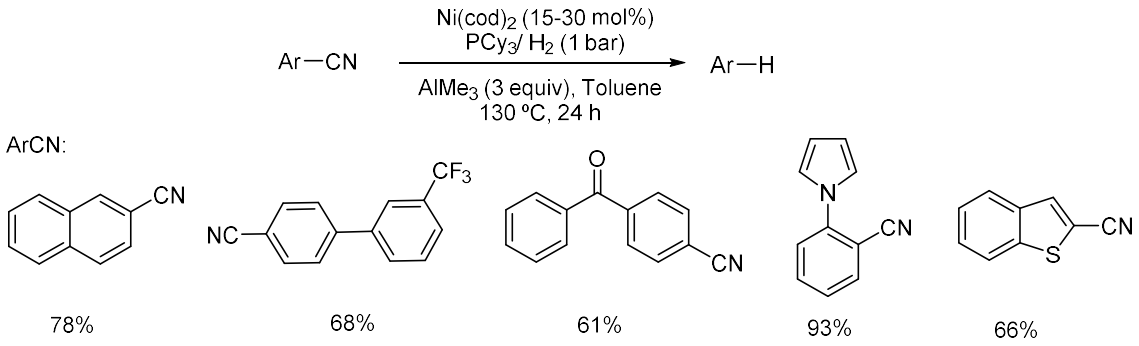

Scheme 1.27: Nickel-catalysed reductive cleavage of C-CN bonds of aromatic cyanides

A related reductive C-CN bond cleavage in aryl and alkyl nitriles was developed by the use of triisopropylsilane as a reductant (Scheme 1.28).[50] The use of a rhodium catalyst combined with a phosphine ligand (either $P(OBu)_3$ or $P(O^iPr)_3$) and triisopropylsilane effectively converted nitriles into decyanated products. A wide variety of nitriles could be cleaved under these conditions including bulky tertiary alkyl nitriles. It is proposed that hydrosilane reacts with the transition metal catalyst to form silyl metal species that initiates the catalytic cycle.[51]

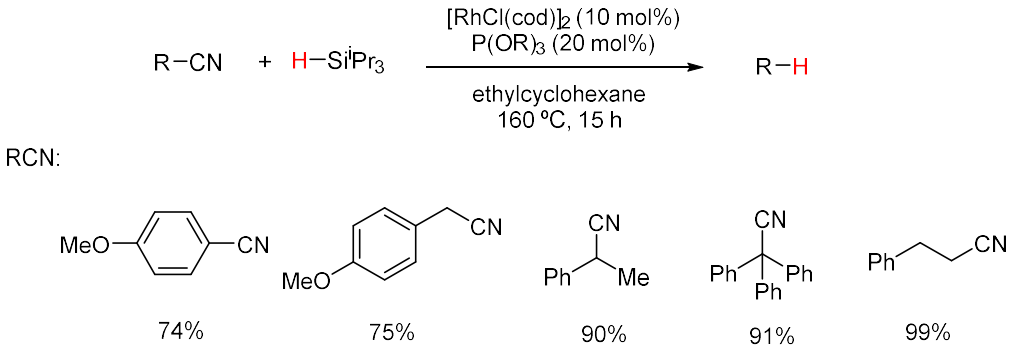

Scheme 1.28: Rhodium-catalysed reductive cleavage of C-CN bonds of aryl and alkyl cyanides

1.4.2. Reductive cleavage of Csp^2-Csp^3 single bonds

Most of the reported examples of catalytic reductive cleavage of Csp^2-Csp^3 single bonds used rhodium catalysts and involved substrates bearing directing groups to facilitate the process. For example, Milstein and coworkers described reductive cleavage of strong Csp^2-Csp^3 bond in a PCP pincer-type substrate assisted by chelating phosphine ligands (Scheme 1.29).[52] The C_{aryl}-C(R) bond between the two phosphines was cleaved by a rhodium catalyst under hydrogen atmosphere to give the dealkylated diphosphine product and methane or ethane. It is proposed that both phosphines coordinate to rhodium prior the oxidative addition into the C-C bond and the subsequent hydrogenolysis delivers the final products.

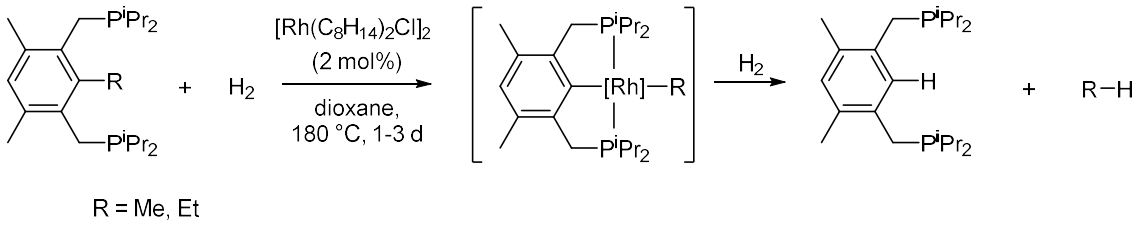

Scheme 1.29: Rh-catalysed hydrogenolysis of a Csp^2-Csp^3 bond in a PCP pincer-type substrate

Later, the same research group developed an analogous reductive Csp^2-Csp^3 bond cleavage in a POCOP pincer-type compound with a cationic rhodium complex at room temperature under hydrogen atmosphere (Scheme 1.30).[53] Similar to the previous example, the rhodium complex undergoes oxidative addition onto the C-C bond directed by coordination with both phosphine ligands. The intermediate alkyl rhodium complex reacts with hydrogen to give the dealkylated rhodium complex and methane.

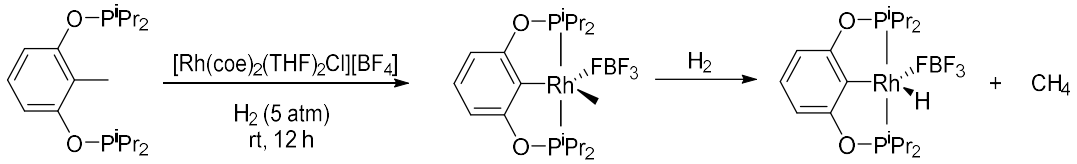

Scheme 1.30: Reductive cleavage of a Csp^2-Csp^3 bond of a POCOP pincer-type substrate

On the other hand, selective reductive cleavage of Csp^2-Csp^3 bonds has been developed for the scission of secondary benzyl alcohols (Scheme 1.31).[54] This reaction was successfully promoted by a rhodium catalyst under H_2 atmosphere to give an aryl and a

benzyl alcohol (Scheme 1.31).[54] Pyrazolyl and pyridinyl groups proved to be efficient functionalities to direct this selective transformation giving moderate to good yields of both products. Various functional groups such as ester, fluoro and methoxy groups were tolerated. The reaction is proposed to occur via β-carbon elimination assisted by Rh^{III}, giving a five-membered rhodacycle and aryl aldehyde. Subsequently, the rhodacycle reacts with H_2 to afford the two cleaved products.

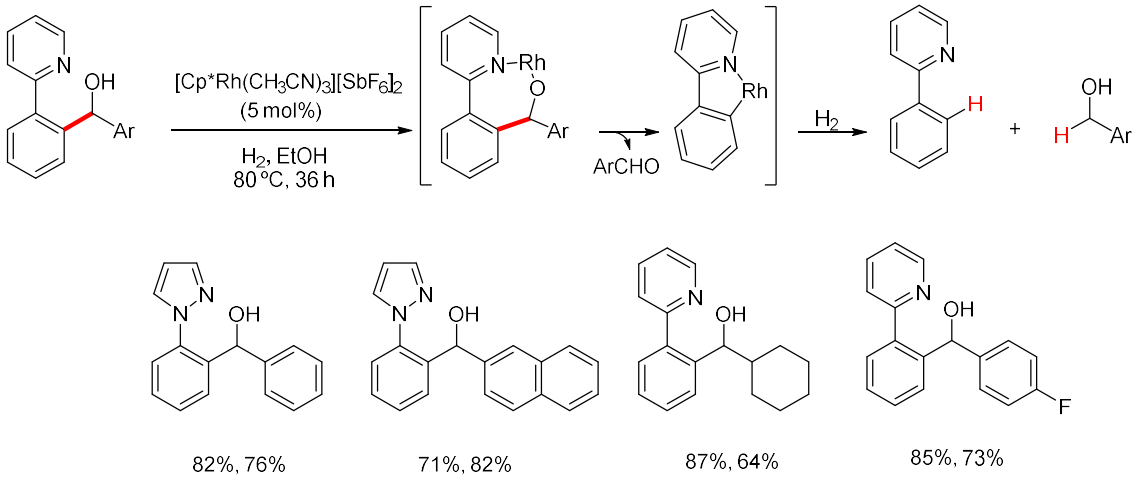

Scheme 1.31: Rh-catalysed selective reductive Csp^2-Csp^3 cleavage of benzyl alcohols directed by N-containing groups

1.4.3. Reductive cleavage of Csp^3-Csp^3 single bonds

Despite being one of the most inert bonds in organic compounds, Csp^3-Csp^3 bonds have been successfully broken *via* catalytic reductive cleavage methods. The majority of the reported examples involve the use of heterogeneous catalytic systems consisting of various types of supported metals. For example, palladium on carbon catalysed the reductive cleavage of Csp^3-Csp^3 bonds of cyclohexadienones (Scheme 1.32).[55] Allylic and benzylic cyclohexadienone derivatives were converted into dealkylated phenols under hydrogen atmosphere in the presence of the Pd/C catalyst. The C-C scission takes place at the quaternary carbon atom bearing an allyl or benzyl substituent. This hydrogenolysis process is proposed to occur via the attack of palladium hydride species that insert into the C-C bond between the allyl group and the quaternary carbon atom.

Subsequently, the protonation of the intermediate palladium species by the polar solvent gives the hydrogenolysis products.

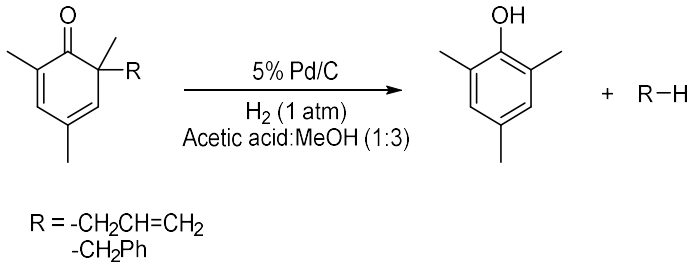

Scheme 1.32: Pd/C-catalysed reductive cleavage of Csp^3-Csp^3 bonds of cyclohexadienones

The effectiveness of Pd/C catalyst for hydrogenolysis of Csp^3-Csp^3 bonds was also shown by Fillion for the cleavage of benzyl Meldrum's acids into tertiary benzylic products (Scheme 1.33).[56] This transformation conducted in the presence of Pd/C under 1 atm of H_2 in MeOH for 24 h at room temperature, gave hydrogenolysed products in good to excellent yields (65-96%). Electronic effects at the aromatic ring play an important role for the reactivity. Substrates bearing *meta*-substituents gave no products whereas *ortho*- and *para*-substituted derivatives underwent reductive cleavage with high yields. Enantioenriched substrates experienced an inversion of the configuration of the asymmetric benzylic centre during the hydrogenolysis reaction. The authors proposed that the reaction occurs through nucleophilic substitution of the Meldrum's acid (S_N2) at the benzylic carbon atom by palladium hydride or Pd^0 to form an organopalladium intermediate which can be transformed into the product by protonation. Deuterium labelling studies showed that both H_2 and MeOH serve as the hydrogen sources in this reaction.

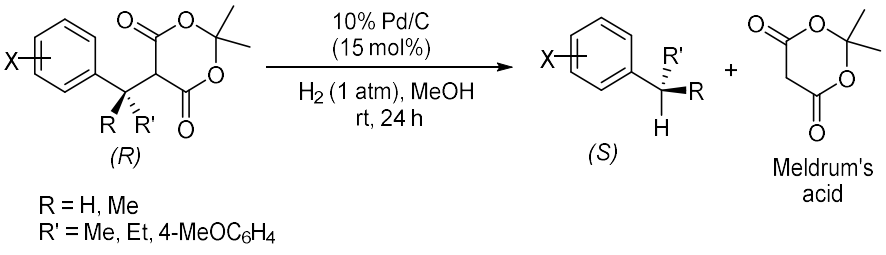

Scheme 1.33: Pd/C-catalysed reductive Csp^3-Csp^3 bond cleavage of Meldrum's acid derivatives

On the other hand, heterogeneous Ziegler-type catalysts[57] mediate the reductive cleavage of saturated hydrocarbons without the assistance of directing groups. An example of Ziegler-type catalysts is the combination of rhenium carbonyl or carbonyl-hydride complexes ($Re_2(CO)_{10}$, $Re_2H_3(CO)_{12}$, $Re_4H_4(CO)_{12}$) with organoaluminium compounds (Et_3Al, $^iBu_2AlH$). This catalytic system mediates the hydrogenolysis of alkanes at 150-180 ºC at 50 atm of H_2 pressure (Scheme 1.34).[58] In this reported example, terminal C-C bonds of linear hydrocarbons such as hexane or octane were reductively cleaved at early stage conversions. Upon longer reaction times, the selectivity of the reaction decreased leading to a range of products of subsequent hydrogenolyses where methane and ethane are the main products. The combination of both rhenium carbonyl complex and organoaluminium compound is essential for the reductive cleavage. Neither organoaluminium species alone nor rhenium complexes showed any activity in alkane cleavage at 180 ºC. Moreover, the activity of the catalyst strongly depends on the ratio of its metal components, which presents the maximum activity for an atomic Re/Al ratio equal to 3.

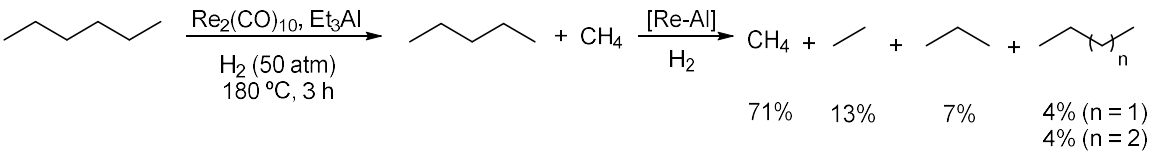

Scheme 1.34: Re/Al-catalysed reductive cleavage of Csp^3-Csp^3 bonds of hydrocarbons

The reductive cleavage of saturated hydrocarbons has also been studied by Basset who utilized silica-supported metal hydrides of hafnium and zirconium as catalysts that can operate at low temperatures. In particular, he showed that hafnium-hydride anchored on a silica surface ($(\equiv Si–O)_3–HfH$) is a an active catalyst for the hydrogenolysis of alkanes such as neopentane (Scheme 1.35).[59] When neopentane is subjected to hydrogenolysis with this hafnium catalyst at 100 ºC and 0.5 atm of H_2 pressure, isobutane and methane are formed in high selectivity as long as conversion is lower than 50%. However, formation of propane and ethane is observed above 50% conversion of the starting alkane indicating further cleavage. At full conversion, mainly methane and ethane are obtained as final products.

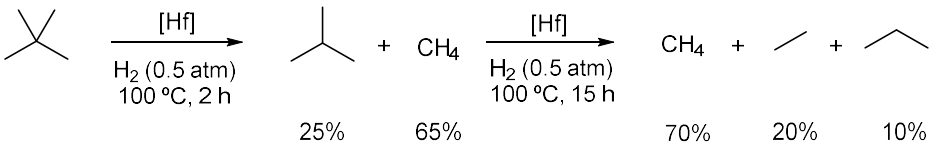

Scheme 1.35: Supported hafnium hydride-catalysed hydrogenolysis of neopentane

Zirconium hydride complexes supported on silica were also shown to catalyse the reductive cleavage of Csp^3-Csp^3 bonds of saturated hydrocarbons (Scheme 1.36). [59–61] In particular, the supported zirconium hydride catalyst [(≡Si–O)$_3$–ZrH] is exceptionally reactive for C_3-C_5 alkane scission. For example, n-butane is transformed into the lower alkanes with the Zr catalyst at 150 ºC and at 1 atm H_2 pressure. At low conversion, propane, ethane and methane were obtained with selectivities of 22%, 56% and 22% respectively. Subsequently, propane is converted into ethane (60%) and methane (40%), when the reaction proceeds further. Similar to the Hf catalyst, the active catalytic species for the hydrogenolysis is the supported zirconium hydride species [(≡Si–O)$_3$–ZrH] as proposed by the authors.

Scheme 1.36: Supported zirconium hydride- catalysed reductive cleavage of n-butane

Both supported hafnium and zirconium catalysts mediate reductive cleavage of saturated hydrocarbons yielding similar mixtures of methane and ethane. Therefore, both supported metal catalysts must operate through similar unselective reaction pathways. To understand the origin of this poor selectivity, Basset studied the mechanism of the reductive cleavage of saturated hydrocarbons using DFT calculations.[62] The hydrogenolysis of n-butane catalysed by silica-supported zirconium hydride species was selected as model reaction for the mechanistic investigations. The studies showed that the poor selectivity can be rationalised by two possible mechanistic pathways (Scheme 1.37). Thus, the zirconium catalyst can insert into a terminal C-H bond of butane (red pathway) leading to the formation of linear butyl-zirconium intermediate that undergoes β-alkyl elimination forming an ethyl-zirconium intermediate and ethylene. Subsequent hydrogenolysis of ethyl-zirconium bond, yields ethane and the zirconium hydride. The

insertion of the zirconium catalyst can also occur into a secondary C-H bond of butane (blue pathway) leading to the formation of a secondary butylzirconium intermediate. This species undergoes β-alkyl elimination to give propylene and the methylzirconium that after cleavage with hydrogen forms methane.

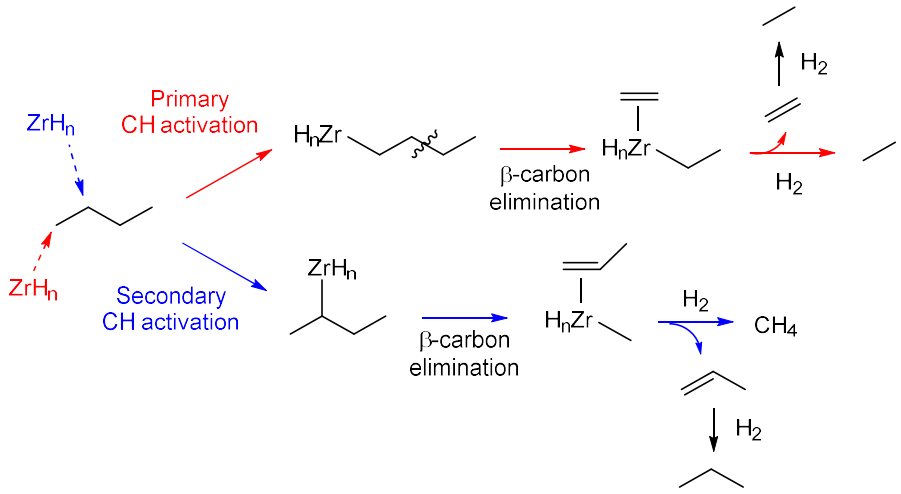

Scheme 1.37: Two possible mechanistic pathways for the supported-zirconium-catalysed hydrogenolysis of n-butane

The released propylene and ethylene are rapidly hydrogenated under these catalytic conditions into propane and ethane. Then, propene can reinsert into the zirconium catalyst and undergo reductive cleavage leading to the formation of ethane and methane via the same mechanism as previously described for n-butane. The DFT calculations reported by Basset prove that the transition states for the primary and the secondary C-H activations are energetically similar. Therefore, both mechanistic pathways are possible leading to a non-selective C-H activation that results in a non-selective C-C single bond cleavage. Intriguingly, the C-C bond cleavage to produce metal-olefin-alkyl intermediates is a very endergonic step. However, the subsequent hydrogenation of the formed olefins by the Zr hydride complex is a highly exergonic step that makes the overall process thermodynamically favourable.

The poor selectivity of reductive Csp^3-Csp^3 bond cleavage catalysed by heterogeneous catalysts led to further investigations for alternative catalytic methods capable of selectively break Csp^3-Csp^3 bonds. These selectivity issues can be addressed by the use of substrates bearing directing groups that enable selective C-H activation and subsequent

faster β-alkyl elimination using a highly active catalyst. The feasibility of this strategy was demonstrated by Murahashi and co-workers who conducted selective C-C bond cleavage in a series of unstrained 1,5-dinitriles and 5-cyanoketones with $Ir(P^iPr_3)_2H_5$ as a homogeneous catalyst (Scheme 1.38).[63] Various nitriles and ketones with different substituents reacted with $Ir(P^iPr_3)_2H_5$ (10 mol%) at 150 ºC to give benzyl nitriles with moderate to excellent yields (38-98%). Murahashi proposed that a free alkene is formed as a second product in these transformations. Substrates bearing terminal nitriles gave better product yields than the corresponding ketones which is explained by the better coordination abilities of nitriles toward the metal centre. Although only substrates with two functionalities were included in this work, this is the first example of catalytic alkene deinsertion through the cleavage of unstrained Csp^3-Csp^3 bonds. Intriguingly, this C-C bond cleavage is proposed to be achieved via β-alkyl elimination at the metal catalyst to give benzyl nitrile and olefin products. However, C-C cleavage through β-alkyl elimination to yield an olefin is an endothermic process as demonstrated by Basset. To successfully drive β-alkyl elimination, the alkene must be removed from the system to drive the equilibrium. Unfortunately, the mechanism of this transformation has not yet been investigated and the driving force that displaces the thermodynamic equilibrium of this process remains unknown. In addition, as discussed above, the selective alkene deinsertion is the key step for selective reductive cleavage of aliphatic C-C bonds. Therefore, the example reported by Murahashi can be used as a starting point for developing selective reductive cleavage of aliphatic C-C bonds.

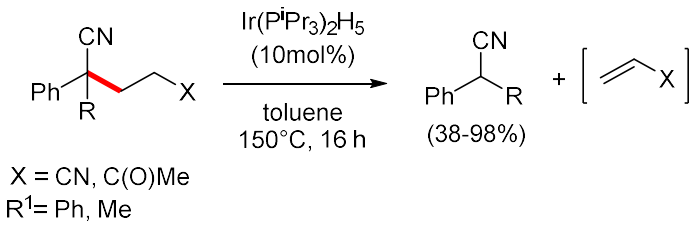

Scheme 1.38: Ir-catalysed reductive cleavage of C-C single bonds of nitriles and ketones

1.5. Summary and objectives

The transition metal catalysed cleavage of C-C single bonds is a highly important transformation involved in various industrial processes such as production of fuels and recycling of plastics. Moreover, this transformation can serve as an innovative synthetic tool for preparation of functionalised organic molecules from readily available chemical feedstock. In view of its important applications, several strategies have been developed to facilitate the cleavage of the thermodynamically and kinetically inert C-C bonds. One common strategy for facilitating C-C bond cleavage relies on the relief of ring strain, but it is limited only to the activation of strained C-C bonds in small cycles. More general strategy involved the use of chelation-assisted C-C bond cleavage, which can be applied for the activation not only for strained, but also for non-strained C-C bonds that are more commonly found in organic molecules. However, this strategy is limited to specific starting materials bearing certain type of functionalities, such as pincer-type moieties, nitrogen-containing groups or tertiary and primary alcohols.

Further investigations of the cleavage of non-strained C-C bonds demonstrated the effectiveness of the employment of reducing agents, such as H_2, to facilitate the endothermic transformation. The catalytic reductive cleavage of Csp-Csp^3, Csp-Csp^2 and Csp^2-Csp^3 bonds is more facile than Csp^3-Csp^3 bonds owing to thermodynamic and kinetic factors. Indeed, there are very few examples of the reductive Csp^3-Csp^3 cleavage and most of these involve heterogeneous catalysts that lead to unselective transformations.

A possible way to enable a selective cleavage of unstrained aliphatic Csp^3-Csp^3 single bonds is to use substrates with directing groups and a highly active transition metal catalyst. Murahashi and co-workers reported the first example of realisation of this strategy by conducting selective Csp^3-Csp^3 bond cleavage in dinitriles and cyanoketones substrates in the presence of $Ir(P^iPr_3)_2H_5$ catalyst. The reaction was proposed to occur via an unusual alkene deinsertion as a result of α-C-H activation and β-carbon elimination. However, experimental data to support this mechanism are lacking. Also, the scope of this intriguing transformation was limited to substrates bearing two functional groups, which leaves the question regarding the role of the functional groups open.

The main aim of this thesis is to investigate the mechanism of the catalytic reductive cleavage of unstrained aliphatic C-C bonds based on the work published by Murahashi. By studying the mechanism of this unique transformation, we aim:

- To provide a better understanding of the basis of the reductive cleavage of unstrained aliphatic C-C bonds catalysed by iridium complexes.

- To study the role of the functional groups which would allow to increase the substrate scope.

- To identify a more efficient catalyst that operates at milder reaction conditions.

- To evaluate the feasibility of selective, catalytic reductive cleavage of non-strained aliphatic C-C bonds using hydrogen and alcohols as reductants.

1.6. References

(1) Kunkes, E. L.; Simonetti, D. A.; West, R. M.; Serrano-Ruiz, J. C.; Gärtner, C. A.; Dumesic, J. A. *Science.* **2008**, *322* (5900), 417–421.

(2) Kaminsky, W.; Hartmann, F. *Angew. Chemie - Int. Ed.* **2000**, *39* (2), 331–333.

(3) Aguado, J.; Serrano, D. P.; Clark, J. H. In *Feedstock recycling of plastic wastes*; Aguado, J., Serrano, D. P., Clark, J. H., Eds.; 1999; pp 161–178.

(4) Murakami, M.; Ishida, N. *J. Am. Chem. Soc.* **2016**, *138* (42), 13759–13769.

(5) Halpern, J. *Acc. Chem. Res.* **1982**, *15* (8), 238–244.

(6) Murakami, M. *Cleavage of carbon-carbon single bonds by transition metals*; Wiley, 2015.

(7) Stephen J. Blanksby, Ellison, G. B. *Acc. Chem. Res.* **2003**, *36* (4), 255–263.

(8) Bryndza, H. E.; Fong, L. K.; Paciello, R. A.; Tam, W.; Bercaw, J. E. *J. Am. Chem. Soc.* **1987**, *109* (5), 1444–1456.

(9) Heck, R. F. *J. Am. Chem. Soc.* **1969**, *91* (24), 6707–6714.

(10) Adams, D. M.; Chatt, J.; Guy, R. G.; Sheppard, N. *J. Chem. Soc.* **1961**, *0* (0), 738–742.

(11) Bart, S. C.; Chirik, P. J. *J. Am. Chem. Soc.* **2003**, *125* (4), 886–887.

(12) Murakami, M.; Amii, H.; Shigeto, K.; Ito, Y. *J. Am. Chem. Soc.* **1996**, *118* (35), 8285–8290.

(13) Perthuisot, C.; Edelbach, B. L.; Zubris, D. L.; Simhai, N.; Iverson, C. N.; Müller, C.; Satoh, T.; Jones, W. D. *J. Mol. Catal. A Chem.* **2002**, *189* (1), 157–168.

(14) Edelbach, B. L.; Lachicotte, R. J.; Jones, W. D. *Organometallics* **1999**, *18* (20), 4040–4049.

(15) Perthuisot, C.; Jones, W. D. *J. Am. Chem. Soc.* **1994**, *116* (8), 3647–3648.

(16) Satoh, T.; Jones, W. D. *Organometallics* **2001**, *20* (13), 2916–2919.

(17) Flood, T. C.; Statler, J. A. *Organometallics* **1984**, *3* (12), 1795–1803.

(18) Crabtree, R. H.; Dion, R. P.; Gibboni, D. J.; McGrath, D. V.; Holt, E. M. *J. Am. Chem. Soc.* **1986**, *108* (23), 7222–7227.

(19) Suggs, J. W.; Jun, C. H. *J. Am. Chem. Soc.* **1986**, *108* (15), 4679–4681.

(20) Suggs, J. W.; Jun, C.-H. *J. Chem. Soc., Chem. Commun.* **1985**, No. 2, 92–93.

(21) Rybtchinski, B.; Vigalok, A.; Ben-David, Y.; Milstein, D. *J. Am. Chem. Soc.* **1996**, *118* (49), 12406–12415.

(22) Chatani, N.; Ie, Y.; Kakiuchi, F.; Murai, S. *J. Am. Chem. Soc.* **1999**, *121* (37), 8645.

(23) Tobisu, M.; Kita, Y.; Chatani, N. *J. Am. Chem. Soc.* **2006**, *128* (25), 8152–8153.

(24) Jun, C.-H.; Lee, H. *J. Am. Chem. Soc.* **1999**, *121* (4), 880–881.

(25) Jun, C.-H.; Lee, D.-Y.; Kim, Y.-H.; Lee, H. *Organometallics* **2001**, *20* (13), 2928–2931.

(26) Terao, Y.; Wakui, H.; Satoh, T.; Miura, M.; Nomura, M. *J. Am. Chem. Soc.* **2001**, *123*, 10407–10408.

(27) Yoshito Terao; Hiroyuki Wakui; Tetsuya Satoh; Masahiro Miura; Nomura, M. *J. Am. Chem. Soc.* **2001**, *123* (42), 10407–10408.

(28) Ozkal, E.; Cacherat, B.; Morandi, B. *ACS Catal.* **2015**, *5* (11), 6458–6462.

(29) Nishimura, T.; Araki, H.; Maeda, Y.; Uemura, S. *Org. Lett.* **2003**, *5* (17), 2997–2999.

(30) Siegbahn, P. E. M. *J. Phys. Chem.* **1995**, *99* (34), 12723–12729.

(31) Hajela, S.; Bercaw, J. E. *Organometallics* **1994**, *13* (4), 1147–1154.

(32) Horton, A. D. *Organometallics* **1996**, *15* (12), 2675–2677.

(33) Beswick, C. L.; Marks, T. J. *J. Am. Chem. Soc.* **2000**, *122* (42), 10358–10370.

(34) Watson, P. L.; Roe, D. C. *J. Am. Chem. Soc.* **1982**, *104* (23), 6471–6473.

(35) Kondo, T.; Kodoi, K.; Nishinaga, E.; Okada, T.; Morisaki, Y.; Watanabe, Y.; Mitsudo, T. *J. Am. Chem. Soc.* **1998**, *120* (22), 5587–5588.

(36) Wang, Y.; Kang, Q. *Org. Lett.* **2014**, *16* (16), 4190–4193.

(37) Chen, Y.-C.; Zhu, M.-K.; Loh, T.-P. *Org. Lett.* **2015**, *17* (11), 2712–2715.

(38) Yorimitsu, H.; Oshima, K. *Bull. Chem. Soc. Jpn.* **2009**, *82* (7), 778–792.

(39) Hayashi, S.; Hirano, K.; Yorimitsu, H.; Oshima, K. *J. Am. Chem. Soc.* **2006**, *128* (7), 2210–2211.

(40) Nečas, D.; Turský, M.; Kotora, M. *J. Am. Chem. Soc.* **2004**, *126* (33), 10222–10223.

(41) Cane, D. E.; Iyengar, R. *Tetrahedron Lett.* **1979**, *20* (31), 2871–2874.

(42) Fan, W.; Jia, M.; Chang, Y.; Xie, M. *Energy & Fuels* **2015**, *29* (5), 3413–3427.

(43) Santikunaporn, M.; Herrera, J. E.; Jongpatiwut, S.; Resasco, D. E.; Alvarez, W. E.; Sughrue, E. L. *J. Catal.* **2004**, *228* (1), 100–113.

(44) Santana, R. C.; Do, P. T.; Santikunaporn, M.; Alvarez, W. E.; Taylor, J. D.; Sughrue, E. L.; Resasco, D. E. *Fuel* **2006**, *85* (5–6), 643–656.

(45) Kubička, D.; Kumar, N.; Mäki-Arvela, P.; Tiitta, M.; Niemi, V.; Karhu, H.; Salmi, T.; Murzin, D. Y. *J. Catal.* **2004**, *227* (2), 313–327.

(46) Aguado, J.; Serrano, D. P.; San Miguel, G.; Castro, M. C.; Madrid, S. *J. Anal. Appl. Pyrolysis* **2007**, *79* (1–2 SPEC. ISS.), 415–423.

(47) Dufaud, V.; Basset, J. M. *Angew. Chemie - Int. Ed.* **1998**, *37* (6), 806–810.

(48) Patra, T.; Agasti, S.; Modak, A.; Maiti, D. *Chem. Commun.* **2013**, *49* (75), 8362.

(49) Patra, T.; Agasti, S.; Akanksha; Maiti, D. *Chem. Commun.* **2013**, *49* (1), 69.

(50) Tobisu, M.; Nakamura, R.; Kita, Y.; Chatani, N. *J. Am. Chem. Soc.* **2009**, *131* (9), 3174–3175.

(51) Tobisu, M.; Nakamura, R.; Kita, Y.; Chatani, N. *Bull. Korean Chem. Soc.* **2010**,

31 (3), 582–587.

(52) Liou, S.-Y.; van der Boom, M. E.; Milstein, D.; Spek, A. L.; Koten, G. van. *Chem. Commun.* **1998**, *35* (6), 687–688.

(53) Salem, H.; Ben-David, Y.; Shimon, L. J. W.; Milstein, D. *Organometallics* **2006**, *25* (9), 2292–2300.

(54) Chen, K.; Li, H.; Lei, Z.-Q.; Li, Y.; Ye, W.-H.; Zhang, L.-S.; Sun, J.; Shi, Z.-J. *Angew. Chemie Int. Ed.* **2012**, *51* (39), 9851–9855.

(55) Miller, B.; Lewis, L. *J. Org. Chem.* **1974**, *39* (17), 2605–2607.

(56) Wilsily, A.; Nguyen, Y.; Fillion, E. *J. Am. Chem. Soc.* **2009**, *131* (43), 15606–15607.

(57) Boor, J. *J. Polym. Sci. Macromol. Rev.* **1967**, *2* (1), 115–268.

(58) Vol'pin, M. E.; Akhrem, I. S.; Reznichenko, S. V.; Grushin, V. V. *J. Organomet. Chem.* **1987**, *334* (1–2), 109–116.

(59) Ornelas, L. d'; Reyes, S.; Quignard, F.; Choplin, A.; Basset, J.-M. *Chem. Lett.* **1993**, *22* (11), 1931–1934.

(60) Lecuyer, C.; Quignard, F.; Choplin, A.; Olivier, D.; Basset, J.-M. *Angew. Chemie Int. Ed.* **1991**, *30* (12), 1660–1661.

(61) Bendjeriou-Sedjerari, A.; Azzi, J. M.; Abou-Hamad, E.; Anjum, D. H.; Pasha, F. A.; Huang, K.-W.; Emsley, L.; Basset, J.-M. *J. Am. Chem. Soc.* **2013**, *135* (47), 17943–17951.

(62) Pasha, F. A.; Bendjeriou-Sedjerari, A.; Huang, K.-W.; Basset, J.-M. *Organometallics* **2014**, *33* (13), 3320–3327.

(63) Terai, H.; Takaya, H.; Murahashi, S. I. *Synlett* **2004**, No. 12, 2185–2187.

Chapter 2

Ir-catalysed selective reductive cleavage of unstrained aliphatic C-C bonds: Insight into the catalytic cycle

2.1. Introduction

As discussed in the previous chapter, the reductive cleavage of C-C bonds promoted by transition metal catalysts is an important process for industrial production of fuels from hydrocarbons and polymer recycling. Furthermore, this transformation is of growing interest in the context of synthetic chemistry as it offers the potential to make valuable chemicals through the functionalisation of C-C bonds in an atom-economical fashion.

However, the existing processes for the reductive cleavage of unstrained aliphatic C-C single bonds employ heterogeneous catalysts which are poorly selective. Based on mechanistic studies conducted by Basset with one of the most active heterogeneous catalysts (Chapter 1, Section 1.4.3), a mechanism for this transformation involves unselective C-H activation followed by β-alkyl elimination which results in an unselective cleavage.[1] An attractive approach to improve the selectivity is the use of substrates with directing groups to enable a selective C-H activation and subsequent faster β-alkyl elimination using highly active catalysts that facilitate both steps. In 2004, Murahashi and co-workers employed this strategy for the selective cleavage of unstrained C-C single bonds of dinitriles and cyanoketones catalysed by the homogeneous $Ir(P^iPr_3)_2H_5$ catalyst, leading to the formation of benzylic nitriles (Scheme 2.1).[2] In addition, the formation of a free alkene was proposed as a second cleavage product. This is a unique transformation as is the first example of catalytic alkene deinsertion *via* the cleavage of non-strained C-C bonds. Indeed, this transformation is typically considered as thermodynamically unfavourable.[1] Previous examples of this process involved stoichiometric β-alkyl eliminations from electrophilic early transition and rare earth metals complexes where the resulting alkene product underwent subsequent irreversible conversion into allyl complexes (Chapter 1, Section 1.3.2).

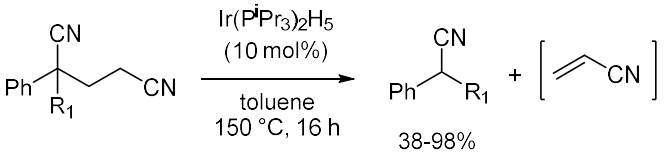

Scheme 2.1: Ir-catalysed C-C single bond cleavage of nitriles

Although with no experimental evidences, the mechanism of this process was proposed to occur *via* Basset-type mechanism involving C-H activation followed by β-alkyl elimination (Scheme 2.2). According to Murahashi, the monocoordinated nitrile substrate undergoes C-H activation to form complex **B**. The subsequent β-alkyl elimination leads to the olefin-coordinated intermediate **C** which after alkene deinsertion and reductive elimination, afford the products of the cleavage. This is an unusual transformation for several reasons. First, alkene deinsertion *via* β-alkyl elimination is typically a thermodynamically unfavourable reaction due to high bond dissociation energy of metal-alkyl bonds, making the products of the β-alkyl elimination less stable than the reactants.[3] Second, in this case β-alkyl elimination occurs faster than β-hydrogen elimination, which is in most cases thermodynamically and kinetically more favourable and takes place preferentially (Chapter 1.1). Third, the scope of this process is limited to substrates bearing two functional groups and the role of the second functional group is unknown.

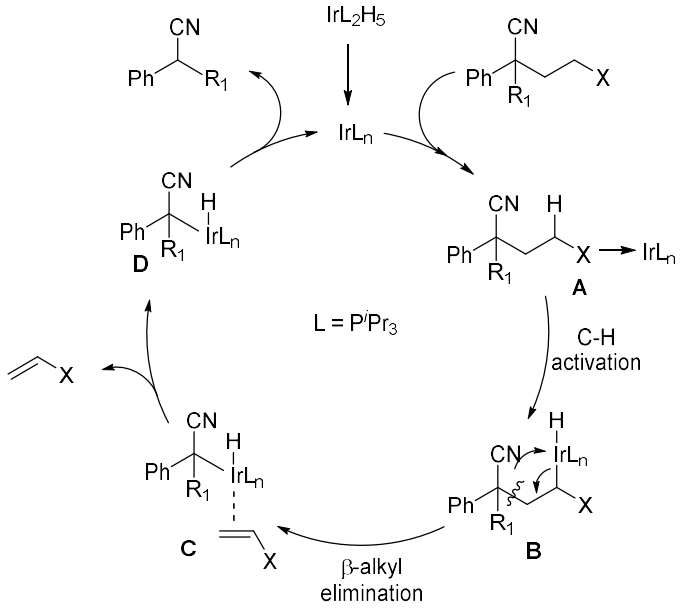

Scheme 2.2: Proposed mechanism by Murahashi, C-C bond cleavage *via* C-H activation followed by β-carbon elimination.

Thus, the mechanism of this reaction as well as the role of directing groups still remain speculative due to the lack of experimental evidences. In this view, we carried out an investigation of the mechanism of this unusual C-C cleavage reaction through a combination of experimental and computational studies. The understanding of this process would help to develop more efficient catalysts and increase the scope of this transformation. Moreover, this mechanistic comprehension would facilitate the design of further C-C functionalisation reactions based on this transformation.

2.2. Ir-catalysed reductive cleavage of unstrained aliphatic C-C bonds of dinitriles: first evidences towards the insight into the catalytic cycle

To get an insight into the mechanism of this transformation, we selected the cleavage of 2,2-diphenylpentanedinitrile **2** (one of the most reactive substrates tested by Murahashi) with 10 mol% of $Ir(P^iPr_3)_2H_5$ in toluene at 150 ºC for 16 h as a model reaction (Scheme 2.1). Initially, the model dinitrile **2** was synthesised *via* Michael addition with diphenylacetonitrile **3** and acrylonitrile **4** with KOH in MeOH in 79% yield (Scheme 2.3).

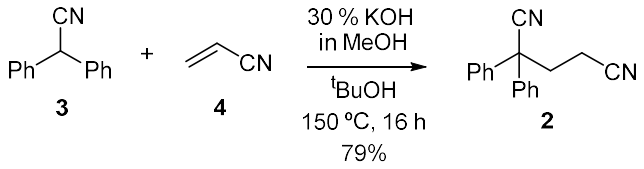

Scheme 2.3: Synthesis of model dinitrile substrate **2**

Carefully analysing the work reported by Murahashi (Scheme 2.1), we realized the intriguing fact that the formation of the second cleavage product – the alkene – was mentioned, but no yields of the alkene products were reported. Considering this fact, we reproduced catalytic conditions employed by Murahashi by heating dinitrile **2** with 10 mol% of $Ir(P^iPr_3)_2H_5$ (**1**) in toluene at 150 °C for 16 h. This reaction led to the formation of diphenylacetonitrile **3** in 75% GC yield at 75% conversion of the starting material, but no expected alkene product was observed. Instead, propionitrile **5** was detected as a second product in 20% yield according to GC and GC-MS analyses (Table 2.1, entry 1). In addition, formation of an insoluble material was observed.

Table 2.1: $Ir(P^iPr_3)_2H_5$-catalysed reductive C-C bond cleavage of dinitrile (**2**)

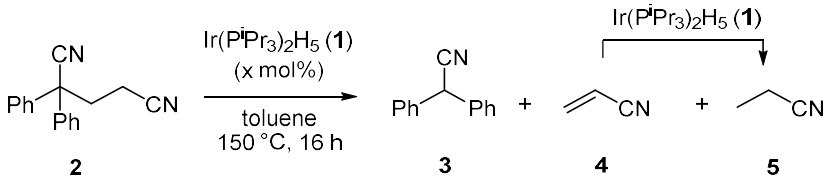

Entry	Catalyst 1, mol%	Conversion 2, %	Yields, %		
			3	**4**	**5**
1	10	75	75	0	20
2	20	95	95	0	45

As the original paper was not certain about the catalyst loading used (10 or 20 mol%), we conducted the model reaction also in the presence of higher catalyst loading (20 mol%). In this case, the reaction gave products **3** and **5** in 95 and 45% yield, respectively, at 95% conversion of **2** (Table 2.1, entry 2). The yield of nitrile **2** is close to that reported by Murahashi (98%).

With all these results in hands, we propose that the propionitrile product that was overlooked in the original paper is the result of rapid hydrogenation of the intermediately formed acrylonitrile **4** by the iridium pentahydride complex **1** (Scheme in Table 2.1).[4] Indeed, this complex can serve as an active hydrogenation catalyst[5] and a "reservoir" of dihydrogen.[6] When 10 mol% of catalyst is used, complex **1** can supply 25 mol% of H_2, which is sufficient to give a 25% yield of propionitrile. To test this hypothesis, we conducted a control experiment with acrylonitrile **4** and 10 mol% of **1** under the standard catalytic conditions (Table 2.2, entry 1). This experiment led to full conversion of acrylonitrile **4** and formation of propionitrile in 22% yield, which is similar to the 20% yield found in the model catalytic reaction with dinitrile **2** (Table 2.1, entry 1). The result of this control experiment confirms our proposal of hydrogenation of the transient acrylonitrile **4** during the C-C cleavage. As a side product, we isolated an insoluble material similar to the one observed after the model catalytic reaction that was identified as polyacrylonitrile (PAN) according to ^1H, ^{13}C-NMR, MS, IR and ICP data. In view of

this, we suggest that acrylonitrile undergoes polymerisation promoted by the iridium catalyst, as supported by literature examples.[4]

Table 2.2: Hydrogenation and polymerisation of acrylonitrile catalysed by $Ir(P^iPr_3)_2H_5$

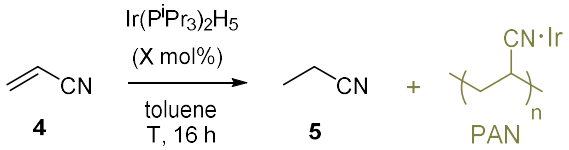

Entry	T, °C	Catalyst 1, mol%	Conversion 4, %	Yield 5, %
1	150	10	100	22
2	150	20	100	20
3	25	10	69	8
4	25	20	98	11

We conducted the hydrogenation of acrylonitrile but using 20 mol% of **1** which, in this case, it can supply 50 mol% of H_2. This reaction afforded propionitrile in 20% yield and polyacrylonitrile, with complete consumption of the starting alkene (Table 2.2, entry 2). In contrast to the corresponding model reaction conducted with 20 mol% of **1** (Table 2.1), the use of higher catalyst loading did not lead to a higher yield of propionitrile **5** (Table 2.2, entries 1 and 2). Although we do not have a clear explanation for this result, we hypothesise that the relative amount of hydrogenation and polymerisation products depends on catalyst speciation. Remarkably, acrylonitrile **4** reacts with catalyst **1** even at room temperature with 69% and 98% conversion in the presence of 10 and 20 mol% of the catalyst, respectively (Table 2.2, entries 3 and 4). These results suggest that the hydrogenation and polymerisation of acrylonitrile occurs much faster than the C-C bond cleavage process and that the alkene product cannot be formed in the C-C bond cleavage reaction reported by Murahashi.

Based on these control experiments, we proposed that the alkene is an unstable intermediate product of the C-C bond cleavage and undergoes rapid hydrogenation and polymerisation reactions in subsequent step. According to the available literature data,[1] the cleavage of C-C single bonds *via* alkene deinsertion (Scheme 2.2) is a

thermodynamically unfavourable process which explains why it has rarely been observed before. To test whether this is the case for our model reaction, we conducted DFT calculations of the free Gibbs energy of the alkene deinsertion of dinitrile substrate **2** in toluene PCM solvent model at 150 °C using Gaussian 09, M06-2X/6-31(d,p) functional (in collaboration with Dr. Neil Berry, University of Liverpool). The results suggest that this process is endergonic with ΔG_{423K}= 25 kJ/mol (Scheme 2.3A). In addition, DFT calculations show that the hydrogenation of acrylonitrile is a favourable process with ΔG_{423K}= -96 kJ/mol (Scheme 2.3B). Remarkably, the coupling of alkene deinsertion with its subsequent hydrogenation makes the entire C-C bond cleavage a highly exergonic process (Scheme 2.3C). These data explain the feasibility of the model reaction and also, are consistent with the higher yields and conversions obtained when higher amounts of dihydrogen are available in the reaction media due to higher catalyst loadings used (10 and 20 mol% of **1**, Table 2.1, entries 1 and 2, respectively). In addition, these computational results are in line with the data for alkene deinsertion from alkanes shown by Basset, as discussed in the previous chapter (Chapter 1, Section 1.4.3).[1,7]

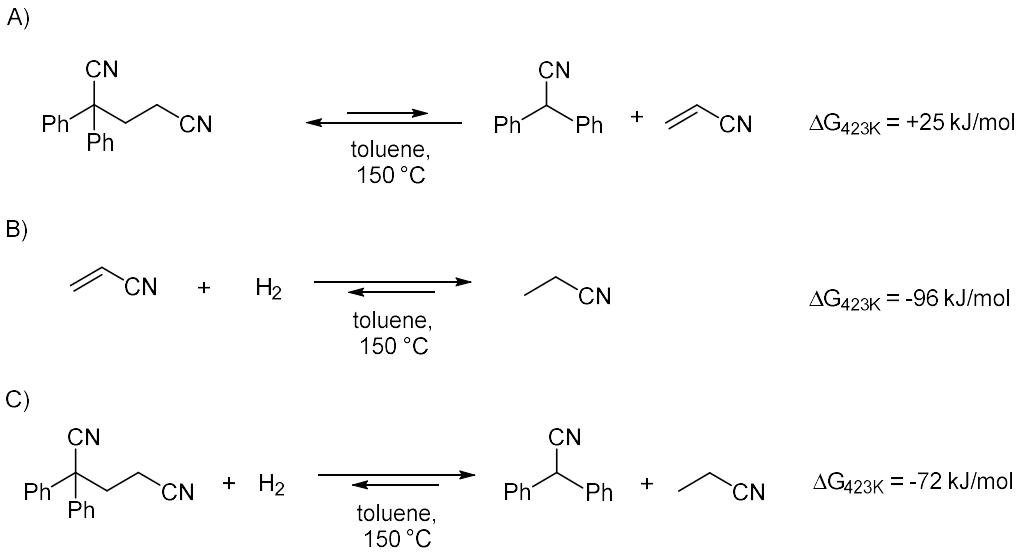

Scheme 2.3: Computed free Gibbs energies for A) Alkene deinsertion from 2,2-diphenylpentanedinitrile; B) Hydrogenation of acrylonitrile; C) Reductive cleavage of 2,2-diphenylpentanedinitrile

On the basis of the obtained data, we propose that the reductive C-C bond cleavage in dinitriles occurs *via* a reversible alkene deinsertion that it is enabled by the irreversible

alkene hydrogenation and polymerisation, which shift the equilibrium towards the products of the cleavage and make feasible the thermodynamically unfavourable alkene deinsertion (Scheme 2.4).

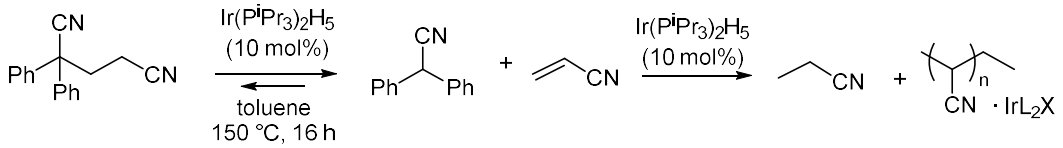

Scheme 2.4: Reductive cleavage of C-C bonds in 2,2-diphenylpentanedinitrile *via* reversible followed by irreversible alkene hydrogenation and polymerisation

To test the reversibility of the alkene deinsertion, we conducted the reaction that is reverse of the C-C bond cleavage by coupling diphenylacetonitrile **3** and acrylonitrile **4** in 1:1 ratio with 10 mol% of $Ir(P^iPr_3)_2H_5$ (**1**) at 150 °C for 16 h. Remarkably, this experiment led to the formation of dinitrile **2** in a 15% yield confirming the reversibility of the process (Table 2.3, entry 1). Note that conversion of **3** was only 15% whereas the acrylonitrile was completely consumed to give hydrogenation and polymerisation products. Based on the observation of fast alkene consumption at 150 °C providing low yields of product **2**, we decided to conduct the same reaction at room temperature. Surprisingly, this experiment afforded product **2** in 69% yield at 71% conversion of **3** and complete conversion of the alkene (Table 2.3, entry 2). As the alkene is fully consumed under these conditions, excess of acrylonitrile (10 equiv) was used to increase the yield of dinitrile **2**. This experiment conducted at 150 °C and at room temperature led to good yields of dinitrile **2**, with 64 and 52% respectively (Table 2.3, entries 3 and 4). These results confirm the reversibility of the alkene deinsertion *via* the C-C cleavage. Moreover, they demonstrate the ability of iridium catalyst **1** to efficiently mediate both reductive C-C bond cleavage and hydroalkylation reaction depending on the reaction conditions. Importantly, we discovered that the catalytic hydroalkylation of acrylonitrile with diphenylacetonitrile can be conducted at room temperature to give dinitrile product **2** in good yield.

Table 2.3: Ir-catalyzed hydroalkylation of acrylonitrile with diphenylacetonitrile (GC yields)

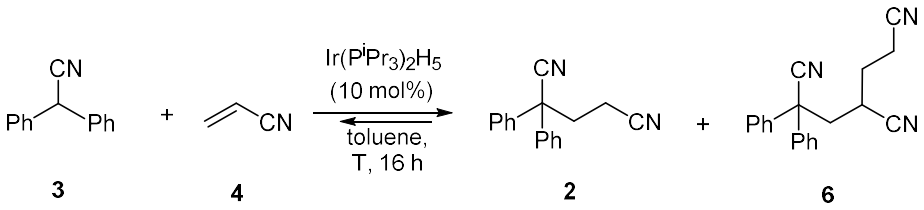

Entry	Ratio 3 : 4	T, °C	Conversion, %		Yield, %	
			3	4[a]	2	6
1	1:1	150	15	100	15	0
2	1:1	25	71	100	69	0
3	1:10	150	88	80	64	21
4	1:10	25	81	59	52	25

[a]: Propionitrile and polyacrylonitrile were formed as side products

Interestingly, the use of large excess of acrylonitrile in the hydroalkylation reaction led to the formation of side product **6** as a result of double alkylation of diphenylacetonitrile. We hypothesise that product **6** is obtained from the alkylation of the dinitrile product **2** *via* α-C-H bond activation of the terminal cyano group (Scheme 2.5).[8]

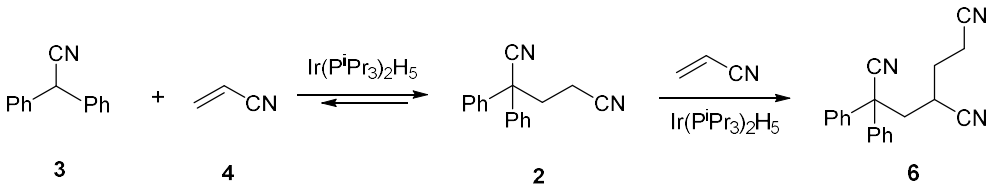

Scheme 2.5: Formation of dialkylation product **6** from dinitrile **2** during the hydroalkylation reaction

Considering the reversibility of the C-C cleavage process of dinitrile **2**, this reaction should be suppressed by the presence of any of the cleavage products, either diphenylacetonitrile **3** or acrylonitrile **4**. Under these conditions, the equilibrium of the reversible cleavage reaction should be shifted towards the reagents according to Le Chatelier's principle. Indeed, when the model cleavage reaction was conducted in the presence of 10-fold excess of diphenylacetonitrile **3** under the standard reaction conditions, the starting dinitrile **2** did not undergo cleavage (Scheme 2.6A). Similarly, this cleavage was also suppressed by the presence of 10-fold excess of acrylonitrile

(Scheme 2.6B). It is noteworthy that in these latter conditions, the product of alkylation of dinitrile **2** with acrylonitrile (Product **6**) was not formed as it does in the reversible reaction (Scheme 2.5). This fact might be explained by a more favourable hydrogenation and polymerisation of acrylonitrile catalysed by complex **1** that compete with α-C-H activation of dinitrile **2** and inhibits the alkylation.

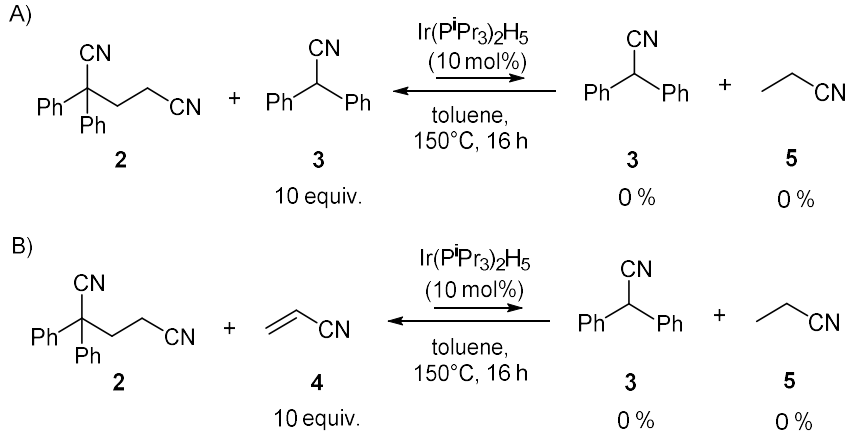

Scheme 2.6: Ir-catalysed cleavage of dinitrile **2** suppressed by diphenylacetonitrile **3** and acrylonitrile **4**

Finally, we conducted an additional control experiment to confirm the irreversibility of the entire reductive C-C cleavage process (Scheme 2.4). With this aim, diphenylacetonitrile **3** and propionitrile **5** were heated at 150 ºC for 16 h in the presence of 10 mol% of catalyst **1** (Scheme 2.7). This reaction did not lead to the formation of dinitrile **2** and the starting materials remained unreacted, evidencing the irreversibility of the C-C cleavage once the transient alkene is consumed.

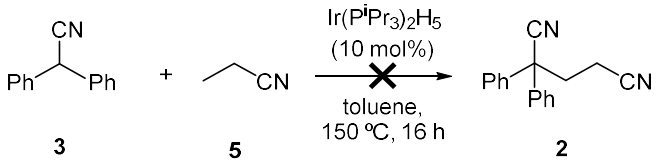

Scheme 2.7: Control experiment to test the irreversibility of C-C cleavage after alkene consumption

In summary, our experimental and computational data indicate that the C-C bond cleavage in dinitirles is a thermodynamically unfavourable process and does not give the free alkene as a second product (as proposed by Murahashi and co-workers). Under

reaction conditions the resulting alkene undergoes rapid irreversible hydrogenation and polymerisation in the presence of the iridium pentahydride catalyst; these processes serve as a driving force for the C-C cleavage process making it thermodynamically favourable. Intriguingly, we showed that the alkene deinsertion process is reversible and its microscopic reverse - hydroalkylation reaction could be efficiently catalysed by the same iridium catalyst under adjusted reaction conditions. That is, we propose that the C-C bond cleavage process in question occurs *via* endergonic reversible alkene deinsertion followed by exergonic irreversible hydrogenation and polymerisation of the transient alkene, and therefore, can be described as a reductive cleavage (hydrogenolysis) of the aliphatic C-C bonds in dinitriles.

2.3. Screening of the catalytic system

Our initial studies on the reductive cleavage of C-C bonds of dinitriles show that this transformation catalysed by $Ir(P^iPr_3)_2H_5$ complex requires high catalyst loadings (10 mol%) and high temperatures (150 °C) which might favour observed undesirable processes, such as alkene polymerisation. To avoid this, we are interested in identifying an alternative highly selective catalyst that can operate under milder conditions than catalyst **1**. With this goal, we conducted a screening of an alternative catalytic system that can mediate the C-C cleavage in comparable yields to the iridium pentahydride complex **1**. Ideally, we also seek a more air-stable catalytic system that would be commercially available to avoid the use of the extremely air-sensitive catalyst **1** and its tedious multistep synthesis.

The selection of catalytic systems for the screening was based on the proposed mechanism of the C-C bond cleavage of dinitriles which was suggested to involve C-H activation as a first step, as shown in Scheme 2.2 (Section 2.1). We hypothesise that the C-H activation might be the rate determining step of the process. Based on this, we chose to focus on metal complexes that might have high activity in C-H activation and therefore, they should facilitate the C-C bond cleavage process. It is well known that the C-H activation is favoured by the use of catalysts based on electron-rich complexes, in particular, metal complexes with electron-donating ligands.[9,10] Herein, we focused on screening iridium

complexes with electron-rich ligands that showed highest activity in known C-H activations: phosphine, phenanthroline and N-heterocyclic carbene iridium complexes. The activity of phosphine iridium complexes for C-H activations was demonstrated in alkane metathesis,[11] borylation of arenes,[12] carbonylation of benzene[13] and deuteration of hydrocarbons.[14] On the other hand, phenanthroline iridium complexes also catalyse C-H borylation of cyclopropanes,[15] and hydrosilylation of primary aliphatic C-H bonds directed by a hydroxyl group.[16] Finally, N-heterocyclic carbene iridium complexes are also able to mediate C-H hydrosilylation of alkynes[17] and deuteration of different organic molecules.[18]

For catalyst screening we used the iridium complexes generated *in situ* from the combination of the corresponding ligand and $[Ir(cod)Cl]_2$ as iridium precursor. This complex was chosen because its cyclooctadiene ligands are easily displaced by other more strongly coordinating ligands making it a versatile precursor for many Ir-catalyzed reactions.[19] To conduct the screening of the catalytic system, the C-C bond cleavage of dinitrile **2** with 5 mol% of $[Ir(cod)Cl]_2$ and ligand (20 mol%) in toluene at 150 °C for 16 h was selected as a model reaction (Scheme 2.8).

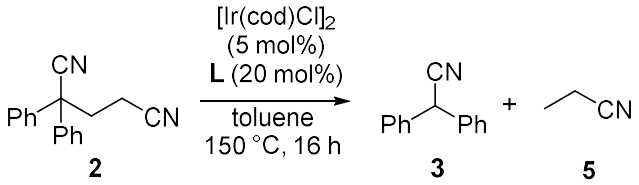

Scheme 2.8: Model C-C cleavage of **2** for the screening of catalysts

Firstly, we screened a set of phosphines with different electronic and steric properties,[20,21] including mono- and bidentate phosphines.[22, 23] The monodentate phosphines (Figure 2.1) included triisopropylphosphine, tricyclohexylphosphine, di(1-adamantyl)-n-butylphosphine, JohnPhos and CyJohnPhos (Table 2.4, entries 1-5). On the other hand, the bidentate phosphines (Figure 2.1) included dppf and rac-BINAP (Table 2.4, entries 6 and 7). Unfortunately, the catalytic system based on $[Ir(cod)Cl]_2$ (5 mol%) with any of the tested phosphines (monodentate: 20 mol%, bidentate: 10 mol%) did not mediate the C-C bond cleavage of the model dinitrile substrate.

Table 2.4: Screening of the catalytic system[a]

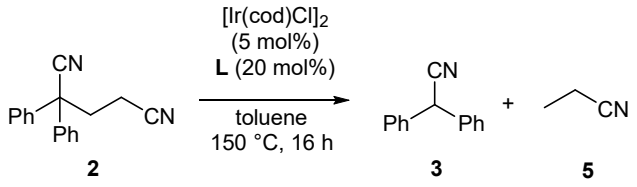

2 3 5

Entry	Ir complex	Ligand	Conversion 2, %	Yield 3, %	Yield 5, %
1	$[Ir(cod)Cl]_2$	P^iPr_3	0	0	0
2	$[Ir(cod)Cl]_2$	PCy_3	0	0	0
3	$[Ir(cod)Cl]_2$	Ad_2P^nBu	0	0	0
4	$[Ir(cod)Cl]_2$	JohnPhos	0	0	0
5	$[Ir(cod)Cl]_2$	CyJohnPhos	0	0	0
6	$[Ir(cod)Cl]_2$	dppf	0	0	0
7	$[Ir(cod)Cl]_2$	rac-BINAP	0	0	0
8	$[Ir(cod)Cl]_2$	tmphen	0	0	0
9[a]	$[Ir(cod)Cl]_2$	IAd·HBF_4	63	63	0
10[a]	$[Ir(cod)Cl]_2$	SIAd·HBF_4	49	48	0
11[a]	$[Ir(cod)Cl]_2$	IBu·HBF_4	33	32	0
12[a]	$[Ir(cod)Cl]_2$	SIMes·HCl	5	5	0
13[a]	$[Ir(cod)Cl]_2$	IPropyl·HBF_4	3	3	0
14[a]	$[Ir(cod)Cl]_2$	SIPr·HCl	29	14	0
15[b]	^{Ad}PCPIrHCl	-	61	58	0
16[b]	^{iPr}PCPIrHCl	-	65	65	0
17[c]	$[Ir(cod)Cl]_2$	IAd·HBF_4	92	92	0
18[d]	^{Ad}PCPIrHCl	-	78	76	0
19[e]	$Ir(P^iPr_3)_2H_5$	-	95	95	45
20[f]	$Ir(P^iPr_3)_2H_5$	-	75	75	20

Conditions: Substrate (1 equiv, 0.2M), $[Ir(cod)Cl]_2$ (5 mol%), ligand (monodentate: 20 mol%, bidentate: 10 mol%), toluene (0.8 ml), dodecane (GC standard). [a]: ^{t}BuONa (22 mol%), [b]: ^{R}PCPIrHCl (10 mol%), ^{t}BuONa (12 mol%). [c]: $[Ir(cod)Cl]_2$ (10 mol%), ligand (40 mol%), base (44 mol%). [d]: ^{Ad}PCPIrHCl (20 mol%), ^{t}BuONa (22 mol%). [e]: $Ir(PiPr_3)_2H_5$ (20 mol%). [f]: $Ir(PiPr_3)_2H_5$ (10 mol%).

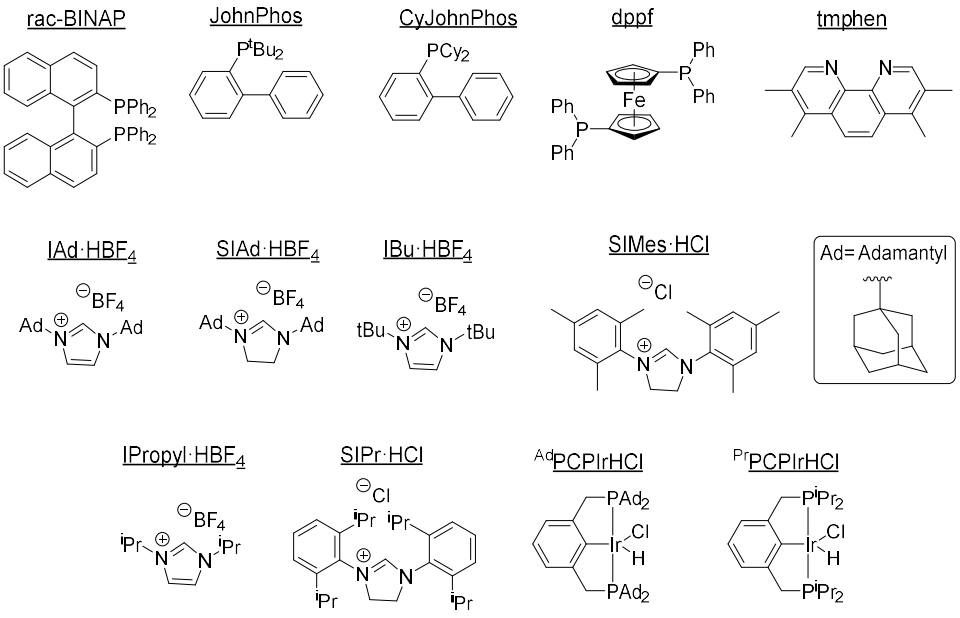

Figure 2.1: Structures of the screened ligands for the C-C bond cleavage

Next, the efficiency of phenanthroline iridium complexes in the C-C cleavage of dinitrile **2** was examined by the use of 20 mol% of 3,4,7,8-tetramethyl-1,10-phenanthroline (tmphen, Figure 2.1) with 5 mol% of $[Ir(cod)Cl]_2$ (Table 2.4, entry 8). This substituted phenanthroline was selected as it is a more electron donating ligand compared to its parent compound 1,10-phenanthroline and it often shows superior catalytic activity.[24] However, the catalytic system based on tmphen did not show any activity in the model reaction and we did not test any other phenanthroline iridium complexes.

Afterwards, N-heterocyclic carbenes (NHC) iridium complexes were screened using $[Ir(cod)Cl]_2$ and different NHC salts as precursors in the presence of bases. Free NHC were generated *in situ* by the deprotonation of NHC salts with sodium *tert*-butoxide. Similar to the approach followed with phosphines, several NHC ligands with different electronic properties were chosen.

Herein, several unsaturated and saturated NHC salts with different substituents at the imidazole ring were selected, as shown in Figure 2.1. The $[Ir(cod)Cl]_2$ (5 mol%) was combined with ^{t}BuONa (22 mol%) and NHC ligands (20 mol%), such as unsaturated adamantyl (IAd·HBF_4), saturated adamantyl (SIAd·HBF_4), *tert*-butyl (IBu·HBF_4), mesitylene (SIMes·HCl), isopropyl (IPropyl·HBF_4) and 2,6-diisopropylphenyl (IPr·HCl) (Table 2.4, entries 9-14). Interestingly, the IAd·HBF_4 with $[Ir(cod)Cl]_2$ and ^{t}BuONa

promoted the cleavage of dinitrile **2** affording diphenylacetonitrile **3** in 63% yield at 63% conversion of the substrate (Table 2.2, entry 9). Then, SIAd·HBF_4, IBu·HBF_4 and IPr·HCl with $[Ir(cod)Cl]_2$ and ^tBuONa mediated the C-C cleavage with 48, 32 and 14% yield of product **3**, respectively (Table 2.4, entries 10, 11 and 14). However, the combination of $[Ir(cod)Cl]_2$ and ^tBuONa with IPropyl·HBF_4 and SIMes·HCl led to very low yields of product **3**, being 5 and 3%, respectively (Table 2.4, entries 12 and 13). It is noteworthy that propionitrile **5** was not detected as a second product of the cleavage when NHC ligands were tested. This fact can be explained by the ability of metal alkoxides, such as sodium *tert*-butoxide, to facilitate the polymerisation of the transient acrylonitrile formed during the cleavage. As a result, the polymerisation of acrylonitrile might occur faster than its hydrogenation, and prevent formation of the propionitrile product.[25,26]

We found that NHC bearing adamantyl substituents (IAd·HBF_4 and SIAd·HBF_4) showed the highest activity for the C-C cleavage which is in line with the higher electron donating abilities of adamantyl compared to other substituents. The electronic properties of N-heterocyclic carbenes have been described using the Tolman electronic parameter (TEP). Originally used for phosphines, the TEP quantifies the electron-donating ability of a ligand by measuring the infrared frequencies of CO of model carbene transition metal complexes with carbonyl ligands. The IR stretching frequency of CO is affected by the electronic properties of the ligand attached to the metal: a more electron-donating ligand makes the metal more electron-rich, which increases the degree of the π-backbonding into the carbonyl and makes the metal-carbon (CO) bond stronger but weakens the C-O bond. This fact is reflected in a decrease in the IR stretching frequency of the CO and likewise, in the TEP which is measured in cm^{-1}.[27] Therefore, the more electron-donating is the ligand, the lower is the TEP value.

Gusev studied the electron properties of NHCs by quantifying the TEP values for various ligands which showed that NHCs with adamantyl substituents are more electron-donating ligand than IBu, SIMes, IPropyl or SIPr (Table 2.5).[28] Remarkably, carbenes bearing adamantyl substituents were found the most active in our catalyst screening, confirming the fact that the more electron-donating is the ligand, the more electron-rich the metal becomes and the resulting complex is more active towards C-H activation. Interestingly,

Gusev's work also shows that NHC ligands are more electron-donating than phosphine ligands which might explain the higher activity of the former.

Table 2.5: DFT calculated TEP values of $[Ni(CO)_3(NHC)]$ [28]

NHC ligand	TEP, cm^{-1}
IAd·HBF$_4$	2048.9
IBu·HBF$_4$	2050.6
SIMes·HCl	2051.2
IPropyl·HBF$_4$	2051.8
SIPr·HCl	2051.5

In conclusion, the combination of $[Ir(cod)Cl]_2$ (5 mol%, being 10 mol% of iridium), IAd·HBF$_4$ (20 mol%) and ^{t}BuONa (22 mol%) led to the formation of diphenylacetonitrile in 66% yield, and it showed the highest activity along all the ligands tested. However, this catalytic system does not promote the C-C bond cleavage in better yields than the original $Ir(P^iPr_3)_2H_5$ and for this reason, we continued the catalyst screening.

In the search of finding a better catalyst for the cleavage of C-C bonds, we also decided to test iridium pincer complexes because they have been proved to be highly efficient in a number of catalytic reactions where C-H activation was the key step,[29,30] such as alkane dehydrogenation reactions.[31] The "pincer ligand" is used to name species of the form $[2,6-(ECH_2)C_6H_3]^-$ (Figure 2.2), where E is a neutral two-electron donor group, particularly PR_2 and NR_2 (called PCP and NCN pincer, respectively). The term "pincer" refers to ligands that generally coordinate in a *mer* tridentate configuration to the metal centre. In general, the tridentate coordination mode of pincer ligands results in strong binding to the metal centre and provides high stability of the pincer-metal unit.[31] Pincer iridium complexes, such as adamantyl- or isopropyl-PCP iridium complexes (Figure 2.1), have been shown to be active catalysts for aliphatic dehydrogenations involving C-H activation.[32,33] Based on these precedents, the adamantly-PCP iridium hydrochloride complex (Figure 2.1) was synthesised and tested in 10 mol% loading for

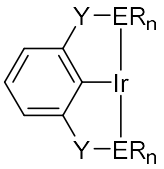

Figure 2.2: Pincer iridium complex (Y = CH_2, O; E = P, N, S, O; R = H, alkyl, aryl)

catalysing the C-C bond cleavage of 2,2-diphenylpentanedinitrile **2** in the presence of ^{t}BuONa (12 mol%) to form free PCP-iridium complex. This reaction led to 58% yield of diphenylacetonitrile **3** (Table 2.4, entry 15). On the other hand, isopropyl-PCP iridium hydrochloride complex (Figure 2.1) was also synthesised and tested using 10 mol% loading in the presence of ^{t}BuONa (12 mol%) which led to the formation of nitrile **3** in 65% yield (Table 2.4, entry 16). Remarkably, propionitrile **5** was not formed after the cleavage reaction catalysed by these PCP iridium complexes in the presence of ^{t}BuONa. As previously observed with the screening of NHC ligands, ^{t}BuONa might cause the polymerisation of the transient acrylonitrile preventing the formation of propionitrile.

To improve the yields of the C-C cleavage reaction, higher loadings of the most active catalysts found during the screening were used in the model catalytic reaction. Thereby, ^{Ad}PCPIrHCl was used in 20 mol% which slightly improved the yield of the reaction compared to the conducted reaction with 10 mol% of this catalyst, affording diphenylacetonitrile **3** in 76% yield (Table 2.4, entry 18). On the other hand, higher catalyst loading of $[Ir(cod)Cl]_2$ (10 mol%, being 20 mol% of iridium) with IAd·HBF_4 (40 mol%) and ^{t}BuONa (44 mol%) mediated the C-C bond cleavage with 92% yield of diphenylacetonitrile **3** (Table 2.4, entry 17), comparable yields to $Ir(P^{i}Pr_3)_2H_5$ when used in a 20 mol% loading (Table 2.4, entry 19).

This screening allowed us to identify $[Ir(cod)Cl]_2$ with IAd·HBF_4, ^{Pr}PCPIrHCl and ^{Ad}PCPIrHCl as alternative catalysts for the C-C bond cleavage that led to the formation of diphenylacetonitrile **3** with good yields. At higher catalyst loadings, $[Ir(cod)Cl]_2$ (10 mol%), IAd·HBF_4 (40 mol%) and ^{t}BuONa (44 mol%) led to 92% yield of nitrile **3**, which is similar to the results obtained with 20 mol% of $Ir(P^{i}Pr_3)_2H_5$ that formed nitrile **3** in 95% yield. However, at lower catalyst loadings (10 mol% of iridium) $Ir(P^{i}Pr_3)_2H_5$ gave nitrile **3** in 75% yield (Table 2.4, entry 20) which is the highest catalyst found and for this reason, we carried on with our investigations of the C-C bond cleavage of dinitriles using this iridium complex.

Before continuing with our research, we conducted several control experiments to test that the $Ir(P^{i}Pr_3)_2H_5$ is indeed the responsible for mediating the C-C bond cleavage. To initiate this process, a free binding site in the 18-electron $Ir(P^{i}Pr_3)_2H_5$ complex is required

for substrate coordination that can be generated *via* ligand dissociation, such as the possible release of free triisopropylphosphine.[34] Free P^iPr_3 is a nucleophilic base that can generate carbanions from relatively C-H acidic compounds.[35] Based on this, we hypothesise that free P^iPr_3 could mediate the retro-Michael addition of dinitrile substrate **2** leading to the products of C-C bond cleavage *via* the deprotonation of the α-position to the terminal nitrile in substrate **2**. To test this hypothesis, triisopropylphosphine (20 mol% which is the highest amount that can be released from 10 mol% of $Ir(P^iPr_3)_2H_5$) was used as a catalyst for the attempted C-C bond cleavage of dinitrile **2** in toluene at 150 °C for 16 h (Scheme 2.9). Absence of conversion of the starting dinitrile in this control experiment indicated that the free phosphine is not able to mediate the C-C bond cleavage.

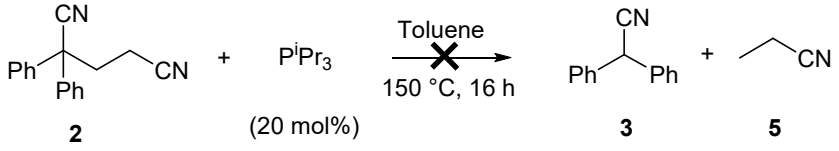

Scheme 2.9: Attempted P^iPr_3-catalyzed C-C cleavage of 2,2-diphenylpentanedinitrile **2**

On the other hand, transition metal catalysts have been found to be able to activate C-H bonds in alkanes *via* radical processes.[36] To study the possibility of the C-C bond cleavage occurring *via* a radical pathway, several control experiments were conducted using radical initiators as catalysts. With this aim, dinitrile **2** was allowed to react with 10 mol% of benzoyl peroxide or azobisisobutyronitrile (AIBN) at 150 °C in toluene (Table 2.6). To avoid too rapid decomposition of the radical initiators at high temperatures, these control experiments were also conducted at 80 °C which is in the range of free-radical initiation temperatures for both initiators.[37] These experiments showed that the cleavage of dinitrile **2** does not occur under these conditions, suggesting that the radical pathway is unlikely. It is noteworthy to mention that additional control experiments with radical scavengers could be conducted to further support the absence of radical pathways. However, these control experiments remain as future work due to the limited time available.

Table 2.6: Control experiments conducted with radical initiators as catalyst (GC yields)

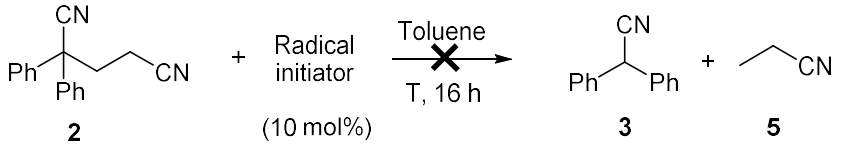

Entry	Radical initiator	T, ºC	Conversion 2, %	Yield 3, %	Yield 5, %
1	Benzoyl peroxide	150	0	0	0
2	AIBN	150	0	0	0
3	Benzoyl peroxide	80	0	0	0
4	AIBN	80	0	0	0

These control experiments show that the $Ir(P^iPr_3)_2H_5$ complex is required to mediate the catalytic C-C bond cleavage and also, provide information with regard to the mechanism in which phosphine- or radical-mediated pathways are unlikely.

2.4. Effect of directing groups in the reductive C-C bond cleavage

After the initial evidences on the reversibility of the reductive cleavage of C-C bonds and the alkene consumption as driving force of the process, we aimed to investigate the mechanism of this reaction in more detail. Initially, we sought to study the role of the directing groups of the dinitrile substrate and their influence on the C-C cleavage which remained unclear from the reported studies by Murahashi (Section 2.1). Particularly, we were interested in studying whether the two nitrile groups are required for the observed reactivity. For this, we replaced each one of the two cyano groups in the model dinitrile substrate **2** by a phenyl group and compared the reactivity of the resulting mononitrile substrates **7** and **8** (Scheme 2.10).

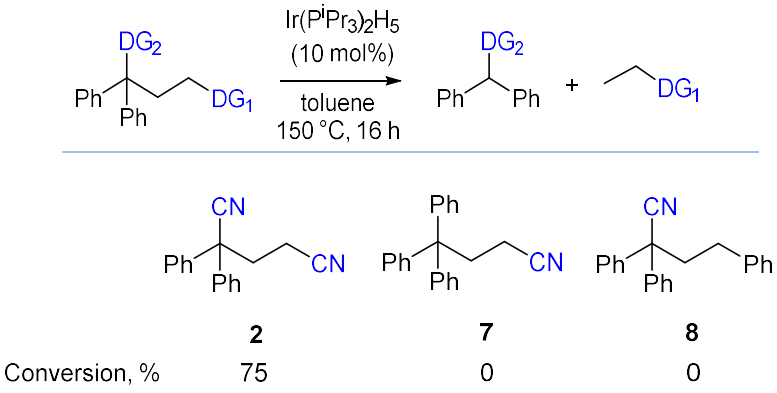

Scheme 2.10: Variation of directing groups in the model substrate

Firstly, the mononitrile substrates were synthesised. Substrate **7** was prepared in a three-step synthesis from 3,3,3-triphenylpropanoic acid (Scheme 2.11).[38] This carboxylic acid was reduced with lithium aluminium hydride to give the corresponding alcohol in 73% yield,[39] which then was converted in 3-iodo-1,1,1-triphenylpropane with red phosphorous and iodine in 86% yield.[40] Finally, the iodide was transformed into the desired mononitrile **7** with sodium cyanide in 30% yield.[41]

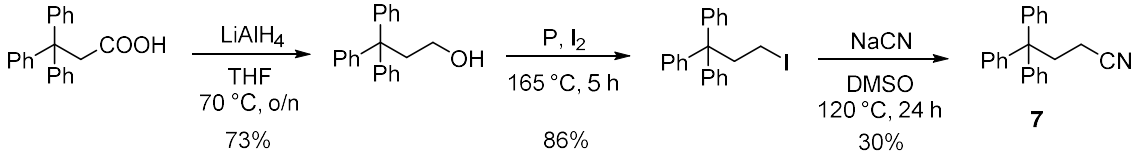

Scheme 2.11: Synthesis of 4,4,4-triphenylbutanenitrile (**7**)

On the other hand, mononitrile **8** was obtained in one-step synthesis from diphenylacetonitrile and 2-phenyl bromoethane with potassium in tert-butanol in 49% yield, following the procedure described in the literature (Scheme 2.12).[42]

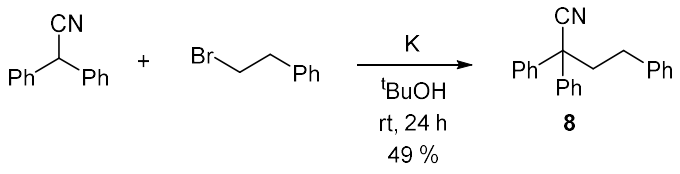

Scheme 2.12: Synthesis of 2,2,4-triphenylbutanenitrile (**8**)

Once these two new substrates were obtained, they were tested in the catalytic C-C bond cleavage reaction under the standard conditions used by Murahashi, using $Ir(P^iPr_3)_2H_5$ (10 mol%) in toluene at 150 °C for 16 h. Whereas the model substrate **2** with two cyano

groups underwent C-C cleavage in 75% conversion, mononitrile substrates **7** and **8** were completely unreactive (Scheme 2.10). These results suggest that two cyano groups are required for the reductive C-C bond cleavage.

The role of two directing groups can be rationalized by two general mechanistic pathways depicted in Scheme 2.13. As Murahashi proposed previously (Section 2.1, Scheme 2.2), Pathway 1 involves the coordination of iridium to the terminal nitrile group to form intermediate **A**, followed by the activation of the adjacent α-C-H bond.[43] Then, β-alkyl elimination would lead to the formation of olefin coordinated complex **C** that after alkene deinsertion and reductive elimination would afford acrylonitrile and diphenylacetonitrile. Finally, acrylonitrile would undergo hydrogenation and polymerisation. Unusually, in this transformation β-alkyl elimination is more favourable than β-hydrogen elimination. This is an intriguing fact as in most aliphatic systems β-hydrogen elimination occurs much faster and typically, β-alkyl elimination cannot be observed.[44]

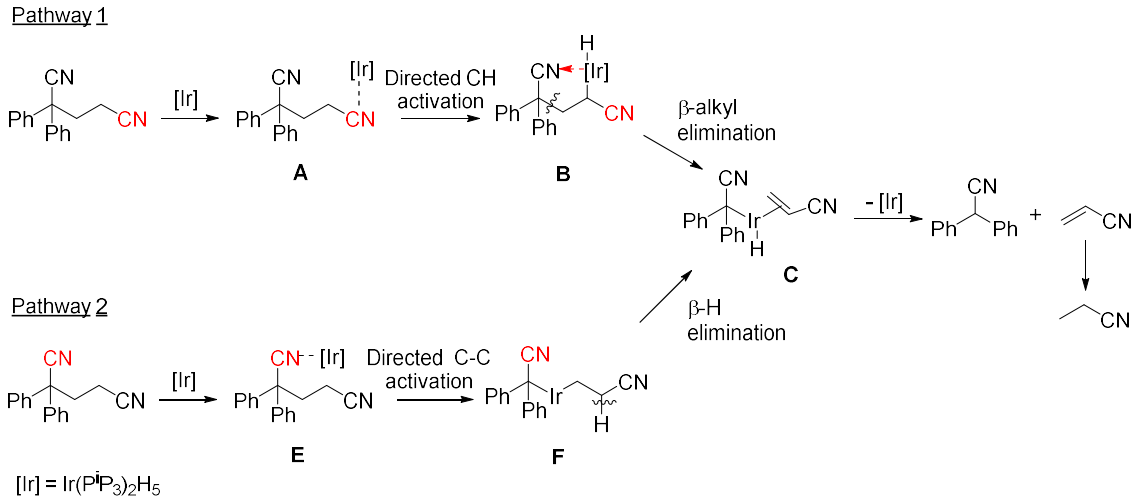

Scheme 2.13: Plausible mechanistic pathways 1) C-H activation followed by β-carbon elimination, 2) directed C-C activation followed by β-hydrogen elimination

However, Murahashi's mechanism does not explain neither the role of the second nitrile group nor the faster β-alkyl elimination observed in this case. We propose that the second CN group is possibly required to stabilize the alkyliridium intermediate **B** by coordination to the metal. This intermediate **B** would facilitate the subsequent β-alkyl elimination as the cleaving C-C and α-C-Ir bonds would be in syn-coplanar arrangement (Figure 2.3), required for β-elimination reactions (Chapter 1, Section 1.1).[44] This conformation of

complex **B** would also explain the favoured β-carbon elimination compared to β-hydrogen elimination.

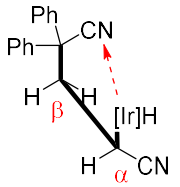

Figure 2.3: Syn coplanar conformation of intermediate complex **B**

Alternatively, we propose a second plausible mechanism – Pathway 2 – that starts with the coordination of iridium to the tertiary cyano group and subsequent insertion of iridium into the adjacent Csp^3-Csp^3 to form intermediate **F** (Scheme 2.13).[45,46] The dialkyl iridium complex **F** would undergo β-hydrogen elimination to form same complex **C** as in Pathway 1. We hypothesise that the terminal CN group in complex **F** would facilitate the β-H elimination by weakening the cleaving C-H bond *via* inductive effect as it is an electron-withdrawing group.[47] Then, the cleavage products would be formed after reductive elimination and alkene deinsertion.

That is, Pathway 1 involves directed C-H activation next to the terminal nitrile whereas Pathway 2 involves directed C-C activation next to the tertiary nitrile. Based on these mechanisms, both cyano groups are engaged with this transformation either through chelate or inductive effect. The study of the role of these two CN groups would help to understand the mechanism of the reductive C-C bond cleavage.

We evaluated the effect of other functionalities on the conversion of the reductive C-C bond cleavage to understand if both CN groups act as chelating groups or any of them serves as electron-withdrawing group. With this aim, we tested other substrates in which either of the two cyano groups was replaced by other functional groups, including coordinating and non-coordinating groups.

Based on the mechanism of the C-C cleavage *via* C-H activation (Pathway 1, Scheme 2.13), we selected various functional groups with coordinating properties that would favour the syn-coplanar arrangement of iridium intermediate complexes. We chose a variety of directing groups that are efficient for transition metal-catalysed C-H activation and functionalisation reactions. For example, different carbonyl groups have been involved in this type of processes, such as aldehyde moieties that are involved in the formation of quinolones *via* C-H activation.[48] Also, ketones and esters are efficient directing groups involved in transition metal-catalysed reactions such as alkylations,

arylations and olefinations of aromatic rings.[49,50] On the other hand, nitrogen-based functionalities, such as pyridine, oxime and oxazoline, are effectively involved in processes like C-H acylation[51] and arylations,[52] alkane acetoxylation[53] and alkenylations.[54] Alternatively, hydroxyls have also been shown efficient directing groups for C-H functionalisations, like hydrosylilations,[16] and C-H cyclisations.[55]

Additionally, our investigation on the effect of other functionalities on the C-C cleavage also included non-coordinating groups with electron-withdrawing properties to study whether either of the two cyano groups of the original dinitrile substrate **2** affects the cleavage based on electronic effects. With this aim, difluoromethyl and methoxy moieties were tested as non-coordinating electron-withdrawing functionalities.

To evaluate the effect of the identity of these functionalities on the cleavage of C-C bonds, we prepared a set of substrates shown in Figure 2.4.

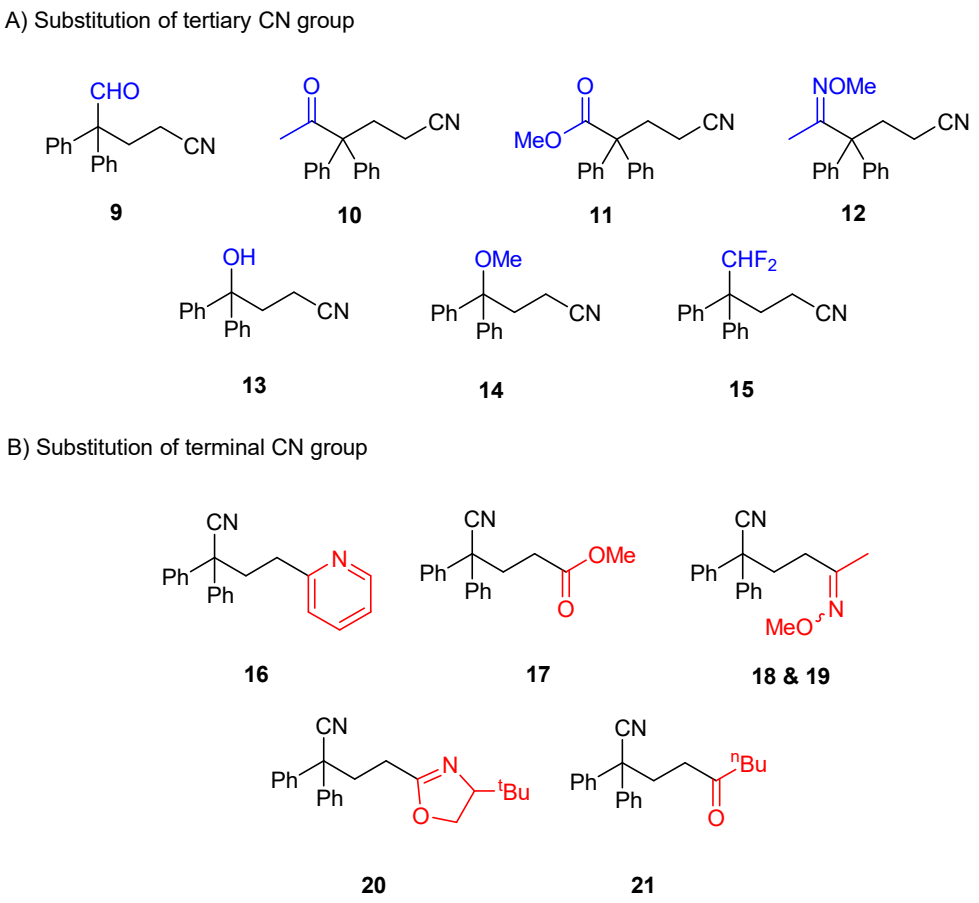

Figure 2.4: Envisioned substrates to study the effect of directing groups in the reductive C-C cleavage reaction

2.4.1. Syntheses of substrates

Substrates **9-21** were synthesised following different approaches. Most of these substrates are novel compounds whose syntheses were designed by this research group. Firstly, substrates **9-15** were obtained via formal replacement of the tertiary cyano group in the dinitrile **2** for different functionalities. Formyl substrate **9** was obtained *via* Michael addition with 2,2-diphenylacetaldehyde and acrylonitrile with DBU in 77% yield (Scheme 2.14).

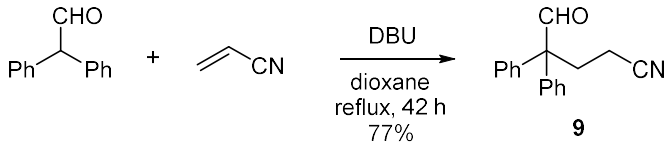

Scheme 2.14: Synthesis of 5-oxo-4,4-diphenylpentanenitrile **9**

Ketone substrate **10** was prepared from 1,1-diphenylacetone and acrylonitrile using benzyltrimethylammonium hydroxide (Triton B) as a base in 54% yield (Scheme 2.15).[56]

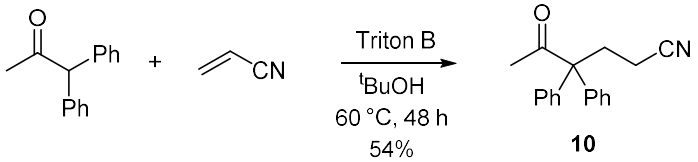

Scheme 2.15: Synthesis of 5-oxo-4,4-diphenylhexanenitrile **10**

The Michael addition of methyl 2,2-diphenylacetate to acrylonitrile in the presence of sodium hydride afforded methoxycarbonyl substrate **11** in 47% yield (Scheme 2.16).[57]

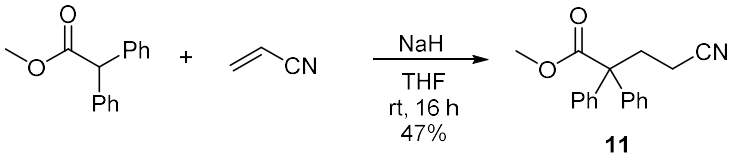

Scheme 2.16: Synthesis of 4-cyano-2,2-diphenylbutanoate **11**

The preparation of oxime **12** was achieved from ketone **10** and methoxyamine hydrochloride in pyridine in 53% yield (Scheme 2.17).

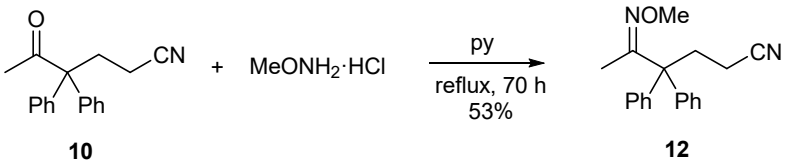

Scheme 2.17: Synthesis of 5-(methoxyimino)-4,4-diphenylhexanenitrile **12**

In addition, 4-hydroxy-4,4-diphenylbutanenitrile **13** was prepared in two-step synthesis: firstly, 3-chloropropiophenone was converted to 3-chloro-1,1-diphenylpropan-1-ol with phenylmagnesium bromide solution in 47% yield. Then, this chloride was mixed with sodium cyanide to obtain the desired alcohol **13** in 63% yield (Scheme 2.18).

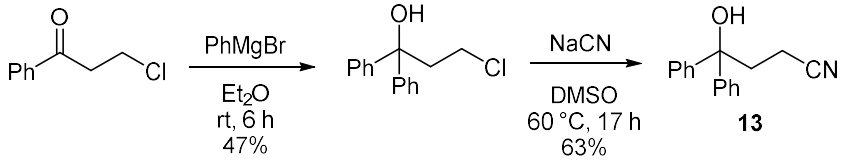

Scheme 2.18: Synthesis of 4-hydroxy-4,4-diphenylbutanenitrile **13**

The synthesised alcohol **13** also served as precursor for preparation of methoxy derivative **14**. Alkylation of **13** with methyl iodide in the presence of sodium hydride gave **14** in 81% yield (Scheme 2.19).

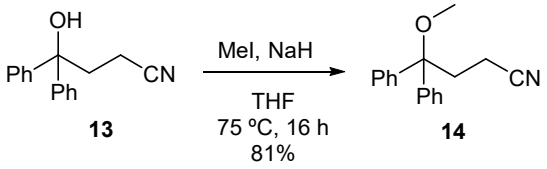

Scheme 2.19: Synthesis of 4-hydroxy-4,4-diphenylbutanenitrile (**14**)

Additionally, difluoromethylated substrate **15** was synthesised from formyl substrate **9** and (diethylamino)sulphur trifluoride (DAST) in 86% yield (Scheme 2.20).

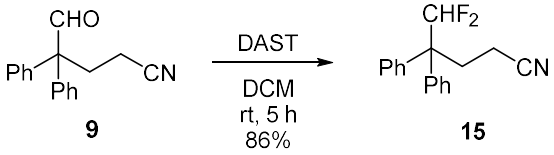

Scheme 2.20: Synthesis of 5,5-difluoro-4,4-diphenylpentanenitrile **15**

Next, we synthesised substrates **16-21** where the terminal nitrile group of dinitrile **2** was replaced by other functionalities (Figure 2.4). Specifically, pyridine **16** was prepared *via* Michael addition with diphenylacetonitrile and 2-vinylpyridine in the presence of KOH solution in MeOH, as described in the literature.[58] The desired pyridine **16** was obtained in 74% yield (Scheme 2.21).

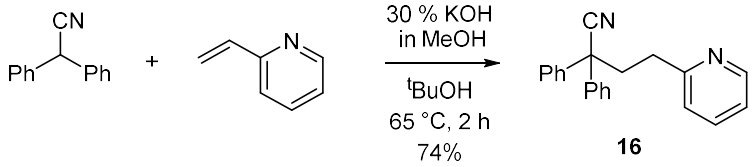

Scheme 2.21: Synthesis of 2,2-diphenyl-4-pyridylbutanenitrile **16**

Similarly, the Michael addition of diphenyacetonitrile to methyl acrylate mediated by KOH in methanol afforded the desired methyl ester **17** in 53% by modifying the literature procedure through applying anhydrous conditions (Scheme 2.22).

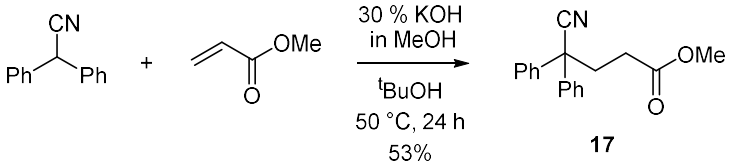

Scheme 2.22: Synthesis of 4-cyano-4,4-diphenylbutanoate **17**

On the other hand, oximes **18** and **19** were obtained in similar way to oxime **12** (Scheme 2.17) but starting with the corresponding ketone precursor, 5-oxo-2,2-diphenylhexanenitrile **18a** (Scheme 2.23). Firstly, this methyl ketone was synthesised in 36% yield *via* Michael-addition with diphenylacetonitrile and methyl vinyl ketone with KOH solution in methanol, as described in the literature.[59] Then, the ketone **18a** was heated in pyridine in the presence of $MeONH_2 \cdot HCl$ to afford oxime isomers **18** and **19** in 63 and 19% yield, respectively.

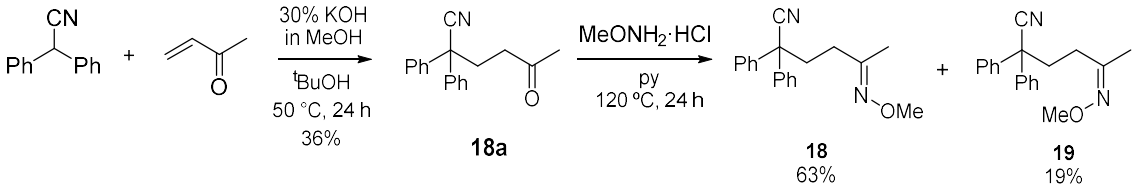

Scheme 2.23: Synthesis of 5-(methoxyimino)-2,2-diphenylhexanenitrile, *E* and *Z* isomers **18** and **19**, respectively

Oxazoline substrate **20** was synthesised from methyl ester **17** and rac-*tert*-leucinol which was obtained from the reduction of the corresponding aminoacid with sodium borohydride and iodine (Scheme 2.24). The desired oxazoline **20** was obtained in 81% yield.

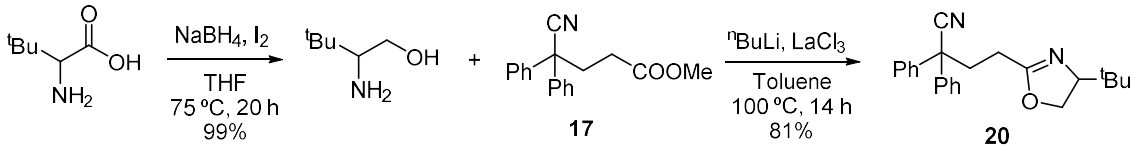

Scheme 2.24: Synthesis of 4-(tert-butyloxazoline)-2,2-diphenylbutanenitrile (**20**)

Finally, butyl ketone **26** was also prepared *via* a Michael addition but in this case, butyl vinyl ketone was used as Michael acceptor. This ketone was obtained from the oxidation of 1-hepten-3-ol with H_2SO_4 and $Na_2Cr_2O_7 \cdot 2H_2O$ in 71% yield.[60] Then, the obtained butyl ketone was treated with diphenylacetonitrile in the presence of KOH in methanol to afford the desired ketone **21** in 4% yield (Scheme 2.25).

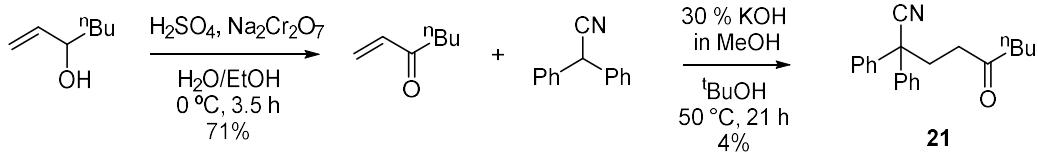

Scheme 2.25: Synthesis of 2,2-diphenylnonanenitrile (**21**)

2.4.2. Ir-catalysed reductive C-C bond cleavage of synthesised substrates

Once the substrates of interest were synthesised, they were tested in the model catalytic C-C bond cleavage reaction. For this study, Murahashi´s standard catalytic conditions were employed, using $Ir(P^iPr_3)_2H_5$ (10 mol%) in toluene at 150 ºC for 16 h (Scheme 2.26).

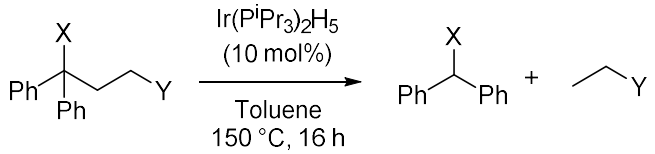

Scheme 2.26: Standard catalytic conditions for substrate screening

Firstly, substrates in which the tertiary cyano group has been replaced by other functionalities, such as carbonyl groups, were tested (Figure 2.5).

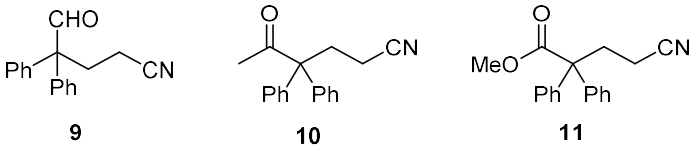

Figure 2.5: Substrate derivatives with replaced tertiary cyano group

Aldehyde **9** reacted with 50% conversion to give 2,2-diphenylacetaldehyde in 4% yield (Table 2.7, entry 2). On the other hand, ketone **10** underwent the cleavage in 87% conversion to afford 1,1-diphenylacetone in 34% yield (Table 2.7, entry 3). Finally, methyl ester **11** was cleaved in 29% conversion to give methyl 2,2-diphenylacetate in 20% yield (entry 4). As one can notice, the catalytic cleavage of aldehyde **9** and ketone **10** occurred with poor material balance as evidenced by a mismatch between conversion of starting material and yield of the diaryl product. This can be explained by the side reactions involving either the starting material or the products under these catalytic conditions, as shown by independent experiments. For example, 2,2-diphenylacetaldehyde (expected cleavage product of formyl substrate **9**) undergoes decarboxylation and hydrogenation in the presence of the Ir catalyst. As a result, diphenylmethane and 2,2-diphenylethan-1-ol were isolated in 17 and 24% yield, respectively, at 50% conversion of the starting aldehyde (Scheme 2.27).

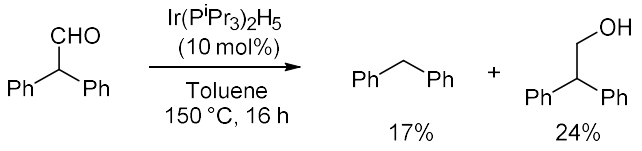

Scheme 2.27: Control experiment with 2,2-diphenylacetaldehyde under the catalytic conditions

On the other hand, ketone substrate **10** produces 1,1-diphenylacetone and 1,1-diphenylethylene in 34 and 11% isolated yield, respectively, under the standard catalytic conditions (Scheme 2.28).

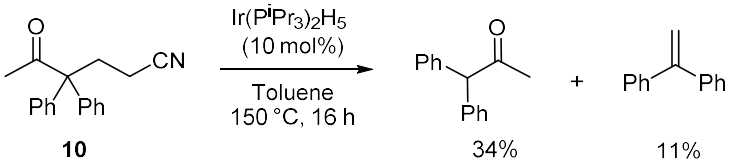

Scheme 2.28: Side product formed during the catalytic cleavage of 5-oxo-4,4-diphenylhexanenitrile **10**

Table 2.7: Screening of substrates [a]

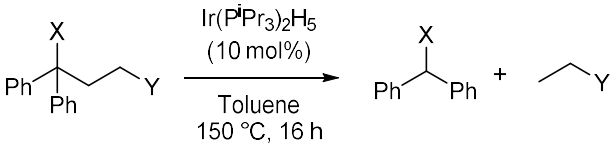

Entry	Substrate	Conversion substrate, %	Yield Ph_2CHX, %	Yield CH_3CH_2Y, %
1	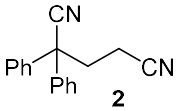 **2**	75	75	20
2	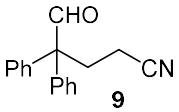 **9**	50	4	13
3	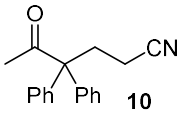 **10**	87	34	10
4[b]	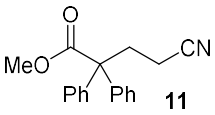 **11**	29	20	12
5	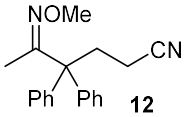 **12**	0	0	0
6	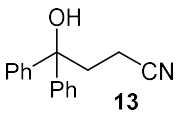 **13**	73	0	0

7	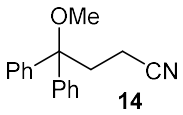 **14**	0	0	0
8	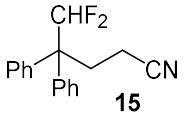 **15**	0	0	0
9	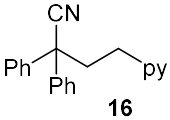 **16**	0	0	0
10	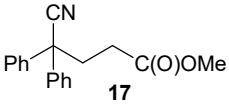 **17**	0	0	0
11	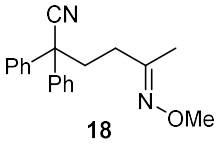 **18**	23	11	0
12	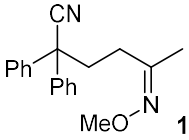 **19**	25	15	0
13	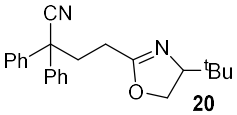 **20**	60	9	0
14	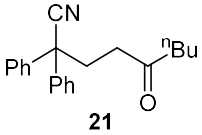 **21**	100	96	34

[a]: Reaction conditions: Substrate (1 equiv, 0.2 M), $Ir(P^iPr_3)_2H_5$ (10mol%), toluene, dodecane (GC standard), 150 °C for 16 h. [b] Experiment conducted for 24 h.

These studies show that various carbonyl groups which are electron-withdrawing and able to coordinate to the metal mediate the C-C bond cleavage reaction. However, these groups are not well tolerated under the reaction conditions.

When oxime **12** was tested in the model reaction, no C-C bond cleavage was observed (Table 2.7, entry 5).

Next, alcohol **13** was subjected to cleavage reaction conditions which led to 71% conversion of the substrate but no expected diphenylmethanol was found (Table 2.7, entry 6). Instead benzophenone was formed as a major product in 57% isolated yield (Scheme 2.29)[61] .

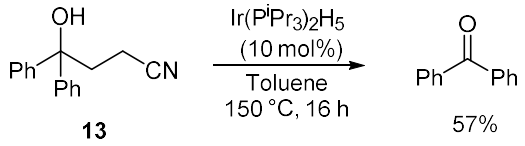

Scheme 2.29: Ir-catalyzed cleavage of 4-hydroxy-4,4-diphenylbutanenitrile

The formation of benzophenone might occur *via* β-alkyl elimination involving an iridium alcoholate (Scheme 2.30). The iridium complex can insert into the O-H bond prior the C-C cleavage step that would form the benzophenone product. This pathway has been proposed for the C-C bond cleavage of unstrained tertiary alcohols, as discussed in Chapter 1, Section 1.3.2.

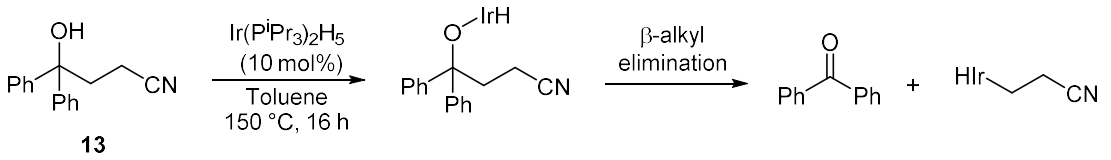

Scheme 2.30: Ir-catalysed cleavage of alcohol **13** *via* β-alkyl elimination involving an iridium alcoholate intermediate

In contrast to alcohol **13**, the methoxy derivative **14** did not undergo C-C cleavage under the standard catalytic conditions (Table 2.7, entry 7). This fact could be rationalised by the plausible mechanism depicted in Scheme 2.30. In case of methoxy **14**, the insertion of iridium complex into the O-Me bond is less favourable than O-H activation. Therefore, this fact could prevent the subsequent β-alkyl elimination that would lead to the products of the cleavage.

At this point, we tested the substrate in which the tertiary nitrile group was replaced by non-coordinating functionalities, such as difluoromethylated substrate **15**. Under these catalytic conditions, this substrate appeared to be completely unreactive (Table 2.7, entry 8), leading to the conclusion that coordinating groups are required at the quaternary carbon for the C-C cleavage.

On the other hand, we also tested those substrates in which the terminal cyano group was replaced by other functionalities, such as pyridine **16**, methyl ester **17**, methoxy oxime **18** and **19** (*E* and *Z* isomers, respectively), oxazoline **20** and butyl ketone **21** (Figure 2.6).

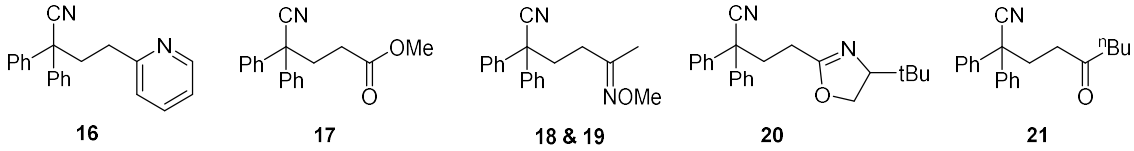

Figure 2.6: Substrates with replaced terminal nitrile group

Among these substrates, butyl ketone **21** underwent C-C cleavage with a 96% yield of diphenylacetonitrile at full conversion (Table 2.7, entry 14). In contrast, low yields of diphenylacetonitrile were obtained with oximes **18** and **19** and oxazoline **20** (Table 2.7, entries 11, 12 and 13, respectively). Pyridine **16** and methyl ester **17** substrates were even less reactive and gave no products of C-C bond cleavage (Table 2.7, entries 9 and 10, respectively).

These results suggest that two directing groups are essential for the C-C bond cleavage to occur. Thus, only electron-withdrawing groups such as cyano, carbonyl, hydroxyl or oxime groups that can coordinate to the metal centre promote C-C bond cleavage. These observations help to clarify the intriguing fact from Murahashi's work regarding the scope limited to substrates bearing two functional groups (Section 2.1). However, further studies are required to elucidate the exact role of these directing groups in the mechanism of this remarkable C-C bond cleavage reaction.

2.5. C-H activation *versus* C-C activation: distinguishing two possible mechanistic pathways

As discussed in the previous section, the presence of two directing groups in the substrate leads to two possible mechanistic pathways for the reductive C-C cleavage as shown in Scheme 2.31. Pathway 1 involves the directed activation of α-C-H bond next to the terminal nitrile group followed by β-alkyl elimination. On the other hand, Pathway 2

involves the C-C bond activation directed by the tertiary nitrile group followed by β-hydrogen elimination.

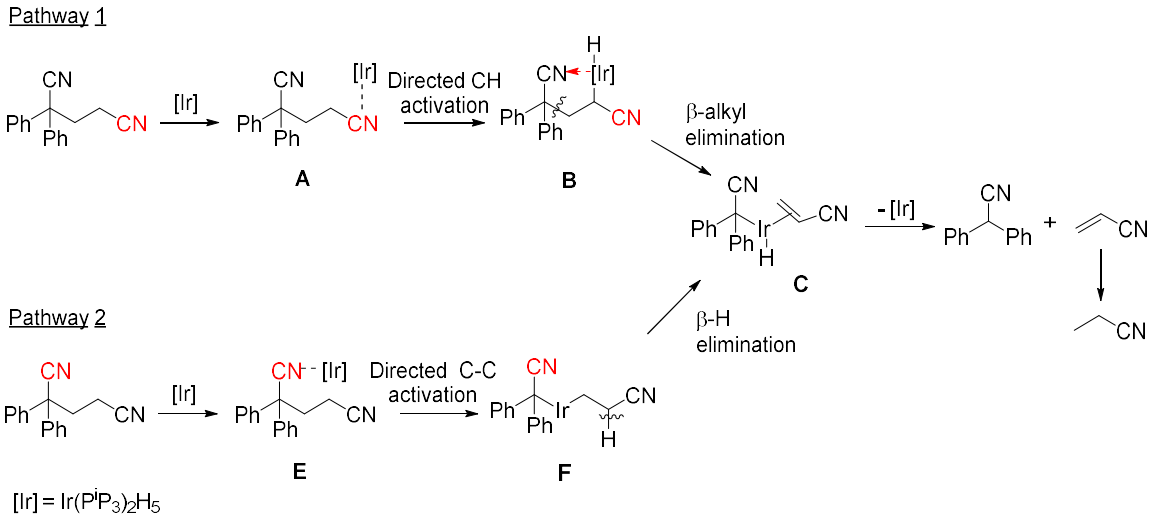

Scheme 2.31: Possible mechanistic pathways of C-C bond cleavage of dinitriles 1) C-H activation followed by β-alkyl elimination and 2) C-C activation followed by β-hydrogen elimination

To distinguish between these two possible mechanistic pathways, we envisioned an experiment with substrate **22**, an α,α-dimethylated analogue of the model dinitrile **2** (Figure 2.7). By using this substrate, Pathway 1 would be supressed as there are no α-C-H bonds available for activation. However, the directed insertion of the iridium centre into the C-C bond would be still possible in the dimethylated substrate (Pathway 2). Therefore, if the dimethylated substrate **22** undergoes C-C cleavage, this result would be consistent with Pathway 2.

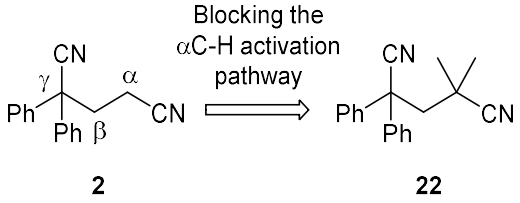

Figure 2.7: The use of dimethylated substrate **22** blocks the α-C-H activation pathway

Substrate **22** can react *via* Pathway 2 by directed insertion of iridium into either C-C bond A or B (Scheme 2.32). The insertion into the C-C bond A would lead to the formation of complex **23**. According to the proposed Pathway 2, the next step after the formation of complex **23** would be the β-hydride elimination which it would not be possible in this

case as there are no hydrogen atoms in β-position. However, if complex **23** is formed and the reaction mixture is treated with hydrochloric acid, the C-Ir bonds in complex **23** would undergo protonolysis[62,63] to give diphenylacetonitrile (**3**) and trimethylacetonitrile (**24**).

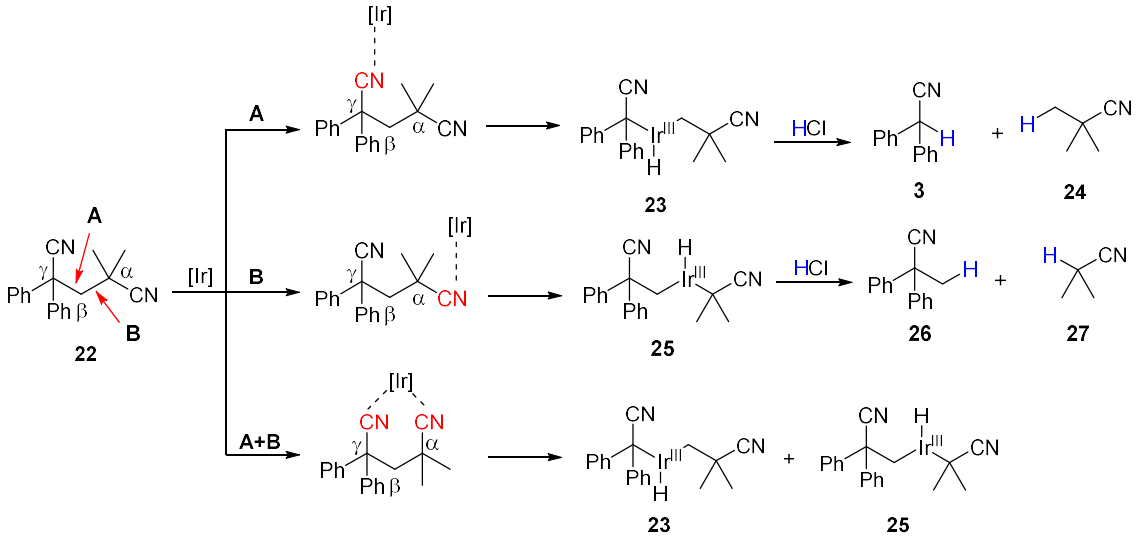

Scheme 2.32: Distinguishing mechanistic pathways using a dimethylated substrate derivative

Alternatively, if the insertion occurs into the C-C bond B, the intermediate complex **25** would be formed (Scheme 2.32). In this case, the β-hydride elimination would not be possible either, but the acidic treatment of complex **25** would lead to the formation of methyldiphenylacetonitrile **26** and isobutyronitrile **27**.

In addition, we envisioned an alternative pathway where the iridium centre would coordinate to both cyano groups to form a N,N-coordinated complex (Scheme 2.32). In this case, iridium could insert into either of A and B C-C bonds to form complexes **23** and **25** that after acidic treatment would form a mixture of products **3**, **24**, **26** and **27**.

Thus, to distinguish between Pathway 1 and 2, we prepared dimethylated substrate **22**. The synthesis of this substrate proved to be a challenging task as the molecule contains two quaternary carbon atoms. Several approaches were attempted to obtain this compound, such as the methylation of dinitrile **2** with iodomethane or the nucleophilic substitution of chloride **28** with diphenylacetonitrile (Scheme 2.33).

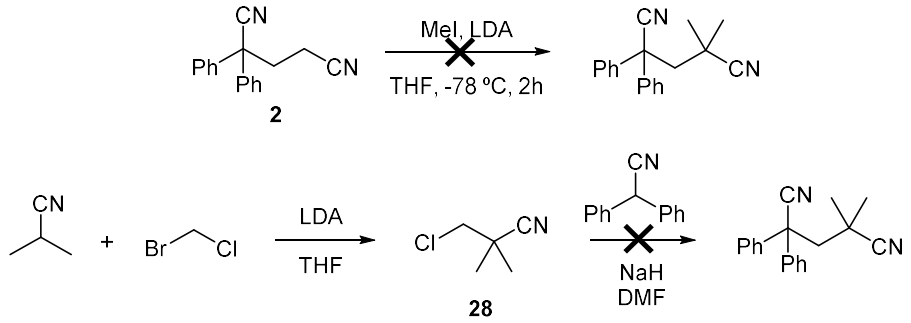

Scheme 2.33: Attempted syntheses of dimethylated substrate **22**

The desired dimethylated substrate **22** was eventually obtained by the two-step synthesis shown in Scheme 2.34. Firstly, bromide **29** was prepared in 78% yield from diphenylacetonitrile and dibromomethane in the presence of sodium hydroxide and tetrabutylammonium bromide. Then, **29** was treated with isobutyronitrile and lithium diisopropylamide to afford the desired product **22** in 49% yield.

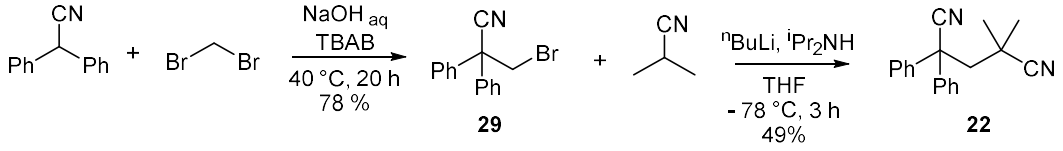

Scheme 2.34: Synthesis of 2,2-dimethyl-4,4-diphenylpentanedinitrile (**22**)

The obtained nitrile **22** was then allowed to react with 1 equivalent of $Ir(P^iPr_3)_2H_5$ in toluene at 150 °C for 16 h (Scheme 2.35). The reaction mixture was subsequently treated with 2M aqueous HCl and then with aqueous NaOH. Considering that the $Ir(P^iPr_3)_2H_5$ complex might mediate the reduction of nitriles to amines,[64] basic treatment was necessary to detect possible amine products that could have been protonated upon the acidic treatment. Notably, according to GC and GC-MS no expected products **3**, **24**, **26** and **27** were detected. Instead, unexpected products **30** and **31** were observed as major products by GC-MS (Scheme 2.35).

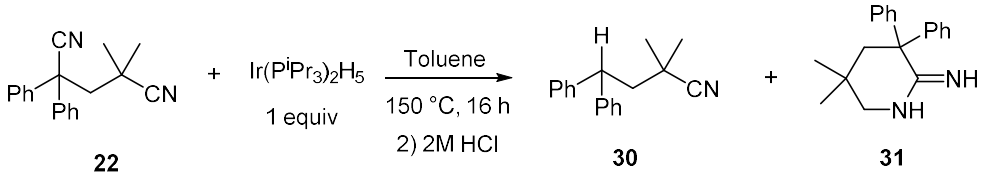

Scheme 2.35: Stoichiometric experiment with Ir pentahydride complex and dinitrile **22**

The isolation of these products by column chromatography yielded the unexpected air stable hydrochloride iridium complexes **32** and **33** in 15 and 8% yield, respectively (Scheme 2.36). The isolation of these complexes suggests that compounds **30** and **31** detected by GC and GC-MS are likely the products of thermal decomposition of complexes **32** and **33** during GC analysis. The low isolated yields of both complexes can be explained by their partial decomposition upon the basic work up. The structure of these complexes was confirmed by X-Ray and NMR data. X-Ray diffraction analyses of complexes **32** and **33** show an octahedral configuration of the Ir(III) centre with the two P^iPr_3 ligands in *trans*-arrangement (Figure 2.8). The equatorial plane of complex **32** consists of a hydride ligand, N-coordinated nitrile **30** and two chlorines in *trans*-arrangement. On the other hand, complex **33** contains hydride, N-coordinated amidine **31** and two *cis*-chloride ligands.

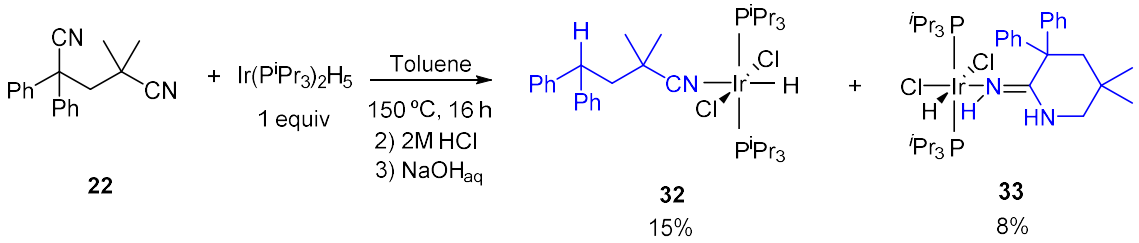

Scheme 2.36: Isolated complexes from stoichiometric experiment with $Ir(P^iPr_3)_2H_5$ and dimethylated substrate **22**

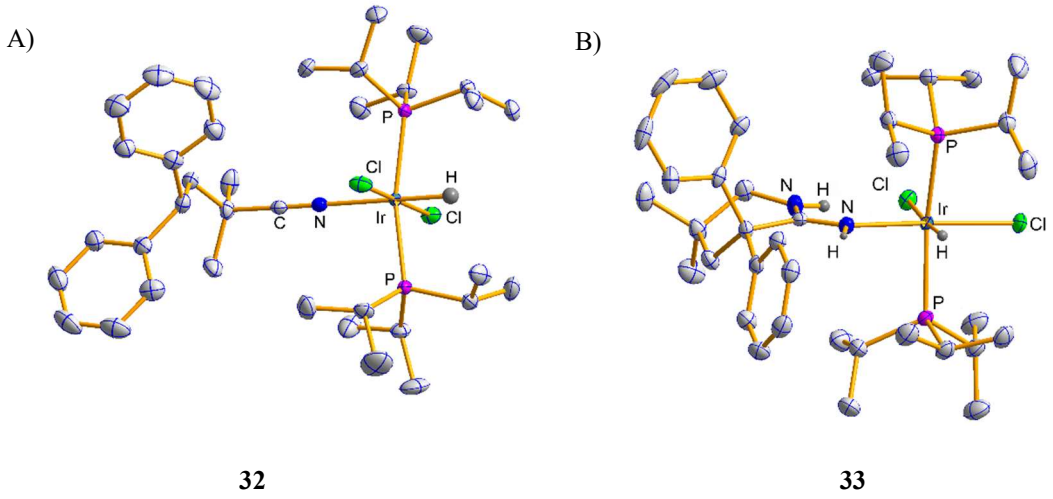

Figure 2.8: X-Ray structure of A) Complex **32** and B) Complex **33**

Complexes **32** and **33** are likely the products of quenching of the corresponding hydride complexes $IrH(P^iPr_3)_2L$ or $IrH_3(P^iPr_3)_2L$ (L= **30** or **31**) with HCl.[65] Complex **32** contains product **30** as ligand which is the product of hydrodecyanation of the dinitrile **22** (Scheme 2.37). The proposed mechanism of formation of complex **32** involves the coordination of the iridium catalyst to the CN group placed at α-C, followed by its insertion into the Ph_2C-CN bond. The reaction proceeds with the reductive elimination of hydrogen cyanide using $Ir(P^iPr_3)_2H_5$ as a hydride source. Then, C-H bond forming reductive elimination leads to the intermediate monohydride complex which after acidic treatment leads to complex **32**.

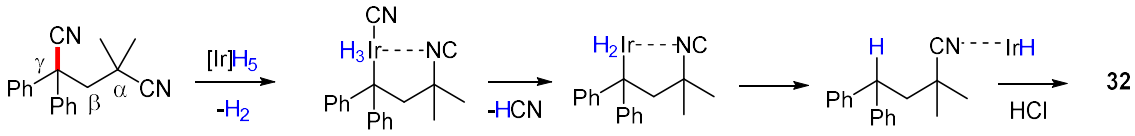

Scheme 2.37: Proposed mechanism of formation of complex **32**

Proposed decyanation process to form product **30** is similar to reported hydrogenolyses of C-CN bonds catalysed by rhodium[66] or nickel[67] in the presence of various reducing agents. In these processes, hydride complexes were suggested as intermediate catalytic species which supports our proposal.

On the other hand, second complex **33** is the result of selective hydrogenation of the α-CN and the subsequent intramolecular cyclization of the substrate. The hydrogenation of the α-CN group affords amine intermediate **34** (Scheme 2.38). Intramolecular nucleophilic attack of the amino group at the benzylic CN[68,69] forms the cyclised intermediate **35** that after the acidic treatment gives complex **33**.

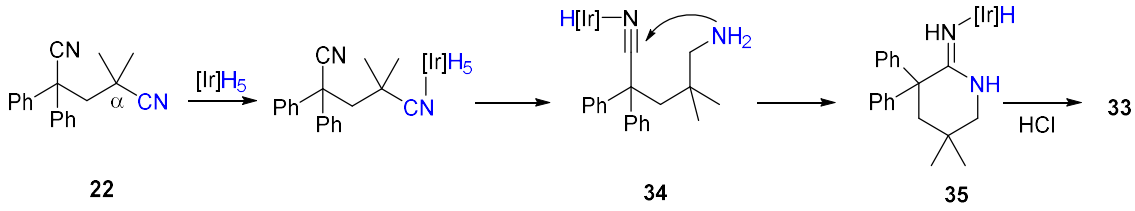

Scheme 2.38: Proposed mechanism of formation of complex **33**

In summary, experiments with dimethylated substrate **22** and complex $Ir(P^iPr_3)_2H_5$ led to the formation of complexes **32** and **33** after the acidic treatment. When the C-H activation pathway is blocked, the iridium complex does not insert into neither C-C bond A nor B of substrate **22** as evidenced by the absence of expected products **3** and **24** or **26** and **27**,

respectively (Scheme 2.32). Therefore, these results suggest that Pathway 2 is unlikely, however, they are consistent with Pathway 1 which involves the directed α-C-H activation followed by β-alkyl elimination (Scheme 2.31).

2.6. Deuterium labelling studies

As evidenced by the results presented in the preceding section, the reductive C-C bond cleavage of dinitriles is likely to occur through C-H activation followed by β-alkyl elimination (Pathway 1). To further investigate the mechanism, we conducted deuterium labelling experiments with dideuterated substrate **2**-d_2 (Scheme 2.39). If the C-C cleavage occurs *via* Pathway 1, then either of the two deuteriums of substrate **2**-d_2 should migrate to the α-position of nitrile product **3**-d and the remaining deuterium should be detected in α-position of propionitrile **5**-d.

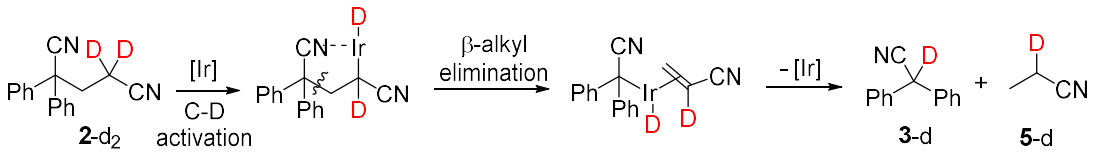

Scheme 2.39: C-H activation followed by β-alkyl elimination with deuterated substrate **2**-d_2

The target deuterated substrate **2**–d_2 was synthesised from dinitrile **2** and a solution of sodium deuteroxide in D_2O under reflux affording the desired product in 78% yield using the modified literature procedure (Scheme 2.40).[70] Substrate **2**–d_2 was obtained in 95% deuterium-purity according to ^{1}H-NMR.

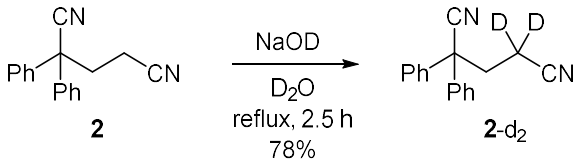

Scheme 2.40: Synthesis of 2,2-dideuterium-4,4-diphenylpentanedinitrile **2**-d_2

Then, studies with substrate **2**–d_2 were conducted under standard catalytic conditions, with $Ir(P^iPr_3)_2H_5$ (10 mol%) in toluene at 150 °C and the deuterium content of the products was estimated by D NMR and GC (Scheme 2.41). The results of this experiment show a preferential incorporation of deuterium at the α-positions of diphenylacetonitrile

and propionitrile. After 1 h, the deuterium content at the α-position of diphenylacetonitrile was 71%. Also, propionitrile was found to contain most of the deuterium in the α-position as evidenced by α-D/β-D ratio of 85%/15% after 1 h of reaction (Scheme 2.41). These observations support the proposed mechanism of α-C-H activation followed by β-alkyl elimination (Scheme 2.31, Pathway 1).

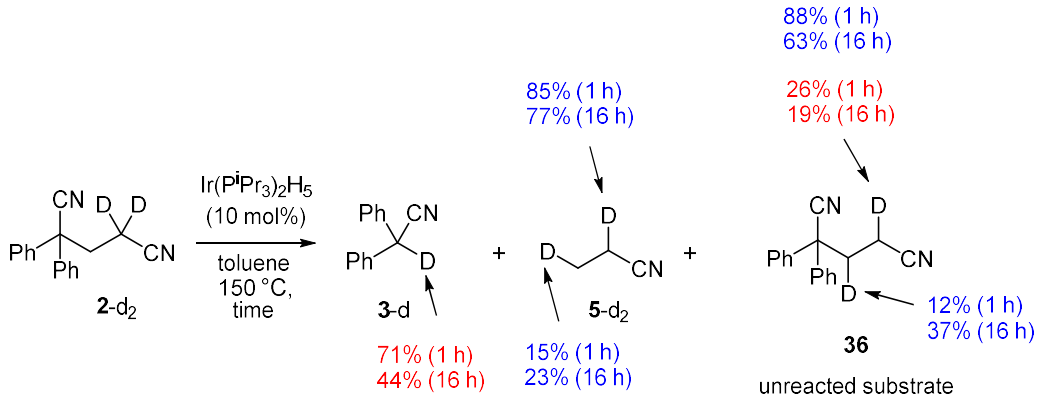

Scheme 2.41: Deuterium labelling experiments with 2,2-dideuterium-4,4-diphenylpentanedinitrile. Numbers in red indicate absolute deuterium content in % and numbers in blue, relative D% content for the α and β-positions of propionitrile and deuterated dinitrile substrate.

However, the deuterium content in diphenylacetonitrile decreased from 71% to 44% after 16 h, which suggests that this compound undergoes H/D exchange in the presence of the iridium catalyst. Similarly, propionitrile was also found to undergo H/D exchange under these conditions as illustrated by the change in the α-D/β-D ratio from 85%/15% (1 h) to 77%/23% after 16 h. On the other hand, when the deuterium content in the unreacted starting substrate was analysed, a decrease in the absolute D content at the α-position from 95% to 26% was observed within 1 h. Moreover, H/D exchange also occurred between α and β-positions where the α-D/β-D ratio was 88%/12% after 1 h and changed to 63%/37% after 16 h. The observed H/D exchange between α and β-positions in the substrate suggests that the C-H activation of the dinitrile substrate is a reversible step. Moreover, C-H activation should occur faster or with comparable yields than the subsequent β-alkyl elimination as otherwise product **36** could not be observed.

On basis of the observed decrease in deuterium content in diphenylacetonitrile, we desired to study possible H/D exchange of this product under the catalytic conditions. To

test this, dipheylacetonitrile **3**-d was synthesised in 90% yield according to the literature procedure from diphenylacetonitrile **3** with ^{n}BuLi followed by the subsequent quenching with D_2O (Scheme 2.42).[71] Compound **3**-d was obtained in 94% deuterium purity according to ^{1}H-NMR.

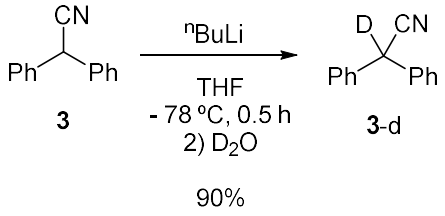

Scheme 2.42: Synthesis of α-deuterated diphenylacetonitrile (**3**-d)

The experiment with nitrile **3**-d under the standard catalytic conditions showed that the deuterium content decreased from 94% at initial time to 71% after 16 h of heating. This experiment confirms the H/D exchange process in diphenylacetonitrile product and the reversibility of C-H activation (Scheme 2.43).

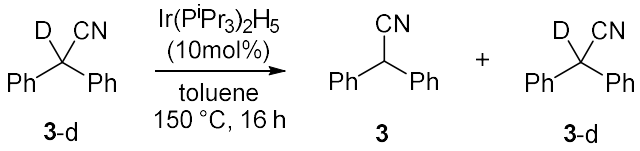

Scheme 2.43: Control experiment with α-deuterated diphenylacetonitrile (**3**-d)

In conclusion, deuterium labelling experiments show the incorporation of deuterium at the α-position of the diphenylacetonitrile and propionitrile which is consistent with the proposed Pathway 1 involving C-H activation followed by β-carbon elimination (Scheme 2.31).

To determine whether the C-H activation step is the rate limiting step of the C-C cleavage process, we attempted to conduct kinetic isotope effect (KIE)[72–74] measurements with the non-deuterated and the deuterated dinitrile substrates (**2** and **2**-d_2). With this purpose, substrates **2** and **2**-d_2 were allowed to react under the standard catalytic conditions at early stages of the reaction (Scheme 2.44). Both reactions were monitored by GC and ^{1}H NMR to compared initial rates (conversion < 20%) of the reactions with deuterated and non-deuterated substrates.

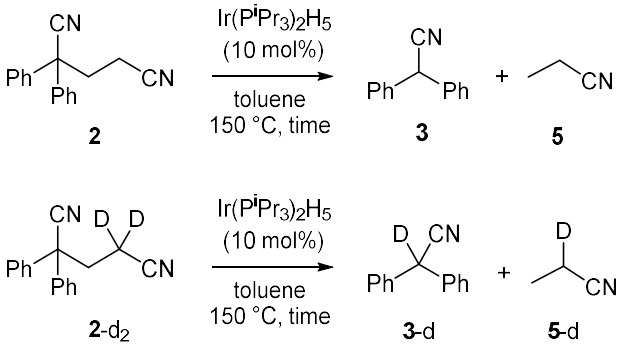

Scheme 2.44: Experiments with non-deuterated and deuterated dinitrile substrates to measure KIE

Initially, the experiments were conducted at 150 ºC but after 5 min of heating, the conversion of substrate **2** was already 37% which was a too high conversion to compare initial rates of these reactions. To slow down the reaction, these experiments were conducted at 80 ºC. The experiment with substrate **2** and $Ir(P^iPr_3)_2H_5$ (10 mol%) at 80 ºC for 15 min led to 6% yield of product **3** at 21% conversion of substrate **2**. After 1 h, product **3** was formed in 12% yield at 29% conversion of the starting material. This poor material balance between product yield and substrate conversion remained after 16 h, where 35% of dinitrile **2** was converted into nitrile **3** in 20% yield. We hypothesised that these discrepancies might be explained by the consumption of product **3** *via* side process(es) under these conditions (see Section 2.7). Therefore, KIE measurements to compare initial rates of the reactions with substrates **2** and **2**-d_2 were not possible due to the issue with the material balance at a lower temperature. Looking into this issue, however, has helped us to identify a catalyst resting state for this process.

2.7. Detection and isolation of catalyst resting state complex 37

As a part of our mechanistic investigations, we focused our studies on the detection of reaction intermediates and their potential isolation. With this goal, the model reaction was monitored by ^1H and ^{31}P NMR to detect possible iridium intermediate complexes. Initially, dinitrile **2** and $Ir(P^iPr_3)_2H_5$ (10 mol%) were heated at 150 °C in d_8-toluene and ^1H and ^{31}P NMR were recorded at different reaction times (calculations of conversions and yields were based on ^1H NMR). The reaction reached 56% conversion in the first 1 h

and gradually reached final conversion of 70% after 19 h, suggesting a progressive decrease in the reaction rate. As shown in the ^{31}P NMR spectra below (Figure 2.8), the singlet of the initial $Ir(P^iPr_3)_2H_5$ at 45.5 ppm almost disappeared after 5 min and a new singlet at 35.5 ppm (phosphorous species **Y**), a triplet at 32 ppm (phosphorous species **Z**) and singlet of free P^iPr_3 (19 ppm) appeared in a ratio of 0.10:1.17:1.15:1.0, respectively. Also, a small signal at 39.9 ppm was detected. Upon heating, the intermediate species are gradually consumed and a final broad singlet at 19 ppm is formed.

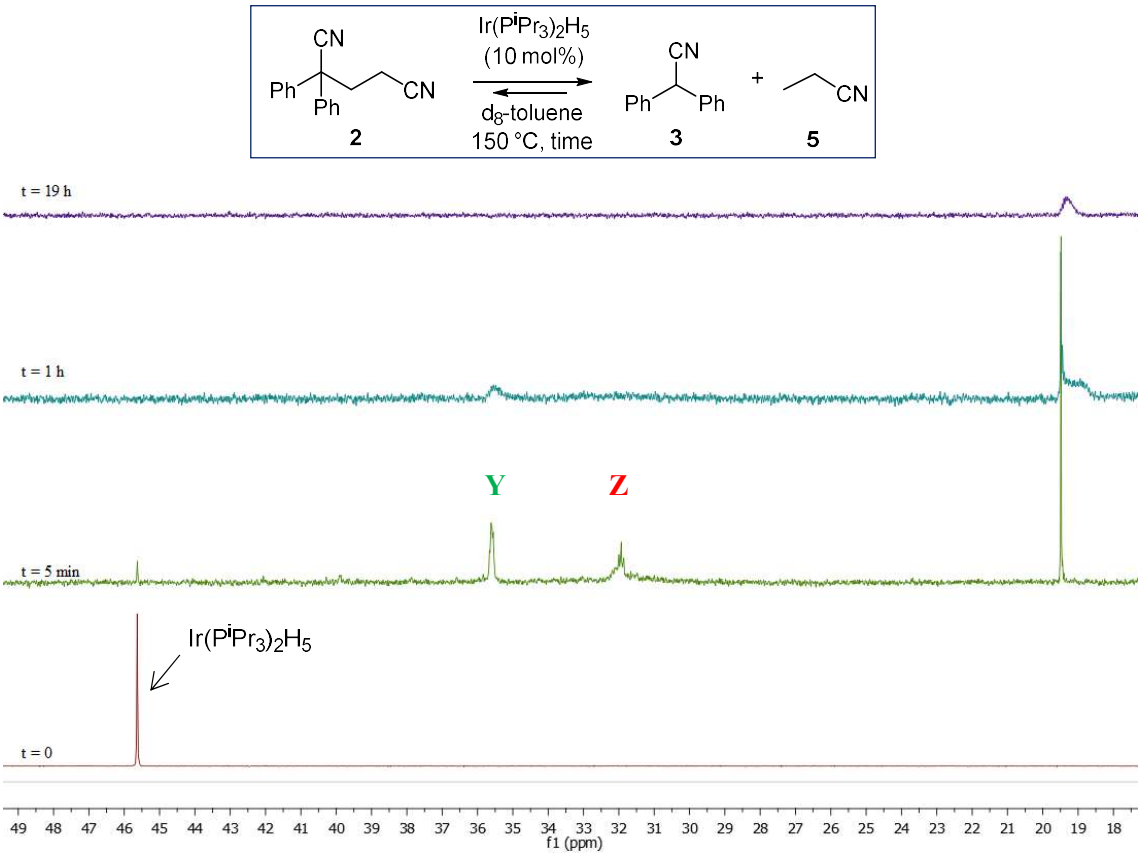

Figure 2.8: ^{31}P-NMR monitoring experiment of model reaction in d_8-toluene at 150 °C

The decrease in size of signals of the species **Y** and **Z** after 1 h coincides with the slowing down of the reaction which might indicate that these species are iridium-phosphine complexes that might be involved in the catalytic cycle. As evidenced in this experiment, species **Z** disappeared faster than species **Y**. We hypothesise that species **Y** could be formed from species **Z**. To check this idea, the catalytic model reaction was monitored at a lower temperature of 80 ºC by ^1H and ^{31}P NMR. After 1 h, the initial $Ir(P^iPr_3)_2H_5$ was

completely consumed (45.5 ppm) and species **Y** and **Z** were formed, as well as an apparent triplet or doublet of doublets at 39.9 ppm (phosphorous species **X**) and a small broad singlet at 36.5 ppm (Figure 2.9). After 2 h, free P^iPr_3 (19 ppm) was also detected.

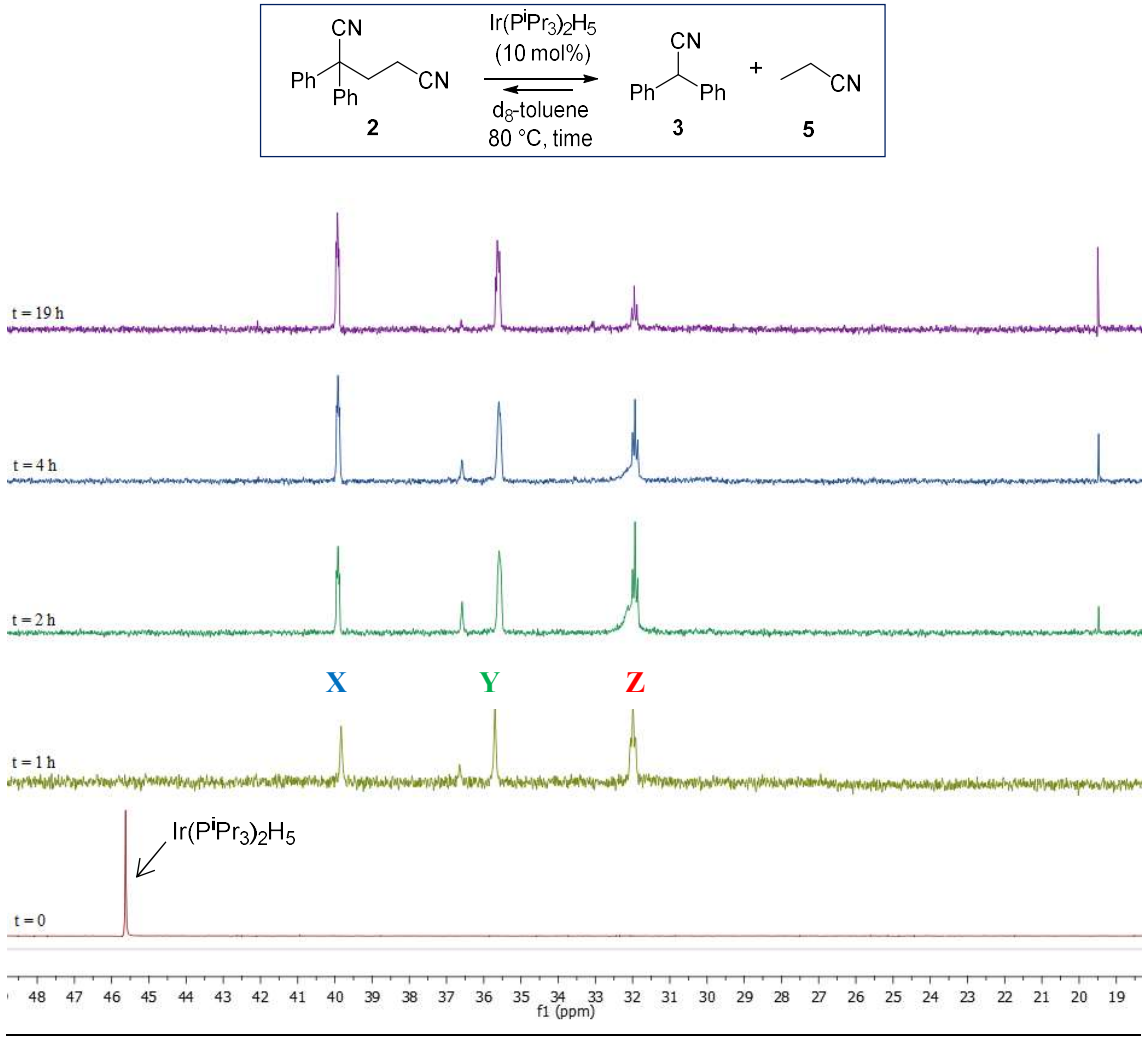

Figure 2.9: ^{31}P-NMR monitoring experiment of model reaction in d_8-toluene at 80 °C

On the other hand, the ^{1}H-NMR of the model reaction showed three new pairs of hydride signals formed upon heating at 80 ºC which we hypothesise that belong to the three dominant complexes **X**, **Y** and **Z** (Figure 2.9). After 4 h (Figure 2.10), the hydride area of ^{1}H-NMR presents two triplets of doublets at -21.8 and -22.3 ppm (hydrides **Z**), two doublets of doublets of triplets at -24.5 and -25.8 ppm and two triplets of doublets at -26.0 and -28.6 ppm (hydrides **X**).

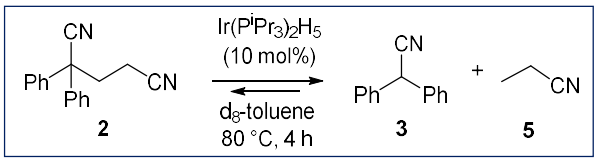

^{1}H NMR:

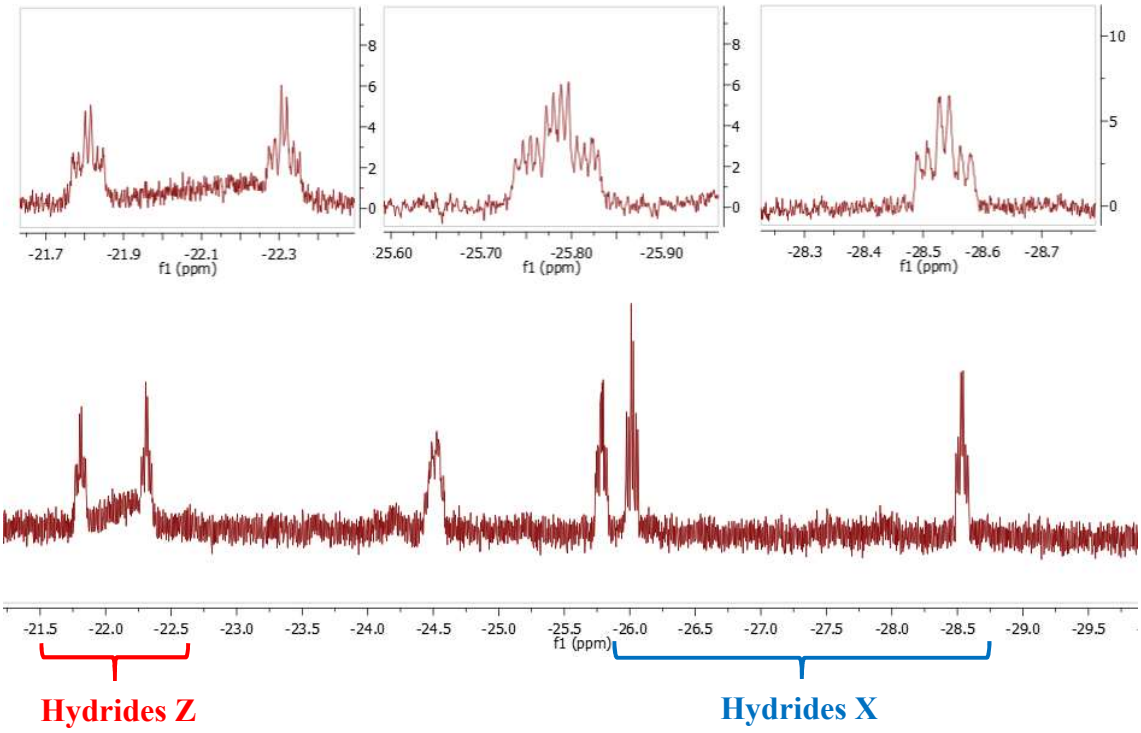

^{31}P NMR:

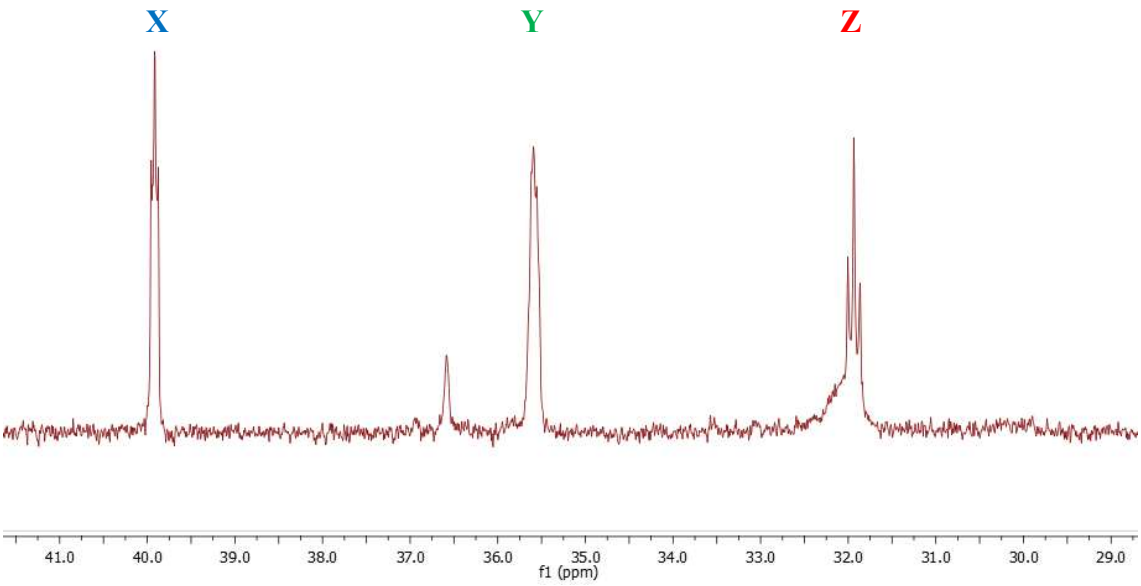

Figure 2.10: ^{1}H NMR (top) and ^{31}P NMR (bottom) spectra of model reaction at 80 ºC for 4 h

The hydride signals at -21.8, -22.3, -24.5, -25.8, -26.0 and -28.6 ppm were formed in a ratio of 1:1.34:1.81:1.54:1.69:1.82, respectively. We propose that the pair of hydride signals at -21.8 (td, J_{PH} = 14 Hz and J_{HH} = 7 Hz) and -22.3 ppm (td, J_{PH} = 14 Hz and J_{HH} = 7 Hz) (hydrides **Z**) correspond to the phosphine species at 32 ppm (t, J_{PH} = 14 Hz, phosphorous signal of **Z**) based on coupling constants values (Figure 2.10). In addition, the monitoring experiment showed that both hydrides and phosphine signals of complex **Z** decrease over the time (see experimental Section 2.13.12.1), whereas phosphorous signal of complexes **X** and **Y** either increased or remained constant (Figure 2.9). This observation further supports our hypothesis that hydride signals **Z** and phosphorous signal **Z** correspond to the same complex. The accurate interpretation of these signals in both ^{1}H and ^{31}P NMR spectra led us to suggest that this complex might correspond to an octahedral Ir(III) phosphine complex of the type of $Ir(P^{i}Pr_3)_2H_2LX$ with the two phosphines in trans position.[75] According to the found $^{2}J_{PH}$ value of 14 Hz, hydride and phosphine ligands are in *cis* arrangement (Figure 2.11), as typical $^{2}J_{PH}$ values for *cis* dispositions are 15 to 30 Hz whereas for trans arrangement are 90 to 200 Hz.[76]

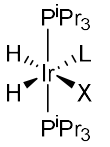

Figure 2.11: Complex of $Ir(P^{i}Pr_3)_2H_2LX$

Further interpretation of these ^{1}H and ^{31}P NMR spectra allowed us to assign the phosphorous signal **X** with hydride signal **X** (Figure 2.10) which multiplicities are analogous to those of phosphorous and hydride signals of complex **Z**, respectively. Therefore, the species **X** could also correspond to a $Ir(P^{i}Pr_3)_2H_2LX$ type complex.

After the analysis of the intermediate species formed during the model reaction at 80 ºC, we focused our attention on product yields established by ^{1}H NMR. After 30 min, the yield of diphenylacetonitrile **3** was 14% at 30% conversion of dinitrile **2**, suggesting the consumption of this product in an unknown side process (similar observation has been mentioned upon discussion of KIE in Section 2.6). Based on this, we speculate that the diphenylacetonitrile product **3** reacted with an active iridium catalyst to form a "dormant" state complex. To test this idea, we conducted the reaction with 1 equiv. of **3** and 1 equiv. of $Ir(P^{i}Pr_3)_2H_5$ at 80 °C and monitored it by ^{1}H and ^{31}P NMR. According to ^{31}P NMR spectrum, the reaction led to the formation of new species at 32 ppm analogous to complex **Z** formed during the model reaction at 150 and 80 ºC (Figure 2.8 and 2.9,

respectively). After 1 h, the reaction stopped at 50% conversion of diphenylacetonitrile **3** suggesting the reversible formation of the dormant state complex. Afterwards, $Ir(P^iPr_3)_2H_5$ was allowed to react with 10-fold excess of nitrile **3** which led to full conversion of starting iridium pentahydride complex and clean formation of the complex **37** in 80% NMR yield after 3.5 h at 80 °C (^{31}P NMR in Figure 2.12).

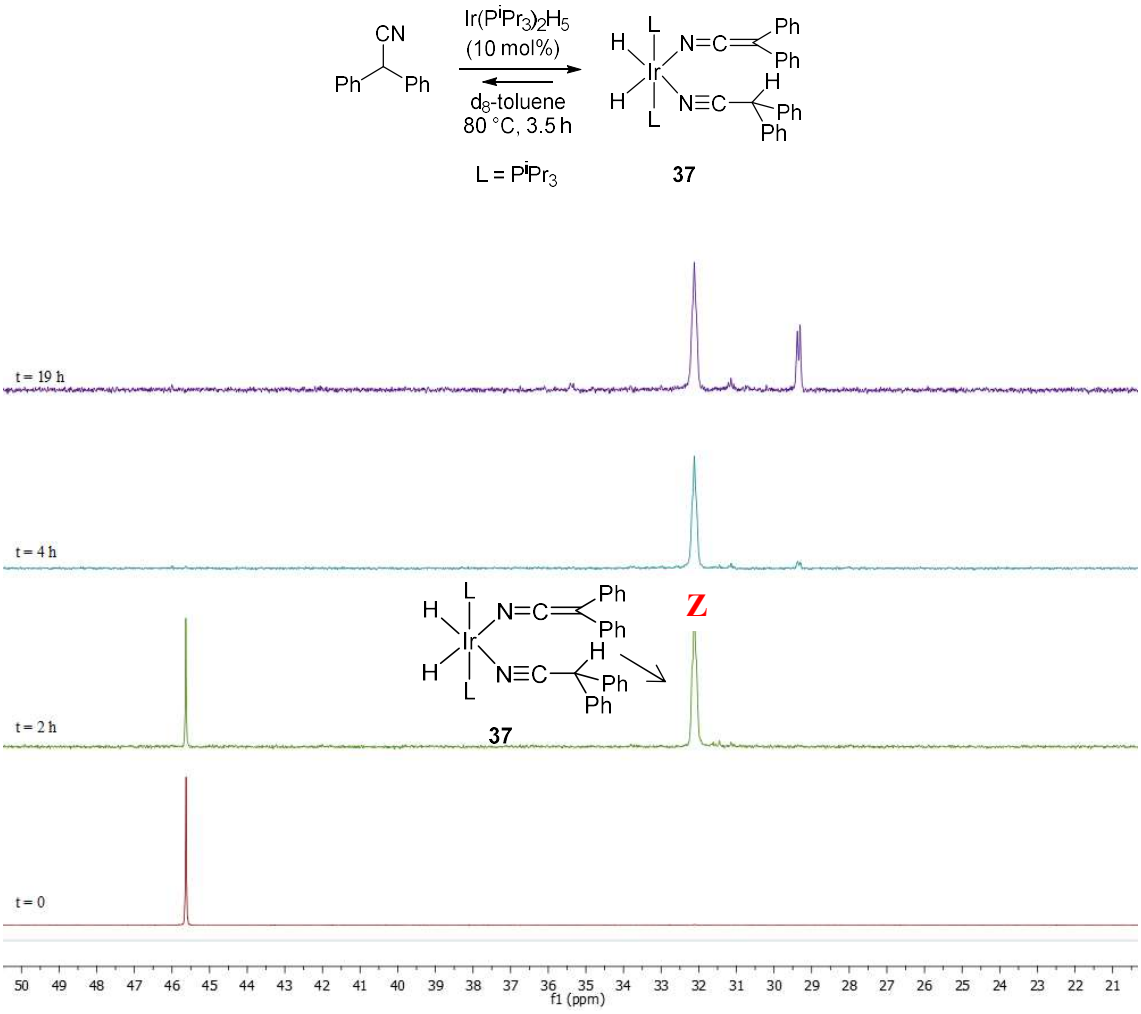

Figure 2.12: ^{31}P-NMR monitoring experiment of diphenylacetonitrile and $Ir(P^iPr_3)_2H_5$ in d_8-toluene at 80 °C

This complex was isolated in 56% yield and the characterisation by NMR, MS, and X-Ray diffraction analysis allowed us to identify it as iridium complex **37 (**Figure 2.12). Complex **37** is an iridium (III) dihydride complex containing two molecules of diphenylacetonitrile, one of which is deprotonated at α-position and can be described as a keteniminate-type ligand.[77] Complex **37** is one of the iridium intermediate species

formed during the model reaction as confirmed by ^{1}H and ^{31}P NMR of the pure complex. These NMR data show hydride signals at -21.8 and -22.3 ppm and a phosphorous signal at 32 ppm that are at the same chemical shifts as hydride and phosphine signals of complex **Z** (Figure 2.10).

The X-Ray diffraction analysis of this novel iridium complex **37** shows an octahedral molecular geometry with the two phosphine ligands placed in axial positions and the equatorial plane formed by two hydrides, diphenylacetonitrile and α-deprotonated diphenylacetonitrile ligands (Figure 2.13). The α-deprotonated diphenylacetonitrile ligand is coordinated *via* the nitrogen atom and exists as a keteniminate ligand $Ph_2C{=}C{=}N$. This ligand has a shorter C4-C3 bond (1.395 Å) and longer C3-N2 bond (1.159 Å) compared to the corresponding bond lengths of free $Ph_2HC{-}C{\equiv}N$ (1.470 and 1.147 Å, respectively).[78] Also, the N2-C3-C4 angle (178.9 º) indicates linear geometry of the keteniminate ligand $Ph_2C{=}C{=}N$. On the other hand, it is noteworthy that P1-Ir-P2 angle (169.1 º) is slightly distorted from linearity which can be explained by the presence of the bulky $Ph_2HC{-}C{\equiv}N$ and $Ph_2C{=}C{=}N$ ligands. The crystal structure of complex **37** supports our hypothesis regarding the structure of this intermediate as a $Ir(P^{i}Pr_3)_2H_2LX$ type complex (Figure 2.11) proposed by the analysis of coupling constants in previous ^{1}H and ^{31}P NMR monitoring experiments. Several examples of keteniminate complexes are reported for various metals such as zirconium,[77] titanium,[79] lithium,[80] gallium or indium,[78] but to the best of our knowledge, **37** is the first reported example of a well-defined iridium keteniminate complex.

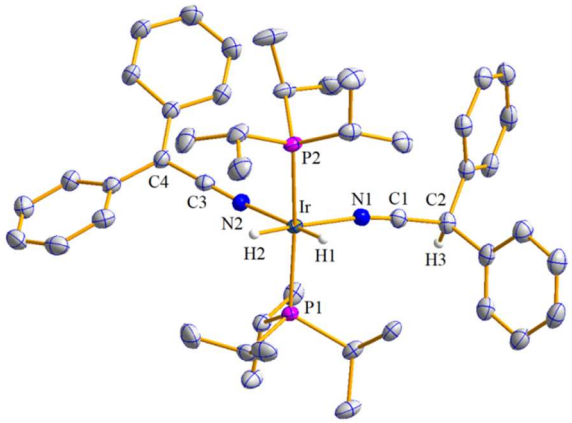

Figure 2.13: Crystal structure of complex **37**. All hydrogen atoms (except H1, H2 and H3) have been omitted for clarity

During our NMR studies of the model reaction with dinitrile **2** conducted at 80 ºC, we observed that the reaction stopped at 30% substrate conversion after 30 min. However, the subsequent heating at 150 °C "restarted" the reaction and led to 75% substrate conversion after 16 h, which suggests the formation of complex **37** as one of the "dormant" states of the catalyst that is reactivated at higher temperature. Therefore, we propose that the "dormant" complex **37** as a possible source of catalytically active species that are generated upon heating this complex at higher temperature. To test this idea, we conducted the cleavage of dinitrile substrate **2** using complex **37** as catalyst.

2.8. Reductive C-C bond cleavage of dinitrile 2 catalysed by complex 37

To examine the ability of complex **37** to mediate the C-C cleavage, a model reaction was conducted with dinitrile substrate **2** and 10 mol% of this complex in toluene at 150 °C for 16 h (Scheme 2.45). Delightfully, this reaction led to the formation of diphenylacetonitrile **3** and propionitrile **5** in 77 and 12% yield, respectively. Therefore, intermediate complex **37** catalyses the C-C cleavage and gives comparable yields of the products as compared to the original $Ir(P^iPr_3)_2H_5$ catalyst, which indicate relevance of **37** to the catalytic cycle.

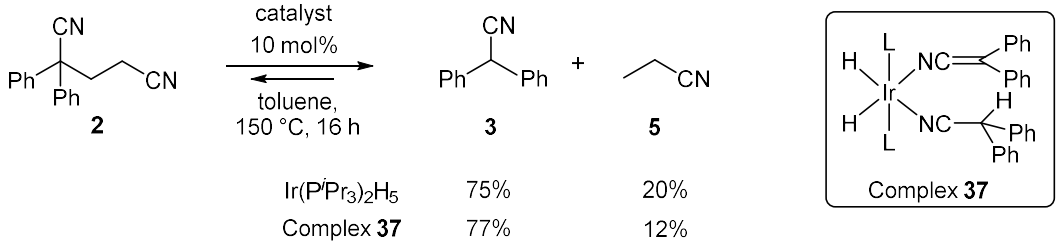

Scheme 2.45: C-C bond cleavage of substrate **2** catalysed by complex **37** compared to $Ir(P^iPr_3)_2H_5$

Previously, we showed that the C-C bond cleavage in dinitrile **2** is a reversible process and the microscopic reverse hydroalkylation reaction of acrylonitrile **4** with diphenylacetonitrile **3** is mediated by the $Ir(P^iPr_3)_2H_5$ catalyst (Section 2.2, Table 2.3). On basis of this, we hypothesised that the catalytically active complex **37** should also catalyse the hydroalkylation reaction. To test this idea, the hydroalkylation of acrylonitrile **4** (1 equiv.) was conducted with diphenylacetonitrile **3** in the presence of 10 mol% of complex **37** in toluene at room temperature (Table 2.9). After 10 min, the

reaction reached full conversion of acrylonitrile **4** and dinitrile **2** was formed in 67% yield, which is comparable to the yield with the pentahydride catalyst (entries 1 and 3). As the alkene was fully consumed under these conditions possibly due to side reactions (Section 2.2, Table 2.2), large excess of acrylonitrile (10 equiv.) was used to improve product yield. Gratifyingly, this reaction led to the formation of dinitrile **2** in a higher yield of 88% (Table 2.9, entry 2), which was also higher than the yield obtained with the $Ir(P^iPr_3)_2H_5$ catalyst (Table 2.9, entry 4). Thus, complex **37** effectively catalyses the microscopic reverse hydroalkylation reaction.

Table 2.9: Ir-catalysed hydroalkylation of acrylonitrile

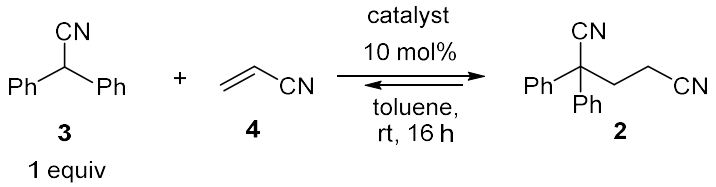

Entry	4, equiv	Catalyst	Conversion 3, %	Conversion 4, %	Yield 2, %
1[a]	1	Complex **37**	70	100	67
2	10	Complex **37**	90	57	88
3	1	$Ir(P^iPr_3)_2H_5$	71	80	69
4[b]	10	$Ir(P^iPr_3)_2H_5$	81	59	52

[a]: Reaction reached full conversion of acrylonitrile after 10 min. [b]: Product of dialkylation of Ph_2CHCN was formed in 26% yield under these conditions.

According to the principle of microscopic reversibility, C-C cleavage and hydroalkylation reactions should occur *via* the same mechanism.[81] Building on this, we devised that we can conduct all steps of the C-C bond cleavage catalytic process in reverse direction, starting from diphenylacetonitrile **3** and acrylonitrile **4**. Indeed, the reaction with $Ir(P^iPr_3)_2H_5$ and diphenylacetonitrile **3** gives the product of C-H activation, which is the deprotonated $Ph_2C{=}C{=}N$ ligand in complex **37** (Scheme 2.46). After the initial C-H activation step, we hypothesised that the next step would be the C-C bond formation step between deprotonated diphenylacetonitrile in complex **37** and acrylonitrile. To test this idea, complex **37** was allowed to react with acrylonitrile at room temperature which led to the formation of dinitrile **2** in 85% NMR yield within 10 min at full conversion of

complex **37** (Scheme 2.46). This experiment further proves the relevance of this complex in the catalytic cycle and the reversibility of the C-C cleavage process.

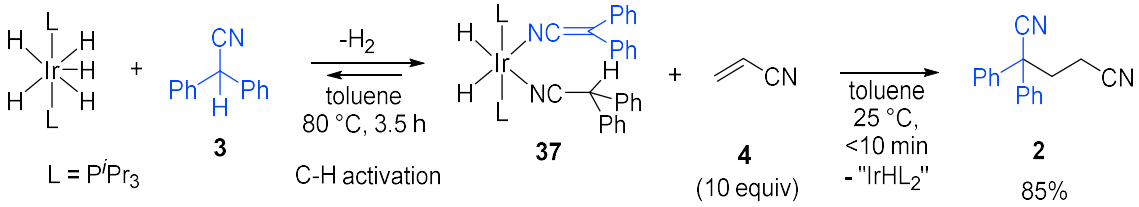

Scheme 2.46: Microscopic reverse of C-C cleavage step: hydroalkylation of **4** with complex **37**

2.9. Computational studies

Our experiments with complex **37** and acrylonitrile further evidenced the reversibility of the C-C cleavage reaction and showed the importance of this complex in the catalytic cycle of both the cleavage and its microscopic reverse – the C-C bond forming hydroalkylation (Scheme 2.46). These studies allowed us to propose initially two possible mechanistic pathways for the C-C bond formation reaction starting from complex **37** (Scheme 2.46), which are also valid for the C-C cleavage process based on the principle of microscopic reversibility. Initially, unsaturated iridium species "IrL$_2$H" (L= P^{i}Pr$_3$) would be formed from precatalyst Ir(P^{i}Pr$_3$)$_2$H$_5$, which would enable the C-H activation of diphenylacetonitrile to form complex **37** (Scheme 2.47). Then, the neutral diphenylacetonitrile would dissociate to form complex **38** creating a free coordination site.

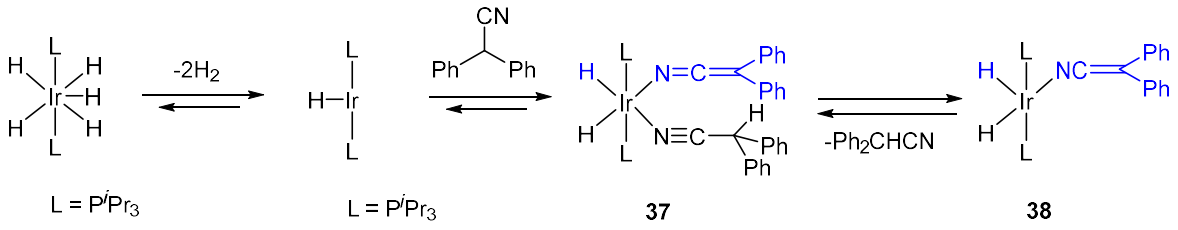

Scheme 2.47: C-H activation of diphenylacetonitrile by precatalyst Ir(P^{i}Pr$_3$)$_2$H$_5$

As shown in Scheme 2.48, the coordination of acrylonitrile to complex **38** would be the next step of the process prior to the intramolecular C-C forming step. Two pathways can

be proposed depending whether acrylonitrile[82] coordinates to iridium through the nitrogen atom (Pathway 1A)[83,84] or the alkene bond (Pathway 2A).[85,86]

Pathway 1A would involve the coordination of acrylonitrile through the C=C bond to give complex **39** (Scheme 2.48). In this complex, the coordinated acrylonitrile would undergo Michael-addition reaction through an intramolecular nucleophilic attack by the α-carbanion centre of N-coordinated deprotonated diphenylacetonitrile. This would lead to N,C-coordinated dinitrile complex **40** that can isomerise to the corresponding monocoordinated complex **41**. Finally, reductive elimination would give the final product **2** and the regenerated "IrL_2H" catalyst.

On the other hand, Pathway 2A would involve the binding of acrylonitrile to complex **38** *via* the nitrogen atom forming complex **42** (Scheme 2.48). Then, the intramolecular C-C bond formation step would give N,N-coordinated dinitrile complex **43** that can isomerise to the corresponding N-monocoordinated complex **44**. Finally, this complex can isomerise to complex **41** and undergo reductive elimination to give the dinitrile product **2**.

To identify the most energetically favourable pathway, we performed DFT calculations (in collaboration with Dr. Neil Berry, University of Liverpool) of the ground state energies of the intermediate complexes involved in the two proposed Pathways 1A and 2A. We also computed the activation energy of the C-C bond formation step for Pathways 1A and 2A, which involved transition state complexes **39TS** and **42TS**, respectively (Figure 2.15). The energy profiles in Figure 2.15 show ground state energies and the energy barrier of only the C-C forming step of each pathway. DFT calculations were performed with Gaussian 09 using M06-2X/6-31(d,p) in toluene PCM solvent model at 298.15 K using rigid rotor and harmonic oscillator approximations.[87]

Initially, we compared the stability of complexes **39** and **42**, resulted from the different coordination modes of acrylonitrile with complex **38**. DFT calculations indicated that the N-bonded complex **42** is more stable than the C-C bonded complex **39** by 13 kcal/mol (Figure 2.15). Although computed activation energies of C-C forming step of pathway 1A and 2A are similar (11.4 and 10.4 kcal/mol, respectively), transition state **42TS** is more stable than **39TS** by 14 kcal/mol.

Scheme 2.48: Proposed mechanistic pathways of C-C bond formation from complex **37** and transition state complexes. Pathway 1A) C-C bond formation through the Ir species with C=C bonded acrylonitrile and 2A) C-C bond formation through the Ir species with N- bonded acrylonitrile.

Pathway 1A

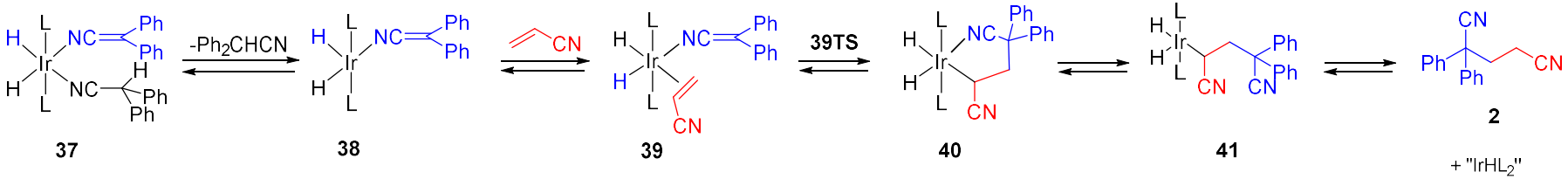

Pathway 2A

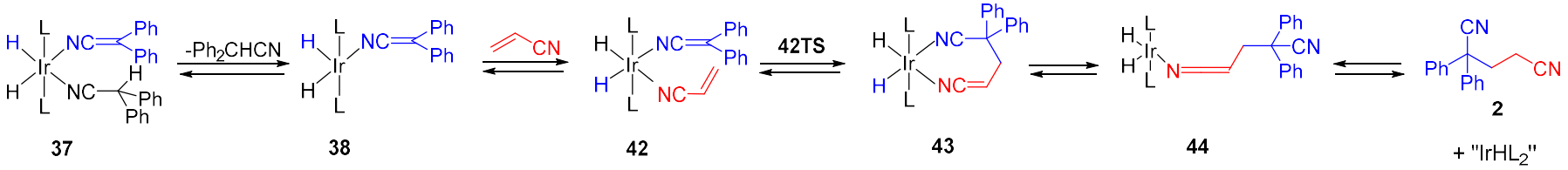

We next compared the ground state energies of complexes formed after the C-C forming step in each pathway. We found that N,C-coordinated dinitrile complex **40** (Pathway 1A) is similar in energy to its isomer in Pathway 2A – the N,N-coordinated dinitrile complex **43** – (Figure 2.15).[88] Finally, the energy of complexes **41** and **44**, formed prior to the reductive elimination step, was also compared. These calculated energies resulted in that the N-monocoordinated dinitrile complex **44** is 3 kcal/mol more stable than the analogous C-bound complex **41**. According to these preliminary computational results, the transition state of Pathway 2A as well as the ground state energy of its intermediate iridium complexes are more stable than the corresponding complexes involved in Pathway 1A. Therefore, considering ground state energies of the intermediates and the activation barrier for the C-C bond forming step, Pathway 2A (in red) is energetically more favourable than Pathway 1A (in blue) as depicted in Figure 2.15.

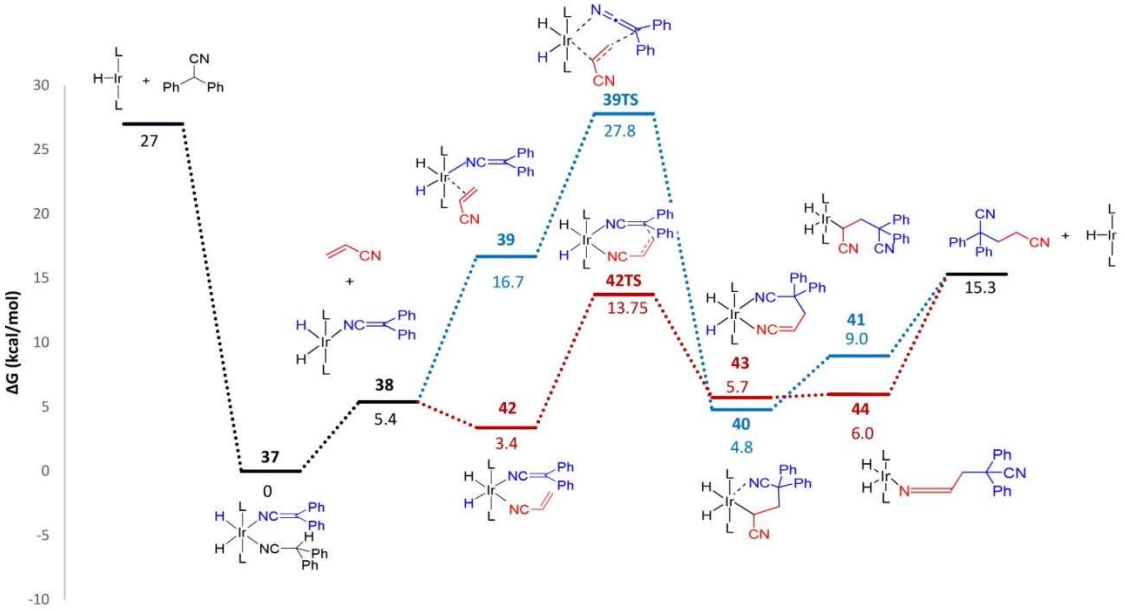

Figure 2.15: Energy profiles of Pathway 1A (blue) and Pathway 2A (red) for the C-C bond formation process (common steps for both pathways are in black). N.b.: These reaction profiles show only ground state energies not energy barriers, except for the C-C forming step of each pathway where corresponding energy barriers *via* transition states **39TS** and **42TS** were calculated.

Interestingly, conducted calculations show different interactions between iridium and the organic ligands in complexes **39** and **42**, those intermediates that undergo the key C-C bond forming step. For example, the optimised structure of complex **42** (Figure 2.16) shows a Ir-N(acrylonitrile) bond length of 2.257 Å which is within the typical length of covalent M-N(acrylonitrile) bond (1.90 - 2.30 Å).[82] In contrast, optimised structure of complex **39** (Figure 2.16) displays a long distance between iridium and the C=C bond of acrylonitrile (3.479 Å) which exceeds typical covalent length for this type of bond (ca. 2.15 Å).[82] Similarly, the optimised structure of complex **40** shows a distance of Ir-N(tertiary CN) of 2.639 Å which is slightly longer compared to the length of this bond in complex **43** (Figure 2.16). Whereas common covalent bond distance of nitriles bound to iridium *via* the N atom is ca. 2.09 Å.[89] The elongated bond distances in complex **39** and **40** might indicate van der Waals interactions between iridium and the corresponding atoms (Figure 2.16, van der Waals interaction represented as a dotted line). This hypothesis is supported by the standard van der Waals distances of Ir-Csp^2 (3.7 Å) and Ir-N (3.5 Å) calculated based on van der Waals radii of Ir (2.0 Å), C (1.7 Å) and N (1.55 Å).[90,91]

In addition to discussed Pathways 1A and 2A, we also envisioned two alternative pathways that involve the C-coordinated analogue of complex **37** – complex **45** – in which deprotonated diphenylacetonitrile binds to iridium through the α-carbon atom (Figure 2.17).[92–94]

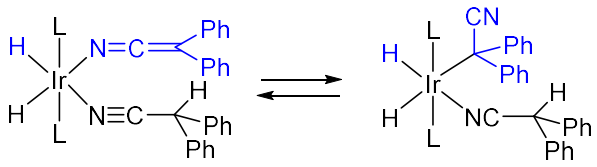

37 **45**

Figure 2.17: N-bonded complex **37** and its plausible isomer, C-bonded complex **45**

Figure 2.16: Optimised structures of complexes **42** and **43** from pathway 2A and complexes **39** and **40** from pathway 1A. Hydrogen atoms (except hydride ligands) have been omitted for clarity. Iridium is represented in dark blue, carbon in black, phosphorous in orange, nitrogen in light blue and hydrogen in white.

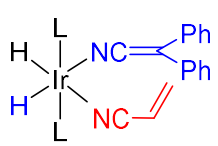

42

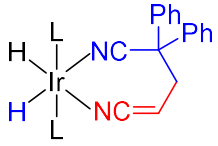

43

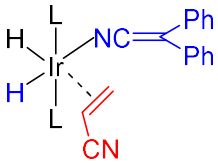

39

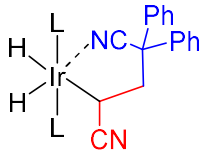

40

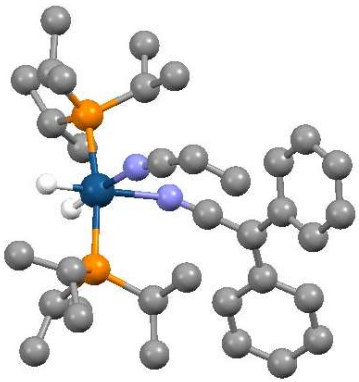

42

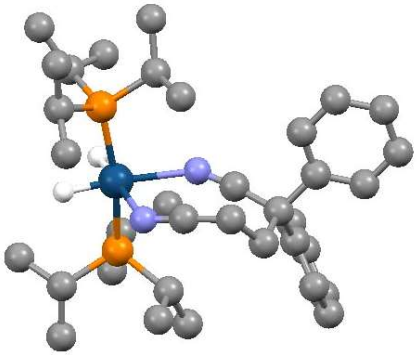

43

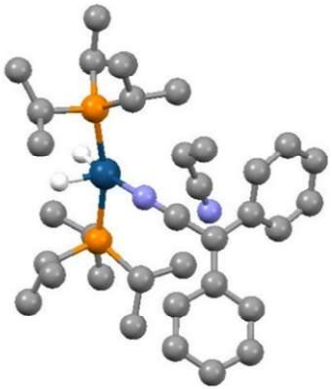

39

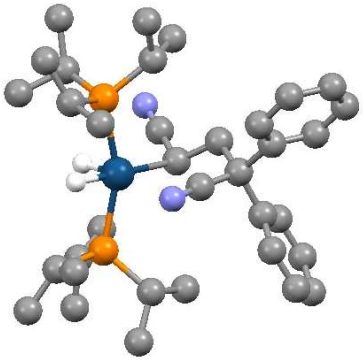

40

It is noteworthy that this coordination mode was proposed by Murahashi to suggest the mechanism of the C-C bond cleavage of dinitriles (Scheme 2.2). Based on this, we studied computationally two additional pathways of C-C forming process that involved C-coordinated intermediates (Scheme 2.49). These Pathways 1B and 2B would start with the deinsertion of neutral diphenylacetonitrile from complex **45** to form complex **46** (Scheme 2.49). Pathway 1B would involve the coordination of acrylonitrile to **46** through the C=C bond to give complex **47**. Subsequently, intramolecular nucleophilic attack of deprotonated diphenylacetonitrile to acrylonitrile would lead to complex **40** with N,C-coordinated deprotonated dinitrile ligand, the same complex as in Pathway 1A. Isomerisation to complex **41** with C-monodentate dinitrile ligand and reductive elimination would form dinitrile product **2** and would regenerate the active "$IrHL_2$" species. Notably, this pathway is the microscopic reverse of the mechanism of the C-C bond cleavage proposed by Murahashi.

Alternatively, Pathway 2B involves the coordination of acrylonitrile *via* the nitrogen atom, which gives complex **48** (Scheme 2.49). The consecutive intramolecular C-C bond forming step leads to complex **43** which isomerises to complex **44**. Reductive elimination through complex **41** gives the dinitrile product **2** and "$IrHL_2$" species.

To study the thermodynamic feasibility of Pathways 1B and 2B and compare them with previous Pathways 1A and 2A, ground state energies of intermediate complexes of these additional pathways were computed. These calculations indicate that C-bound forms of intermediate complexes (Pathways 1B and 2B) involved in the C-C forming steps are less stable than the corresponding N-bonded complexes (Pathways 1A and 2A). For instance, C-bound complex **45** is higher in energy than its N-bound analogous complex **37** by 18 kcal/mol (Figure 2.18). This is in good agreement with the ^{13}C NMR data of complex **37** which indicates that it exists exclusively in N-coordinated form in solution. The ^{13}C NMR spectra shows a characteristic peak at δ 145.4 ppm which is a singlet and it is assigned to the carbon adjacent to the nitrogen in the $Ph_2C=C=N$ moiety. This chemical shift is comparable with those found in the reported N-coordinated complexes $[Ph_2C=C=NGaMe_2]_2$ (140.0 ppm) or $[Ph_2C=C=NInMe_2(THF)]_2$ (143.8 ppm).[78]

Scheme 2.49: Proposed mechanistic pathways for C-C bond formation from complex **45**. Pathway 1B: C-C bond formation through the Ir species with C=C bound acrylonitrile. Pathway 2B: C-C bond formation through the Ir species with N-bound acrylonitrile.

Pathway 1B

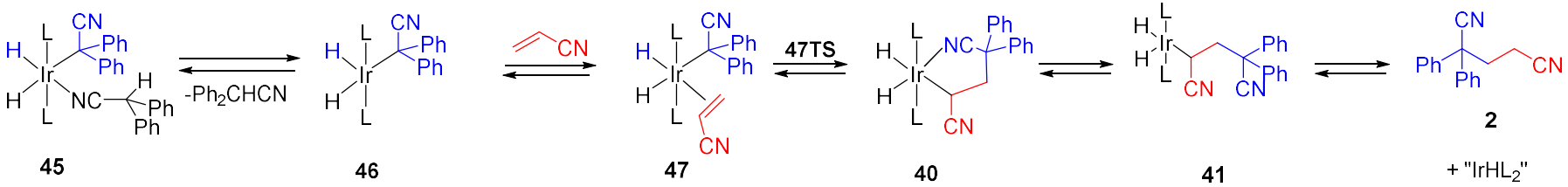

Pathway 2B

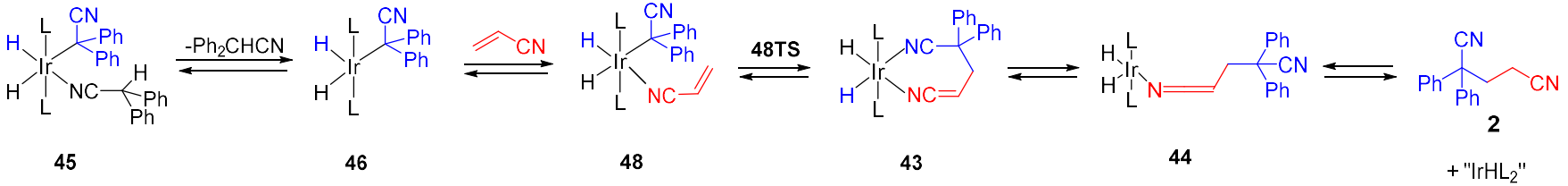

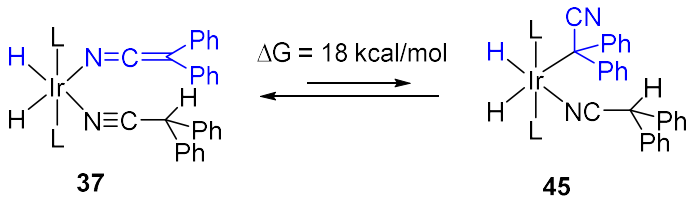

Figure 2.18: Relative energies of N-bound complex **37** and C-bound complex **45**

Similarly, C-bound complex **46** is less stable than its corresponding N-isomer complex **38** by 12 kcal/mol (Figure 2.19), which is in line with reported studies on C- and N-bound isomers of ruthenium α-cyanocarbanions where it is demonstrated that bulky phosphine ligands, such as P^iPr_3, favour the N-coordination of anionic alkyl nitriles.[95]

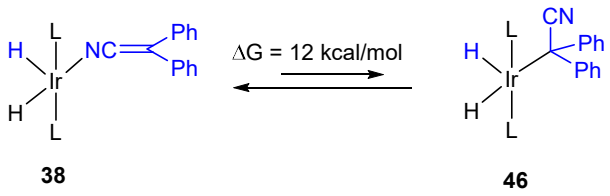

Figure 2.19: Relative energies of N-bound complex **38** and C-bound complex **46**

As part of our computational studies, energy barriers of the C-C forming step in Pathways 1B and 2B were also calculated. Remarkably, optimisation of geometry for transition states **47TS** and **48TS** corresponding to Pathways 1B and 2B respectively, led to transition state **42TS** that corresponds to Pathway 2A (Figure 2.20). This result may imply that the C-C bond forming steps in Pathways 1B and 2B are energetically unfavourable and converge into the more favourable Pathway 2A.

Additional evidence that supports this idea is found in the results of the optimised structure for complex **46**. In this complex, the iridium centre is surrounded by sterically demanding ligands, which blocks the coordination of acrylonitrile. This is illustrated by the optimized structures of the subsequent complexes **47** and **48**, (involved in Pathway 1B and 2B, respectively), in which acrylonitrile is not coordinated to iridium in any of these complexes as indicated by its large distance to iridium (Figure 2.21). The distance between iridium atom and the terminal carbon atom of acrylonitrile in complex **47** is of 4.71 Å whereas typical distances for a covalent Ir-C (C=C) bond with alkenyl nitrile ligands is ca. 2.2 Å.[96] Likewise, structure of complex **48** shows a long Ir-N (acrylonitrile)

Figure 2.20: Optimised structures of complexes 47TS, 52TS and 53TS. Hydrogen atoms (except hydride ligands) have been omitted for clarity. Iridium is represented in dark blue, carbon in black, phosphorous in orange, nitrogen in light blue and hydrogen in white.

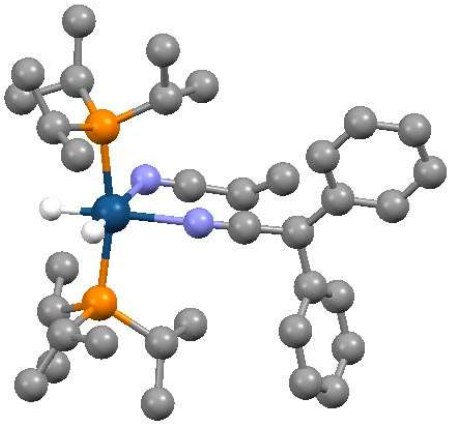

47TS

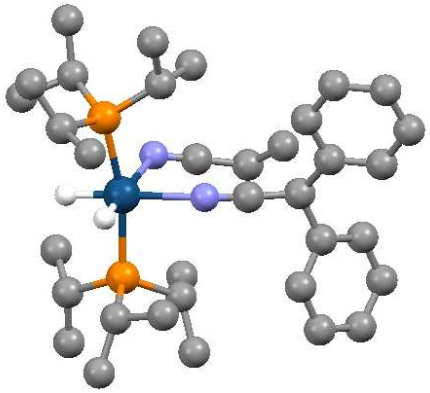

52TS

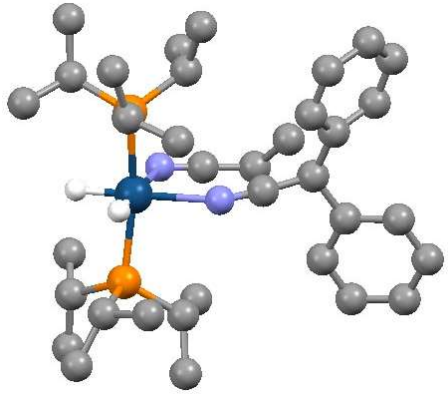

53TS

distance of 4.69 Å compared to common covalent M-N(acrylonitrile) bond length (1.90 - 2.30 Å).[82]

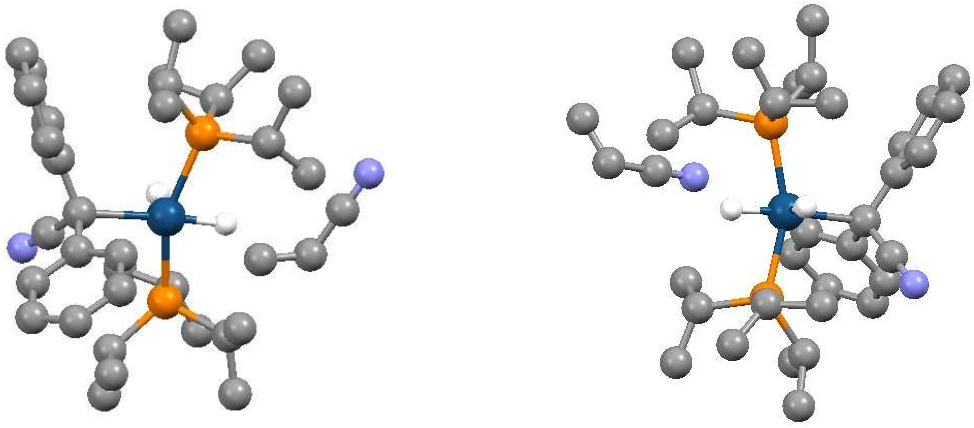

47 **48**

Figure 2.21: Optimised structures of complexes **47** and **48**. Hydrogen atoms (except hydride ligands) have been omitted for clarity. Iridium is represented in dark blue, carbon in black, phosphorous in orange, nitrogen in light blue and hydrogen in white.

In addition to the considered four mechanisms that involved intramolecular C-C bond formation, we additionally hypothesised a fifth mechanism involving an intermolecular C-C forming step (Pathway 3, Scheme 2.50). The intermolecular pathway has been hypothesised as a plausible mechanism for various reported Michael additions catalysed by transition metals.[43,97,98] This additional Pathway 3 would involve the intermolecular nucleophilic attack of the deprotonated α-carbon of diphenylacetonitrile in complex **37** at acrylonitrile to generate complex **49** *via* transition state **37TS**. The corresponding DFT calculations show a high activation barrier of 31 kcal/mol, suggesting a more energetically demanding route compared to the intramolecular pathways.

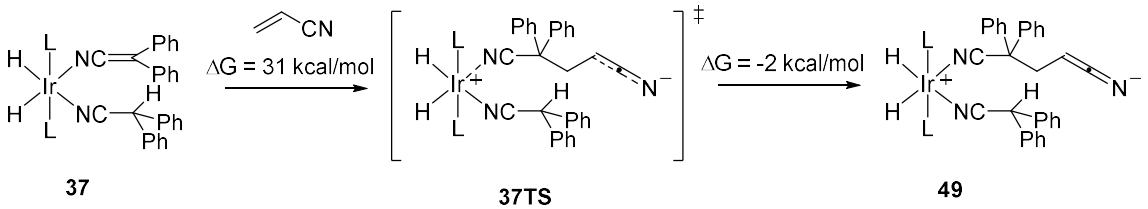

Scheme 2.50: Pathway 3, Intermolecular pathway of C-C bond formation between complex **37** and acrylonitrile

In view of computational results and the experimental observation of the facile room temperature hydroalkylation between complex **37** and acrylonitrile, we consider that the intermolecular Pathway 3 is unlikely due to the high energy barrier obtained.

In conclusion, five potential pathways for the C-C bond formation were considered in this computational study: one intermolecular pathway (3) and four intramolecular pathways (1A, 1B, 2A, and 2B). The computational results suggest that intermolecular Pathway 3 is unfavourable owing to the high activation energy of the C-C forming step. Regarding intramolecular pathways, computational data present evidences that Pathways 1B and 2B that involve C-C bond formation from complexes with C-coordinated deprotonated diphenylacetonitrile are not feasible and converge in Pathway 2A. Notably, the C-C bond forming step in Pathway 1B, a microscopic reverse of the C-C cleavage step in the Murahashi's mechanism, – is not realistic and therefore the catalytic cycle for the C-C cleavage of dinitriles suggested by Murahashi does not seem valid. More energetically favourable pathways are Pathways 1A and 2A that include C-C bond formation in iridium complexes with N-bonded deprotonated diphenylacetonitrile ligand. Among these, Pathway 2A involving species with N-coordinated acrylonitrile is more favourable than Pathway 1A involving species with C-C bonded acrylonitrile (Figure 2.15). Thus, the obtained data allow to identify the privileged mechanism for the C-C bond formation step from complex **37**. However, to reach a more comprehensive conclusion regarding the distinguishing between the proposed routes, calculations of activation barriers for all steps in these mechanisms are being performed. It is worth mentioning, that this is the first example of computational study of the C-C bond formation in iridium-mediated Michael-type hydroalkylations.

2.10. Proposed mechanism of Ir-catalysed reductive cleavage of unstrained C-C bond of dinitriles

Our preliminary DFT computational results of the mechanism of the C-C bond forming hydroalkylation reaction provide also insight regarding the C-C bond cleavage process according to the principle of microscopic reversibility. Based on the DFT results and our experimental findings, we propose a mechanism of iridium-catalysed reductive cleavage

of C-C single bonds of dinitriles (Scheme 2.51). In contrast to Murahashi and co-workers, we suggest that this mechanism occurs through N-coordinated iridium species in which the C-H activated dinitrile substrate coordinates *via* the two nitrile groups to the iridium prior to the cleavage step. Herein, our proposed catalytic cycle is described step by step.

The catalytic cycle starts with the formation of coordinatively unsaturated iridium species from the 18-electron $Ir(P^iPr_3)_2H_5$ complex to coordinate the dinitrile substrate. We propose that the unsaturated iridium species are generated *via* the release of two molecules of dihydrogen.[6,99,100] As a result, IrL_2H type complexes will be formed as catalytically active species, which have been previously proposed as reactive intermediates.[101]

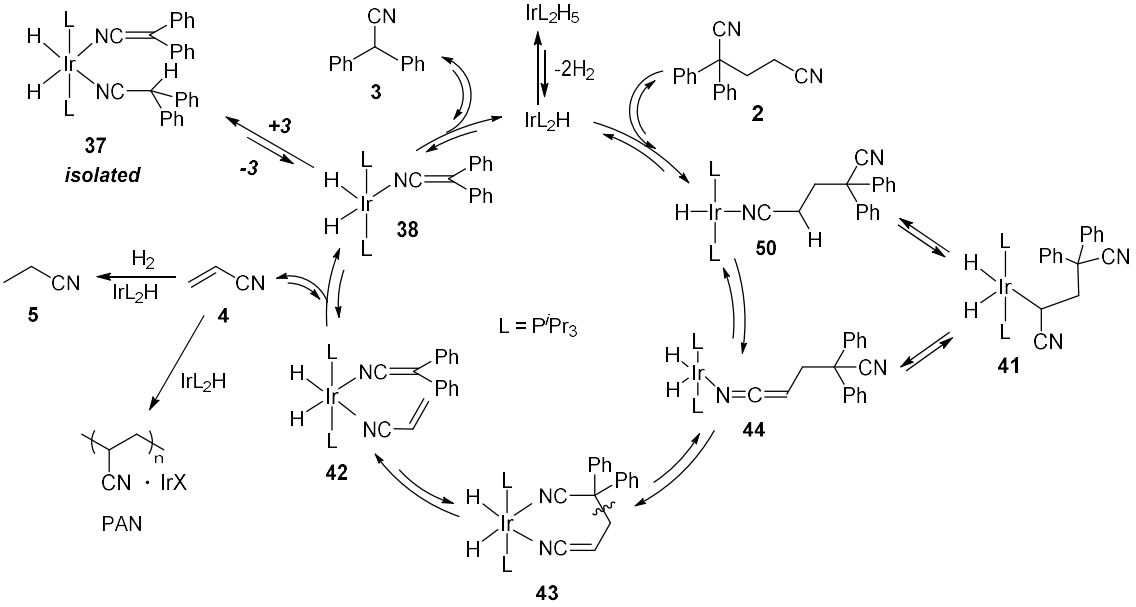

Scheme 2.51: Proposed catalytic cycle of the Ir-catalysed reductive cleavage of C-C single bonds of dinitriles

Once the active species are formed, dinitrile **2** would coordinate to iridium centre through the terminal nitrile group to produce intermediate **50**. This proposed coordination mode of dinitrile substrate **2** is supported by additional DFT computations. The ground state energies of N-coordinated dinitrile iridium complex **50** and N,N-coordinated dinitrile iridium complex **50a** were calculated to understand the most favourable coordination

mode of the dinitrile substrate **2** (Figure 2.22). Optimisation of geometry for the N,N-bound complex **50a** led to N-bound complex **50**, suggesting that a bidentate coordination of the dinitrile substrate is energetically unfavourable.

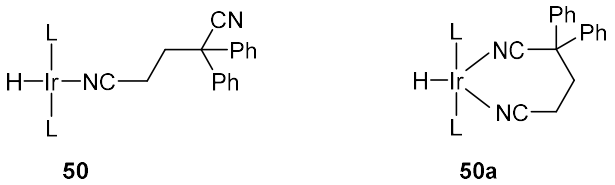

Figure 2.22: Modes of coordination of dinitrile **2** to iridium

Subsequently, iridium complex **50** would convert into α-deprotonated complex **44** (Scheme 2.51). In this regard, the mechanism of C-H activation of α-C-H bonds in nitriles has not yet been studied but it can occur *via* two general pathways. Complex **50** can undergo intramolecular deprotonation of the α-C-H bond by the iridium centre to give **44**. Alternatively, iridium can insert into the C-H bond to give complex **41**.[8,43] To gain insight into the C-H activation step, these mechanisms are currently being calculated by DFT. We suggest that C-coordinated complex **41** and its N-isomer complex **44** could be in equilibrium,[88] as these complexes are similar in energy according to DFT computations (Figure 2.15). At the same time, complex **44** can easily interconvert to N,N-coordinated dinitrile iridium complex **43**, as their ground state energy are also similar (Figure 2.15). As evidenced by our studies on the role of two functionalities in the substrate (Section 2.4), two directing groups are required for the C-C bond cleavage step which supports the proposal of N,N-coordinated dinitrile iridium complex **43** prior to the breaking step.

The next step in the catalytic cycle is the cleavage of the aliphatic C-C bond. On the basis of DFT calculations of the microscopic reverse step (Scheme 2.48, Pathway 2A), we propose that the C-C cleavage is occurring *via* a retro-Michael type reaction. Thus, N,N-coordinated complex **43** is converted to complex **42**, which contains N-coordinated deprotonated diphenylacetonitrile and N-coordinated acrylonitrile.

Next, the dissociation of acrylonitrile leads to formation of N-coordinated deprotonated diphenylacetonitrile iridium complex **38** driven by the irreversible consumption of acrylonitrile through hydrogenation and polymerisation. Our proposal of alkene consumption as a driving force of the process is in good agreement with mechanistic

studies conducted by Basset on C-C hydrogenolysis of alkanes (Chapter 1, Section 1.4.3).[1]

Finally, complex **38** reductively eliminates diphenylacetonitrile **3** and regenerates the initial active catalyst "IrL_2H". Complex **38** can coordinate a second molecule of diphenylacetonitrile **3** forming the previously observed iridium dinitrile complex **37** (Section 2.7). The reductive elimination could occur directly from the N-coordinated complex **38** or through initial isomerisation into the C-coordinated complex **46** (Scheme 2.52). As discussed previously, DFT calculations indicated that complex **38** is more stable than complex **46** by 12 kcal/mol. However, a more detailed mechanistic study would be required to explain how this reductive elimination occurs as the mechanism of its microscopic reverse reaction – the C-H activation of nitriles – has not yet been investigated.

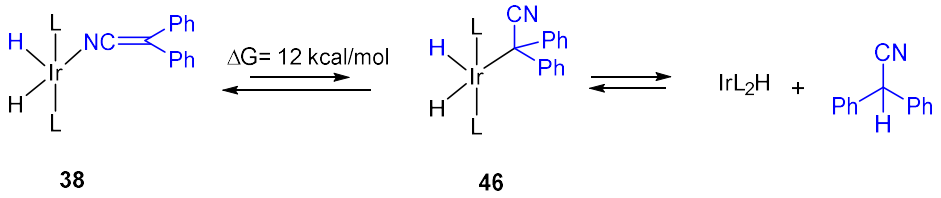

38 **46**

Scheme 2.52: N- and C-coordinated C-H activated diphenylacetonitrile iridium complexes **43** and **46**

The structure of intermediate iridium complexes in the proposed catalytic cycle, such as complexes **42** and **43**, is in line with the hypothesis of formation of $Ir(P^iPr_3)_2H_2LX$ type intermediate complexes (L= neutral ligand) detected during our NMR monitoring experiments (Section 2.7, Figures 2.8 and 2.11). To further support the proposed catalytic cycle, we attempted to intercept these intermediate complexes or resting states of catalyst. With this aim, dinitrile **2** (1 equiv) and $Ir(P^iPr_3)_2H_5$ complex (1 equiv) were heated at 150 °C in d_8-toluene and the reaction was monitored by ^1H and ^{31}P NMR until full conversion of the starting iridium complex. After 10 min, the ^{31}P NMR indicated formation of complex **37** as a major intermediate species together with two minor phosphine iridium complexes at 33.8 and 40.3 ppm. Once the $Ir(P^iPr_3)_2H_5$ was completely consumed after 1 h, the reaction mixture was treated with 2 M aqueous solution of HCl. Acidic treatment was necessary to convert sensitive hydride complexes into more stable hydrochlorinated

iridium derivatives that could be isolated by column chromatography or crystallisation. This reaction after subsequent acidic treatment led to isolation of complex **51** in a 10% yield (Scheme 2.53). The characterisation by NMR, MS, IR and X-Ray diffraction analysis allowed us to identify complex **51** as an iridium monohydride complex containing N-coordinated diphenylacetonitrile, two phosphines and two chloride ligands.

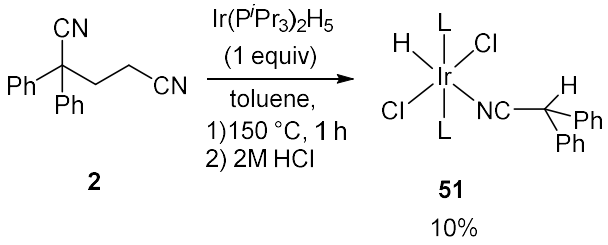

2 **51**

10%

Scheme 2.53: Formation of complex **51** from the acidic treatment of the stoichiometric experiment of dinitrile substrate and Ir(P^{i}Pr$_3$)$_2$H$_5$.

The X-Ray diffraction analysis shows an octahedral geometry of complex **51** with both phosphines in apical positions and the equatorial plane constituted by a hydride, the N-bonded diphenylacetonitrile and the two chlorides in *trans*-arrangement (Figure 2.23). The X-Ray analysis reveals a N1-C1 bond length of 1.146 Å which is analogous to the C≡N bond distance for free diphenylacetonitrile (1.147 Å). It is noteworthy that the P1-Ir-P2 angle (165 º) is slightly distorted from linearity which might be due to the presence of the bulky diphenylacetonitrile ligand.

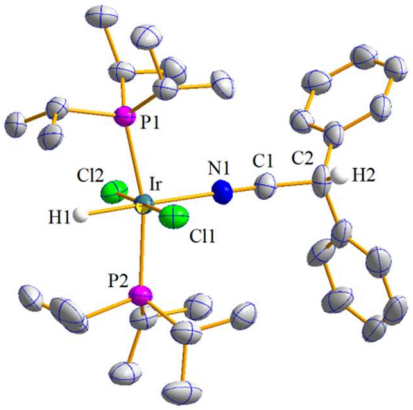

Figure 2.23: X-Ray structure of complex **51**. All hydrogen atoms (except H1 and H2) have been omitted for clarity

We propose that complex **51** is formed by hydrochlorination of intermediate catalytic species generated during the cleavage reaction. In particular, complex **51** could be formed from the intermediate complex **37** that was observed by NMR as major species. To probe this idea, the isolated complex **37** was dissolved in toluene and treated with 4 M HCl in dioxane. After 10 min at room temperature, the formation of complex **51** was confirmed by ^{1}H and ^{31}P NMR at complete conversion of the complex **37** (Scheme 2.54). Complex **51** was isolated in 61% yield. The formation of complex **51** from the acidic treatment of complex **37** as well as from the previous stoichiometric experiment (Scheme 2.53) further confirms participation of complex **37** in the catalytic cycle as resting state.

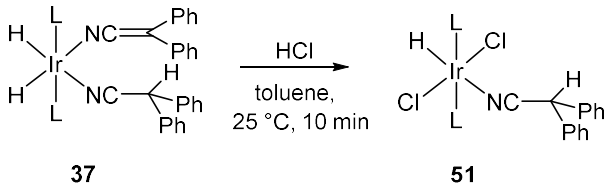

37 **51**

Scheme 2.54: Formation of complex **51** from acidic treatment of complex **37**

We suggest that complex **51** is a result of protonation of coordinated deprotonated diphenylacetonitrile and protonolysis of one of the Ir-H bonds by HCl in **37** (Scheme 2.55). The structure of complex **37** can be respresented by the two resonance structures **37** and **52**. The latter structure illustrates the carbanionic character of the α-carbon atom of the keteniminate ligand. Protonation of the keteniminate ligand at the nucleophilic α-carbon atom would give the cationic Ir(III) intermediate that after release of diphenylacetonitrile and coordination of chloride anion will yield the dihydride complex **53**.[102] Protonolysis of one of the Ir-H bonds in **53** with a second molecule of HCl will give final complex **51**.

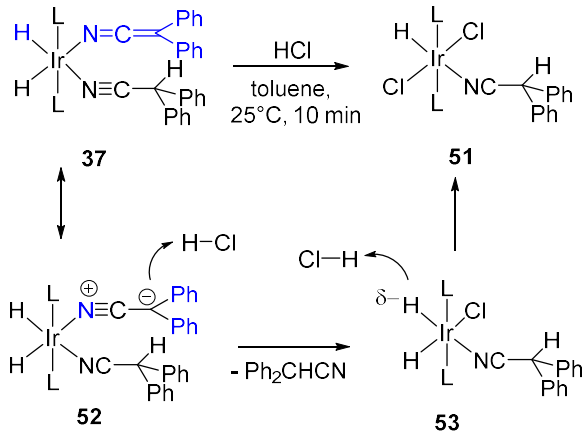

Scheme 2.55: Proposed mechanism of formation of complex **51** from complex **37**

Finally, we also looked at potential pathways for deactivation of the iridium catalyst. During our studies of the Ir-catalysed C-C bond cleavage of the dinitrile substrate **2**, formation of polyacrylonitrile oligomer was observed as side product (Section 2.2). This product is as a result of polymerisation of the transient acrylonitrile catalysed by $Ir(P^iPr_3)_2H_5$ (Scheme 2.56).[4]

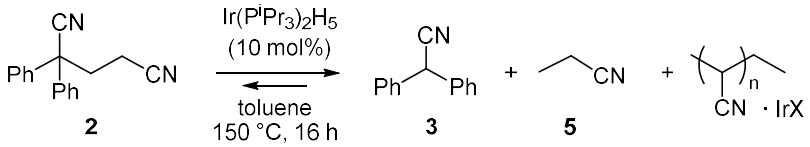

Scheme 2.56: Ir-catalysed reductive cleavage of C-C bond in dinitrile **2**

The ICP analysis of the isolated polyacrylonitrile revealed the presence of iridium in 15 w/w% that suggests the trapping of iridium catalyst by the polymer. The capture of iridium is one of the catalyst deactivation pathways that might explain the need of a high catalyst loading to achieve high yields of the cleavage products. However, the 15 w/w% of iridium captured by this polymer represents only the 20% of the total amount of iridium present in the reaction mixture. This fact suggests that the catalyst trapping is a minor route for catalyst decomposition and led us to hypothesise the existence of an additional pathway.

During our NMR monitoring experiments of the model reaction with dinitrile **2** at 150 °C, we observed the formation of phosphine iridium species that appear at 20 ppm (^{31}P NMR) as a broad singlet at late reaction times (Section 2.7, Figure 2.8). When the model

reaction stopped after 16 h and 25% of the starting amount of dinitrile **2** remained unreacted, the broad singlet at 20 ppm was observed as the only signal in the ^{31}P NMR spectrum. This may indicate that this signal belongs to a catalytically inactive complex or a product of catalyst decomposition. In view of this, we proposed that this decomposition product might be formed *via* P-C bond cleavage or cyclometallation in the phosphine ligand of the active catalyst. Indeed these two processes are common pathways for deactivation of homogeneous catalysts with phosphorous ligands.[103–105] To check this idea, we attempted the isolation of these phosphine iridium species by precipitation from the model reaction mixture after heating at 150 °C for 16 h. Unfortunately, no phosphine iridium species were isolated after several attempts.

In summary, a novel proposal for the mechanism of Ir-catalysed reductive cleavage of unstrained C-C bonds has been presented on the basis of experimental and computational evidences. As discussed in the introduction of this chapter, our mechanistic studies were based on the unique C-C bond cleavage reported by Murahashi.[2] In his article, Murahashi proposed a tentative mechanism that involved the C-H activation of dinitrile **2** by the iridium catalyst involving a C-bound intermediate complex (Scheme 2.2). Then, the subsequent C-C cleavage was proposed to occur *via* β-carbon elimination forming a C-bound olefin iridium complex that after alkene dissociation and reductive elimination formed diphenylacetonitrile **3**. In contrast to the proposed mechanism by Murahashi and to our first hypothesis, our experimental and computational evidences indicate that the C-C cleavage step does not occur through a classical β-carbon elimination but *via* a singular retro-Michael type reaction. Our studies also indicated that this transformation is driven by the irreversible consumption of the transient acrylonitrile. Thus, our investigations provide evidences regarding the feasibility of this unfavourable process and the nature of the second cleavage product, that remained unclear from Murahashi's work (Section 2.1).

2.11. Progress towards the development of a more general reductive C-C bond cleavage of dinitriles: sequential C-C cleavage and alkene hydrogenation reaction

Our mechanistic studies on reductive cleavage of C-C bonds of dinitriles evidence the reversibility of the process which is driven by the irreversible hydrogenation of the transient alkene. However, according to our results, the yield of the second cleavage product – propionitrile – is low, which is explained by the fact that there is no enough hydrogen in the system to allow full hydrogenation of the transient acrylonitrile. As previously discussed, iridium pentahydride catalyst can only supply 25 to 50 mol% of H_2 when 10 or 20 mol% of the catalyst is used, respectively (Section 2.2). Furthermore, other possible reason of low yield of propionitrile is the competing polymerisation of acrylonitrile.

To address the issue of low yields of propionitrile, we conducted the C-C cleavage of dinitriles in the presence of an added reductant, such as hydrogen (Scheme 2.57). The presence of higher concentration of reductant would facilitate the relative rate of hydrogenation of the intermediate acrylonitrile with respect to polymerisation and would help to increase the yield of propionitrile. Moreover, we believe that the increase of the relative rate of hydrogenation would increase the conversions of dinitrile **2** by displacing the equilibrium of the C-C cleavage step towards the products.

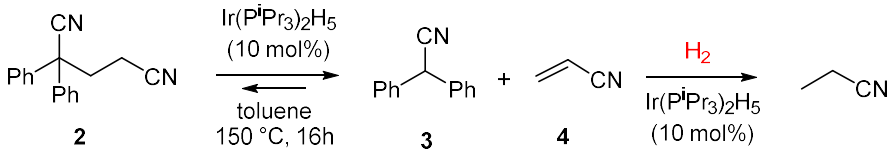

Scheme 2.57: Cleavage of C-C bonds with subsequent functionalization of the alkene

The sequential C-C cleavage and functionalisation of the alkene was inspired by recent reported examples on reductive cleavage of C-C σ bonds involving hydrogenolysis reactions, such as the cleavage of pincer-type substrates under hydrogen pressure[106,107] as discussed in the previous Chapter 1 (Section 1.4.2). In case of hydrogenolysis of hydrocarbons, only examples of unselective processes are reported which lead to mixtures of products (Chapter 1, Section 1.4.3).[108] However, selective hydrogenolysis of unstrained aliphatic C-C single bonds have not yet been investigated.

2.11.1. Ir-catalysed hydrogenolysis of C-C single bonds of dinitriles with H_2

Initially, we envisioned the hydrogenolysis of C-C bonds of 2,2-diphenylpentanedinitrile **2** using hydrogen as a reducing agent and $Ir(P^iPr_3)_2H_5$ complex as a catalyst to hydrogenate the transient acrylonitrile (Scheme 2.59).

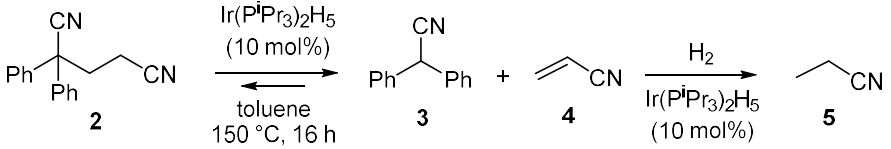

Scheme 2.59: Ir-catalysed hydrogenolysis of **2** with H_2

Thereby, substrate **2** was heated with $Ir(P^iPr_3)_2H_5$ (10 mol%) under H_2 (1 atm) in toluene at 150 °C for 16 h (Scheme 2.60). This reaction led to the formation of diphenylacetonitrile **3** and propionitrile **5** in 17 and 33% yield respectively at 90% conversion of **2**. In addition, a third product was formed which was identified as 2,2-diphenylethan-1-amine (**54**), according to GC, GC-MS and ^{1}H-NMR data.

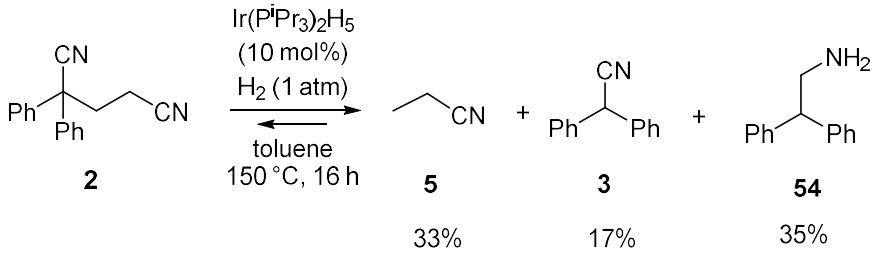

Scheme 2.60: Ir-catalysed C-C cleavage of 2,2-diphenylpentanedinitrile under hydrogen atmosphere

Formation of product **7** and low yield of nitrile **3** might suggest that the amine product **54** is the result of hydrogenation of the cyano group of the diphenylacetonitrile **3**. Indeed, iridium complexes have been demonstrated to mediate the reduction of nitriles to amines under H_2.[109] To test this idea, diphenylacetonitrile **3** was heated with $Ir(P^iPr_3)_2H_5$ (10 mol%) under the same reaction conditions. According to GC analysis, the reaction gave amine **54** in 93% yield at 95% conversion of **3** (Scheme 2.61), which is in agreement with our proposal.

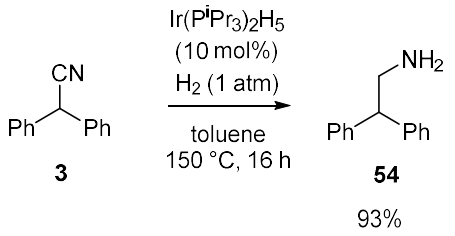

Scheme 2.61: Ir-catalysed hydrogenation of diphenylacetonitrile **3**

The Ir-catalysed hydrogenolysis of 2,2-diphenylpentanedinitrile **2** led to higher conversions of the model substrate and slightly higher yield of propionitrile compared to the catalytic model reaction conducted in the absence of hydrogen atmosphere. Therefore, these results further evidences that the consumption of the transient alkene facilitates the C-C bond cleavage. However, to address the issue with the side reactions that occurred with nitrile **3** under hydrogen atmosphere, we turned to hydrogenolysis of unstrained C-C single bonds in **2** using alternative reducing agents.

2.11.2. Ir-catalysed transfer hydrogenolysis of unstrained aliphatic C-C bonds of dinitriles

As an alternative methodology, we envisioned a transfer C-C bond hydrogenolysis using a hydrogen-transfer agent as an alternative hydrogen source. This transfer hydrogenation might help to avoid further hydrogenation reactions as it typically occurs under mild conditions and does not require a large excess of reducing agent. In this regard, secondary alcohols are a common source of hydrogen in transfer hydrogenations.[110,111]

Based on this, our devised strategy involves the reductive cleavage of C-C bonds using secondary alcohols as a source of hydrogen. The selection of this hydrogen donor was based on a reported example of the dehydrogenation of saturated secondary alcohols to the corresponding ketones catalysed by $Ir(P^iPr_3)_2H_5$ in the absence of a hydrogen acceptor (Scheme 2.62).[61]

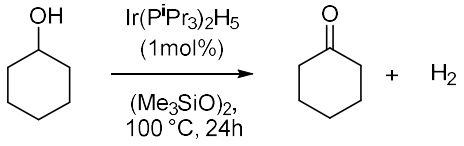

Scheme 2.62: Ir-catalysed acceptorless dehydrogenation of cyclohexanol

This precedent inspired us to probe Ir-catalysed transfer hydrogenolysis of dinitrile **2** in the presence of cyclohexanol (Scheme 2.63). The $Ir(P^iPr_3)_2H_5$ catalyst will mediate the alkene deinsertion from dinitrile **2** and in parallel, the dehydrogenation of cyclohexanol. The hydrogen produced from the latter reaction will be involved in the hydrogenation of acrylonitrile **4**.

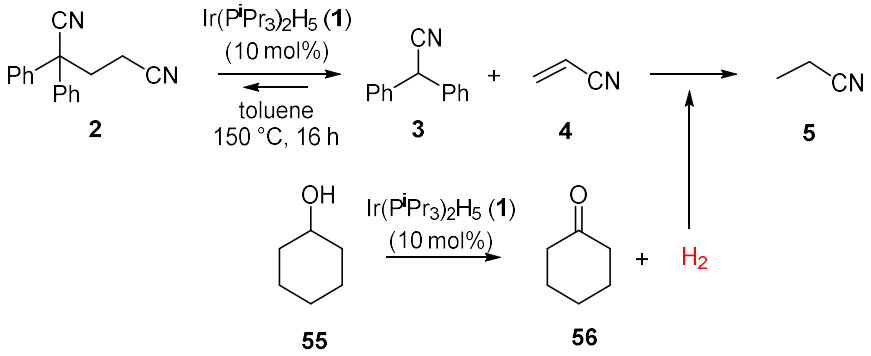

Scheme 2.63: Strategy for Ir-catalysed transfer C-C bond hydrogenolysis of dinitrile **2**

With this designed experiment in mind, 2,2-diphenylpentanedinitrile **2** was allowed to react with 2 equivalents of cyclohexanol **55** and $Ir(P^iPr_3)_2H_5$ (10 mol%) in toluene at 150 °C for 16 h (Scheme 2.64). For our delight, this reaction led to diphenylacetonitrile **3** and propionitrile **5** in 95% and 74% yield, respectively, at full conversion of the starting dinitrile **2**.

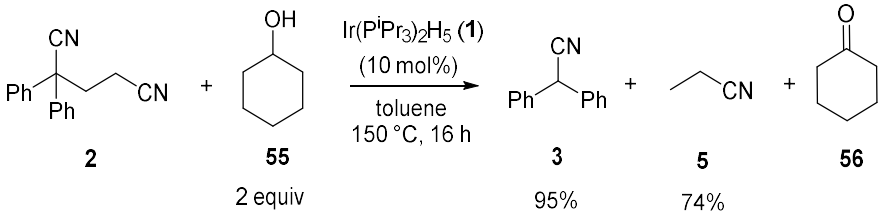

Scheme 2.64: Ir-catalysed transfer C-C bond hydrogenolysis of dinitrile **2** with cyclohexanol

This experiment showed that our transfer hydrogenolysis reaction leads to higher conversions and yields of both products compared to the original procedure studied by Murahashi (Section 2.1). To the best of our knowledge, this is the first example of selective transfer hydrogenolysis of unstrained aliphatic C-C bonds.

2.12. Conclusions

The mechanism of the Ir-catalysed reductive cleavage of unstrained aliphatic C-C bonds of dinitriles has been studied. We propose that this process occurs through directed C-H activation followed by alkene deinsertion *via* a retro-Michael type reaction as the key C-C breaking steps (Scheme 2.51). The catalytic cycle involves the formation of C-H activated N,N-coordinated dinitrile complex **43** which leads to Ir species with N-bound deprotonated diphenylacetonitrile and N-bound acrylonitrile, according to preliminary DFT calculations. Our proposed mechanism explains the need for two directing groups in the substrate to promote the C-C cleavage step *via* alkene deinsertion. This was confirmed by examination of the role of chelating groups where substrates bearing only one cyano group appeared to be unreactive.

We showed that the alkene deinsertion is a reversible process which is driven by the irreversible alkene hydrogenation and polymerisation. Thus, the irreversible consumption of the alkene enables the thermodynamically unfavourable alkene deinsertion.

Relevant monitoring experiments by NMR permitted the detection and the successive isolation of the catalytically active intermediate complex **37**. This complex was found to catalyse both the reductive C-C cleavage in dinitrile **2** and its reverse C-C forming hydroalkylation with product yields comparable to those of the original pentahydride catalyst. Subsequent experiments with complex **37** and acrylonitrile led to dinitrile **2**, further evidencing the reversibility of the C-C cleavage process. Remarkably, the complex **37** constitutes the first example of a well-defined iridium keteniminate complex.

Our investigation provides novel experimental and computational evidences for the mechanistic understanding of this unusual transformation *via* alkene deinsertion. Furthermore, it resolves the uncertainties of Murahashi's work. Specifically, our studies reveal the nature of the second cleavage product (propionitrile), the driving force of the process and the role of the directing groups.

In addition, we evaluated the feasibility of selective, catalytic reductive cleavage of non-strained aliphatic C-C bonds using hydrogen and alcohols as reductants. These studies allowed us to showcase the first example of selective transfer hydrogenolysis of

unstrained C-C single bonds with excellent yields of the cleaved products using cyclohexanol as a transfer hydrogenation agent.

Importantly, our proposed catalytic cycle is not only valid for the C-C bond cleavage but also for the corresponding reverse C-C bond formation according to the principle of microscopic reversibility. In particular, the pentahydride iridium catalyst as well as complex **37** were found to be excellent catalysts for Michael-type hydroalkylation reactions under mild conditions. This finding allowed us to initiate a second research project on catalytic hydroalkylation reactions. As described in the next chapter, we have developed a new method for the alkylation of cyclic α,β-unsaturated ketones with non-activated aryl alkyl nitriles catalysed by $Ir(P^iPr_3)_2H_5$.

2.13. Experimental section

2.13.1. General Experimental Information

Equipment and methods

All air-sensitive reactions were set up in an inert atmosphere of argon in Innovative Technologies glovebox and conducted using standard Schlenk techniques under argon. All glassware was heated up in an oven at 120 °C and cooled under vacuum prior to use.

Nuclear magnetic resonance (NMR) spectra were recorded on Bruker AVIII-HD 500 MHz and Bruker AVI 400 MHz spectrometers. Chemical shifts are reported in ppm relative to a peak of a residual solvent (CDCl3, δ 7.26 ppm for ^{1}H and 77 ppm for ^{13}C. d_8-toluene δ 2.11 ppm for ^{1}H and 21.3 ppm for ^{13}C. d_8-THF 1.79 ppm for ^{1}H and 26.1 ppm for ^{13}C). The splitting patterns are designated as follows: s (singlet), d (doublet), t (triplet), q (quartet), m (multiplet), dd (doublet of doublets), dt (doublet of triplets), br. s (broad singlet).

Gas chromatography analyses were obtained on an Agilent 7890 Gas Chromatograph equipped with an HP-5 30 m x 0.32 mm ID x 0.25 μm capillary column and an FID detector. The following GC oven temperature program was used: 50 °C hold for 5 min, ramp 5 °C/min to a final temperature of 80 °C, hold for 5 min, ramp 40 °C/min to a final temperature of 250 °C and hold for 10 min. The injector temperature was held at 250 °C.

GC-MS analyses were obtained on an Agilent 7820A Gas Chromatograph equipped with an HP-5 30 m x 0.25 mm x 0.25 μm capillary column. The GC was directly interfaced to an Agilent 5975 mass selective detector (EI). The following GC oven temperature program was used 50 °C hold for 5 min, ramp 5 °C/min to a final temperature of 80 °C, hold for 5 min, ramp 40 °C/min to a final temperature of 250 °C and hold for 15 min.

IR spectra were acquired on a Perkin Elmer FT-IR Spectrum 100 spectrometer and on a Bruker alpha FT-IR platinum ATR spectrometer.

Analytical thin-layer chromatography (TLC) was performed on Whatman F254 precoated silica gel plates (250 μm thickness) visualizing with UV light (254 nm) and/or submersion

in aqueous potassium permanganate solution followed by brief heating. Column chromatography was performed using Whatman Silica Gel 60 Å (230-400 mesh).

Solvents and reagents

Unless otherwise noted, all chemicals were obtained from commercial suppliers and used without further purification. Iridium (III) chloride hydrate ($IrCl_3 \cdot x\ H_2O$) was purchased from Pressure Chemicals, bis(1,5-cyclooctadiene)diiridium (I) dichloride ($[Ir(cod)Cl]_2$) and chlorobis(cyclooctene)iridium(I)dimer ($[Ir(coe)_2Cl]_2$) were purchased from Aldrich. $Ir(P^iPr_3)_2H_5$, ^{iPr}PCPIrHCl and ^{Ad}PCPIrHCl were prepared according to the literature procedures (Section 2.13.2). All reactions with iridium complexes were conducted under dry conditions and under argon atmosphere as these complexes are air-sensitive. Syntheses of substrates used are described below. All solvents used were thoroughly dried over the appropriate drying agents and made free of oxygen by distillation under argon; THF, diethyl ether, toluene, and hexane were distilled using sodium ketyl; Methanol and dichloromethane was distilled over CaH_2. All distilled solvents were stored in either Sure-Store flasks under argon or in the glovebox. ^{i}PrOH and deuterated NMR solvents (used for air-sensitive compounds) were degassed by freeze-pump-thaw technique (3 cycles) and dried over molecular sieves. Acrylonitrile was purified by passing through basic aluminium oxide to remove the stabilizer and used immediately in a catalytic reaction. Cyclohexanol was degassed *via* freeze-pump-thaw and kept under argon atmosphere prior to use.

2.13.2. Syntheses of Iridium complexes

2.13.2.1. Synthesis of $Ir(P^iPr_3)_2H_5$ (1)

Prepared according to literature procedure.[112]

Synthetic route:

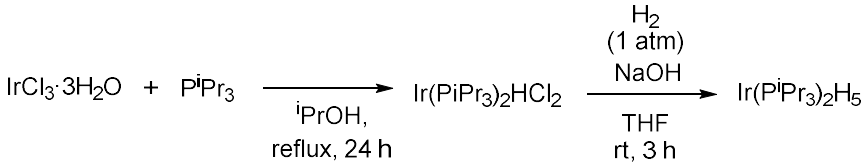

Synthesis of $Ir(P^iPr_3)_2HCl_2$

To an argon filled 50 ml Schlenk bomb containing $IrCl_3 \cdot 3H_2O$ (0.25 g, 0.7 mmol) and triisopropylphosphine (465 µl, 2.12 mmol) was added ^{i}PrOH (1.6 ml). The reaction mixture was refluxed under argon atmosphere for 24 h. The reaction mixture was allowed to return to room temperature and the purple solids were collected by filtration using a cannula. The product was washed with ^{i}PrOH (3x1 ml) and the pure complex was dried under vacuum and obtained as a purple solid (0.28 g) in 68 % yield. **^{1}H NMR** (500 MHz, $CDCl_3$) δ 3.33- 2.86 (m, 6H, CH), 1.35 (dd, J = 13.9, 7.1 Hz, 36H, CH_3), -49.13 (t, J = 11.4 Hz, 1H, hydride). **^{31}P{^{1}H} NMR** (202 MHz, $CDCl_3$) δ 31.9 (s, P^iPr_3).

NMR data in accordance with the literature data.[112]

Synthesis of $Ir(P^iPr_3)_2H_5$

$Ir(P^iPr_3)_2HCl_2$ (0.26 g, 0.45 mmol) and NaOH (1.90 g, 47.5 mmol) were mixed in THF (21 ml). Hydrogen (1 atm) was bubbled through the reaction mixture under vigorous stirring at room temperature for 3 h. Then the solvent was removed under vacuum. The yellow solid was washed with degassed water and dried under vacuum overnight. The desired complex was obtained as a yellowish solid (0.191 g) in 82% yield. **^{1}H NMR** (400 MHz, C_6D_6) δ 1.93 – 1.57 (m, 6H, CH), 1.12 (dd, J = 13.6, 6.9 Hz, 36H, CH_3), -10.87 (t, J = 12.2 Hz, 5H, hydrides). **^{31}P{^{1}H} NMR** (400 MHz, C_6D_6) δ 45.4 (s, P^iPr_3).

NMR data in accordance with the literature data.[112]

2.13.2.2. Synthesis of ^{iPr}PCPIrHCl

Synthetic route:

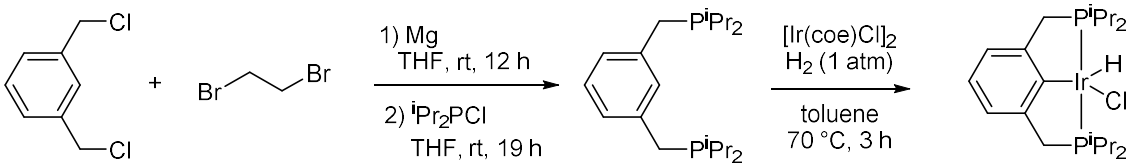

Synthesis of 1,3-Bis[(diisopropylphosphino)methyl]benzene

Prepared according to literature procedure.[113]

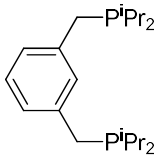

An argon filled 500 ml three-neck flask equipped with an addition funnel and condenser was charged with Mg turnings (60.8 mmol, 1.49 g), THF (21 ml) and a magnetic stir bar. To this mixture was added 1,2-dibromoethane (2.32 mmol, 0.2 ml) at room temperature. The mixture was gently heated until ethylene evolution was observed. Then, *m*-dichloro-xylene in THF (190 ml) was added dropwise and 16.5 ml of THF was added. The reaction mixture was stirred for 12 h at room temperature. Filtration to remove excess Mg followed by titration of this solution with n-butanol and menthol using 1,10-phenanthroline as an indicator revealed formation of the desired 1,3-bis[(chloromagnesio)methyl]benzene product in 92% yield. The resulting Grignard reagent (14.4 mmol, 4.5 g) was added at 0 °C to a solution of $^{i}Pr_2PCl$ (28.8 mmol, 4.50 g) in THF (91.5 ml). At the end of the addition, the mixture was allowed to warm to room temperature and stirred for additional 19 h. The solvent was removed under vacuum and the crude product was extracted with dry ether (3 x 100 ml). The solution was filtrated through Celite to remove $MgCl_2$. The crude product was purified by vacuum distillation, bp: 105 °C ($2 \cdot 10^{-3}$ mm Hg). The desired product was obtained as an orange oil (3.44 g) in 71% yield. **^{1}H NMR** (250 MHz, $CDCl_3$) δ 7.23 – 6.93 (m, 4H, Aromatic H), 1.77 – 1.53 (m, 4H, CH), 1.08 – 0.88 (m, 24H, CH_3). **^{31}P{^{1}H} NMR** (101 MHz, $CDCl_3$) δ 11.1 (s, P^iPr_2).

NMR data in accordance with the literature data.[113]

Synthesis of ^{iPr}PCPIrHCl

Prepared according to literature procedure.[114]

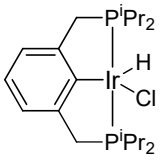

Chlorobis(cyclooctene)iridium(I)dimer (0.44 mmol, 0.40 g) was added to a solution of 1,3-Bis[(di-isopropylphosphino)methyl]-benzene (0.93 mmol, 0.31 g) in tolunene (18.5 ml). The mixture was stirred at 70 °C under H_2 atmosphere (1 atm) for 3 h. Solvent was removed under vaccum and the resulting solid was washed with hexane (2 x 5 ml). The desired product was obtained after recrystallization in hexane as a dark red solid (52 mg) in 21% yield. **^{1}H NMR** (500 MHz, $CDCl_3$) δ 6.92 (d, *J* = 7.4 Hz, 2H, Aromatic H), 6.73 (dd, *J* = 29.2, 21.7 Hz, 1H, Aromatic H), 3.18 (ddt, *J* = 47.8, 17.3, 4.1 Hz, 4H, bridging- CH_2), 2.95 – 2.80 (m, 2H, 2CH), 2.47 – 2.32 (m, 2H, 2CH), 1.34 – 1.23 (m, 24H, 8CH_3). **^{31}P{^{1}H} NMR** (500 MHz, $CDCl_3$) δ 55.2 (P^iPr_2).

NMR data in accordance with the literature data.[114]

2.13.2.3. Synthesis of ^{Ad}PCPIrHCl

Prepared by Claudia Gatti according to literature procedure.[32]

Synthetic route:

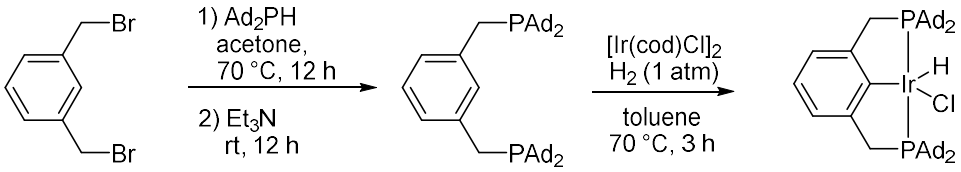

Synthesis of 1,3-Bis[(di-adamantylphosphino)methyl]-benzene (^{Ad}PCP-H)

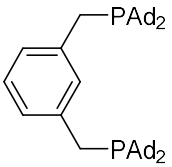

Under argon atmosphere, a mixture of di-1-adamantylphosphine (1.5 g, 5.02 mmol) and 1,3-dibromoxylene (0.65 g, 2.48 mmol) in degassed acetone (60 mL) was heated to reflux for 24 h. The resulting white suspension was cooled to room temperature, the solvent was removed via cannula and the white precipitate (phosphonium salt) was dried under vacuum. Then, benzene (60 mL) and Et_3N (0.54 g, 5.37 mmol) were added and the mixture was stirred

overnight. The yellowish solution was then separated by cannula filtration to remove the $Et_3N{\cdot}HBr$ salt. The mother liquor was evaporated to dryness to obtain a light yellow solid. The solid (770 mg) was dissolved in chloroform (15 mL), then methanol (40 mL) was added and the resulting solution cooled in an ice-bath to precipitate the phosphine out. The supernatant solution was then removed via cannulation and the remaining solid was washed with methanol to yield the product as a white crystalline solid (521 mg) in 67% yield. **^{1}H NMR** (500 MHz, d_8-Toluene): δ 7.74 (s, 1H, ipsoAromatic H), 7.34 (d, *J* =7.6 Hz, 2H, Aromatic H), 7.22 (t, *J* =7.5 Hz, 1H, Aromatic H), 2.85 (d, *J* =2.4 Hz, 4H, bridging-CH_2), 1.95 (s, 24H, 12Ad-CH_2), 1.88 (s, 12H, 12Ad-CH), 1.69 (s, 24H, 12Ad-CH_2). **^{31}P{^{1}H} NMR** (500 MHz, d_8-Toluene): δ 28.5 (s, PAd_2).

Synthesis of ^{Ad}PCPIrHCl

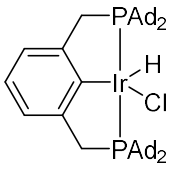

A mixture of ^{Ad}PCP-H (209 mg, 0.296 mmol) and $[Ir(cod)Cl]_2$ (99 mg, 0.15 mmol) in toluene (8.5 mL) was heated at 70 °C for 3 h under hydrogen atmosphere (1 atm). After cooling the resulting dark red solution to room temperature, the solvent was removed under vacuum to yield a dark brown-red solid (280 mg) in 99% yield. **^{1}H NMR** (500 MHz, C_6D_6): δ 7.01-7.01 (m, 3H, Aromatic H), 3.29 (d, J=17.5 Hz, 2H, CH_2), 3.12 (d, J =17.4 Hz, 2H, CH_2), 2.16-2.57 (m, 24H, Ad-CH_2), 1.81-1.87 (m, 12H, Ad-CH), 1.51-1.69 (m, 24H, Ad-CH_2), -43.15 (t, J =11.95 Hz, 1H, Ir-H). **^{31}P{^{1}H} NMR** (500 MHz, C_6D_6): δ 57.4 (d, J =25.3 Hz).

NMR data in accordance with the literature data. [32]

2.13.3. Syntheses of substrates

2,2-Diphenylpentanedinitrile (2)

Prepared according to the literature procedure.[115]

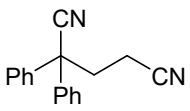

In an argon filled 100 ml round bottom flask equipped with a condenser, diphenylacetonitrile (5.00 g, 25.9 mmol) was dissolved in ^{t}BuOH (13 ml). KOH in MeOH 30% solution (0.5 ml, 1.3 mmol of KOH) was

added and the mixture was stirred for 20 min. Then, acrylonitrile (2.06 g, 38.8 mmol) was added dropwise and reaction mixture was stirred at 50 °C for 2.5 h. Water (20 ml) was poured into reaction mixture and the product precipitated out. The solid was purified by recrystallization from warm ethanol (3 ml) to give the pure product in 79% yield as a white solid (5.04 g). **^{1}H NMR** (400 MHz, $CDCl_3$) δ 7.49 – 7.30 (m, 10H, Aromatic H), 2.90 – 2.73 (m, 2H, $C_{quaternary}$-C**H$_2$**), 2.54 – 2.37 (m, 2H, C**H$_2$**-CN). **^{13}C{^{1}H} NMR** (101 MHz, $CDCl_3$) δ 138.1 (C), 129.3 (CH), 128.7 (CH), 126.6 (CH), 120.7 (CH), 118.0 (CH), 50.9 (CH), 35.4 (CH_2), 14.1 (CH_2). **HRMS** (CI^+) m/z 264.1507 $(M+NH_4)^+$ (264.1495 calcd for $C_{17}H_{18}N_2$ $(M+NH_4)^+$). **IR** 3053, 2960, 2944, 2252, 2236, 1491, 1447, 754, 699 cm $^{-1}$.

4,4,4-Triphenylbutanenitrile (7)

Prepared according to an adapted literature procedure, following the synthetic route:[38]

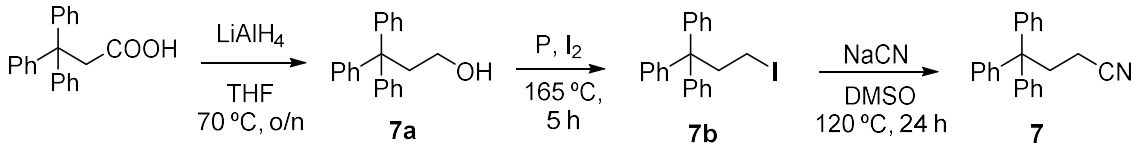

- **Synthesis of 3,3,3-triphenylpropan-1-ol (7a)**

Prepared according to an adapted literature procedure.[39]

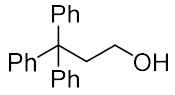

$LiAlH_4$ (614.9 mg, 16.20 mmol) was dissolved in THF (16.1 ml) and the solution was cooled down to 0 °C. A solution of triphenylpropionic acid (1.99 g, 6.90 mmol) in THF (14.6 ml) was added dropwise to the $LiAlH_4$ solution. After 5 h at room temperature, the reaction mixture was heated at 70 °C overnight. The reaction mixture was quenched with water (15 ml) and with 2 M NaOH aqueous solution (10 ml). Then, the reaction mixture was filtrated, extracted with Et_2O (3 x 10 ml) and the combined organic layers were washed with a saturated aqueous solution of $NaHCO_3$ (8 ml), H_2O (8 ml) and brine (8 ml). The organic layer was dried over Na_2SO_4 and the solvent was removed under vacuum. Product **7a** (1.39 g) was obtained as a white solid in 73% yield and was used in the next step without purification. **^{1}H NMR** (500 MHz, $CDCl_3$) δ 7.42 – 7.10 (m, 15H, Aromatic H), 3.52 (s, 2H, $C_{quaternary}$-C**H$_2$**), 3.05 – 2.86 (m, 2H, C**H$_2$**-OH).

- **Synthesis of 3-iodo-1,1,1-triphenylpropane (7b)**

Prepared according to literature procedure.[40]

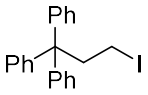

A 50 ml Schlenk flask equipped with a condenser and stir bar was charged with 3,3,3-triphenylpropan-1-ol (1.21 g, 4.19 mmol), red phosphorous (42.4 mg, 1.26 mmol) and iodine (0.62 g, 4.2 mmol). The reaction mixture was then heated at 165 °C for 5 h, cooled down and diethyl ether (100 ml) was added. The mixture was then washed with water (60 ml) and 5% NaOH aqueous solution (50 ml). The crude product was extracted with diethyl ether (3x 100 ml). The combined organic layers were dried over $MgSO_4$. After removal of solvent under vacuum product **7b** was obtained as a white solid (1.44 g) in 86% yield. **^{1}H NMR** (500 MHz, $CDCl_3$) δ 7.53 – 7.11 (m, 15H, Aromatic H), 3.39 – 3.12 (m, 2H, $C_{quaternary}$-C**H$_2$**), 3.01 – 2.79 (m, 2H, C**H$_2$**-I).

- **Synthesis of 4,4,4-triphenylbutanenitrile (7)**

Prepared according to an adapted literature procedure.[41]

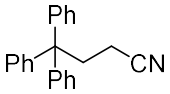

In an argon filled 25 ml two neck round bottom flask, 3-iodo-1,1,1-triphenylpropane (0.85 g, 2.1 mmol) and NaCN (0.18 g, 3.44 mmol) were dissolved in DMSO (10 ml). The reaction mixture was heated at 120 °C for 24 h, then cooled down and treated with water (15 ml). The crude product was extracted with diethyl ether (4 x 16 ml). The combined organic layers were treated with 6 M aqueous HCl (50 ml), washed with brine and dried over $MgSO_4$, and the solvent was removed under vacuum. The crude product was purified by recrystallization in ethanol to give product **7** (0.19 g) in 30% yield. **^{1}H NMR** (500 MHz, $CDCl_3$) δ 7.38 – 7.19 (m, 15H, Aromatic H), 3.02 (dd, J = 9.4, 7.2 Hz, 2H, $C_{quaternary}$-C**H$_2$**), 2.11 (dd, J = 9.1, 7.4 Hz, 2H, C**H$_2$**-CN). **^{13}C{^{1}H} NMR** (126 MHz, $CDCl_3$) δ 145.3 (C), 130.2 (CH), 128.7 (CH), 128.3 (CH), 127.6 (CH), 126.5 (CH), 119.9 (CN), 56.0 (C), 36.0 (CH_2), 14.1 (CH_2). **Elemental Analysis** Calcd for ($C_{22}H_{19}N$): C, 88.85; H, 6.44; N, 4.71; Found C, 88.44; H, 6.46; N, 4.48. **HRMS** (CI^+) m/z 315.1856 $(M+NH_4)^+$ (315.1856 calcd for $C_{22}H_{19}N$ $(M+NH_4)^+$). **IR** 3053, 3033, 2959, 2248, 1490, 1445, 653 cm $^{-1}$.

2,2,4-Triphenylbutanenitrile (8)

Prepared according to literature procedure.[42]

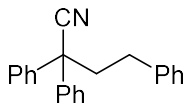

In an argon filled 100 ml Schlenk flask, potassium (0.680 g, 17.4 mmol) was dissolved in ^{t}BuOH (25.6 ml). To the resulting clear solution, diphenylacetonitrile (3.26 g, 16.8 mmol) was added and reaction mixture turned yellow. Then, 2-phenyl bromoethane (2.30 ml, 16.8 mmol) was added and the mixture was stirred at room temperature for 24 h. The reaction mixture was then neutralized with 0.7 M H_2SO_4 (15 ml) and after addition of water (25 ml) a white solid precipitated out. The solid was recrystallized from methanol (2 ml) to give the desired product **8** in 49% yield (2.45 g). **^{1}H NMR** (250 MHz, $CDCl_3$) δ 7.53 – 7.09 (m, 15H, Aromatic H), 2.91 – 2.55 (m, 4H, $2CH_2$). **^{13}C{^{1}H} NMR** (101 MHz, $CDCl_3$) δ 140.6 (C), 139.9 (C), 128.9 (CH), 128.6 (CH), 128.3 (CH), 127.9 (CH), 126.8 (CH), 126.3 (CH), 122.2 (CN), 51.7 (CH), 41.7 (CH_2), 32.0 (CH_2). **HRMS** (CI^+) m/z 315.1863 $(M+NH_4)^+$ (315.1856 calcd for $C_{22}H_{19}N$ $(M+NH_4)^+$). **IR** 3058, 3025, 3001, 2958, 2935, 2864, 2235, 1447, 752, 695 cm $^{-1}$.

5-Oxo-4,4-diphenylpentanenitrile (9)

Prepared according to literature procedure.[116]

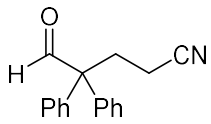

2,2-diphenylacetaldehyde (2.75 g, 14.0 mmol,) and acrylonitrile (0.901 g, 16.9 mmol) were dissolved in dioxane (31 ml) in a 50 ml two-neck round bottom flask equipped with a condenser and stir bar. DBU (2.5 g, 16.4 mmol) was added dropwise by a syringe at room temperature. The reaction was heated at 120 °C for 42 h and cooled down. After evaporation of solvent in vacuum, the resulting crude product was purified by flash column chromatography (silica gel, eluent: hexane:EtOAc, 95:5) to give **9** was as a white solid (2.69 g) in 77% yield. **^{1}H NMR** (500 MHz, $CDCl_3$) δ 9.79 (s, 1H, CHO), 7.50 – 7.21 (m, 10H, Aromatic H), 2.76 – 2.64 (m, 2H, $C_{quaternary}$-**CH_2**), 2.14 – 2.05 (m, 2H, **CH_2**-CN). **^{13}C{^{1}H} NMR** (101 MHz, $CDCl_3$) δ 197.0 (CO), 138.3 (C), 129.3 (CH), 128.62 (CH), 119.4 (CN), 62.7 (C), 30.1 (CH_2), 13.4 (CH_2). **HRMS** (CI^+) m/z 267.1501 $(M+NH_4)^+$ (267.1492 calcd for $C_{17}H_{15}NO$

$(M+NH_4)^+$). **IR** 3060, 3025, 3002, 2833, 2728, 2252, 1710, 1693, 1491, 1443, 760 cm^{-1}.

5-Oxo-4,4-diphenylhexanenitrile (10)

Prepared according to an adapted literature procedure.[56]

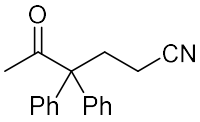

In a 10 ml round bottom flask, 1,1-diphenylacetone (2.02 g, 9.6 mmol) was dissolved in tert-butanol (3.2 ml) and then, 40% benzyltrimethylammonium hydroxide aqueous solution (55 µl, 4.1 mmol) was added. After stirring for 30 min, acrylonitrile (0.55 g, 10.5 mmol) was added and the mixture was stirred at 60 °C for 48 h. The reaction mixture was then cooled down and treated with H_2SO_4, which led to precipitation of a white solid. The solid was washed with cold ^{i}PrOH and dried to give product **10** as a white solid (1.36 g) in 54% yield. **^{1}H NMR** (500 MHz, $CDCl_3$) δ 7.41 (m, 6H, Aromatic H), 7.27 (m, 4H, Aromatic H), 2.67 (m, 2H, $C_{quaternary}$-C**H₂**), 2.04 (s, 3H, CH_3), 2.03 (m, 2H, CH_2-CN). **^{13}C{^{1}H} NMR** (126 MHz, $CDCl_3$) δ 207.3 (CO), 139.6 (C), 128.9 (CH), 127.9 (CH), 119.7 (CN), 65.5 (C), 34.0 (CH_2), 27.6 (CH_3), 13.7 (CH_2). **HRMS** (ES^+) m/z 286.1204 $(M+Na)^+$ (286.1208 calcd for $C_{18}H_{21}N_2ONa$ $(M+Na)^+$). **IR** 3060, 3035, 3003, 2961, 2937, 2251, 1696, 703 cm^{-1}.

Methyl 4-cyano-2,2-diphenylbutanoate (11)

Prepared according to an adapted literature procedure.[57]

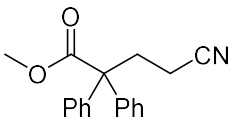

In a 100 ml Schlenk flask under argon atmosphere, sodium hydride (113.2 mg in 60 % suspension in oil, 5.4 mmol) was dissolved in dry THF (52 ml) and methyl 2,2-diphenylacetate (1.01 g, 4.5 mmol) was added dropwise. The mixture was stirred at 0 °C for 30 min. Then acrylonitrle (0.28 g, 5.3 mmol) was added dropwise at 0 °C. The mixture was warmed up to room temperature and stirred for 16 h, then treated with saturated solution of NH_4Cl (17 ml) and extracted with dichloromethane (3 x 11 ml). The combined organic layers were dried over $MgSO_4$. The crude product was purified by column chromatography (eluent: hexane:EtOAc, 4:1)

to give product **11** (0.58 g) as a white solid in 47% yield. **^{1}H NMR** (500 MHz, $CDCl_3$) δ 7.33 (m, 6H), 7.22 (m, 4H), 3.72 (s, 3H), 2.77 (m, 2H), 2.14 (m, 2H). **^{13}C{^{1}H} NMR** (101 MHz, $CDCl_3$) δ 173.6 (CO), 141.1 (C), 128.5 (CH), 128.4 (CH), 127.6 (CH), 119.6 (CH), 59.5 (C), 52.7 (CH_3), 34.5 (CH_2), 13.9 (CH_2). **Elemental Analysis** Calcd for ($C_{18}H_{17}NO_2$): C, 77.40; H, 6.13; N, 5.01; Found C, 77.15; H, 6.10; N, 5.05. **HRMS** (CI^+) m/z 297.1608 $(M+NH_4)^+$ (297.1598 calcd for $C_{18}H_{21}N_2O_2$ $(M+NH_4)^+$). **IR** 3060, 3037, 2956, 2253, 1715, 1429, 1244, 1224, 703 cm^{-1}.

5-(Methoxyimino)-4,4-diphenylhexanenitrile (12)

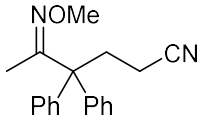

In an argon filled 50 ml three neck round bottom flask equipped with a condenser and magnetic stir bar, methoxyamine hydrochloride (0.75 g, 8.98 mmol) was dissolved in anhydrous pyridine (5.8 ml). Then, 5-oxo-4,4-diphenylhexanenitrile **10** (1.79 g, 6.81 mmol) was added as a solid under stirring. The reaction mixture was refluxed for 70 h, treated with water (10 ml) and extracted with diethyl ether (3 x 10 ml). The combined organic layers were washed with brine (15 ml) and dried over $MgSO_4$. The solvent was removed under vacuum and crude product was purified by column chromatography (eluent: hexane:EtOAc, 10:1). Product **12** was obtained (1.06 g) as a yellowish solid in 53% yield. **^{1}H NMR** (500 MHz, $CDCl_3$) δ 7.40-7.37 (m, 4H, Aromatic H), 7.34-7.31 (m, 2H, Aromatic H), 7.26-7.23 (m, 4H, Aromatic H), 3.97 (s, 3H, OCH_3), 2.78 (m, 2H, $C_{quaternary}$-C**H$_2$**), 2.10 (m, 2H, C**H$_2$**-CN), 1.62 (s, 3H, CH_3). **^{13}C{^{1}H} NMR** (101 MHz, $CDCl_3$) δ 158.0 (C=N), 141.75(C), 128.8 (CH), 128.5 (CH), 127.2 (CH), 120.5 (CN), 61.9 (OCH_3), 57.9 (C), 35.7 (CH_2), 14.5 (CH_3), 14.1 (CH_2). **Elemental Analysis** Calcd for ($C_{19}H_{20}N_2O$): C, 78.05; H, 6.89; N, 9.58; Found C, 78.03; H, 6.85; N, 9.34. **HRMS** (CI^+) m/z 293.1653 $(M+NH_4)^+$ (293.1648 calcd for $C_{19}H_{25}N_3O$ $(M+NH_4)^+$). **IR** 3078, 3025, 3002, 2967, 2937, 2900, 2247, 1598, 1442, 702 cm^{-1}.

4-Hydroxy-4,4-diphenylbutanenitrile (13)

Synthetic route:

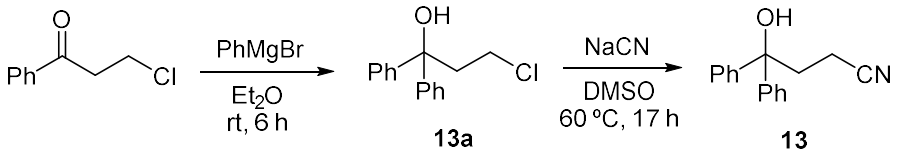

- **3-Chloro-1,1-diphenylpropan-1-ol (13a)**

Prepared according to literature procedure.[117]

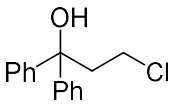

In an argon-filled 250ml Schlenk flask, 3-chloropropiophenone (3.01 g, 17.9 mmol) was dissolved in diethyl ether (30 ml). The reaction mixture was cooled down to -10 °C and then phenylmagnesium bromide solution in Et_2O (58.5 mmol, 43 ml) was added dropwise over a period of 35 min. The reaction mixture was stirred at -10 °C for 40 min, warmed up to room temperature and stirred for 6 h. Then to the reaction mixture was slowly added cold saturated solution of NH_4Cl (20 ml). The aqueous layer was separated and extracted with dichloromethane (2 x 15ml). The combined organic layers were treated with saturated solution of $NaHCO_3$ (10 ml) and dried over Na_2SO_4. After filtration and concentration in vacuum, the crude product was purified by column chromatography (silica gel, eluent: petroleum ether: EtOAc, 25:1) to give **13a** as a white solid (2.08 g) in 47% yield. **^{1}H NMR** (500 MHz, $CDCl_3$) δ 7.41 (d, *J*= 7.6 Hz, 4H, Aromatic H), 7.36 (t, *J*= 7.7, 15.3 Hz, 4H, Aromatic H), 7.28 (t, *J*= 6.6, 14.3 Hz, 2H, Aromatic H), 3.52 (m, 2H, $C_{quaternary}$-C**H$_2$**), 2.82 (m, 2H, C**H$_2$**-Cl), 2.25 (s, 1H, OH). **^{13}C{^{1}H} NMR** (101 MHz, $CDCl_3$) δ 145.8 (C), 128.4 (CH), 127.3 (CH), 125.8 (CH), 77.7 (C), 44.8 (CH_2), 40.5 (CH_2). **HRMS** (CI^+) m/z 229.0787 ($M-H_2O+H^+$), (229.0779 calcd for $C_{15}H_{13}Cl$ $[M-H_2O]^+$). **IR** 3354, 3530, 3086, 3055, 3026, 3003, 2961, 1445 cm^{-1}.

- **4-Hydroxy-4,4-diphenylbutanenitrile (13)**

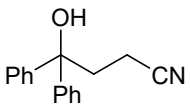

In an argon filled 250 ml two-neck round bottom flask, 3-chloro-1,1-diphenylpropan-1-ol (2.04 g, 8.3 mmol) was dissolved in DMSO (52 ml). Then, sodium cyanide (1.99 g, 40.6 mmol) was added as a solid and the reaction mixture was stirred at 60 °C for 17 h. The mixture was cooled down,

treated with water (35 ml) and extracted with ethyl acetate (3 x 20 ml). The combined organic layers were washed with brine (20 ml), dried over $MgSO_4$ and solvent was removed in vaccum. The crude product was purified by column chromatography (eluent: hexane:EtOAc, 20:1) to give **13** as a white solid (1.24 g) in 63% yield. **^{1}H NMR** (500 MHz, $CDCl_3$) δ 7.36 (s, 8H, Aromatic H), 7.28 (s, 2H, Aromatic H), 2.67 (m, 2H, $C_{quaternary}$-C**H$_2$**), 2.31 (m, 2H, C**H$_2$**-CN), 2.09 (s, 1H, OH). **^{13}C{^{1}H} NMR** (101 MHz, $CDCl_3$) δ 145.1 (C), 128.6 (CH), 127.6 (CH), 125.8 (CH), 120.2 (CN), 53.4 (C), 37.7 (CH_2), 12.2 (CH_2). **Elemental Analysis** Calcd for ($C_{16}H_{15}NO$): C, 80.98; H 6.37; N 5.90; Found C, 80.71; H, 6.39; N, 5.50. **HRMS** (CI^+) m/z 238.1228 ($M+H^+$) (238.1226 calcd for $C_{16}H_{15}NO$ $(M+H)^+$). **IR** 3414, 3059, 3027, 2929, 2258, 1447, 696 cm^{-1}.

4-Methoxy-4,4-diphenylbutanenitrile (14)

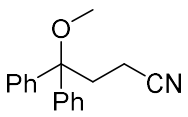

To an argon filled 25 ml Schlenk flask containing sodium hydride (0.39 g in 60% dispersion in mineral oil, 10.08 mmol), a solution of 4-hydroxy-4,4-diphenylbutanenitrile **13** (1.20 g, 5.05 mmol) in dry THF (9.5 ml) was added dropwise at 0 °C. After stirring the mixture at this temperature for 10 min, methyl iodide (1.49 g, 10.5 mmol) was added dropwise and the reaction mixture was allowed to warm up to room temperature and heated at 75 °C for 16 h. Then the reaction mixture was cooled to 0 °C and quenched with water (20 ml). After removal of the solvent under vacuum, the crude product was extracted with ethyl acetate (3 x 15 ml). The combined organic layers were washed with brine (15 ml) and dried over $MgSO_4$. The solvent was evaporated in vacuum and the crude product was purified by column chromatography (silica, eluent: hexane:EtOAc, 5:1) to give **14** as a white solid (1.03 g) in 81% yield. **^{1}H NMR** (400 MHz, $CDCl_3$) δ 7.35-7.25 (m, 10H, Aromatic H), 3.05 (s, 3H, CH_3), 2.70 (m, 2H, $C_{quaternary}$-C**H$_2$**), 2.13 (m, 2H, C**H$_2$**-CN). **^{13}C{^{1}H} NMR** (101 MHz, $CDCl_3$) δ 143.3 (C), 128.31 (CH), 127.3 (CH), 126.7 (CH), 120.1 (CN), 81.4 (C), 50.3 (CH_3), 31.3 (CH_2), 11.5 (CH_2). **MS** (CI^+) m/z 220.1 $(M\text{-}MeOH)^+$ (220.1 calcd for $C_{16}H_{14}N$ $[M\text{-}MeOH]^+$). **IR** 3086, 3026, 3000, 2928, 2247, 1264 cm^{-1}.

5,5-Difluoro-4,4-diphenylpentanenitrile (15)

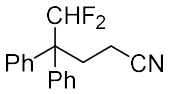

In a 50 ml Schlenk flask under argon, 5-oxo-4,4-diphenylpentanenitrile (1.5 g, 6.07 mmol) was dissolved in dry dichloromethane (25 ml). The solution was cooled down to 0 °C and (diethylamino)sulphur trifluoride (2.2 g, 13.6 mmol) was added dropwise. The resulting yellow mixture was allowed to stir at room temperature for 5 h, quenched with water (15 ml). The aqueous layer was extracted with dichloromethane (3 x 10 ml). After drying the combined organic layers over $MgSO_4$, the solvent was removed under vacuum and crude product was purified by column chromatography (eluent: 5-25 % ethyl acetate in hexane) to give **15** (1.42 g) as a yellowish solid in 86% yield as a mixture of diastereomers. **^{1}H NMR** (500 MHz, $CDCl_3$) δ 7.37-7.24 (m, 6H, Aromatic H), 7.16 (m, 2H, Aromatic H), 7.05 (d, J= 7.1 Hz, 2H, Aromatic H), 5.55 (dd, J= 5.57, 5.50 Hz, 1H, CHF_2), 2.80 (m, 1H, $C_{quaternary}$-CH_2), 2.60-2.35 (m, 2H, CH_2-CN), 2.14 (m, 1H, $C_{quaternary}$-CH_2). **^{13}C{^{1}H} NMR** (126 MHz, $CDCl_3$) δ 128.8 (C, d, *J* = 1.3 Hz), 128.7 (CH, s), 128.6 (CH, d, *J* = 1.9 Hz), 127.7 (CH, s), 127.2 (CH, dd, *J* = 7.4, 1.6 Hz), 125.2 (d, *J* = 10.3 Hz), 119.0 (CN, s), 98.0 (C, dd, J= 188.39, 22.95 Hz), 96.2 (CHF_2, dd, *J* = 186.6, 24.0 Hz), 31.1 (CH_2, dd, *J* = 22.5, 4.1 Hz), 11.5 (CH_2, d, *J* = 5.1 Hz). **Elemental Analysis** Calcd for ($C_{17}H_{15}NF_2$): C, 75.26; H, 5.57; N, 5.16; Found C, 75.34; H, 5.54; N, 5.28. **HR-MS** (CI^+) m/z 289.1508 $(M+NH_4)^+$ (289.1511 calcd for $C_{17}H_{19}N_2F_2$ $(M+NH_4)^+$). **IR** 3062, 3032, 2958, 2252, 1450 cm^{-1}.

2,2-Diphenyl-4-pyridylbutanenitrile (16)

Prepared according to literature procedure.[58]

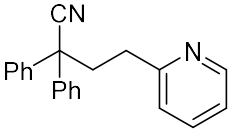

In a 100 ml round bottom flask equipped with a condenser and stir bar, diphenylacetonitrile (1.19 g, 6.15 mmol) was dissolved in ^{t}BuOH (25 ml). A 30% solution of KOH in MeOH (57 µl, 0.30 mmol of KOH) was then added and mixture was stirred for 20 min. Then, 2-vinylpyridine (1 ml, 9.27 mmol) was added dropwise and reaction mixture was stirred at 65 °C for 2 h. After cooling to room temperature, water (50 ml) was added to the reaction mixture and a white solid precipitated out. The white solid was purified by recrystallization from ethanol (1.5 ml) to give **16** in 74% yield (1.36 g). **^{1}H NMR** (400 MHz, $CDCl_3$) δ 8.64 – 8.43 (m, 1H,

Aromatic H), 7.57 (td, J = 7.7, 1.8 Hz, 1H, Aromatic H), 7.51 – 7.43 (m, 4H, Aromatic H), 7.41 – 7.33 (m, 4H, Aromatic H), 7.32 – 7.23 (m, 2H, Aromatic H), 7.16 – 7.08 (m, 2H, Aromatic H), 3.08 – 2.76 (m, 4H, $2CH_2$). **$^{13}C\{^1H\}$ NMR** (101 MHz, $CDCl_3$) δ 160.1 (CH), 149.3 (CH), 139.9 (CH), 136.4 (CH), 128.9 (CH), 127.9 (CH), 126.9 (CH), 123.1 (CH), 122.2 (CH), 121.4 (CN), 51.6 (C), 39.0 (CH_2), 34.3 (CH_2). **HRMS** (CI^+) m/z 299.1553 $(M+NH_4)^+$ (299.1543 calcd for $C_{21}H_{15}N$ $(M+NH_4)^+$). **IR** 3031, 3003, 2962, 2928, 2857, 2235, 1469, 700.54 cm $^{-1}$.

Methyl 4-cyano-4,4-diphenylbutanoate (17)

Prepared according to the literature procedure, but by applying anhydrous conditions.[59]

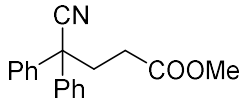

In an argon filled 100 ml Schlenk flask, diphenylacetonitrile (3.0 g, 15.5 mmol) was dissolved in *tert*-butanol (8 ml). A 30% solution of KOH in MeOH (0.15 ml, 0.05 mmol of KOH) was added and mixture was stirred for 20 min. Then, methyl acrylate (1.33 g, 15.5 mmol) was added dropwise and reaction mixture was stirred at 50 °C for 24 h. After cooling to room temperature, water (15 ml) was added to the reaction mixture. The aqueous layer was extracted with diethyl ether (3x 8 ml) and the combined organic layers were dried over $MgSO_4$. The crude product was purified by column chromatography (silica gel, eluent: hexane:EtOAc, 8:1) to give **17** as a white solid (2.20 g) in 53% yield. **^{1}H NMR** (300 MHz, $CDCl_3$) δ 7.50 – 7.22 (m, 10H, Aromatic H), 3.66 (s, 3H, CH_3), 2.83 – 2.41 (m, 4H, $2CH_2$). **$^{13}C\{H\}$ NMR** (75 MHz, $CDCl_3$) δ 194.6 (CO), 139.2 (CH), 129.0 (CH), 128.1 (CH), 126.8 (CH), 115.4 (CN), 51.7 (C), 34.4 (CH_2), 30.4 (CH_2). **Elemental Analysis** Calcd for ($C_{18}H_{17}NO_2$): C, 77.40; H 6.13; N 5.01; Found C, 78.99; H, 6.15; N, 5.01. **MS** (CI^+) m/z 297.2 $(M+NH_4)^+$ (297.1 calcd for $C_{18}H_{21}N_2O_2$ $(M+NH_4)^+$). **IR** 2236, 1734, 1200, 1175 cm^{-1}.

(E) and (Z)-5-(methoxyimino)-2,2-diphenylhexanenitrile (18 & 19)

Synthetic route:

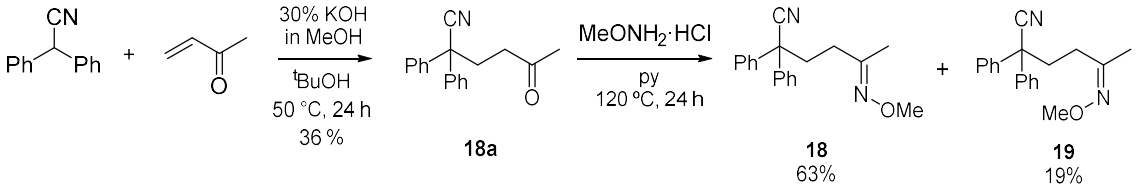

- **5-Oxo-2,2-diphenylhexanenitrile (18a)**

Prepared according to literature procedure.[59]

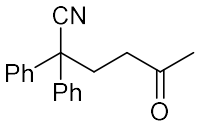

In an argon filled 100 ml Schlenk flask, diphenylacetonitrile (1 g, 5.2 mmol) was dissolved in *tert*-butanol (16 ml). A freshly prepared solution of 30% KOH in MeOH (1.1 equiv) was added and the mixture was stired for 20 min. Methyl vinyl ketone (0.36 g, 5.2 mmol) was then added dropwise and the mixture was heated at 50 °C for 24 h. The reaction mixture was treated with water (10 ml). The crude product was extracted with diethyl ether (3 x 8 ml) and the combined organic layers were washed with brine, dried over $MgSO_4$ and concentrated in vacuum. The crude product was purified by column chromatography (hexane:EtOAc, 8:1) to give **18a** as a white solid in 36% yield (0.46 g). **^{1}H NMR** (400 MHz, $CDCl_3$) δ 7.38-7.30 (m, 10H, Aromatic H), 2.70-2.58 (m, 2H, $C_{quaternary}$-CH_2), 2.42-2.67 (m, 2H, C**H$_2$**-COMe), 2.10 (s, 3H, CH_3). **^{13}C{^{1}H} NMR** (101 MHz, $CDCl_3$) δ 206.6 (CO), 139.5 (C), 129.0 (CH), 128.1 (CH), 126.7 (CH), 121.9 (CN), 50.7 (C), 33.0 (CH_2), 30.9 (CH_2), 30.1 (CH_3). **Elemental Analysis** Calcd for ($C_{21}H_{23}NO$): C, 82.10; H 6.51; N 5.32; Found C, 82.69; H, 6.54; N, 5.21. **MS** (CI^+) m/z 281.2 ($M+NH_4^+$) (281.1 calcd for $C_{18}H_{21}N_2O$ $(M+NH_4)^+$). **IR** 3005, 2961, 2236, 1714, 1492, 1498 cm^{-1}.

- **(E) and (Z)-5-(methoxyimino)-2,2-diphenylhexanenitrile (18 & 19)**

In an argon filled 50 ml 3 neck round bottom flask equipped with a condenser, methoxyamine hydrochloride (0.16 g, 1.92 mmol) was dissolved in anhydrous pyridine (1.3 ml) and then ketone **18a** (0.39 g, 1.50 mmol) was added as a solid. The reaction mixture was stirred at 120 °C for 24 h, cooled to room temperature, treated with water (10 ml) and extracted with diethyl ether (3 x 10 ml). The combined organic layers were

washed with brine (15 ml) and dried over $MgSO_4$. Solvent was removed under vacuum and the crude product was purified by column chromatography (silica gel, eluent: hexane:EtOAc, 4:1) to give **18** (*E*-isomer) and **19** (*Z*-isomer) as white solids in 63% and 19% yields, respectively. The configuration E and Z of the products was determined by 2D NOESY.

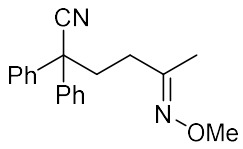

(E)

18. **^{1}H NMR** (500 MHz, $CDCl_3$) δ 7.44 – 7.34 (m, 8H, Aromatic H), 7.33 – 7.28 (m, 2H, Aromatic H), 3.82 (s, 3H, CH_3), 2.74 – 2.54 (m, 2H, $C_{quaternary}$-CH_2), 2.38 – 2.23 (m, 2H, N=C-C**H_2**), 1.81 (s, 3H, CH_3). **^{13}C{^{1}H} NMR** (75 MHz, $CDCl_3$) δ 156.2 (C=N), 139.5 (C), 128.9 (CH), 128.0 (CH), 126.8 (CH), 121.9 (CN), 61.2 (CH_3), 51.7 (C), 35.1 (CH_2), 26.6 (CH_2), 20.2 (CH_3). **Elemental Analysis** Calcd for ($C_{19}H_{20}N_2O$): C, 78.05; H, 6.90; N, 9.58; Found C, 78.08; H, 6.94; N, 9.50. **IR** 3004, 2941, 2231, 1598, 1495, 1446 cm^{-1}.

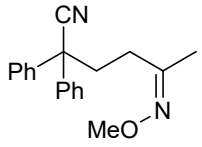

(Z)

19. **^{1}H NMR** (500 MHz, $CDCl_3$) 7.45 – 7.39 (m, 4H, Aromatic H), 7.39 – 7.34 (m, 4H, Aromatic H), 7.34 – 7.27 (m, 2H, Aromatic H), 3.80 (s, 3H, CH_3), 2.58 – 2.50 (m, 2H, $C_{quaternary}$-CH_2), 2.45 – 2.37 (m, 2H, N=C-C**H_2**), 1.86 (s, 3H, CH_3). **^{13}C {H} NMR** (75 MHz, $CDCl_3$) δ 155.5 (C=N), 139.7 (C), 128.9 (CH), 128.0 (CH), 126.8 (CH), 122.0 (CN), 61.2 (CH_3), 51.3 (C), 35.6 (CH_2), 32.3 (CH_2), 14.7 (CH_3). **IR** 3030, 2938, 2236, 1598, 1493, 1449 cm^{-1}.

In the NOESY spectrum of isomer (Z), the signal of the CH_3 of the methoxy group at δ 3.80 ppm shows correlation with the signal of the aromatic protons at δ 7.34-7.27 ppm which allowed us to identify this isomer as (Z).

4-(tert-butyloxazoline)-2,2-diphenylbutanenitrile (20)

Synthetic route:

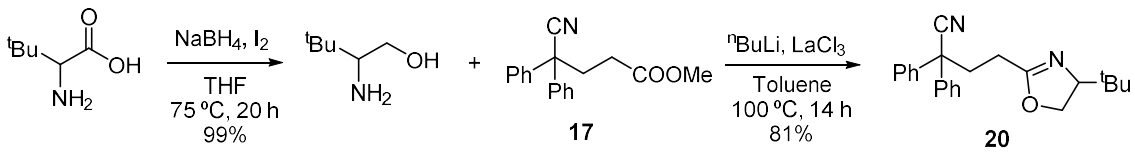

- **Synthesis of *tert*-leucinol**

Prepared according to literature procedure.[118]

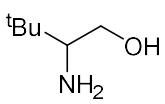

In an argon filled 250 ml three-neck round bottom flask equipped with a condenser and stir bar, L-*tert*-leucine (2.99 g, 16.5 mmol) was added to a mixture of $NaBH_4$ (1.52 g, 40.2 mmol) in dry THF (47.7 ml) at 0 °C. The reaction mixture was stirred for 15 min and then a solution of iodine (4.18 g, 16.5 mmol) in dry THF (13 ml) was added dropwise at 0 °C. The white mixture was stirred at 0 °C until hydrogen evolution ceased and then heated to 75 °C for 20 h The reaction mixture was cooled to 0 °C and methanol (15 ml) was added cautiously until the reaction mixture became clear. After stirring for 20 min at 0 °C, the solvent was evaporated to give a white paste. The white paste was treated with 20% aqueous solution of KOH (50 ml) and the resulting mixture stirred at room temperature overnight. The mixture was extracted with dichloromethane (4 x 25 ml) and the combined organic layers were dried over Na_2SO_4. The solvent was removed under vacuum and *tert*-leucinol was obtained without further purification (1.92 g) in 99% yield. **^{1}H NMR** (500 MHz, $CDCl_3$) δ 3.72 (dd, *J* = 10.2, 3.9 Hz, 1H, C**H**$_2$-OH), 3.21 (t, *J* = 10.2 Hz, 1H, C**H**$_2$-OH), 2.51 (dd, *J* = 10.1, 3.9 Hz, 1H, CH), 1.80 (bs, 1H, OH), 0.91 (s, 9H, $3CH_3$). **^{13}C{^{1}H} NMR** (101 MHz, $CDCl_3$) δ 62.3 (CH_2), 61.7 (CH), 33.2 (C), 26.2 (CH_3). **HRMS** (CI^+) m/z 118.1227 $(M+H)^+$ (118.1226 calcd for $C_6H_{16}NO$ $(M+H)^+$). **IR** 3301 (broad), 2953, 2869, 1364, 1042 cm^{-1}.

- **Synthesis of 4-(tert-butyloxazoline)-2,2-diphenylbutanenitrile (20)**

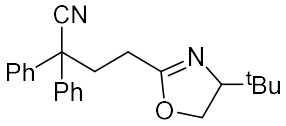

In an argon filled 50 ml Schlenk flask, *tert*-leucinol (0.47 g, 4.01 mmol) was added to a solution of lanthanum (III) chloride (41.2 mg, 0.17 mmol) in dry toluene (16 ml) and the mixture was cooled down to 0 °C. Then, n-butyl lithium (2 ml, 1.6 M in hexanes) was added dropwise and the mixture was stirred at 0 °C for 15 min. Methyl 4-cyano-4,4-diphenylbutanoate **22** (0.47 g, 1.68 mmol) was subsequently added and the mixture became dark brown. The reaction mixture was stirred at 100 °C for 14 h. The resulting yellow reaction mixture was cooled down, treated with concentrated solution of NH_4Cl (15 ml) and extracted with chloroform (3 x 15 ml). The combined organic layers were washed with brine, dried over Na_2SO_4 and the solvent was removed under vacuum. The crude product was purified by

column chromatography (eluent: petroleum ether:EtOAc, 25:1) to give **20** as a white solid (0.43 g) in 81% yield. **^{1}H NMR** (500 MHz, $CDCl_3$) δ 7.42-7.39 (m, 4H, Aromatic H), 7.38-7.34 (m, 4H, Aromatic H), 7.32-7.28 (m, 2H, Aromatic H), 5.66 (d, *J* = 8.7 Hz, 1H, NH due to isomerism), 3.81 (m, 2H, CH_2), 3.51 (m, 1H, CH), 2.79 (m, 2H, CH_2), 2.38 (m, 2H, CH_2), 0.92 (s, 9H, $3CH_3$). **^{13}C{^{1}H} NMR** (101 MHz, $CDCl_3$) δ 172.3 (C), 139.4 (C), 129.0 (CH), 128.1 (CH), 126.8 (CH), 122.1 (CH), 63.2 (CH_2), 59.8 (CH), 51.1 (C), 34.8 (CH_2), 33.4 (C), 32.8 (CH_2), 26.9 (CH_3). **Elemental Analysis** Calcd for ($C_{23}H_{26}N_2O$): C, 79.73; H 7.53; N 8.09; Found C, 74.77; H, 7.69; N, 7.27. **HRMS** (CI^+) m/z 347.2125 $(M+H)^+$ (347.2118 calcd for $C_{23}H_{27}N_2O$ $(M+H)^+$). **IR** 3360, 3279, 2963, 2937, 2235, 1652, 1562 cm^{-1}.

5-oxo-2,2-diphenylnonanenitrile (21)

Synthetic route:

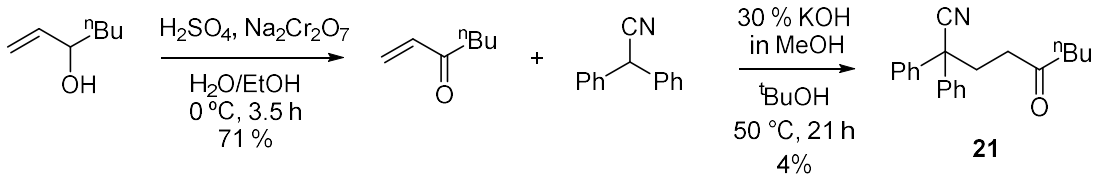

- **Synthesis of butyl vinyl ketone**

Prepared according to literature procedure.[60]

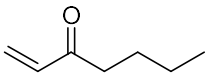

In a 25 ml round bottom flask, concentrated sulphuric acid (3.2 ml) was added dropwise at 0 °C to a solution of sodium dichromate dihydrate (4.36 g, 14.6 mmol) in water (9.9 ml). The mixture was added at 0 °C to a solution of 1-hepten-3-ol (3.01 g, 26.4 mmol) in ethanol (9.9 ml) in a 50ml round bottom flask. The resulting black biphasic mixture was stirred vigorously at 0 °C for 3.5 h and then extracted with diethyl ether (3 x 20 ml). The combined organic layers were washed with saturated aqueous solution $NaHCO_3$ (50 ml), water (50 ml) and brine (50 ml) and dried over Na_2SO_4. Butyl vinyl ketone was obtained as a colourless oil (2.11 g) in a 71% yield and used further without purification. **^{1}H NMR** (400 MHz, $CDCl_3$) δ 6.27 (ddd, *J* =

18.9, 17.7, 5.9 Hz, 2H, 2CH), 5.80 (dd, *J* = 10.5, 1.2 Hz, 1H, CH), 2.57 (t, J= 14.9, 7.4 Hz, 2H, CH_2), 1.59 (quint, *J* = 30.9, 15.1, 15.1, 7.7 Hz, 2H, CH_2), 1.33 (sext, *J* = 14.6, 7.4 Hz, 1H, CH_2), 0.91 (t, *J* = 14.6, 7.3 Hz, 3H, CH_3). **^{13}C{^{1}H} NMR** (101 MHz, $CDCl_3$) δ 201.0 (CO), 136.6 (H**C**=CH_2), 127.7 (HC=**C**H_2), 39.3 (CH_2), 26.1 (CH_2), 22.3 (CH_2), 15.2 (CH_2), 13.8 (CH_3).

- **5-oxo-2,2-diphenylnonanenitrile (21)**

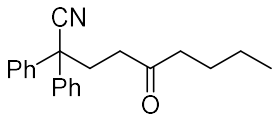

In an argon filled 50 ml two-neck round bottom flask equipped with a condenser, a 30% solution of KOH in methanol (0.1 ml) was added to a diphenylacetonitrile (1.21 g, 6.26 mmol) in dry dioxane (4 ml) and stirred for 30 min. Butyl vinyl ketone (1.02 g, 9.04 mmol) was added dropwise and the mixture was heated at 50 °C for 21 h. The reaction mixture was then cooled to room temperature, treated with water (10 ml) and extracted with diethyl ether (3 x 10 ml). The combined organic layers were washed with brine (15 ml) and dried over $MgSO_4$. The crude product was purified by column chromatography (eluent: hexane:EtOAc, 8:1) and recrystallization by slow addition of hexane to concentrated solution of **21** in dichloromethane (dichloromethane:hexane, 1:3, v/v) to give product **21** as a white solid (0.35 g) in 4% yield. **^{1}H NMR** (400 MHz, $CDCl_3$) δ 7.43 – 7.33 (m, 8H, Aromatic H), 7.33 – 7.27 (m, 2H, Aromatic H), 2.70 (m, 2H, CH_2), 2.55 (m, 2H, CH_2), 2.35 (t, *J* = 7.5 Hz, 2H, CH_2), 1.50 (m, 2H, CH_2), 1.27 (m, 2H, CH_2), 0.87 (t, *J* = 7.3 Hz, 3H, CH_3). **^{13}C{^{1}H} NMR** (101 MHz, $CDCl_3$) δ 209.1 (CO), 139.6 (C), 129.0 (CH), 128.0 (CH), 126.8 (CH), 122.0 (CN), 50.8 (C), 42.7 (CH_2), 38.8 (CH_2), 33.0 (CH_2), 25.8 (CH_2), 22.2 (CH_2), 13.7 (CH_3). **Elemental Analysis** Calcd for ($C_{21}H_{23}NO$): C, 82.58; H 7.59; N 4.59; Found C, 82.14; H, 7.53; N, 4.51. **HRMS** (CI^+) m/z 306.1862 ($M+H^+$) (306.1852 calcd for $C_{21}H_{24}NO$ $[M+H]^+$). **IR** 3061, 3031, 3004, 2965, 2939, 2248, 1714, 1492, 769 cm^{-1}.

Synthesis of 2,2-dimethyl-4,4-diphenylpentandinitrile (22)

Synthetic route:

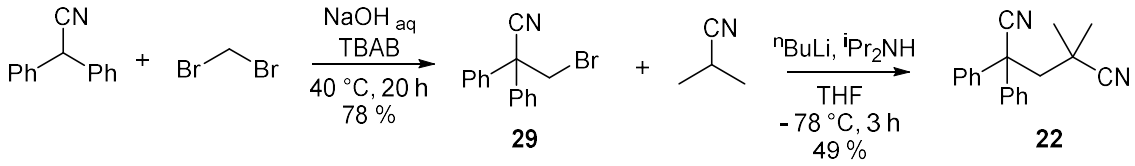

- **2,2-Diphenyl-3-bromopropionitrile (29)**

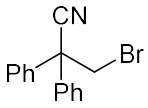

In a 50 ml Schlenk flask under argon atmosphere, diphenylacetonitrile (3.05 g, 15.8 mmol), dibromomethane (12.77 g, 74.3 mmol) and tetrabutylammonium bromide (0.41 g, 1.3 mmol) were mixed with 50% aqueous solution of NaOH (7.5 ml) and heated at 40 °C for 20 h under vigorous stiring. The reaction mixture was then cooled down, treated with water (10 ml), extracted with ethyl acetate (3 x 10ml) and dried over $MgSO_4$. The product **29** was obtained as a white solid (3.51 g) in a 78% yield and used without further purification. **^{1}H NMR** (400 MHz, $CDCl_3$) δ 7.44-7.32 (M, 10H, Aromatic H), 4.09 (s, 2H, CH_2). **^{13}C{^{1}H} NMR {H}** (101 MHz, $CDCl_3$) δ 137.5 (C), 129.1 (CH), 128.7 (CH), 127.1 (CH), 120.8 (CN), 54.0 (C), 36.1 (CH_2). **HRMS** (CI^+) m/z 303.0496 $(M+NH_4)^+$ (303.0491 calcd for $C_{15}H_{16}N_2Br$ $[M+NH_4]^+$). **IR** 3059, 3032, 3093, 2979, 2254, 643, 611 cm^{-1}.

- **2,2-Dimethyl-4,4-diphenylpentandinitrile (22)**

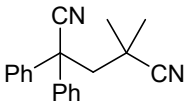

In a 50 ml Schlenk flask under argon atmosphere, diisopropylamine (0.72 ml, 5.1 mmol) was dissolved in THF (3.4 ml) and the solution was cooled down to -78 °C. n-Butyl lithium (3.2 ml, 1.6 M in hexanes) was added dropwise and the mixture was stirred at -78 °C for 30 min. Then, a solution of isobutyronitrile (0.34 g, 4.94 mmol) in THF (3.4 ml) was added and the mixture turned yellow. To this solution, 2,2-diphenyl-3-bromopropionitrile **29** (2.02 g, 7.1 mmol) in dry THF (3.1 ml) was added dropwise at -78 °C and the mixture became intense red. The mixture was stirred for 3 h at room temperature. Then, 2M HCl (10 ml) was added at room temperature and the aqueous layer was extracted with ethyl acetate (3 x 10 ml). The combined organic layers were treated with $NaHCO_3$ (10 ml), water (10 ml), brine (10 ml)

and dried over $MgSO_4$. The crude product was purified by column chromatography (silica gel, eluent: hexane:EtOAc, 10:1) to give **22** as a white solid (0.66 g) in 49% yield. **^{1}H NMR** (400 MHz, $CDCl_3$) δ 7.50 – 7.31 (m, 10H, Aromatic H), 2.75 (s, 2H, CH_2), 1.48 (s, 6H, CH_3). **^{13}C{^{1}H} NMR** (101 MHz, $CDCl_3$) δ 139.4 (C), 129.1 (CH), 128.5 (CH), 127.1 (CH), 122.9 (CN), 48.4 (C), 47.4 (C), 31.0 (CH_2), 28.5 (CH_3). **Elemental Analysis** Calcd for ($C_{19}H_{18}N_2$): C, 83.18; H 6.61; N 10.21; Found C, 82.84; H, 6.66; N, 10.23. **HRMS** (CI^+) m/z 275.1543 $(M+H)^+$ (275.1543 calcd for $C_{19}H_{18}N_2$ $[M+H]^+$). **IR** 3062, 3029, 2991, 2942, 2233, 194, 697 cm^{-1}.

Synthesis of 2,2-dideuterium-4,4-diphenylpentanedinitrile (2-d_2)

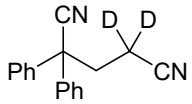

In an argon filled 50 ml two-neck round bottom flask equipped with a condenser, 2,2-diphenylpentanedinitrile (1.05 g, 4.1 mmol) was dissolved in deuterium oxide (2.6 ml). Then, a solution of sodium deuteroxide (0.05 ml, 40 wt% in D_2O) was added and the reaction mixture was refluxed for 2.5 h. After cooling to room temperature, the reaction mixture was extracted with dichloromethane (2 x 5 ml) and the combined organic layers were concentrated under vacuum. The residue was dissolved in deuterium oxide (2.6 ml) and a solution of sodium deuteroxide (0.05 ml, 40 wt% in D_2O) was added and the mixture was refluxed for 2 h. The reaction mixture was extracted with dichloromethane (3 x 5 ml) and the combined organic layers were treated with brine and dried over $MgSO_4$. Product **2**-d_2 (0.83 g) was obtained as a white solid in a 78% yield and was used without further purification. Deuterium purity was 95%, determined by ^{1}H NMR. **^{1}H NMR** (400 MHz, $CDCl_3$) δ 7.43-7.32 (m, 10H, Aromatic H), 2.79 (s, 2H, CH_2). **^{2}H NMR** (400 MHz, d_8-toluene) δ 2.09 (bs, CD_2). **^{13}C{^{1}H} NMR** (101 MHz, $CDCl_3$) δ 138.1 (C), 129.3 (CH), 128.7 (CH), 126.6 (CH), 120.7 (CN), 118.0 (CN), 50.8 (C), 35.2 (CH_2), 13.7 (CD_2). **Elemental Analysis** Calcd for ($C_{17}H_{12}N_2D_2$): C, 82.23; H+D 6.49; N 11.28; Found C, 82.00; H+D, 6.49; N, 11.26. **HRMS** (CI^+) m/z 266.1632 $(M+NH_4)^+$ (266.1621 calcd for $C_{17}H_{16}N_3D_2$ $[M+NH_4]^+$). **IR** 3053, 2978, 2942, 2252, 2236, 1447, 700.

Synthesis of 2-deuterium-2,2-diphenylacetonitrile (3-d)

Prepared according to the literature procedure.[71]

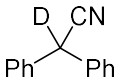

In a 50 ml Schlenk flask under argon atmosphere, diphenylacetonitrile (0.52 g, 2.69 mmol) was dissolved in dry THF (12 ml) and was cooled down to -78 °C. Then, n-butyllithium (1.8 ml, 1.6 M in hexanes) was added dropwise and the mixture was stirred at -78 °C for 30 min. Deuterium oxide (1 ml) was added and the mixture was stirred for 25 min and then allowed to warm up to room temperature. The mixture was extracted with diethyl ether (3 x 5 ml) and the combined organic layers were washed with brine and dried over $MgSO_4$. After removal of solvent under vacuum, product **3**-d was obtained as a white solid (0.47 g) in 90% yield. D% purity was 94% as determined by ^{1}H NMR. **^{1}H NMR** (400 MHz, d_6-acetone) δ 7.51-7.44 (m, 8H, Aromatic H), 7.41-7.37 (m, 2H, Aromatic H). **^{13}C{^{1}H} NMR** (101 MHz, Acetone) δ 136.9 (C), 129.1 (CH), 128.0 (CH), 127.6 (CH), 119.7 (CN), 41.6 (CH). **HRMS** (CI^+) m/z 212.1291 $(M+NH_4)^+$ (212.1293 calcd for $C_{14}H_{14}N_2D$ $[M+NH_4]^+$).

2.13.4. Iridium-catalysed reductive cleavage of unstrained aliphatic C-C bonds with $Ir(P^iPr_3)_2H_5$

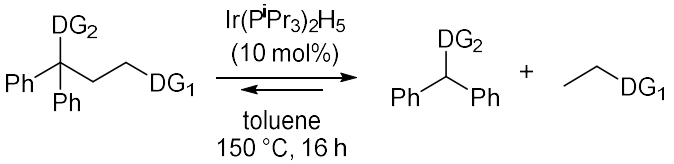

In a glovebox, a stock solution was prepared from nitrile substrate (0.20 mmol), dodecane (24.5 mg, 0.14 mmol, GC standard) and toluene (1 ml). From this stock solution, 0.8 ml was added into a 10 ml Schlenk bomb charged with $Ir(P^iPr_3)_2H_5$ catalyst (8.3 mg, 0.016 mmol, 10 mol% or 16.6 mg, 0.0321 mmol, 20 mol%) and a magnetic stir bar. The Schlenk bomb was then sealed, removed from the glovebox and the reaction mixture was heated in an oil bath at 150 °C for 16 h. Then, the reaction mixture was cooled down and was passed through a short silica gel column (5 ml plastic syringe filled with a 3 cm layer of silica gel) eluting with 15 ml of EtOAc. The treated reaction mixture was analysed by GC. The products were all known compounds that were identified using GC-MS and GC by comparison of the mass spectra and retention times with those of authentic standard.

2.13.5. Screening of the catalytic system for reductive cleavage of unstrained aliphatic C-C bonds in dinitriles

2.13.5.1. Catalytic reductive cleavage of unstrained aliphatic C-C bonds with $[Ir(cod)Cl]_2$ and phosphine, phenanthroline or NHC ligands

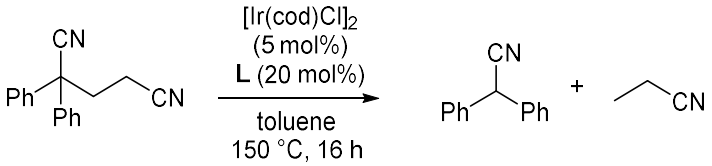

The reaction was conducted according to the general procedure described in Section 2.13.4. using $[Ir(cod)Cl]_2$ (5.2 mg, 0.008 mmol, 5 mol%), a ligand (0.032 mmol, 20 mol%) and 0.8 ml of a stock solution prepared from 2,2-diphenylpentanedinitrile **2** (49.9 mg, 0.202 mmol), dodecane (24.2 mg, 0.142 mmol, GC standard) and toluene (1 ml). Note, for N-heterocyclic carbene ligands, ^{t}BuONa (3.7 mg, 0.04 mmol, 22 mol%) was

added. For bidentate phosphine and phenanthroline ligands, 10 mol% of ligand was used. The reaction mixture was heated at 150 °C for 16 h. GC analyses of the reaction mixtures showed the yields and conversions summarised in Table 2.4.

2.13.5.2. Catalytic reductive cleavage of unstrained aliphatic C-C bonds with iridium pincer ligands (^{R}PCPIrHCl)

The reaction was conducted according to the general procedure described in section 2.13.4. using ^{R}PCPIrHCl complex (10 mol%, R = Ad or ^{i}Pr), ^{t}BuONa (12 mol%) and 0.8 ml of a stock solution prepared from 2,2-diphenylpentanedinitrile **2** (49.2 mg, 0.200 mmol), dodecane (23.9 mg, 0.140 mmol, GC standard) and toluene (1 ml). The reaction mixture was heated at 150 °C for 16 h. GC analyses of the reaction mixtures showed the yields and conversions summarised in Table 2.4.

2.13.5.3. Control experiments of catalytic reductive cleavage of unstrained aliphatic C-C bonds of dinitrile 2 with P^{i}Pr$_3$

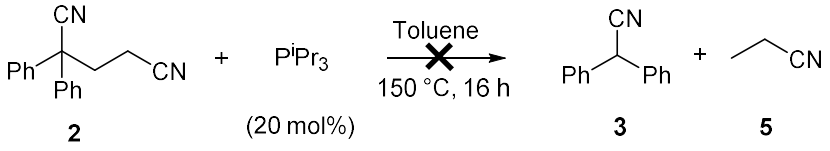

The reaction was conducted according to the general procedure described in section 2.13.4. using P^{i}Pr$_3$ (7.1 mg, 0.044 mmol, 20 mol%) and 0.8 ml of a stock solution prepared from dinitrile **2** (50.0 mg, 0.203 mmol), dodecane (24.5 mg, 0.14 mmol, GC standard) and toluene (1 ml). The reaction mixture was heated at 150 °C for 16 h. The reaction mixture was allowed to cold down and a 0.1 ml aliquot of the mixture was dissolved in 1 ml of EtOAc for GC analysis. The GC analysis of the reaction mixture showed that dinitrile **2** does not undergo C-C bond cleavage in the presence of catalytic amounts of P^{i}Pr$_3$ under these reaction conditions.

2.13.5.4. Control experiments of catalytic reductive cleavage of unstrained aliphatic C-C bonds of dinitrile with benzoyl peroxide or AIBN

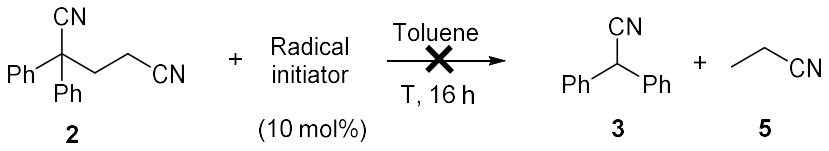

The reaction was conducted according to the general procedure described in Section 2.13.4. using benzoyl peroxide (4.1 mg, 0.017 mmol, 10 mol%) and 0.8 ml of a stock solution prepared from dinitrile **2** (50.0 mg, 0.203 mmol), dodecane (24.5 mg, 0.14 mmol, GC standard) and toluene (1 ml). Note, for reactions with azobisisobutyronitrile (AIBN), 80 µl (2.62 mg, 0.0160 mmol) of a solution of this radical initiator (16.3 mg, 0.099 mmol) in toluene (0.5 ml) was used. The reaction mixture was heated at 150 °C or at 80 °C for 16 h. The reaction mixture was allowed to cold down and a 0.1 ml aliquot of the mixture was dissolved in 1 ml of EtOAc for GC analysis. The GC analyses of the reaction mixture showed that dinitrile **2** does not undergo C-C bond cleavage in the presence of catalytic amounts of benzoyl peroxide or AIBN neither at 150 °C nor at 80 °C.

2.13.6. Study on the effect of directing groups in the reductive C-C bond cleavage

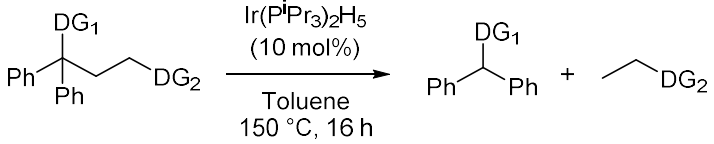

Reductive C-C bond cleavage of 5-oxo-4,4-diphenylpentanenitrile 9

The reaction was conducted according to the general procedure described in Section 2.13.4. using $Ir(P^iPr_3)_2H_5$ catalyst (8.2 mg, 0.016 mmol, 10 mol%) and 0.8 ml of a stock solution prepared from 5-oxo-4,4-diphenylpentanenitrile **9** (49.1 mg, 0.197 mmol), dodecane (24.2 mg, 0.142 mmol, GC standard) and toluene (1 ml). The reaction mixture was heated at 150 °C for 16 h. The GC analysis of the reaction mixture showed 50%

conversion of aldehyde **9** and formation of 2,2-diphenylacetaldehyde and propionitrile in 4 and 13% yield, respectively.

To understand the origin of poor material balance between conversion of aldehyde **9** and yield of 2,2-diphenylacetaldehyde, the following control experiment was conducted:

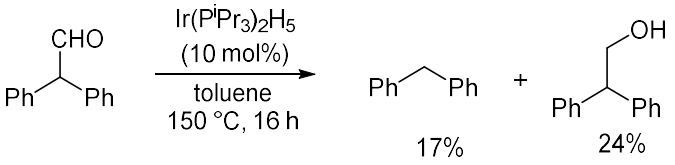

This experiment was conducted following the general procedure described in section 2.13.4 using 2,2-diphenylacetaldehyde (187.7 mg, 0.95 mmol) and $Ir(P^iPr_3)_2H_5$ catalyst (49.2 mg, 0.0950 mmol, 10 mol%) in toluene (4.8 ml). After heating at 150 ºC for 16 h, the reaction mixture was cooled down and the solvent was removed under vacuum. Diphenylmethane and 2,2-diphenylethan-1-ol were isolated by column chromatography (eluent: hexane:EtOAc, 95:5). The conversion of the starting 2,2-diphenylacetaldehyde was 50% determined by isolation of the remaining starting material (93.7 mg).

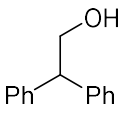

2,2-diphenylethan-1-ol, white solid (46 mg), 24% isolated yield. **^{1}H NMR** (400 MHz, $CDCl_3$) δ 7.34-7.22 (m, 10H, Aromatic H), 4.24-4.16 (m, 1H+2H, OH + CH_2), 1.46 (t, J = 6.1 Hz, 1H, CH). **^{13}C{^{1}H} NMR** (101 MHz, $CDCl_3$) δ 141.3 (C), 128.7 (CH), 128.3 (CH), 126.8 (CH), 66.1 (CH), 53.6 (CH_2). **HR-MS** (CI) m/z 181.1010 $[M-H_2O]^+$ (181.1012 calcd for $C_{14}H_{13}^+$).

NMR data in accordance with the literature data.[119]

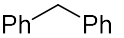

Diphenylmethane, white solid (28 mg), 17% isolated yield. **^{1}H NMR** (400 MHz, $CDCl_3$) δ 7.27-7.19 (m, 10H, Aromatic H), 3.98 (s, 2H, CH_2). **^{13}C{^{1}H} NMR** (101 MHz, $CDCl_3$) δ 141.1 (C), 128.9 (CH), 128.5 (CH), 126.1 (CH), 41.9 (CH_2). **GC-MS** m/z 167.1 $[M-H]^+$ (167.1 calcd for $C_{13}H_{11}^+$).

NMR data in accordance with the literature data.[120]

Reductive C-C bond cleavage of 5-oxo-4,4-diphenylhexanenitrile 10

The reaction was conducted according to the general procedure described in Section 2.13.4. using $Ir(P^iPr_3)_2H_5$ catalyst (8.7 mg, 0.016 mmol, 10 mol%) and 0.8 ml of a stock solution prepared from 5-oxo-4,4-diphenylhexanenitrile **10** (53.2 mg, 0.202 mmol), dodecane (24.8 mg, 0.145 mmol, GC standard) and toluene (1 ml). The reaction mixture was heated at 150 °C for 16 h. The GC analysis of the reaction mixture showed 87% conversion of ketone **10** and formation of 1,1-diphenylacetone and propionitrile in 34 and 10% yield, respectively.

To understand the origin of poor material balance between conversion of ketone **10** and yield of 1,1-diphenylacetone, the catalytic reductive cleavage of ketone **10** was conducted in a larger scale to isolate the products formed:

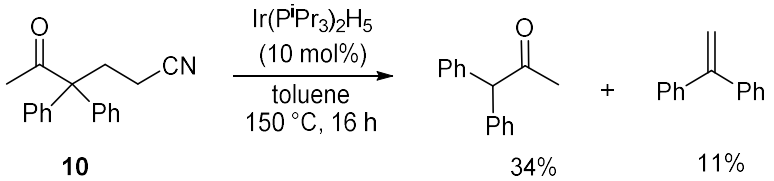

10 34% 11%

This experiment was conducted following the general procedure described in section 2.13.4 using the carbonyl compound **10** (201.2 mg, 0.7646 mmol), $Ir(P^iPr_3)_2H_5$ catalyst (39.1 mg, 0.0764 mmol, 10 mol%) and toluene (3.8 ml). After heating at 150 ºC for 16 h, the reaction mixture was cooled down and the solvent was removed under vacuum. The crude mixture was purified by column chromatography (eluent: hexane:EtOAc, 30:1). The conversion of the starting aldehyde was 70% determined by isolation of the remaining starting material (60.4 mg). Two products were isolated:

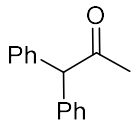

1,1-diphenylpropan-2-one, white solid (54.4 mg), 34% isolated yield. **^{1}H NMR** (400 MHz, $CDCl_3$) δ 7.35-7.22 (m, 10H, Aromatic H), 5.11 (s, 1H, CH), 2.24 (s, 3H, CH_3). **^{13}C{^{1}H} NMR** (101 MHz, $CDCl_3$) δ 206.5 (CO), 138.3 (C), 129.0 (CH), 128.7 (CH), 127.2 (CH), 65.0 (CH), 30.1 (CH_3).

NMR data in accordance with the literature data.[121]

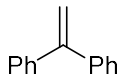

1,1-diphenylethylene, white solid (15.4 mg), 11% isolated yield. **^{1}H NMR** (400 MHz, $CDCl_3$) δ 7.34 (s, 10H, Aromatic H), 5.46 (s, 2H, CH_2=C). **^{13}C{^{1}H}**

NMR (101 MHz, $CDCl_3$) δ 150.0 (C), 141.4 (C), 128.2 (CH), 128.1 (CH), 127.7 (CH), 114.3 (CH_2).

NMR data in accordance with the literature data.[122]

Reductive C-C bond cleavage of methyl 4-cyano-2,2-diphenylbutanoate 11

The reaction was conducted according to the general procedure described in Section 2.13.4. using $Ir(P^iPr_3)_2H_5$ catalyst (8.4 mg, 0.016 mmol, 10 mol%) and 0.8 ml of a stock solution prepared from methyl 4-cyano-2,2-diphenylbutanoate **11** (56.1 mg, 0.201 mmol), dodecane (24.7 mg, 0.145 mmol, GC standard) and toluene (1 ml). The reaction mixture was heated at 150 °C for 24 h. The GC analysis of the reaction mixture showed 29% conversion of ester **16** and formation of methyl 2,2-diphenylacetate and propionitrile in 20 and 12% yield, respectively.

Reductive C-C bond cleavage of 5-(methoxyimino)-4,4-diphenylhexanenitrile 12

The reaction was conducted according to the general procedure described in Section 2.13.4. using $Ir(P^iPr_3)_2H_5$ catalyst (8.2 mg, 0.016 mmol, 10 mol%) and 0.8 ml of a stock solution prepared from 5-(methoxyimino)-4,4-diphenylhexanenitrile **12** (58.5 mg, 0.200 mmol), dodecane (24.7 mg, 0.145 mmol, GC standard) and toluene (1 ml). The reaction mixture was heated at 150 °C for 16 h. The GC analysis of the reaction mixture showed no conversion of oxime **12**.

Reductive C-C bond cleavage of 4-hydroxy-4,4-diphenylbutanenitrile 13

The reaction was conducted according to the general procedure described in Section 2.13.4. using $Ir(P^iPr_3)_2H_5$ catalyst (8.1 mg, 0.016 mmol, 10 mol%) and 0.8 ml of a stock solution prepared from 4-hydroxy-4,4-diphenylbutanenitrile **13** (47.2 mg, 0.199 mmol), dodecane (24.7 mg, 0.145 mmol, GC standard) and toluene (1 ml). The reaction mixture was heated at 150 °C for 24 h. The GC analysis of the reaction mixture showed 73% conversion of alcohol **13** but the expected diphenylmethanol was not detected.

To understand what products were formed during the cleavage of alcohol **13**, this experiment was conducted in larger scale:

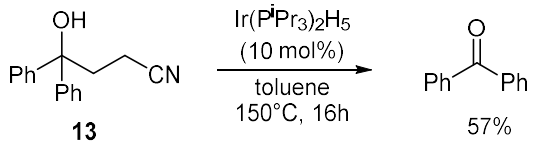

This experiment was conducted following the general procedure described in section 2.13.4 using alcohol **13** (180.3 mg, 0.760 mmol), $Ir(P^iPr_3)_2H_5$ catalyst (39.5 mg, 0.0763 mmol, 10 mol%) and toluene (3.8 ml). After heating at 150 ºC for 16 h, the reaction mixture was cooled down and the solvent was removed under vacuum. The crude mixture was purified by column chromatography (eluent: hexane:EtOAc, 7:1). The conversion of the starting alcohol was 71% as determined by isolation of the remaining starting material (51.9 mg). Two products were isolated:

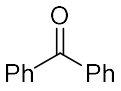

Benzophenone, white solid, 57% GC yield. **^{1}H NMR** (400 MHz, $CDCl_3$) δ 7.85-7.81 (m, 4H, Aromatic H), 7.67-7.63 (m, 2H, aromatic H), 7.56-7.51 (m, 4H, aromatic H). **GC-MS** m/z 182.1 ($C_{13}H_{10}O$) (182.1 calcd for $C_{13}H_{10}O$).

NMR data in accordance with the literature data.[123]

Attempted reductive C-C bond cleavage of 4-methoxy-4,4-diphenylbutanenitrile 14

The reaction was conducted according to the general procedure described in Section 2.13.4. using $Ir(P^iPr_3)_2H_5$ catalyst (8.5 mg, 0.016 mmol, 10 mol%) and 0.8 ml of a stock solution prepared from 4-methoxy-4,4-diphenylbutanenitrile **14** (50.1 mg, 0.199 mmol), dodecane (23.9 mg, 0.140 mmol, GC standard) and toluene (1 ml). The reaction mixture was heated at 150 °C for 16 h. The GC analysis of the reaction mixture showed no conversion of **14**.

Attempted reductive C-C bond cleavage of 5,5-difluoro-4,4-diphenylpentanenitrile 15

The reaction was conducted according to the general procedure described in Section 2.13.4. using $Ir(P^iPr_3)_2H_5$ catalyst (8.7 mg, 0.017 mmol, 10 mol%) and 0.8 ml of a stock

solution prepared from 5,5-difluoro-4,4-diphenylpentanenitrile **15** (54.7 mg, 0.201 mmol), dodecane (24.7 mg, 0.145 mmol, GC standard) and toluene (1 ml). The reaction mixture was heated at 150 °C for 16 h. The GC analysis of the reaction mixture showed no conversion of fluorinated substrate **15**.

Attempted reductive C-C bond cleavage of 2,2-diphenyl-4-pyridylbutanenitrile 16

The reaction was conducted according to the general procedure described in Section 2.13.4. using $Ir(P^iPr_3)_2H_5$ catalyst (8.2 mg, 0.016 mmol, 10 mol%) and 0.8 ml of a stock solution prepared from 2,2-diphenyl-4-pyridylbutanenitrile **16** (44.6 mg, 0.202 mmol), dodecane (24.6 mg, 0.144 mmol, GC standard) and toluene (1 ml). The reaction mixture was heated at 150 °C for 16 h. The GC analysis of the reaction mixture showed no conversion of **16**.

Attempted reductive C-C bond cleavage of methyl 4-cyano-4,4-diphenylbutanoate 17

The reaction was conducted according to the general procedure described in Section 2.13.4. using $Ir(P^iPr_3)_2H_5$ catalyst (8.8 mg, 0.017 mmol, 10 mol%) and 0.8 ml of a stock solution prepared from methyl 4-cyano-4,4-diphenylbutanoate **17** (55.1 mg, 0.197 mmol), dodecane (24.1 mg, 0.141 mmol, GC standard) and toluene (1 ml). The reaction mixture was heated at 150 °C for 16 h. The GC analysis of the reaction mixture showed no conversion of ester **17**.

Reductive C-C bond cleavage of (*E*)-5-(methoxyimino)-2,2-diphenylhexanenitrile 18

The reaction was conducted according to the general procedure described in Section 2.13.4. using $Ir(P^iPr_3)_2H_5$ catalyst (8.2 mg, 0.016 mmol, 10 mol%) and 0.8 ml of a stock solution prepared from (E)-5-(methoxyimino)-2,2-diphenylhexanenitrile **18** (58.4 mg, 0.200 mmol), dodecane (23.5 mg, 0.138 mmol, GC standard) and toluene (1 ml). The reaction mixture was heated at 150 °C for 16 h. The GC analysis of the reaction mixture

showed 23% conversion of oxime **18** and formation of diphenylacetonitrile in 11% yield. No (*E*)-butan-2-one O-methyl oxime was detected.

Reductive C-C bond cleavage of (*Z*)-5-(methoxyimino)-2,2-diphenylhexanenitrile 19

The reaction was conducted according to the general procedure described in Section 2.13.4. using $Ir(P^iPr_3)_2H_5$ catalyst (8.3 mg, 0.016 mmol, 10 mol%) and 0.8 ml of a stock solution prepared from (Z)-5-(methoxyimino)-2,2-diphenylhexanenitrile **19** (58.1 mg, 0.199 mmol), dodecane (25.0 mg, 0.147 mmol, GC standard) and toluene (1 ml). The reaction mixture was heated at 150 °C for 16 h. The GC analysis of the reaction mixture showed 25% conversion of oxime **19** and formation of diphenylacetonitrile in 15% yield. No (*Z*)-butan-2-one O-methyl oxime was detected.

Reductive C-C bond cleavage of 4-(tert-butyloxazoline)-2,2-diphenylbutanenitrile 20

The reaction was conducted according to the general procedure described in Section 2.13.4. using $Ir(P^iPr_3)_2H_5$ catalyst (8.4 mg, 0.016 mmol, 10 mol%) and 0.8 ml of a stock solution prepared from 4-(tert-butyloxazoline)-2,2-diphenylbutanenitrile **20** (69.8 mg, 0.201 mmol), dodecane (23.8 mg, 0.140 mmol, GC standard) and toluene (1 ml). The reaction mixture was heated at 150 °C for 16 h. The GC analysis of the reaction mixture showed 69% conversion of oxazoline **20** and formation of diphenylacetonitrile in 9% yield. No 4-(tert-butyl)-2-ethyl-4,5-dihydrooxazole was detected.

Reductive C-C bond cleavage of 5-oxo-2,2-diphenylnonanenitrile 21

The reaction was conducted according to the general procedure described in Section 2.13.4. using $Ir(P^iPr_3)_2H_5$ catalyst (8.2 mg, 0.016 mmol, 10 mol%) and 0.8 ml of a stock solution prepared from 5-oxo-2,2-diphenylnonanenitrile **21** (61.2 mg, 0.200 mmol), dodecane (24.7 mg, 0.145 mmol, GC standard) and toluene (1 ml). The reaction mixture was heated at 150 °C for 16 h. The GC analysis of the reaction mixture showed full

conversion of ketone **21** and formation of diphenylacetonitrile and heptan-3-one in 96 and 34% yields, respectively.

2.13.7. Ir-catalysed reductive cleavage of C-C single bond of unstrained dinitriles in the presence of diphenylacetonitrile or acrylonitrile

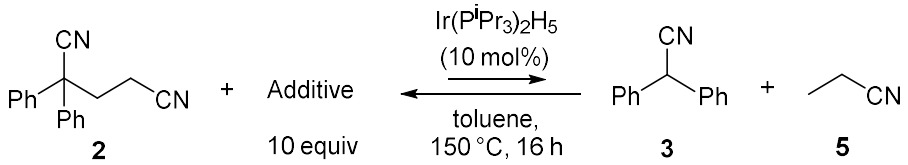

Additive: diphenylacetonitrile

The reaction was conducted according to the general procedure described in Section 2.13.4. using $Ir(P^iPr_3)_2H_5$ catalyst (8.2 mg, 0.016 mmol, 10 mol%) and 0.8 ml of a stock solution prepared from dinitrile **2** (49.9 mg, 0.203 mmol), diphenylacetonitrile **3** (231.7 mg, 1.199 mmol), dodecane (23.9 mg, 0.142 mmol, GC standard) and toluene (1 ml). The reaction mixture was heated at 150 °C for 16 h. The GC analysis of the reaction mixture showed no conversion of dinitrile **2**.

Additive: acrylonitrile

In a glovebox, a stock solution was prepared containing dinitrile **2** (49.3 mg, 0.200 mmol), dodecane (24.6 mg, 0.144 mmol, GC standard) in toluene (1 ml). From this stock solution, 0.8 ml was added into a 10 ml Schlenk bomb charged with $Ir(P^iPr_3)_2H_5$ catalyst (8.7 mg, 0.016 mmol, 10 mol%) and a magnetic stir bar. Then, acrylonitrile (84.9 mg, 1.6 mmol) was added. The Schlenk bomb was sealed, removed from the glovebox and the reaction mixture was heated in an oil bath at 150 °C for 16 h. The GC analysis of the reaction mixture showed no conversion of dinitrile **2**.

2.13.8. Iridium-catalysed hydrogenation and polymerization of acrylonitrile

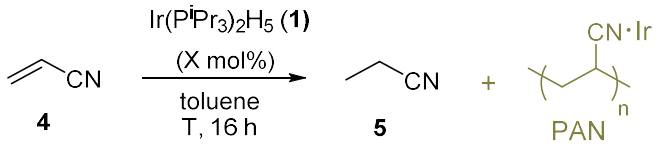

In a glovebox, $Ir(P^iPr_3)_2H_5$ (8.4 mg, 0.015 mmol, 10 mol% or 16.7 mg, 0.0322 mmol, 20 mol%), dodecane (9.9 mg, 0.06 mmol, GC standard) were dissolved in toluene (0.8 ml). Then, acrylonitrile (9.0 mg, 0.16 mmol) was added to the solution, the mixture was stirred for 5 min at room temperature and then transferred into a 10 ml Schlenk bomb. The Schlenk bomb was removed from the glovebox and the reaction mixture was stirred for 16 h at 150 ºC or at room temperature. The reaction vessel with orange solution and a dark orange precipitate was then cooled down and brought back into the glovebox to isolate the solid. A dark orange precipitate (acrylonitrile oligomer) formed during reaction was filtered off, washed with toluene, dried in vacuum and analysed by ^{1}H NMR, MS, EA, IR and ICP. The filtered orange reaction mixture was passed through a short silica gel column (5 ml plastic syringe filled with a 3 cm layer of silica gel) eluting with EtOAc (15 ml) outside the glovebox and was analysed by GC. Propionitrile was identified using GC by comparison of retention times with those of authentic standard. The GC yields and conversions of these experiments at different catalyst loadings and temperatures are shown in Table 2.10.

Table 2.10: Ir-catalysed hydrogenation of acrylonitrile **4**

Entry	T, °C	Catalyst **1**, mol%	Conversion **4**, %	Yield **5**, %
1	150	10	100	22
2	150	20	100	20
3	25	10	69	8
4	25	20	98	11

Polyacrylonitrile. The acrylonitrile oligomer was isolated in 37% yield (based on the starting acrylonitrile). **^{1}H NMR** (500 MHz, DMSO-d_6) δ 2.88-2.55 (br. s, CH), 1.00-1.45 (bs, CH_2). **Elemental Analysis** C, 52.54; H, 5.80; N, 13.70. **MS** (CI^+) m/z 179.0

$(M+NH_4)^+$ (179.1 calcd for trimer $C_9H_{15}N_4$ $(M+ NH_4)^+$). **IR** 3356, 2925, 2871, 2192, 1430, 1230 cm^{-1}. **ICP-OES:** Ir: 53.35 ppm (15 w/w% iridium).

NMR data is in accordance with reported literature data.[124,125]

2.13.9. $Ir(P^iPr_3)_2H_5$-catalysed hydroalkylation of acrylonitrile with diphenylacetonitrile

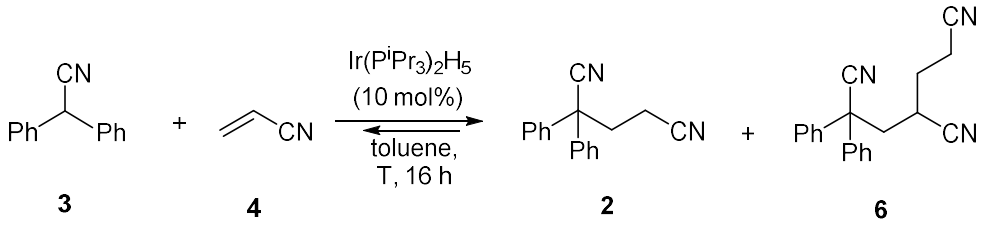

In a glovebox, a stock solution was prepared from diphenylacetonitrile (38.4 mg, 0.198 mmol), acrylonitrile (10.2 mg, 0.192 mmol), dodecane (24.5 mg, 0.143 mmol, GC standard) and toluene (1 ml). From this stock solution, 0.8 ml was added into a 10 ml Schlenk bomb charged with $Ir(P^iPr_3)_2H_5$ catalyst (8.3 mg, 0.016 mmol, 10 mol%) and a magnetic stir bar. The Schlenk bomb was sealed, removed from the glovebox and the reaction mixture was stirred for 16 h at room temperature or at 150 °C in an oil bath. Then, the reaction mixture was cooled down and passed through a short silica gel column (5 ml plastic syringe filled with a 3 cm layer of silica gel) eluting with 15 ml of EtOAc. The treated reaction mixture was analysed by GC.

Note, for experiment with 10-fold excess of acrylonitrile, the alkene was added (102.00 mg, 2.00 mmol) to a 10 ml Schlenk bomb containing 0.8 ml of a solution prepared from diphenylacetonitrile (37.9 mg, 0.196 mmol), dodecane (24.5 mg, 0.143 mmol, GC standard), $Ir(P^iPr_3)_2H_5$ catalyst (8.3 mg, 0.016 mmol, 10 mol%) and toluene (1 ml).

Results of GC analyses of the treated reaction mixtures are shown in Table 2.11.

Table 2.11: Ir-catalysed hydroalkylation of acrylonitrile **4** with diphenylacetonitrile **3**

Entry	Ratio **3** : **4**	T, °C	Conversion, %		Yield, %	
			3	**4**	**2**	**6**
1	1:1	150	15	100	15	0
2	1:1	25	71	100	69	0
3	1:10	150	88	80	64	21
4	1:10	25	81	59	52	25

[a]: Propionitrile and polyacrylonitrile were formed as side products

2.13.9.1. $Ir(P^iPr_3)_2H_5$-catalysed hydroalkylation of acrylonitrile with diphenylacetonitrile: scaled-up experiment for the isolation of trinitrile 6

When the hydroalkylation experiment was conducted with 10 equiv. of acrylonitrile, trinitrile **6** was formed according to GC-MS analyses. To isolate this product, the catalytic hydroalkylation of acrylonitrile (10 equiv) with diphenylacetonitrile (1 equiv) was conducted in larger scale:

The reaction was conducted according to the general procedure using diphenylacetonitrile (78.4 mg, 0.406 mmol) and $Ir(P^iPr_3)_2H_5$ catalyst (20.6 mg, 0.0398 mmol, 10 mol%) dissolved in toluene (2 ml). Acrylonitrile (209.7 mg, 3.95 mmol) was subsequently added to the mixture. The reaction mixture was heated at 150 °C in an oil bath for 16 h, cooled down and concentrated under vacuum. The crude reaction mixture was purified by column chromatography (silica gel, eluent: 10-30% EtOAc in hexane) which gave dinitrile **2** (59.9 mg) and trinitrile **6** (13.9 mg) as white solids in 60% and 12% yield, respectively. The conversion of diphenylacetonitrile was 80% determined by isolation of the remaining starting material (15.7 mg).

Both products **2** and **6** were identified by NMR spectroscopy and HRMS (in case of product **6**).

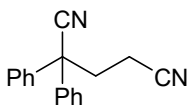

2

2. **^{1}H NMR** (400 MHz, $CDCl_3$) δ 7.51 – 7.29 (m, 10H, Aromatic H), 2.90 – 2.72 (m, 2H, CH_2), 2.55 – 2.37 (m, 2H, CH_2).

^{1}H NMR data in accordance with the characterisation data of the synthesised dinitrile **2** (Section 2.13.3).

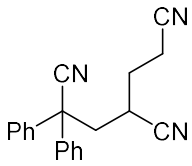

6

6. ^{1}**H NMR** (500 MHz, $CDCl_3$) δ 7.48 – 7.34 (m, 10H, aromatic H), 2.99 (dd, *J* = 14.1, 7.8 Hz, 1H, 1 Ph_2C-C**H**$_2$), 2.87 – 2.80 (m, 1H, CN-**CH**), 2.64 (dd, J= 14.2, 4.2 Hz, 1H, 1 Ph_2C-C**H**$_2$), 2.60 (ddd, J= 17.0, 7.8 Hz, 1H, CN-CH_2-C**H**$_2$), 2.49 (dt, 17.0, 8.0, 8.0 Hz, 1H, CN-CH_2-C**H**$_2$), 2.13 – 1.97 (m, 2H, CN-C**H**$_2$-CH_2). ^{13}**C{**^{1}**H} NMR** (101 MHz, $CDCl_3$) δ 138.7 (C), 137.5 (C), 129.4 (CH), 129.4 (CH), 129.0 (CH), 128.8 (CH), 126.9 (CH), 126.6 (CH), 120.9 (CN), 118.6 (CN), 117.4 (CN), 50.3 (CH), 41.2 (CH_2), 29.1 (CH), 27.9 (CH_2), 15.1 (CH_2). **HRMS** (CI+) m/z 317.1766 $(M+NH_4)^+$ (317.1761 calcd for $C_{20}H_{17}N_3$ $(M+NH_4)^+$).

2.13.10. Stoichiometric experiment with dimethylated substrate 22 and Ir(P^{i}Pr$_3$)$_2$H$_5$ complex

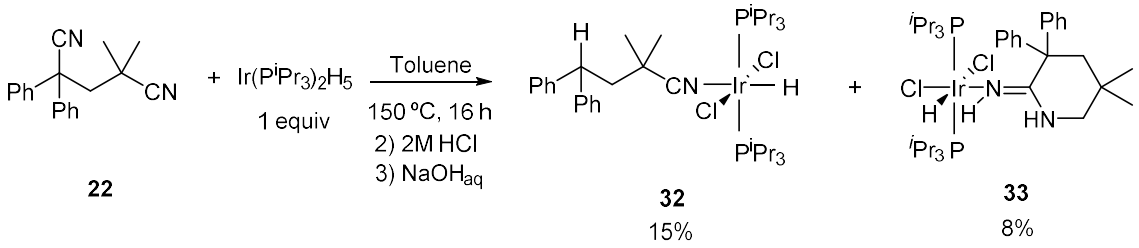

22 32 15% 33 8%

In a glovebox, Ir(P^{i}Pr$_3$)$_2$H$_5$ (80.7 mg, 0.159 mmol), dinitrile substrate **22** (43.9 mg, 0.16 mmol), toluene (0.8 ml) and a magnetic stir bar were placed into a 10 ml Schlenk bomb. The Schlenk bomb was sealed, and the reaction mixture was stirred for 5 min at room temperature. Then the Schlenk bomb was removed from the glovebox and the reaction mixture was heated in an oil bath at 150 °C for 16 h. The reaction mixture was then cooled down, treated with 2M aqueous solution of HCl (2 ml) and stirred for 10 min. Then, 1M aqueous solution of NaOH (1M) was added until reaching pH = 10 and the mixture was extracted with toluene (3 x 1 ml). The combined organic layers were dried over $MgSO_4$ and the products were isolated by column chromatography (silica gel, eluent: 5-50% ethyl acetate in hexane).

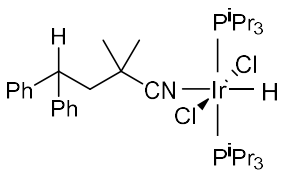

Complex **32**. Yellowish solid (20.4 mg). 15% isolated yield. **^{1}H NMR** (400 MHz, $CDCl_3$) δ 7.32 (d, *J* = 7.4 Hz, 4H, aromatic H), 7.26 (t, J= 7.6 Hz, 4H, aromatic H), 7.16 (t, J= 7.2 Hz, 2H, aromatic H), 4.37 (t, J= 6.7 Hz, 1H, CH), 2.88 (m, 6H, 6CH), 2.46 (d, *J* = 6.8 Hz, 2H, CH_2), 1.33 (q, *J* = 13.4, 6.7 Hz, 36H, $12CH_3$), 1.22 (s, 6H, $2CH_3$), -23.90 (m, 1H, hydride). **^{13}C{^{1}H} NMR** (101MHz, $CDCl_3$) δ 144.8 (C), 128.9 (CH), 127.8 (CH), 126.7 (CH), 120.9 (CN), 48.7 (CH_2), 45.7 (CH), 38.1 (C), 27.4 ($2CH_3$), 22.1 (**C**H-P), 19.0 (**C**H_3-CH-P) **^{31}P {^{1}H} NMR** (400 MHz, $CDCl_3$) δ 6.63. **MS** (EI^+) m/z 249.1 [M-Ir($PiPr_3$)$_2Cl_2H$]$^+$ (249.1 calcd for $C_{18}H_{19}N$) **Elemental Analysis** Calcd for ($C_{36}H_{62}Cl_2IrNP_2$): C, 51.85; H, 7.49; N, 1.68; Found C, 51.57; H, 7.48; N, 1.83. **X-Ray** structure in Section 2.13.17.1.

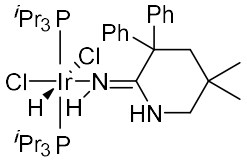

Complex **33**. Yellowish solid (11.0 mg). 8% isolated yield. **^{1}H NMR** (500 MHz, d_8-toluene) δ 11.05 (bs, 1H, NH), 6.87-7.03 (m, 10H, aromatic H), 5.13 (bs, 1H, NH), 2.72 (d, J = 4.06 Hz, 2H, CH_2), 2.60 (m, 6H, 6CH), 2.03 (s, 2H, CH_2), 1.24 (m, 36H, $12CH_3$), 0.61 (s, 6H, $2CH_3$), -25.28 (t, J= 13.57 Hz, 1H, hydride). **^{31}P {^{1}H} NMR** (202 MHz, d_8-toluene) δ 2.96 ppm **MS** (ES+) m/z 791.4 [M-HCl-Cl] (791.4 calcd for $C_{37}H_{64}IrN_2P_2$). **X-Ray** structure in Section 2.13.17.2.

2.13.11. Deuterium labelling studies

2.13.11.1. Deuterium labelling experiments with 2,2-dideuterium-4,4-diphenylpentanedinitrile (2-d_2)

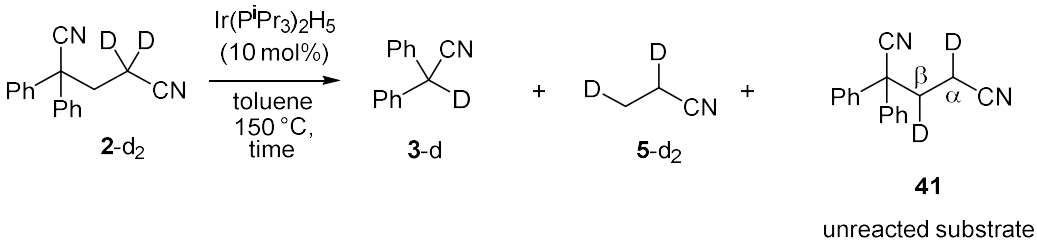

The reaction was conducted according to the general procedure described in Section 2.13.4. using Ir(P^iPr_3)$_2H_5$ catalyst (6.4 mg, 0.012 mmol, 10 mol%), 2,2-dideuterio-4,4-diphenylpentanedinitrile **2-**d_2 (30.8 mg, 0.12 mmol), *p*-dimethoxybenzene (11.9 mg, GC

standard) and toluene (0.6 ml). After heating the reaction mixture at 150 ºC for the specified time, (1 or 16 h), d_8-THF (3.0 mg, ^{2}H NMR standard) was added to the reaction mixture inside a glovebox and the mixture was transferred into a J Young tube to record ^{2}H NMR. After recording ^{2}H NMR spectrum, the reaction mixture from the NMR sample was passed through short silica gel column (5 ml plastic syringe filled with 3 cm of silica gel) eluting with EtOAc (15 ml). The resulting solution was analysed by GC.

Absolute D % contents were determined based on the ratio of ^{2}H NMR and GC yields (^{2}H NMR yield corresponds to the yield of deuterated compound and GC yield corresponds to the total yield of deuterated and non-deuterated compound). Relative D % contents were determined based on ^{2}H NMR, as the ratio of (D integration area of the signal of interest)/(total D integration area of compound), e.g. for propionitrile, the relative D% content of CH_3 group was calculated based on (integral D of CH_3)/(sum of integrals D of CH_3 and CH_2). The ^{2}H NMR and GC analyses of these experiments are shown in Table 2.12 and 2.13.

Table 2.12: ^{2}H NMR conversions and yields (The experiment was duplicated at 1 h and 16 h)

Reaction code	Time, h	Conversion **2**-d_2, %	Yield **3**-d, %	Yield **5**-d_2 , % "CH_2"	"CH_3"	Yield **41** (β-position), %
MFG365	1	81	22	23	3	4
MFG377	1	84	23	22	6	6
MFG369	16	92	20	31	9	8
MFG375	16	88	28	32	9	15

Table 2.13: GC conversions and yields (Reported yields and conversions correspond to total amount of deuterated and non-deuterated compound)

Reaction code	Time, h	Conversion (**2** + **2**-d_2 + **41**), %	Yield (**3** + **3**-d), %	Yield (**5** + **5**-d_2), %
MFG365	1	33	33	18
MFG377	1	32	31	20
MFG369	16	58	46	14
MFG375	16	63	62	23

Absolute (in red) and relative (in blue) deuterium content in %

MFG365

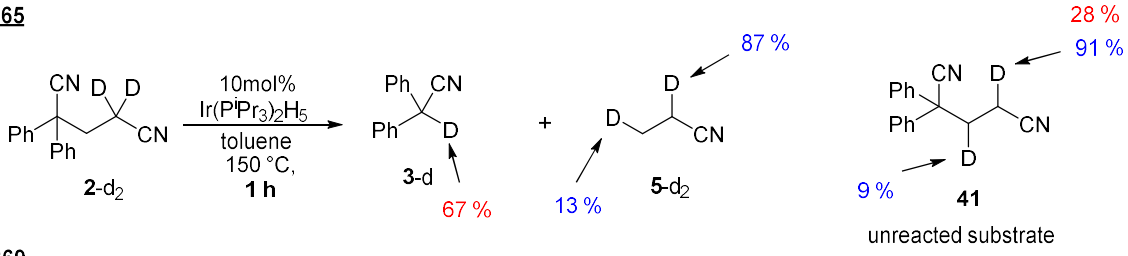

MFG369

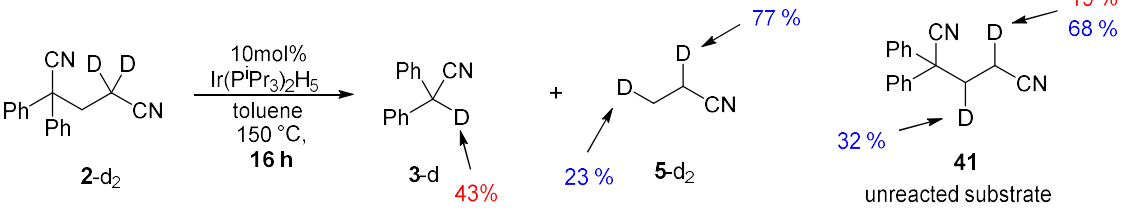

MFG377

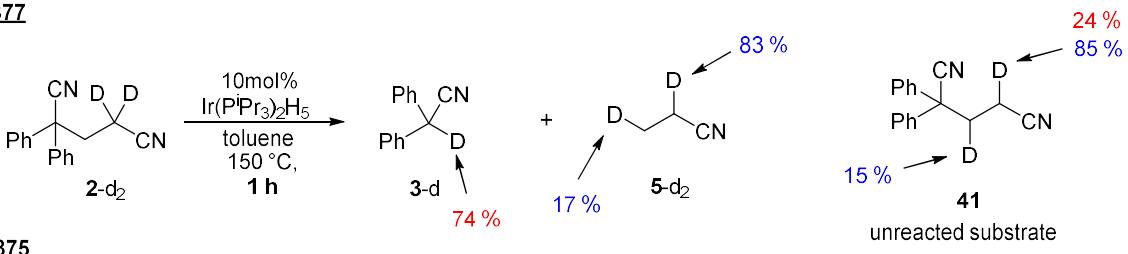

MFG375

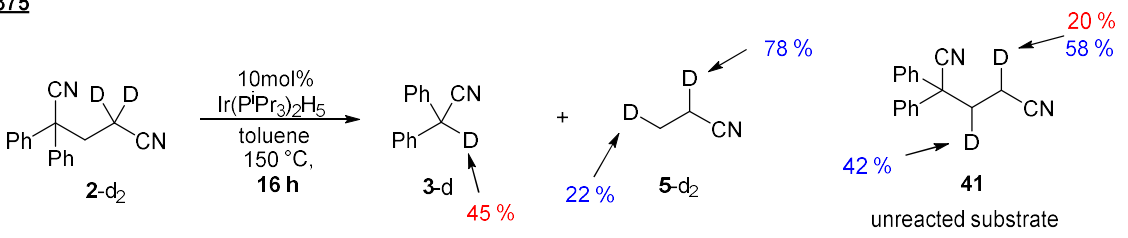

Average absolute and relative deuterium content in %

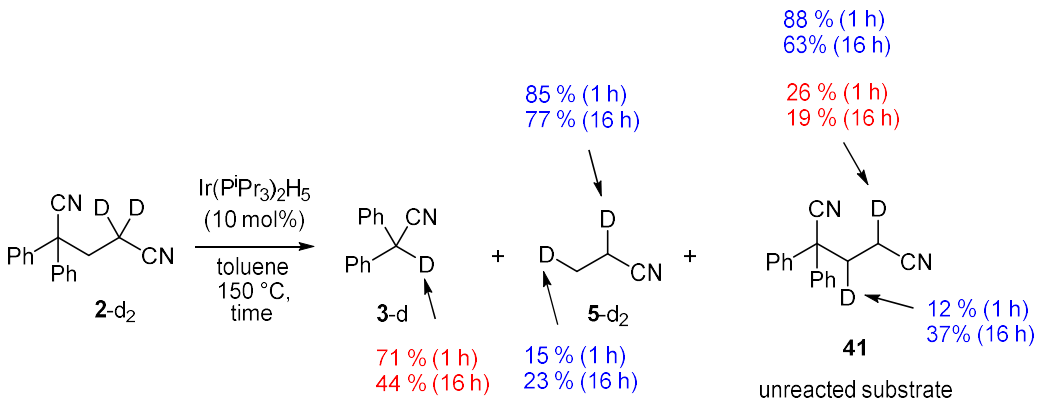

2.13.11.2. Deuterium labelling experiments with 2-deuterium-2,2-diphenylacetonitrile (3-d)

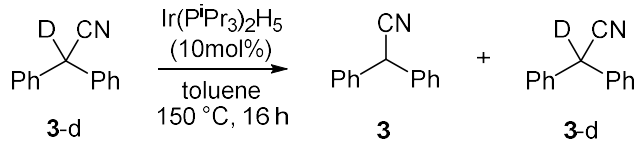

The reaction was conducted according to the general procedure described in Section 2.13.4. using $Ir(P^iPr_3)_2H_5$ catalyst (6.2 mg, 0.012 mmol, 10 mol%), 2-deuterio-2,2-diphenylacetonitrile **3**-d (23.2 mg, 0.12 mmol), *p*-dimethoxybenzene (11.9 mg, GC standard) and toluene (0.6 ml). After heating the reaction mixture at 150 ºC for the specified time, (1 or 16 h), d_8-THF (3.0 mg, ^2H NMR standard) was added to the reaction mixture inside a glovebox and it was transferred to a J Young tube to record ^2H NMR. After recording ^2H NMR spectrum, the reaction mixture from the NMR sample was passed through short silica gel column (5 ml plastic syringe filled with 3 cm of silica gel) eluting with EtOAc (15 ml). The treated reaction mixture was analysed by GC (Table 2.14).

Table 2.14: Absolute deuterium content of **3**-d based on ^2H NMR (this experiment was triplicated)

Reaction code	Time, h	D content **3**-d, %
MFG385	16	72
MFG386	16	71
MFG369	16	69

Average D content **3**-d = 71%

2.13.12. General procedure for NMR monitoring of iridium-catalysed reactions

In a glovebox, $Ir(P^iPr_3)_2H_5$ catalyst (6.70 mg, 0.01 mmol), nitrile substrate (0.12 mmol) and *p*-dimethoxybenzene (3.2 mg, 0.023 mmol, NMR standard) were dissolved in d_8-toluene (0.6 ml) and transferred to a J Young tube. Experiments performed at temperatures up to 100 °C were conducted in the J Young tube and heated in an oil bath or inside the NMR instrument (specified in each experiment). Experiments performed at temperatures above 100 °C were conducted in a 10 ml Schlenk bomb. The reaction mixtrures were heated in an oil bath for specified time, cooled down and transferred to a J Young tube inside a glovebox. After recording ^1H and ^{31}P NMR spectra, the NMR tube was brought back into the glovebox and the solution was transferred back into a Schlenk bomb for continuing heating and recording NMR at subsequent reaction times.

2.13.12.1. NMR monitoring experiment of $Ir(P^iPr_3)_2H_5$-catalysed cleavage of C-C bond of dinitrile 2

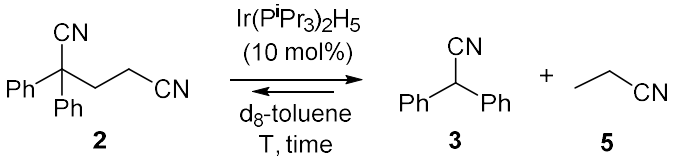

The reaction was conducted according to the general procedure described in Section 2.13.12. using $Ir(P^iPr_3)_2H_5$ catalyst (6.5 mg, 0.013 mmol), dinitrile **2** (32.1 mg, 0.13 mmol), *p*-dimethoxybenzene (3.3 mg, 0.023 mmol, NMR standard) and d_8-toluene (0.6 ml). Tables 2.15, 2.16 and 2.17 show ^1H NMR yields and conversions of the model catalytic C-C cleavage reaction with substrate **2** at different temperatures and times.

Table 2.15: ^1H NMR yields and conversions of the Ir-catalysed cleavage of dinitrile **2** at 150 °C

Time	Conversion **2**, %	Yield **3**, %	Yield **5**, %
0	0	0	0
5 min	37	34	15
30 min	54	54	19
1 h	54	54	19
22 h	68	68	19
42h	70	68	19

Table 2.16: ^{1}H NMR yields and conversions of the Ir-catalysed cleavage of dinitrile **2** at 80 °C (J Young tube heated in an oil bath)

Time, h	Conversion **2**, %	Yield **3**, %	Yield **5**, %
0	0	0	0
0.5	27	12	12
1	29	12	12
2	30	12	12
4	34	16	14
6	35	20	14
19	35	20	14
21	35	20	14

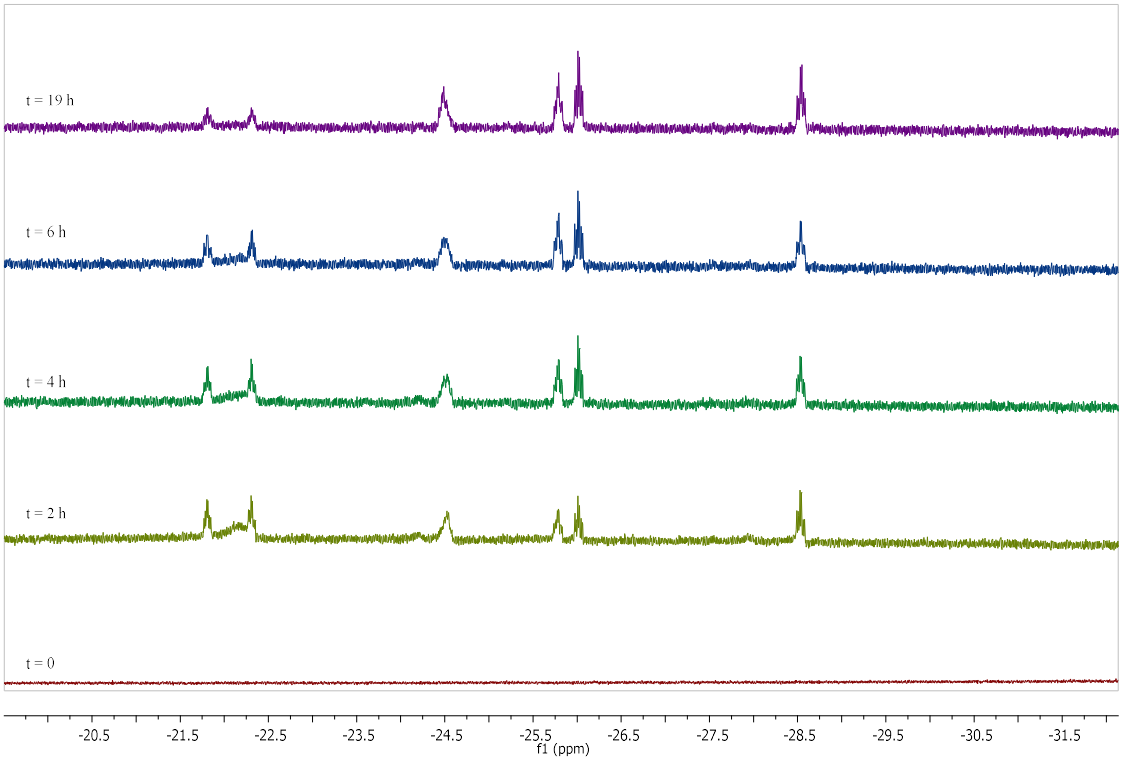

Figure 2.25: Stacked ^{1}H NMR spectra of model reaction conducted at 80 °C (hydride region)

Table 2.17: ^{1}H NMR yields and conversions of the Ir-catalysed cleavage of dinitrile **2** at 80 °C (16 h) followed by subsequent heating at 150 °C (16 h)

T, °C	Time, h	Conversion **2**, %	Yield **3**, %	Yield **5**, %
80	16	35	20	13
150	16	68	68	21

2.13.12.2. NMR monitoring of the reaction of diphenylacetonitrile and $Ir(P^iPr_3)_2H_5$

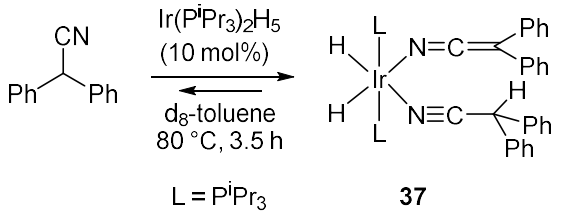

The reaction was conducted according to the general procedure described in Section 2.13.12. using $Ir(P^iPr_3)_2H_5$ catalyst (6.4 mg, 0.012 mmol), diphenylacetonitrile **3** (23.2 mg, 0.12 mmol), *p*-dimethoxybenzene (3.4 mg, 0.025 mmol, NMR standard) and d_8-toluene (0.6 ml) at 80 °C. Tables 2.18 and 2.19 show ^{1}H NMR yields of **37** and conversions of the starting complex and **3**:

Table 2.18: ^{1}H NMR yields and conversions of the reaction of diphenylacetonitrile and $Ir(P^iPr_3)_2H_5$

Time, h	Conversion $Ir(P^iPr_3)_2H_5$, %	Conversion **3**, %	Yield complex **37**, %
0	0	0	0
2	80	11	80
4	99	28	79
6	100	31	75
19	100	31	55
21	100	31	51

Table 2.19: ^{1}H NMR yields and conversions of the reaction of diphenylacetonitrile and $Ir(P^{i}Pr_3)_2H_5$ at earlier times:

Time, h	Conversion $Ir(P^{i}Pr_3)_2H_5$, %	Conversion **3**, %	Yield complex **37**, %
0	0	0	0
0.5	40	10	42
1	60	16	60
2	91	28	86
2.5	95	29	89
3	98	27	80
3.5	100	27	80

2.13.12.3. NMR monitoring of the reaction of acrylonitrile with complex 37

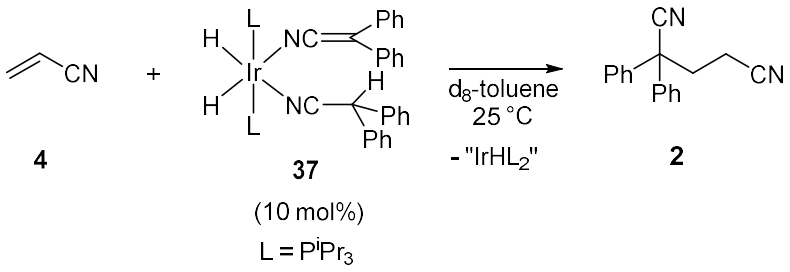

The reaction was conducted according to the general procedure described in Section 2.13.12. using complex **37** (10.8 mg, 0.012 mmol), *p*-dimethoxybenzene (3.6 mg, 0.026 mmol, NMR standard) and d_8-toluene (0.6 ml). ^{1}H and ^{31}P NMR were recorded at time zero before the addition of acrylonitrile. Then, the sample was brought inside the glovebox and acrylonitrile **4** (6.4 mg, 0.12 mmol) was added. Table 2.20 shows ^{1}H NMR yields and conversions of the experiment conducted at room temperature.

Table 2.20: ^{1}H NMR yields and conversions of the reaction of acrylonitrile and complex **37** at rt

Time, h	Conversion **4**, %	Conversion complex **37**, %	Yield **2**, %	Yield **5**, %
0 (before addition of acrylonitrile)	0	0	0	0
10 min	66	100	85	0
1	70	100	85	0
2	75	100	89	0
16	90	100	90	0

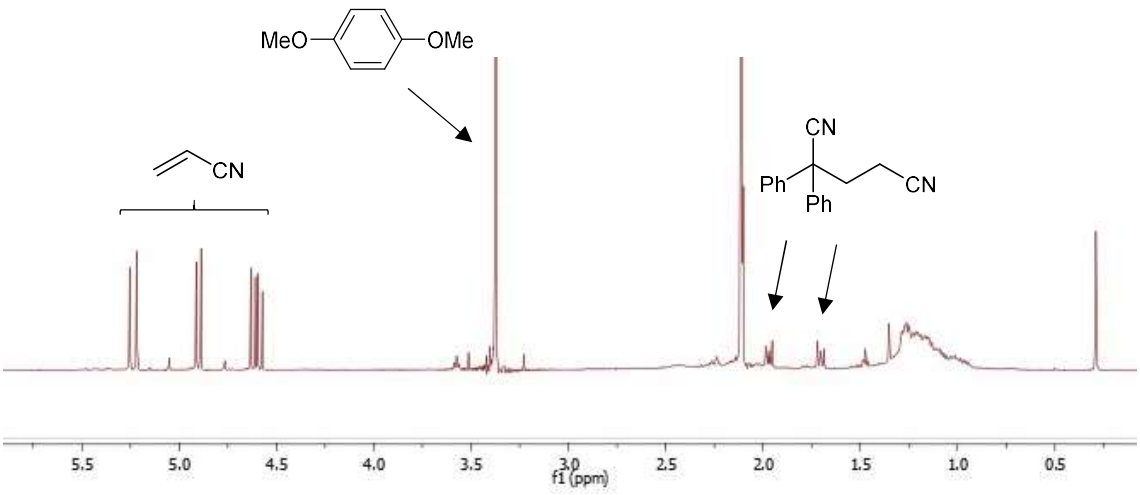

Figure 2.26: ^{1}H NMR spectrum of experiment with complex **37** and acrylonitrile at room temperature (t= 10 min)

2.13.12.4. NMR monitoring experiment of the reaction of acrylonitrile and $P^{i}Pr_3$ with complex 37

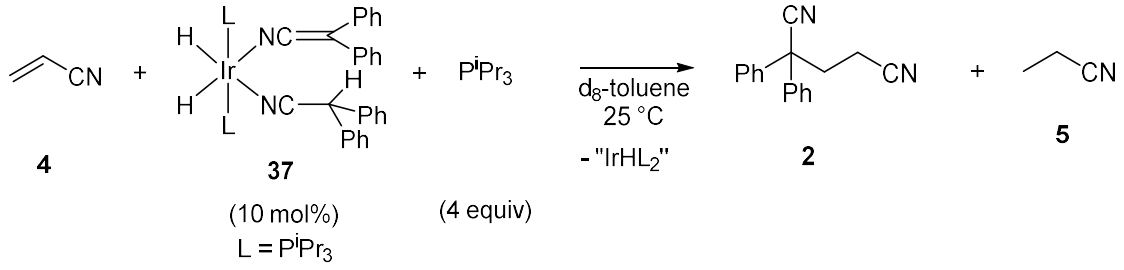

The reaction was conducted according to the general procedure described in Section 2.13.12. using complex **37** (10.8 mg, 0.0119 mmol), $P^{i}Pr_3$ (7.72 mg, 0.0482 mmol) and *p*-dimethoxybenzene (3.6 mg, 0.026 mmol, NMR standard) and d_8-toluene (0.6 ml). Then, acrylonitrile **4** (6.5 mg, 0.12 mmol) was added. Firstly, the reaction was conducted at room temperature but no new phosphine species were observed. For this reason, the reaction mixture was heated at 80 °C. Table 2.21 shows ^{1}H NMR yields and conversions of the experiment conducted at room temperature and the subsequent heating of the same sample at 80 ºC.

Table 2.21: ^{1}H NMR yields and conversions of the reaction of acrylonitrile and complex **37** at rt and the subsequent heating at 80 ºC.

Time	T, °C	Conversion **4**, %	Conversion complex **37**, %	Yield **2**, %	Yield **5**, %
10 min	25	79	100	80	0
1 h	25	80	100	92	0
2 h	25	82	100	92	0
30 min	80	95	100	100	8
1 h	80	96	100	100	8
2 h	80	98	100	100	13
16 h	80	100	100	100	18

2.13.12.5. NMR monitoring of the reaction of 2,2-diphenylpentanedinitrile with $Ir(P^{i}Pr_3)_2H_5$ (1 equiv)

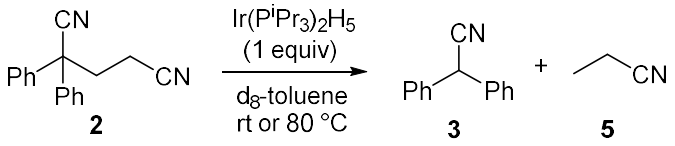

In a glovebox, $Ir(P^{i}Pr_3)_2H_5$ complex (80.7 mg, 0.16 mmol) and 2,2-diphenylpentanedinitrile **2** (38.2 mg, 0.16 mmol) were dissolved in d_8-toluene (0.7 ml). The mixture was transferred into a J Young tube. ^{1}H and ^{31}P NMR were recorded at room temperature at time zero. The J Young tube was placed inside the NMR instrument and the reaction was monitored by NMR at room temperature or 80 ºC.

T = 80 °C

The shifted chemical shifts from t = 5 min is explained by the difference of chemical shifts of the starting iridium complexes at room temperature and 80 °C.

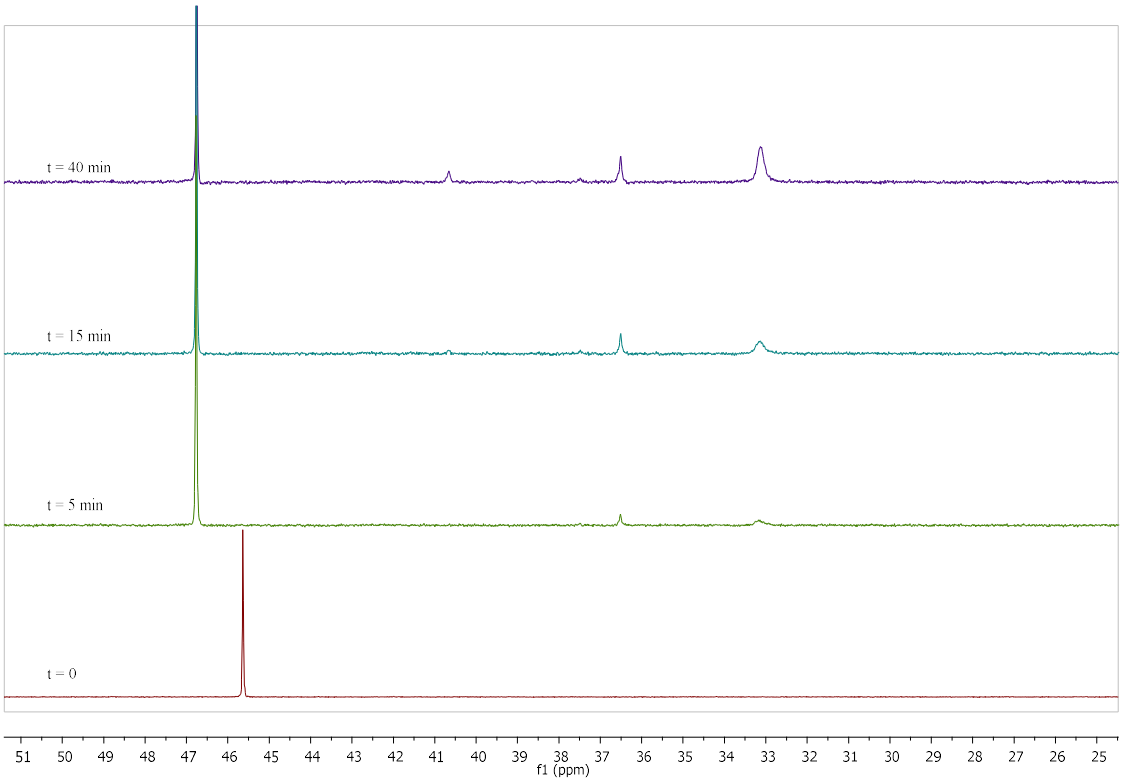

Figure 2.28: Stacked ^{31}P NMR spectra of the reaction mixture of dinitrile **2** and $Ir(P^iPr_3)_2H_5$ (1 equiv) at 80 °C. The spectrum at t = 0 min was recorded at room temperature.

T = room temperature

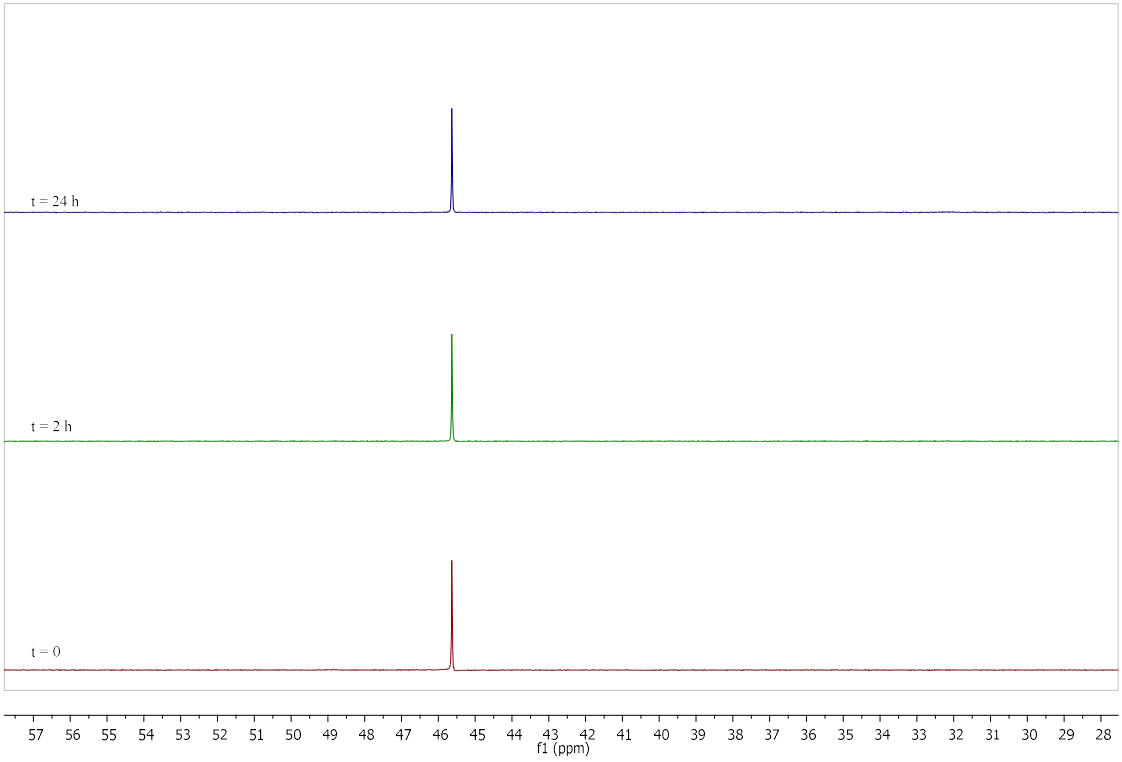

Figure 2.29: Stacked ^{31}P NMR spectra of the reaction mixture of dinitrile **2** and $Ir(P^iPr_3)_2H_5$ (1 equiv) at room temperature

2.13.13. Independent synthesis and isolation of intermediate complexes

2.13.13.1. Synthesis of complex 37

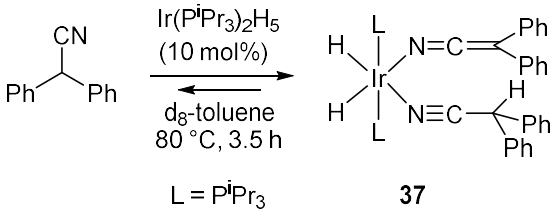

In a glovebox, a 10 ml Schlenk bomb was charged with $Ir(P^iPr_3)_2H_5$ complex (40.3 mg, 0.08 mmol), diphenylacetonitrile (150.5 mg, 0.80 mmol) and toluene (3 ml). The Schlenk bomb was removed from the glovebox and the reaction mixture was heated at 80 °C for 3.5 h. The reaction vessel with an orange solution was then cooled down and brought

back into the glovebox. The reaction mixture was concentrated under vacuum to give crude **37** as yellow solid. The complex was obtained after recrystallization from addition of hexane to a solution of the complex in toluene (Toluene:Hexane, 1:3, v/v) as dark orange crystals (39.4 mg) in 56% yield. **^{1}H-NMR** (500 MHz, d_8-THF, - 60 °C) δ 7.45 (m, 10H, aromatic H), 7.25 (d, 7.9 Hz, 4H, aromatic H), 6.92 (t, 7.7 Hz, 4H, aromatic H), 6.42 (t, 7.15 Hz, 2 H, aromatic H), 6.20 (s, 1H, CH), 2.24 (m, 6H, 6CH), 1.16 (quint, 7.0 Hz, 14.0 Hz, 36 H, 12CH_3), -21.72 (td, 8 Hz, 16 Hz, 1H, hydride), -22.12 (td, 8 Hz, 16 Hz, 1H, hydride). **^{13}C{^{1}H} NMR** (126 MHz, d_8-THF) δ 145.4 (N=**C**=C), 130.7 (CH), 129.8 (CH), 129.5 (CH), 128.8 (CH), 123.3 (CH), 117.8 (CN), 58.7 (N=C=**C**), 44.4 (C-P), 20.7 (CH_3). **^{31}P NMR** (202 MHz, d_8-THF, - 60 °C) 31.9 ppm. **Elemental Analysis** Calcd for ($C_{46}H_{65}IrN_2P_2$): C, 61.38; H, 7.28; N, 3.11; Found C, 61.52; H, 7.14; N, 3.19. **MS** (ES+) m/z 708.3 (M-Ph_2C=C=N)$^+$ (708.3 calcd for $C_{32}H_{55}NIrP_2$ (M-Ph_2C=C=N)$^+$). **X-Ray** structure in Section 2.13.17.3.

2.13.13.2. Stoichiometric reaction of 2,2-diphenylpentanedinitrile with Ir(P^{i}Pr$_3$)$_2$H$_5$

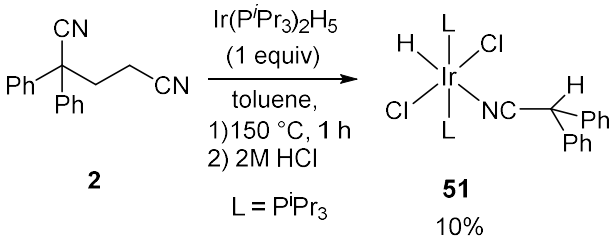

2 **51**

10%

In a glovebox, a 10 ml Schlenk bomb was charged with Ir(P^{i}Pr$_3$)$_2$H$_5$ complex (80.7 mg, 0.16 mmol), 2,2-diphenylpentanedinitrile **2** (38.2 mg, 0.16 mmol) and toluene (0.7 ml). The Schlenk bomb was removed from the glovebox and the reaction mixture was heated at 150 °C for 1 h. The reaction mixture was cooled down, treated with 2 M HCl aqueous solution (2 ml), neutralized with 1M NaOH aqueous solution until reaching a pH=10. The mixture was extracted with ethyl acetate (3 x 2 ml) and the combined extracts were dried over $MgSO_4$. The product was isolated by column chromatography (0-50% ethyl acetate in hexane) as a yellowish solid (11.2 mg) in 10% yield.

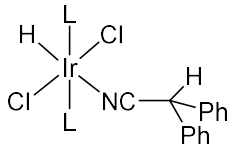

Complex **51**. Isolated yield 10%. **^{1}H NMR** (400 MHz, $CDCl_3$) δ 7.42-7.25 (m, 10H, aromatic H), 5.36 (bs, 1H, CH), 2.81 (m, 6H, 6CH), 1.24 (q, *J* = 6.7 Hz, 7.0 Hz, 36H, $12CH_3$), -23.93 (t, 12.97 Hz, 1H, hydride). **^{13}C{^{1}H} NMR** (101 MHz, $CDCl_3$) δ 134.8 (C), 129.2 (CH), 128.4 (CH), 128.1 (CH), 120.9 (CN), 43.4 (CH), 21.7 (CH), 18.6 (CH_3). **^{31}P{^{1}H} NMR** (162 MHz, $CDCl_3$) δ 6.01 (d, J= 11.1 Hz). **Elemental Analysis** Calcd for ($C_{33}H_{57}Cl_2IrNP_2$): C, 49.99; H, 7.25; N, 1.77; Found C, 50.57; H, 7.10; N, 1.98. **HRMS** (ESI) m/z 742.3022 [M-Cl] (742.3049 calcd for $C_{32}H_{54}IrClNP_2$ [M-Cl]). **IR** 2957, 2923, 2869, 2287 cm^{-1}. **X-Ray** structure in Section 2.13.17.4.

2.13.13.3. NMR monitoring of the reaction mixture of complex 37 with hydrochloric acid

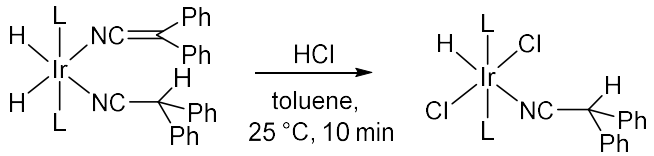

37 **51**

Complex **37** (6.5 mg, 7.2 mmol) was dissolved in d_8-toluene (0.7 ml) and ^{1}H and ^{31}P NMR were recorded. Then, 4 M HCl in dioxane solution (0.01 ml) was added into the reaction mixture under argon atmosphere and ^{1}H and ^{31}P NMR were recorded after 10 min and 1 h. In a glovebox, the reaction mixture was concentrated under vacuum and was cooled down in a freezer at -28 °C to allow precipitation. The resulting yellowish crystals were dried under vacuum and were obtained in 61% isolated yield (3.48 mg). **^{1}H NMR** (400 MHz, d_8-toluene) δ 7.15-6.94 (m, 10H, aromatic H), 4.38 (br. s, 1H, CH), 2.39 (m, 6H, 6CH), 1.34-1.22 (m, 36H, $12CH_3$), -23.47 (br. s, 1H, hydride). **^{31}P{^{1}H} NMR** (162 MHz, d_8-toluene) δ 7.01 (d, J= 11.1 Hz).

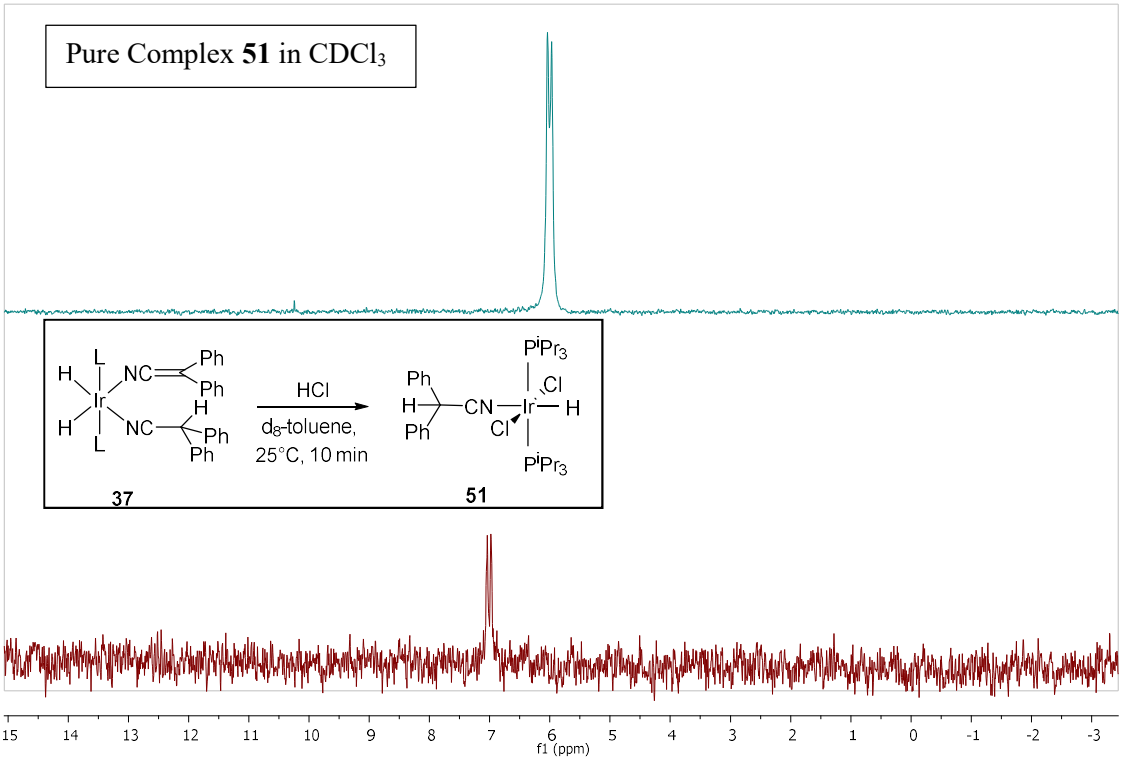

Figure 2.27: Stacked ^{31}P NMR of pure complex **51** in $CDCl_3$ and complex **51** obtained from acidic treatment of complex **37**

2.13.14. Iridium-catalyzed C-C hydrogenolysis of 2,2-diphenylpentanedinitrile in the presence of hydrogen

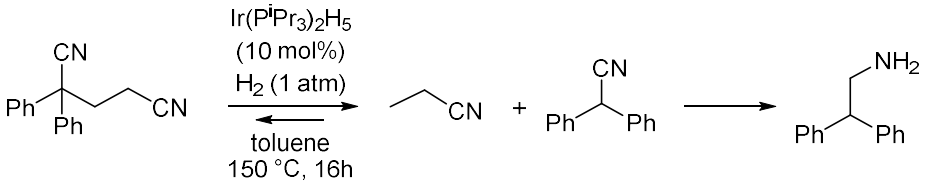

In a glovebox, a stock solution was prepared containing 2,2-diphenylpentanedinitrile **2** (49.3 mg, 0.200 mmol), dodecane (24.7 mg, 0.14 mmol, GC standard) and toluene (1 ml). From this stock solution, 0.8 ml was added into a 10 ml Schlenk bomb charged with $Ir(P^iPr_3)_2H_5$ catalyst (8.3 mg, 0.016 mmol, 10 mol%) and a magnetic stir bar. The Schlenk tube was sealed and removed from the glovebox. The reaction mixture was degassed through two cycles of freeze-pump-thaw and the tube was pressurized with 1 atm of hydrogen at room temperature. The reaction mixture was heated in an oil bath at 150 °C

for 16 h. Then, the reaction mixture was cooled down and was passed through a short silica gel column (5 ml plastic syringe filled with a 3 cm layer of silica gel) eluting with 15 ml of EtOAc. The resulting solution was analysed by GC and GC/MS. All products were known compounds and were identified using GC-MS and GC by comparison of retention times and the mass spectra with those of authentic standard. GC and GC/MS analyses showed 90% conversion of the dinitrile **2** and formation of diphenylacetonitrile and propionitrile in 17 and 33% yields, respectively. In addition, 2,2-diphenylethan-1-amine was formed in 35% yield.

2.13.14.1. Iridium-catalysed hydrogenation of diphenylacetonitrile

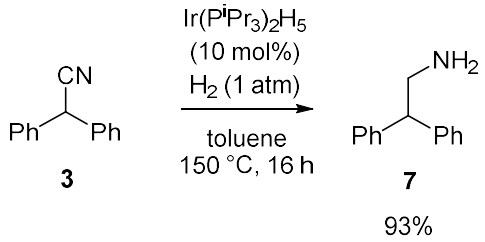

This experiment was conducted according to the procedure described in Section 2.13.14 using $Ir(P^iPr_3)_2H_5$ catalyst (8.5 mg, 0.016 mmol, 10 mol%) and 0.8 ml of a stock solution prepared from diphenylacetonitrile (38.6 mg, 0.20 mmol), dodecane (19.5 mg, GC standard) and toluene (1 ml). The reaction mixture was heated at 150 °C for 16 h. The GC-MS analysis of the reaction mixture revealed the formation of 2,2-diphenylethan-1-amine which according to the GC, it was formed in 93% yield at 95% conversion of diphenylacetonitrile.

This experiment was repeated to be analysed by NMR. The experiment was conducted according to the procedure described in Section 2.13.14 using $Ir(P^iPr_3)_2H_5$ catalyst (8.2 mg, 0.016 mmol, 10 mol%), diphenylacetonitrile (31.2 mg, 0.161 mmol) and d_8-toluene (0.8 ml). After heating at 150 ºC for 16 h, the reaction vessel was cooled down and brought back into the glovebox. The reaction mixture was transferred into a J Young tube and analysed by ^1H NMR. This analysis confirmed the formation of the 2,2-

diphenylethan-1-amine: **^{1}H NMR** (400 MHz, d_8-toluene) δ 3.70 (t, J= 7.3 Hz, 1H, CH), 3.05 (m, 2H, NH_2), 0.55 (m, 2H, CH_2). (aromatic H are overlapped with toluene signals).

NMR data in accordance with the literature data.[126]

2.13.15. Iridium-catalyzed transfer hydrogenation of 2,2-diphenylpentanedinitrile with cyclohexanol

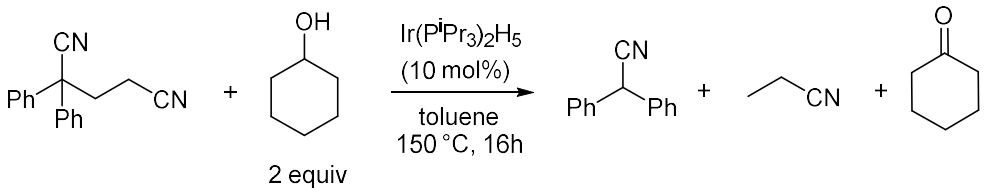

In a glovebox, a stock solution was prepared from 2,2-diphenylpentanedinitrile **2** (49.8 mg, 0.202 mmol), dodecane (25.1 mg, 0.147 mmol, GC standard) and toluene (1 ml). From this stock solution, 0.8 ml was added into a 10 ml Schlenk bomb charged with $Ir(P^iPr_3)_2H_5$ catalyst (8.1 mg, 0.016 mmol, 10 mol%) and a magnetic stir bar. The Schlenk tube was sealed and removed from the glovebox. Cyclohexanol (34 µl, 0.32 mmol) was then added into the Schlenk flask under argon atmosphere. The reaction mixture was heated in an oil bath at 150 °C for 16 h, cooled down and was passed through a short silica gel column (5 ml plastic syringe filled with a 3 cm layer of silica gel) eluting with 15 ml of EtOAc. The resulting solution was analysed by GC. All products were known compounds and identified using GC by comparison of the retention times with those of authentic standard. GC analysis showed full conversion of the dinitrile **2**, and formation of diphenylacetonitrile and propionitrile in 95 and 74% yields, respectively.

2.13.16. Crystallographic experimental details

Single crystals were mounted on a Mitegen using Paratone-N oil and were cooled under a stream of nitrogen. Crystal data were collected on a Rigaku Oxford Diffraction SuperNova diffractometer using Mo or Cu Kα radiation; the structures were solved by direct methods using ShelXT and refined by least squares using ShelXL. Metal bound hydrogen atoms were located in the difference map and refined isotropically. Figures and tables were generated using OLEX2. For complex **32** two reflections (-1 -2 6 and -6 -4 5) were omitted from the last refinement cycles due to poor agreement.

2.13.16.1. Crystallographic data and structure refinement for complex 32

Identification code	**Complex 32**
Empirical formula	$C_{36}H_{62}Cl_2IrNP_2$
Formula weight	833.90
Temperature/K	99.9(4)
Crystal system	triclinic
Space group	P-1
a/Å	11.1318(2)
b/Å	11.33316(20)
c/Å	17.5536(3)
α/°	71.9421(16)
β/°	85.7072(16)
γ/°	63.2385(19)
Volume/Å^3	1874.47(7)
Z	2
ρ_{calc} g/cm^3	1.477
μ/mm^{-1}	3.814
F(000)	852.0
Crystal size/mm^3	0.167 × 0.149 × 0.122
Radiation	MoKα (λ = 0.71073)
2Θ range for data collection/°	4.896 to 59.408
Index ranges	-15 ≤ h ≤ 14, -15 ≤ k ≤ 15, -24 ≤ l ≤ 23
Reflections collected	63702
Independent reflections	9770 [R_{int} = 0.0414, R_{sigma} = 0.0313]
Data/restraints/parameters	9770/0/397
Goodness-of-fit on F^2	1.102
Final R indexes [I>=2σ (I)]	R_1 = 0.0225, wR_2 = 0.0451
Final R indexes [all data]	R_1 = 0.0257, wR_2 = 0.0463
Largest diff. peak/hole / e Å^{-3}	0.91/-0.94

$R_1 = \Sigma ||Fo|-|Fc| / \Sigma |Fo|$; $wR_2 = [\Sigma (w(Fo^2 - Fc^2)^2 / \Sigma w(Fo^2)^2]^{1/2}$

2.13.16.1.1. Crystal structure of complex 32

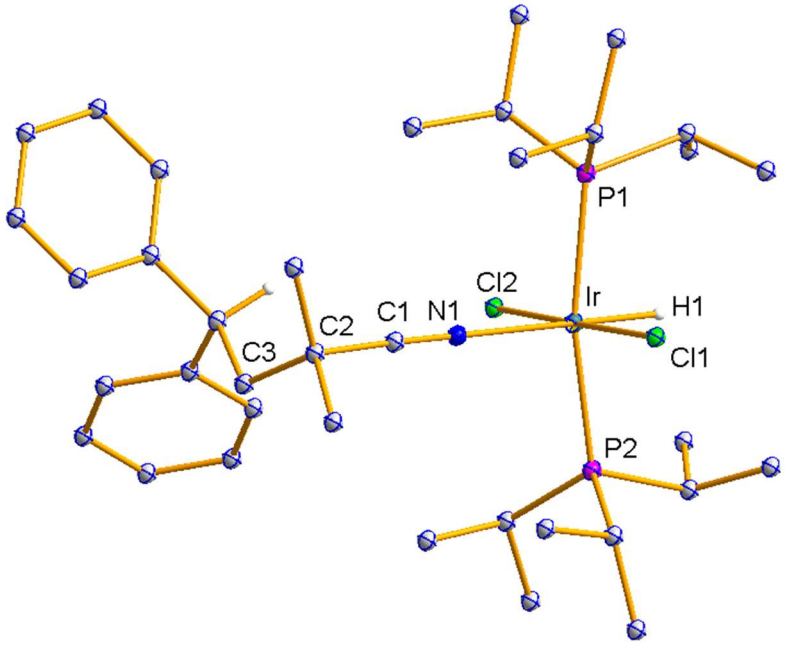

Hydrogen atoms have been omitted for clarity (except H1).

2.13.16.1.2. Table of selected bond length and angles for complex 32

Bonds lengths (Å)		**Bond and torsion angles (°)**	
Ir-P1	2.357	P1-Ir-P2	167.1
Ir-P2	2.358	H1-Ir-N1	178.8
Ir-H1	1.568	Cl1-Ir-Cl2	178.9
Ir-N1	2.127	P1-Ir-H1	83.4
N1-C1	1.144	P1-Ir-Cl1	88.7
C1-C2	1.482	N1-C1-C2	177.8
C2-C3	1.542	C1-C2-C3	108.1

2.13.16.2. Crystallographic data and structure refinement for complex 33

Identification code	**Complex 33**
Empirical formula	$C_{37}H_{65}Cl_2IrN_2P_2$
Formula weight	862.95
Temperature/K	99.9(5)
Crystal system	monoclinic
Space group	$P2_1/n$
a/Å	12.83575(8)
b/Å	14.09538(8)
c/Å	22.00910(12)
α/°	90
β/°	91.3956(5)
γ/°	90
Volume/Å^3	3980.81(4)
Z	4
ρ_{calc} g/cm^3	1.440
μ/mm^{-1}	8.677
F(000)	1768.0
Crystal size/mm^3	0.292 × 0.156 × 0.094
Radiation	CuKα (λ = 1.54184)
2Θ range for data collection/°	7.448 to 154.624
Index ranges	$-15 \leq h \leq 16$, $-17 \leq k \leq 17$, $-27 \leq l \leq 27$
Reflections collected	51026
Independent reflections	8392 [R_{int} = 0.0222, R_{sigma} = 0.0127]
Data/restraints/parameters	8392/0/419
Goodness-of-fit on F^2	1.133
Final R indexes [I>=2σ (I)]	R_1 = 0.0151, wR_2 = 0.0373
Final R indexes [all data]	R_1 = 0.0153, wR_2 = 0.0374
Largest diff. peak/hole / e Å^{-3}	0.41/-0.73

$R_1 = \Sigma \, ||Fo|-|Fc|| \, / \, \Sigma \, |Fo|$; $wR_2 = [\Sigma \, (w(Fo^2 - Fc^2)^2 \, / \, \Sigma \, w(Fo^2)^2]^{1/2}$

2.13.16.2.1. Crystal structure of complex 33

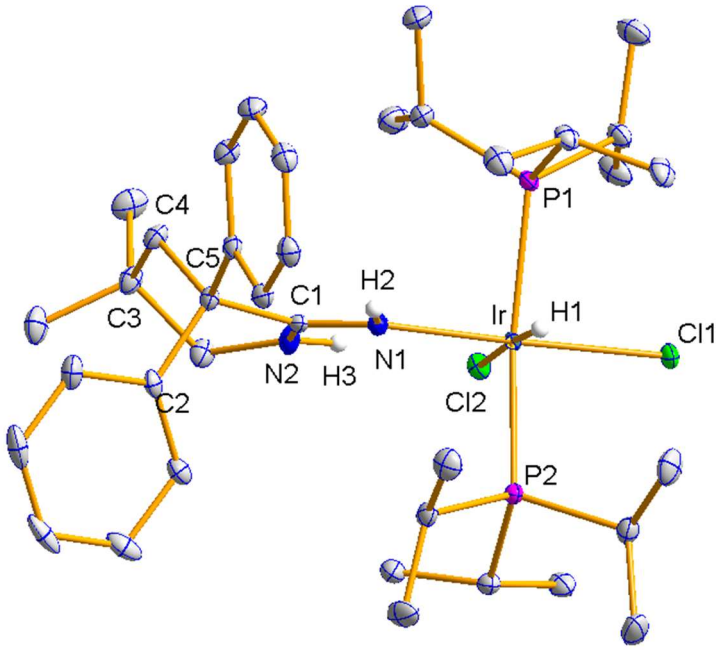

Hydrogen atoms have been omitted for clarity (except for H1, H2 and H3).

2.13.16.2.2. Table of selected bond length and angles for complex 33

Bonds lengths (Å)		**Bond and torsion angles (°)**	
Ir-P1	2.349	P1-Ir-P2	163.6
Ir-P2	2.367	P1-Ir-H1	80.1
Ir-H1	1.475	P1-Ir-Cl1	88.9
Ir-Cl1	2.388	P1-Ir-Cl2	98.7
Ir-Cl2	2.531	Cl1-Ir-Cl2	85.9
Ir-N1	2.084	Cl1-Ir-N1	177.5
N1-C1	1.302	Ir-N1-C1	136.4
C1-N2	1.337	N1-C1-N2	121.5
N2-C2	1.457	N2-C1-C5	122.8
C2-C3	1.545	C1-C5-C4	105.2
C1-C5	1.546		

2.13.16.3. Crystallographic data and structure refinement for complex 37

Identification code	**Complex 37**
Empirical formula	$C_{46}H_{65}IrN_2P_2$
Formula weight	900.14
Temperature/K	99.9(5)
Crystal system	triclinic
Space group	P-1
a/Å	12.6583(2)
b/Å	13.8629(2)
c/Å	14.6122(3)
α/°	113.1144(17)
β/°	107.9793(16)
γ/°	95.8219(15)
Volume/Å^3	2169.33(7)
Z	2
ρ_{calc} g/cm^3	1.378
μ/mm^{-1}	6.885
F(000)	924.0
Crystal size/mm^3	0.281 × 0.188 × 0.148
Radiation	CuKα (λ = 1.54184)
2Θ range for data collection/°	7.114 to 154.876
Index ranges	$-15 \leq h \leq 15$, $-16 \leq k \leq 17$, $-18 \leq l \leq 17$
Reflections collected	43726
Independent reflections	9130 [R_{int} = 0.0276, R_{sigma} = 0.0191]
Data/restraints/parameters	9130/0/480
Goodness-of-fit on F^2	1.069
Final R indexes [I>=2σ (I)]	R_1 = 0.0190, wR_2 = 0.0484
Final R indexes [all data]	R_1 = 0.0196, wR_2 = 0.0488
Largest diff. peak/hole / e Å^{-3}	0.91/-1.32

$R_1 = \Sigma \, ||Fo|-|Fc|| \, / \, \Sigma \, |Fo|$; $wR_2 = [\Sigma \, (w(Fo^2 - Fc^2)^2 \, / \, \Sigma \, w(Fo^2)^2]^{1/2}$

2.13.16.3.1. Crystal structure of complex 37

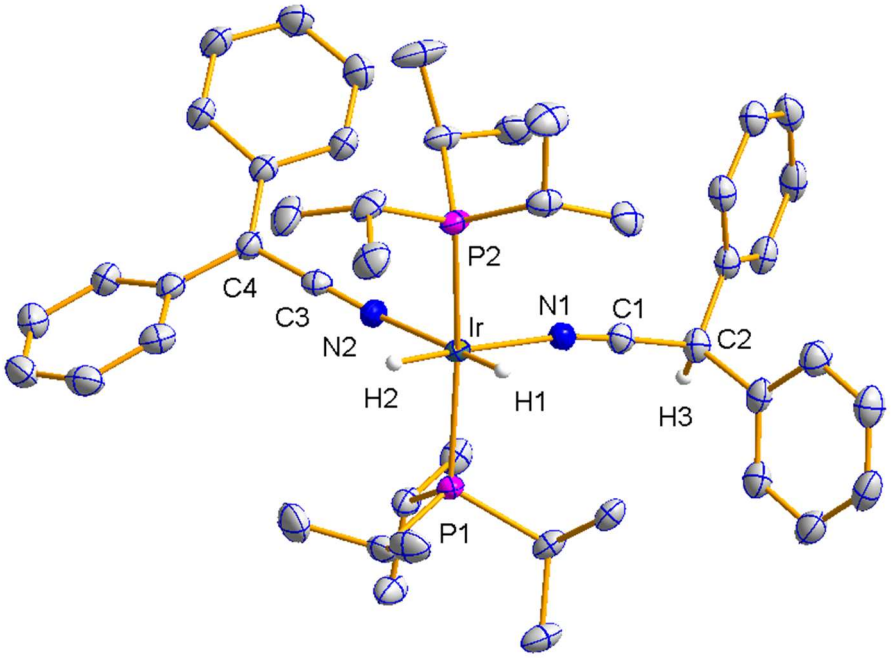

Hydrogen atoms are omitted for clarity (except H1, H2 and H3).

2.13.16.3.2. Table of selected bond length and angles for complex 37

Bonds lengths (Å)		**Bond and torsion angles (°)**	
Ir-P1	2.314(6)	P2-Ir-P1	169.0
Ir-P2	2.315(6)	P2-Ir-N1	99.0
Ir-N1	2.125(2)	P2-Ir-H1	83.6
Ir-N2	2.139(2)	H1-Ir-H2	84.3
Ir-H1	1.36(3)	N1-C1-C2	177.1
Ir-H2	1.33(5)	N2-C3-C4	178.9
N1-C1	1.138(3)	Ir-N2-C3	158.7
C1-C2	1.479(3)	Ir-N1-C1	171.4
C2-H3	0.980		
N2-C3	1.159(2)		
C3-C4	1.395(2)		

2.13.16.4. Crystallographic data and structure refinement for complex 51

Identification code	**Complex 51**
Empirical formula	$C_{32}H_{54}Cl_2IrNP_2$
Formula weight	777.80
Temperature/K	100.01(10)
Crystal system	monoclinic
Space group	$P2_1/c$
a/Å	9.1059(2)
b/Å	18.1800(4)
c/Å	20.9058(5)
α/°	90
β/°	94.940(2)
γ/°	90
Volume/Å^3	3448.02(13)
Z	4
ρ_{calc} g/cm^3	1.498
μ/mm^{-1}	9.945
F(000)	1576.0
Crystal size/mm^3	0.128 × 0.083 × 0.029
Radiation	CuKα (λ = 1.54184)
2Θ range for data collection/°	6.454 to 153.27
Index ranges	$-11 \leq h \leq 9$, $-19 \leq k \leq 22$, $-23 \leq l \leq 26$
Reflections collected	27737
Independent reflections	7200 [R_{int} = 0.0539, R_{sigma} = 0.0444]
Data/restraints/parameters	7200/1/359
Goodness-of-fit on F^2	1.033
Final R indexes [I>=2σ (I)]	R_1 = 0.0417, wR_2 = 0.1059
Final R indexes [all data]	R_1 = 0.0490, wR_2 = 0.1126
Largest diff. peak/hole / e Å^{-3}	1.63/-3.42

$R_1 = \Sigma \, ||Fo|-|Fc|| \, / \, \Sigma \, |Fo|$; $wR_2 = [\Sigma \, (w(Fo^2 - Fc^2)^2 \, / \, \Sigma \, w(Fo^2)^2]^{1/2}$

2.13.16.4.1. Crystal structure of complex 51

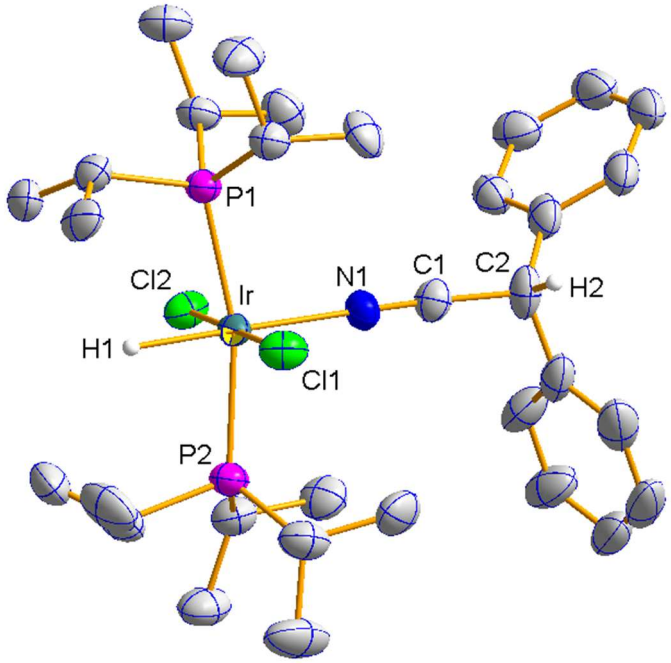

Hydrogen atoms have been omitted for clarity (except for H1 and H2).

2.13.16.4.2. Table of selected bond length and angles for complex 51

Bonds lengths (Å)		**Bond and torsion angles (°)**	
Ir-P1	2.352(1)	P1-Ir-P2	164.9
Ir-P2	2.355(1)	P1-Ir-N1	96.9
Ir-N1	2.133(4)	P2-Ir-N1	98.1
Ir-H1	1.73(2)	P1-Ir-H1	83.7
Ir-Cl1	2.377(1)	P1-Ir-Cl1	81.1
Ir-Cl2	2.377(1)	H1-Ir-N1	179.0
N1-C1	1.146(7)	Ir-N1-C1	90.2
C1-C2	1.479(7)	Ir-N1-C2	89.5
C2-H1	0.98	N1-C1-C2	177.0

2.13.17. DFT calculations

All stationary points were fully optimized with Gaussian 09 using M06-2X/6-31(d,p).[87] Harmonic vibrational frequencies were computed for all optimized structures to verify that they were either minima or transition states, possessing zero imaginary frequencies and one imaginary frequency respectively. Calculations were performed with M06-2X functional, which is constructed to include nonlocal effects of electronic dispersion and is found to give good estimates for reaction enthalpies in bond-forming reactions. Toluene as the solvent was modelled using the PCM method.[127]

Ground state energies of relevant complexes from section 2.10 at T= 298.15 K

Compound	Ground state energy (au)
$Ir(P^iPr_3)_2H_5$ (**1**)	-1500.53
2,2-diphenylpentanedinitrile (**2**)	-765.186
Diphenylacetonitrile (**3**)	-594.437
Acrylonitrile (**4**)	-170.732
"$Ir(P^iPr_3)_2H$"	-1498.17
H_2	-1.16838
Complex **37**	-2687.08
Complex **37TS**	-2857.78
Complex **38**	-2092.64
Complex **39**	-2263.35
Complex **39TS**	-2263.33
Complex **40**	-2263.37
Complex **41**	-2263.36
Complex **42**	-2263.37
Complex **42TS**	-2263.35
Complex **43**	-2263.37
Complex **44**	-2263.37
Complex **45**	-2687.05
Complex **46**	-2092.62
Complex **47**	-2263.33
Complex **47TS**	-2263.35
Complex **48**	-2263.34
Complex **48TS**	-2263.35
Complex **49**	-2857.78
Complex **50**	-2263.36
Complex **50a**	-2263.36

2.13.17.1. Optimised geometries of complexes relevant to proposed mechanistic pathways 1A, 2A, 1B, 2B and intermolecular mechanism

Iridium is represented in dark blue, carbon in black, phosphorous in orange, nitrogen in light blue and hydrogen in white. Hydrogens have been omitted for clarity (except for hydride ligands).

$Ir(P^iPr_3)_2H_5$ (**1**)

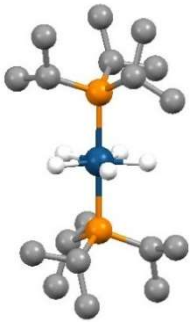

Complex "$Ir(P^iPr_3)_2H$"

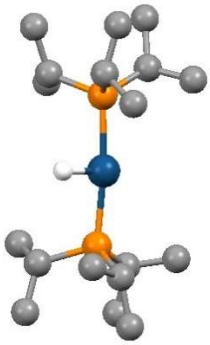

Complex **37**

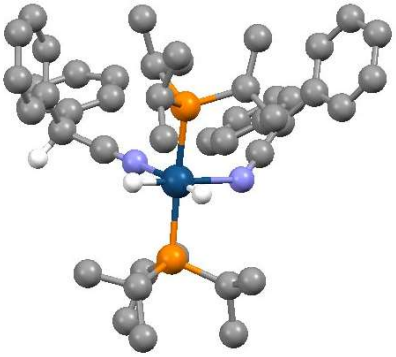

Complex **37TS**

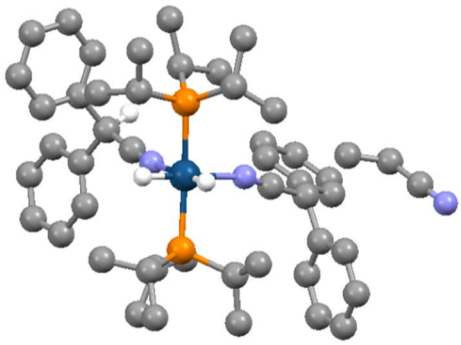

Complex **38**

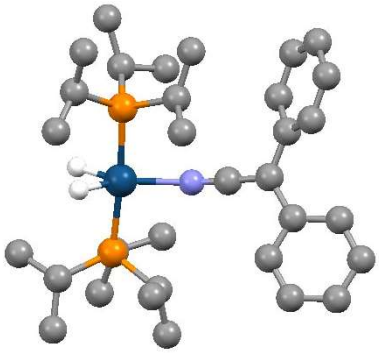

Complex **39**

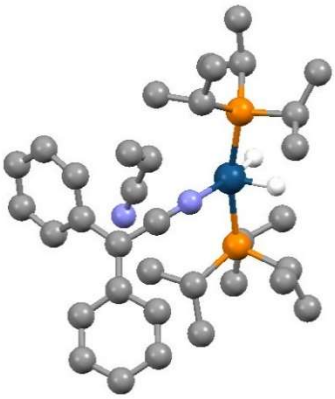

Complex **39TS**

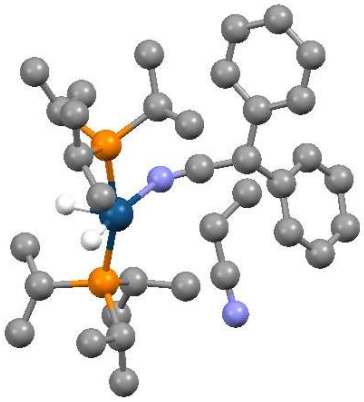

Complex **40**

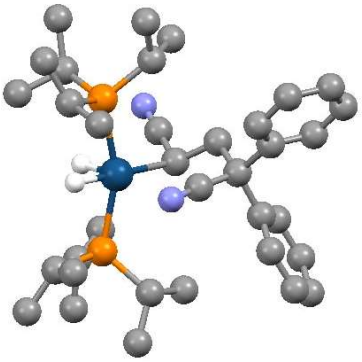

Complex **41**

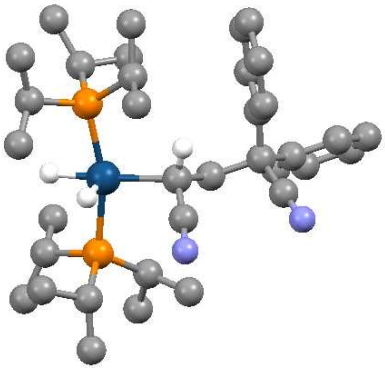

Complex **42**

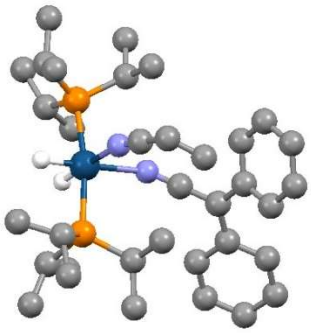

Complex **42TS**

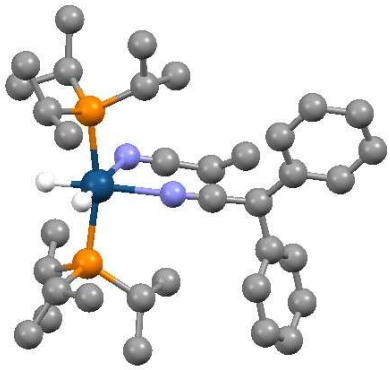

Complex **43**

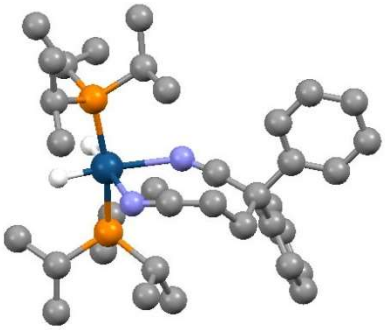

Complex **44**

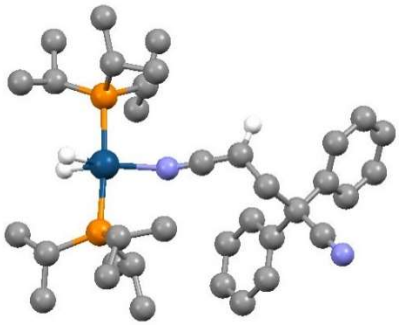

Complex **45**

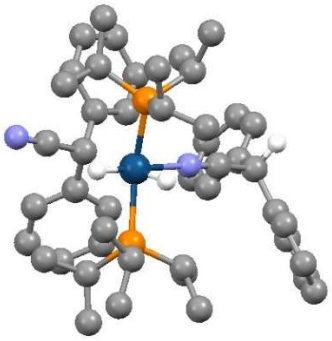

Complex **46**

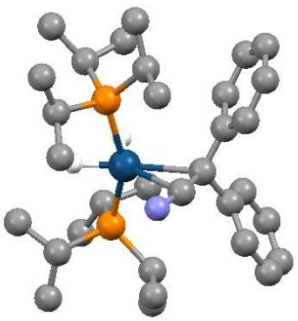

Complex **47**

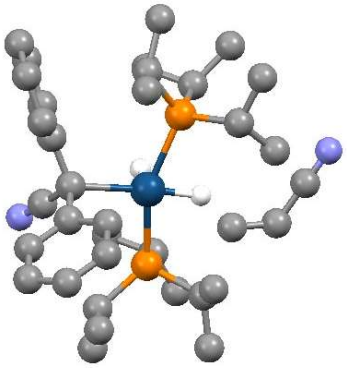

Complex **47TS**

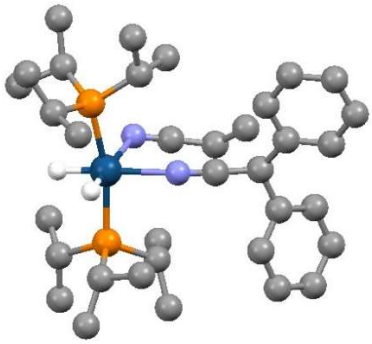

Complex **48**

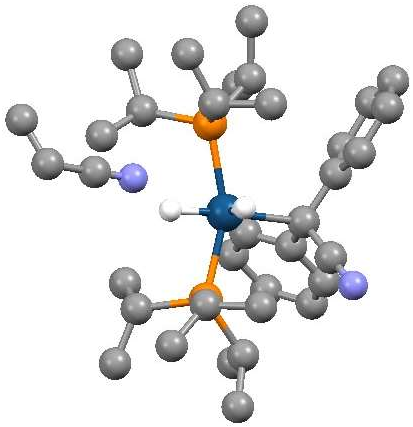

Complex **48TS**

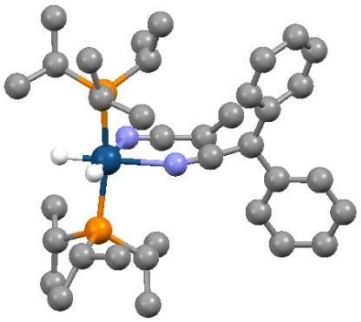

Complex **49**

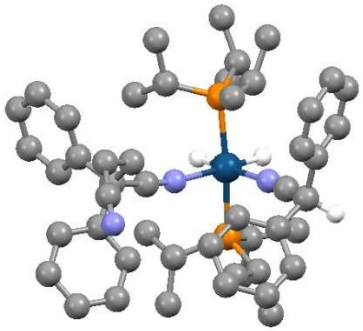

Complex **50**

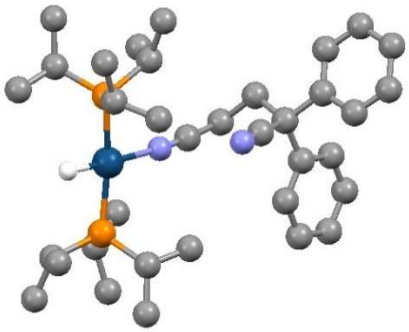

Complex **50a**

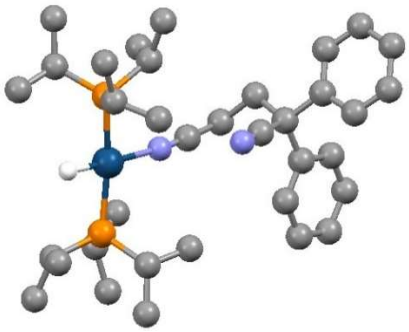

2.14. References

(1) Pasha, F. A.; Bendjeriou-Sedjerari, A.; Huang, K.-W.; Basset, J.-M. *Organometallics* **2014**, *33* (13), 3320–3327.

(2) Terai, H.; Takaya, H.; Murahashi, S. I. *Synlett* **2004**, No. 12, 2185–2187.

(3) Schock, L. E.; Marks, T. J. *J. Am. Chem. Soc.* **1988**, *110* (23), 7701–7715.

(4) Chin, C. S.; Moon, C. J. *J. Korean Chem. Soc.* **1982**, *26*, 253–254.

(5) Clerici, M. G.; Di Gioacchino, S.; Maspero, F.; Perrotti, E.; Zanobi, A. *J. Organomet. Chem.* **1975**, *84* (3), 379–388.

(6) Goldman, A. S.; Halpern, J. *J. Am. Chem. Soc.* **1987**, *109* (24), 7537–7539.

(7) Lecuyer, C.; Quignard, F.; Choplin, A.; Olivier, D.; Basset, J.-M. *Angew. Chemie Int. Ed.* **1991**, *30* (12), 1660–1661.

(8) Takaya, H.; Naota, T.; Murahashi, S.-I. *J. Am. Chem. Soc.* **1998**, *120*, 4244–4245.

(9) Thompson, W. H.; Sears, C. T. *Inorg. Chem.* **1977**, *16* (4), 769–774.

(10) Mann, G.; Shelby, Q.; Roy, A. H.; Hartwig, J. F. *Organometallics* **2003**, *22* (13), 2775–2789.

(11) Arndtsen, B. A.; Bergman, R. G. *Science (80-.).* **1995**, *270*, 1970.

(12) Cho, J.-Y.; Tse, M. K.; Holmes, D.; Maleczka, R. E.; Smith, M. R. *Science (80-.).* **2002**, *295*, 305.

(13) Kunin, A. J.; Eisenberg, R. *J. Am. Chem. Soc* **1986**, *108*, 535–536.

(14) Klei, S. R.; Tilley, T. D.; Bergman, R. G. *Organometallics* **2002**, *21*, 4905–4911.

(15) Liskey, C. W.; Hartwig, J. F. *J. Am. Chem. Soc.* **2013**, *135* (9), 3375–3378.

(16) Simmons, E. M.; Hartwig, J. F. *Nature* **2012**, *483* (7387), 70–73.

(17) Mas-Marzá, E.; Poyatos, M.; Sanaú, M.; Peris, E. *Inorg. Chem.* **2004**, *43*, 2213–2219.

(18) Corberán, R.; Sanaú, M.; Peris, E. *J. Am. Chem. Soc* **2006**, *128*, 3974–3979.

(19) Herde, J. L.; Lambert, J. C.; Senoff, C. V.; Cushing, M. A. In *Inorganic Syntheses*; John Wiley & Sons, Inc., 2007; pp 18–20.

(20) Tolman, C. A. *Chem. Rev.* **1977**, *77* (3), 313–348.

(21) Bilbrey, J. A.; Kazez, A. H.; Locklin, J.; Allen, W. D. *J. Comput. Chem.* **2013**, *34* (14), 1189–1197.

(22) Kendall, A. J.; Zakharov, L. N.; Tyler, D. R. *Inorg. Chem.* **2016**, *55* (6), 3079–3090.

(23) Dierkes, P.; van Leeuwen, P. W. N. M.; Higuchi, T.; Hirotsu, K.; Fukuyo, E.; Yanagi, K.; Fraanje, J.; Schenk, H.; Bo, C. *J. Chem. Soc. Dalt. Trans.* **1999**, *334* (10), 1519–1530.

(24) Zhu, L.; Altman, R. A. In *Encyclopedia of Reagents for Organic Synthesis*; John Wiley & Sons, Ltd: Chichester, UK, 2013; pp 1–4.

(25) Zilkha, A.; Feit, B.-A.; Frankel, M. *J. Chem. Soc.* **1959**, 928.

(26) Zilkha, A.; Feit, B.-A. *J. Appl. Polym. Sci.* **1961**, *5* (15), 251–260.

(27) Hopkinson, M. N.; Richter, C.; Schedler, M.; Glorius, F. *Nature* **2014**, *510* (7506), 485–496.

(28) Gusev, D. G. *Organometallics* **2009**, *28* (22), 6458–6461.

(29) Gupta, M.; Hagen, C.; Kaska, W. C.; Cramer, R. E.; Jensen, C. M. *J. Am. Chem. Soc.* **1997**, *119* (4), 840–841.

(30) Morales-Morales, D.; Grause, C.; Kasaoka, K.; Redón, R.; Cramer, R. E.; Jensen, C. M. *Inorganica Chim. Acta* **2000**, *300*, 958–963.

(31) Gupta, M.; Hagen, C.; Flesher, R. J.; Kaska, W. C.; Jensen, C. M. *Chem. Commun.* **1996**, *15* (17), 2083–2084.

(32) Punji, B.; Emge, T. J.; Goldman, A. S. *Organometallics* **2010**, *29* (12), 2702–2709.

(33) Liu, F.; Pak, E. B.; Singh, B.; Jensen, C. M.; Goldman, A. S. *J. Am. Chem. Soc.* **1999**, *121* (eq 1), 4086–4087.

(34) Faller, J. W.; Smart, C. J. *Organometallics* **1989**, *8* (3), 602–609.

(35) Methot, J. L.; Roush, W. R. *Adv. Synth. Catal.* **2004**, *346* (910), 1035–1050.

(36) Sherry, A. E.; Wayland, B. B. *J. Am. Chem. Soc.* **1990**, *112* (3), 1259–1261.

(37) Sandler, S. R.; Karo, W. *Polymer syntheses. Volume 3*.

(38) Wilt, J. W.; Lundquist, J. A. *J. Org. Chem.* **1964**, *29* (4), 921–925.

(39) Hille, U. E.; Zimmer, C.; Vock, C. A.; Hartmann, R. W. *ACS Med. Chem. Lett.* **2011**, *2* (1), 2–6.

(40) McPhee, W. D.; Lindstrom, G. *J. Am. Chem. Soc.* **1943**, *65*, 2177–2180.

(41) Friedman, L.; Shechter, H. *J. Org. Chem.* **1960**, *25*, 877–879.

(42) Kluiber, R. W. *J. Org. Chem.* **1965**, *30* (6), 2037–2041.

(43) Murahashi, S. I.; Naota, T.; Taki, H.; Mizuno, M.; Takaya, H.; Komiya, S.; Mizuho, Y.; Oyasato, N.; Hiraoka, M.; Hirano, M.; Fukuoka, A. *J. Am. Chem. Soc.* **1995**, *117* (50), 12436–12451.

(44) Hartwig, J. F. *Organotransition metal chemistry: from bonding to catalysis*; University Science Books, 2010.

(45) Chatani, N.; Ie, Y.; Kakiuchi, F.; Murai, S. *J. Am. Chem. Soc.* **1999**, *121* (37), 8645.

(46) Rathbun, C. M.; Johnson, J. B. *J. Am. Chem. Soc.* **2011**, *133* (7), 2031–2033.

(47) Macomber, R. S. *Organic chemistry*; University Science Books, 1996.

(48) Liu, X.; Li, X.; Liu, H.; Guo, Q.; Lan, J.; Wang, R.; You, J. *Org. Lett.* **2015**, *17* (12), 2936–2939.

(49) Huang, Z.; Lim, H. N.; Mo, F.; Young, M. C.; Dong, G.; Protsuk, N. I.; Mikhaleva, A. I. *Chem. Soc. Rev.* **2015**, *44* (21), 7764–7786.

(50) Rao, Y.; Shan, G.; Yang, X. *Sci. China Chem.* **2014**, *57* (7), 930–944.

(51) Maiti, S.; Burgula, L.; Chakraborti, G.; Dash, J. *European J. Org. Chem.* **2017**, *2017* (2), 332–340.

(52) Chen, K.; Li, Z.-W.; Shen, P.-X.; Zhao, H.-W.; Shi, Z.-J. *Chem. - A Eur. J.* **2015**, *21* (20), 7389–7393.

(53) Desai, L. V.; Hull, K. L.; Sanford, M. S. *J. Am. Chem. Soc.* **2004**, *126* (31), 9542–9543.

(54) Parthasarathy, K.; Jeganmohan, M.; Cheng, C.-H. *Org. Lett.* **2008**, *10* (2), 325–328.

(55) Wang, X.; Lu, Y.; Dai, H.-X.; Yu, J.-Q. *J. Am. Chem. Soc.* **2010**, *132* (35), 12203–12205.

(56) Robins, R. K. *Chem. Eng. News* **1986**, *64* (July), 28–40.

(57) Michael, J. P.; de Koning, C. B.; van der Westhuyzen, C. W.; Fernandes, M. a. *J. Chem. Soc. Perkin Trans. 1* **2001**, No. 17, 2055–2062.

(58) Barry, R. H.; Clark, J. R.; Walter, L. A. Alpha-phenyl-upsilon-(2-pyridyl)-butyronitriles. US2713050A, 1953.

(59) Kaupp, J.; Nolte, F. Verfahren zur Herstellung von am zentralen Kohlenstoffatom substituierten Diarylacetonitrilen. 894394, 1949.

(60) Mcleod, M. C.; Singh, G.; Plampin Iii, J. N.; Rane, D.; Wang, J. L.; Day, V. W.; Aubé, J. *Nat. Chem.* **2014**, *6*, 133–140.

(61) Lin, Y.; Ma, D.; Lu, X. *Tetrahedron Lett.* **1987**, *28* (27), 3115–3118.

(62) Zuckerman, J. J. *Inorganic reactions and methods. Volume 1. The formation of bonds to hydrogen (Part 1)*; VCH Publishers, 1986.

(63) Ong, C. M.; Jennings, M. C.; Puddephatt, R. J. *Can. J. Chem.* **2003**, *81* (11), 1196–1205.

(64) Chin, C. S.; Lee, B. *Catal. Letters* **1992**, *14* (1), 135–140.

(65) Janser, P.; Venanzi, L. M.; Bachechi, F. *J. Organomet. Chem.* **1985**, *296* (1–2), 229–242.

(66) Tobisu, M.; Nakamura, R.; Kita, Y.; Chatani, N. *Bull. Korean Chem. Soc.* **2010**, *31* (3), 582–587.

(67) Patra, T.; Agasti, S.; Modak, A.; Maiti, D. *Chem. Commun.* **2013**, *49* (75), 8362.

(68) Amodio, C. A.; B. Nolan, K. *Inorganica Chim. Acta* **1986**, *113* (1), 27–30.

(69) Buckingham, D. A.; Morris, P.; Sargeson, A. M.; Zanella, A. *Inorg. Chem.* **1977**, *16* (8), 1910–1923.

(70) Ohhara, T.; Harada, J.; Ohashi, Y.; Tanaka, I.; Kumazawa, S.; Niimura, N.; IUCr; M., H.; N., M.; Y., M. *Acta Crystallogr. Sect. B Struct. Sci.* **2000**, *56* (2), 245–253.

(71) Aikawa, K.; Maruyama, K.; Honda, K.; Mikami, K. *Org. Lett.* **2015**, *17* (19), 4882–4885.

(72) Gómez-Gallego, M.; Sierra, M. A. *Chem. Rev.* **2011**, *111* (8), 4857–4963.

(73) Jones, W. D. *Acc. Chem. Res.* **2003**, *36* (2), 140–146.

(74) Simmons, E. M.; Hartwig, J. F. *Angew. Chemie Int. Ed.* **2012**, *51* (13), 3066–3072.

(75) Casey, C. P.; Rutter, E. W. *Inorg. Chem.* **1990**, *29* (12), 2333–2335.

(76) Crabtree, R. H. In *Encyclopedia of Inorganic Chemistry*; John Wiley & Sons, Ltd: Chichester, UK, 2006.

(77) Zhao, J.; Zhang, S.; Zhang, W.-X.; Xi, Z. *Organometallics* **2011**, *30* (13), 3464–3467.

(78) Iravani, E.; Neumüller, B. *Organometallics* **2003**, *22* (20), 4129–4135.

(79) Becker, L.; Burlakov, V. V.; Arndt, P.; Spannenberg, A.; Baumann, W.; Jiao, H.; Rosenthal, U. *Chem. - A Eur. J.* **2013**, *19* (13), 4230–4237.

(80) Boche, G.; Marsch, M.; Harms, K. *Angew. Chemie Int. Ed. English* **1986**, *25* (4),

373–374.

(81) Burwell, R. L.; Pearson, R. G. *J. Phys. Chem.* **1966**, *70* (1), 300–302.

(82) Bryan, S. J.; Hugget, P. G.; Wade, K. *Chem. Soc. Rev.* **1982**, *44*, 149–189.

(83) Groux, L. F.; Weiss, T.; Reddy, D. N.; Chase, P. A.; Piers, W. E.; Ziegler, T.; Parvez, M.; Benet-Buchholz, J. *J. Am. Chem. Soc* **2005**, *127* (6), 1854–1869.

(84) Wu, F.; Foley, S. R.; Burns, C. T.; Jordan, R. F. *J. Am. Chem. Soc* **2005**, *127* (6), 1841–1853.

(85) Baddley, W. H.; Fraser, M. S. *J. Am. Chem. Soc.* **1969**, *91* (13), 3661–3663.

(86) Baddley, W. H. *J. Am. Chem. Soc.* **1968**, *90* (14), 3705–3710.

(87) Zhao, Y.; Truhlar, D. G. *Theor. Chem. Acc.* **2008**, *120* (1–3), 215–241.

(88) Naota, T.; Tannna, A.; Kamuro, S.; Murahashi, S. I. *J. Am. Chem. Soc.* **2002**, *124* (24), 6842–6843.

(89) Chin, C. S.; Chong, D.; Lee, B.; Jeong, H.; Won, G.; Do, Y.; Park, Y. J. *Organometallics* **2000**, *19* (4), 638–648.

(90) Batsanov, S. S. *Inorg. Mater.* **2001**, *37* (9), 871–885.

(91) Nag, S.; Banerjee, K.; Datta, D. *New J. Chem.* **2007**, *31* (6), 832.

(92) Boche, G.; Harms, K.; Marsch, M. *J. Am. Chem. Soc.* **1988**, *110* (20), 6925–6926.

(93) Alburquerque, P. R.; Pinhas, A. R.; Krause Bauer, J. A. *Inorganica Chim. Acta* **2000**, *298* (2), 239–244.

(94) Del Pra, A.; Forsellini, E.; Bombieri, G.; Michelin, R. A.; Ros, R. *J. Chem. Soc. Dalt. Trans.* **1979**, No. 12, 1862.

(95) Naota, T.; Tannna, A.; Murahashi, S.-I. *J. Am. Chem. Soc.* **2000**, *122* (12), 2960–2961.

(96) Mcginnety, J. A.; Ibers, J. A. *Chem. Commun.* **1968**, 235–237.

(97) Alvarez, S. G.; Hasegawa, S.; Hirano, M.; Komiya, S. *Tetrahedron Lett.* **1998**, *39* (29), 5209–5212.

(98) Hirano, M.; Kiyota, S.; Imoto, M.; Komiya, S. *Chem. Commun.* **2000**, No. 17, 1679–1680.

(99) Cameron, C. J.; Felkin, H.; Fillebeen-Khan, T.; Forrow, N. J.; Guittet, E. *J. Chem. Soc., Chem. Commun.* **1986**, No. 10, 801–802.

(100) Klabunde, U.; Parshall, G. W. *J. Am. Chem. Soc.* **1972**, *94* (26), 9081–9087.

(101) Millard, M. D.; Moore, C. E.; Rheingold, A. L.; Figueroa, J. S. *J. Am. Chem. Soc.* **2010**, *132* (26), 8921–8923.

(102) Panetier, J. A.; Macgregor, S. A.; Whittlesey, M. K. *Angew. Chemie Int. Ed.* **2011**, *50* (12), 2783–2786.

(103) Leeuwen, P. W. van; Chadwick, J. C. *Homogeneous catalysts : activity-stability-deactivation*; Wiley-VCH Verlag, 2011.

(104) Crabtree, R. H. *Chem. Rev.* **2015**, *115* (1), 127–150.

(105) Bruce, M. I. *Angew. Chemie Int. Ed. English* **1977**, *16* (2), 73–86.

(106) To, C. T.; Chan, K. S. *Tetrahedron Lett.* **2016**, *57* (42), 4664–4669.

(107) Liou, S.-Y.; van der Boom, M. E.; Milstein, D.; Spek, A. L.; Koten, G. van. *Chem. Commun.* **1998**, *35* (6), 687–688.

(108) Dufaud, V.; Basset, J. M. *Angew. Chemie - Int. Ed.* **1998**, *37* (6), 806–810.

(109) Chin, C. S.; Lee, B. *Catal. Letters* **1992**, *14* (1), 135–140.

(110) Aranyos, A.; Csjernyik, G.; Szabó, K. J.; Bäckvall, J.-E. *Chem. Commun.* **1999**, *0* (4), 351–352.

(111) Noyori, R.; Hashiguchi, S. *Acc. Chem. Res.* **1997**, *30* (2), 97–102.

(112) Shaun E. Landau; Kai E. Groh; Alan J. Lough, A.; Morris*, R. H. *Inorg. Chem.* **2002**, *41* (11), 2995–3007.

(113) Rybtchinski, B.; BenDavid, Y.; Milstein, D. *Organometallics* **1997**, *16* (17), 3786–3793.

(114) Zhu, K.; Achord, P. D.; Zhang, X.; Krogh-Jespersen, K.; Goldman, A. S. *J. Am. Chem. Soc.* **2004**, *126* (40), 13044–13053.

(115) Chase, B. H.; Hey, D. H. *J. Chem. Soc.* **1952**, 553.

(116) Kaneyoshi Kato, H.; Yoshihiro Sugiura, N.; Koichi Kato, I. Amine compounds, their production and use, 1997.

(117) Mohrle, H.; Engelsing, R. *Monatshefte fur Chemie* **1971**, *102* (1), 233–244.

(118) Shimizu, H.; Holder, J. C.; Stoltz, B. M. *Beilstein J. Org. Chem.* **2013**, *9* (1), 1637–1642.

(119) Gómez, C.; Maciá, B.; Lillo, V. J.; Yus, M. *Tetrahedron* **2006**, *62* (42), 9832–9839.

(120) Peña-López, M.; Ayán-Varela, M.; Sarandeses, L. A.; Pérez Sestelo, J. *Chem. - A Eur. J.* **2010**, *16* (32), 9905–9909.

(121) Fernández-Mateos, A.; Madrazo, S. E.; Teijón, P. H.; González, R. R. *European J. Org. Chem.* **2010**, *2010* (5), 856–861.

(122) Xu, L.; Li, B.-J.; Wu, Z.-H.; Lu, X.-Y.; Guan, B.-T.; Wang, B.-Q.; Zhao, K.-Q.; Shi, Z.-J. *Org. Lett.* **2010**, *12* (4), 884–887.

(123) Yuan, Y.; Shi, X.; Liu, W. *Synlett* **2011**, *2011* (4), 559–564.

(124) Kummerlöwe, G.; Behl, M.; Lendlein, A.; Luy, B. *Chem. Commun.* **2010**, *46* (43), 8273–8275.

(125) Brar, A. S.; Kaur, S. *J. Polym. Sci. Part A Polym. Chem.* **2005**, *43* (23), 5906–5922.

(126) Klumpp, D. A.; Sanchez, G. V.; Aguirre, S. L.; Zhang, Y.; Leon, S. de. *J. Org. Chem.* **2002**, *67* (14), 5028–5031.

(127) Tomasi, J.; Mennucci, B.; Cammi, R. *Chem. Rev.* **2005**, *105* (8), 2999–3094.

Chapter 3

Ir-catalysed Michael-type hydroalkylation of alkyl aryl nitriles to cyclic α,β-unsaturated ketones

3.1. Introduction

The Michael addition of carbon nucleophiles to activated olefins is one of the most important reactions for the formation of C-C bonds. Typically, these additions are catalysed by strong bases such as alkali hydroxides and alkoxides.[1] Despite the effectivity of these processes, the strong basic conditions generate side products as a result of competing reactions. To avoid side reactions, catalysis mediated by transition metals that work under neutral conditions has emerged as an efficient alternative to based-catalysed Michael addition reactions.

Over the last years, there have been reported many examples of transition metal catalysed Michael additions of substrates featuring activated C-H bonds.[2] Typically, these substrates contain at least two electron-withdrawing groups (EWG) that make the C-H bond at the α-carbon atom considerably acidic and highly reactive (Scheme 3.1). These substrates include β-ketoesters, β-diketones, malonates, cyanoacetates etc.

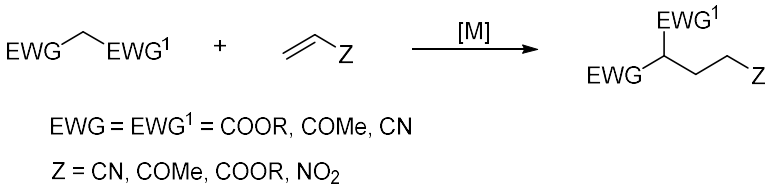

Scheme 3.1: Transition metal-catalysed Michael addition of C-H activated nucleophiles

One of the first examples was the Michael addition catalysed by [Ni(acac)$_2$] reported by Nelson *et al*.[3] They described the addition of various β-dicarbonyl compounds to a range of activated alkenes (Scheme 3.2).

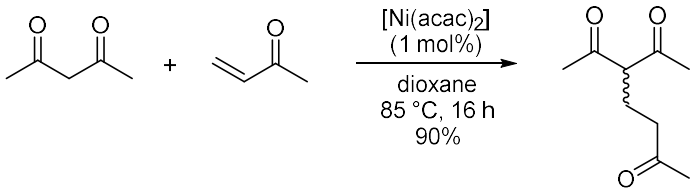

Scheme 3.2: An early example of Michael addition catalysed by $[Ni(acac)_2]$

Michael additions of β-dicarbonyl compounds have been also mediated by a cheap and environmentally-friendly catalyst such as $FeCl_3$ (Scheme 3.3).[4] Thus, the iron-catalyzed addition of β-diketones to styrene derivatives afforded addition products in good to excellent yields (52-96%).

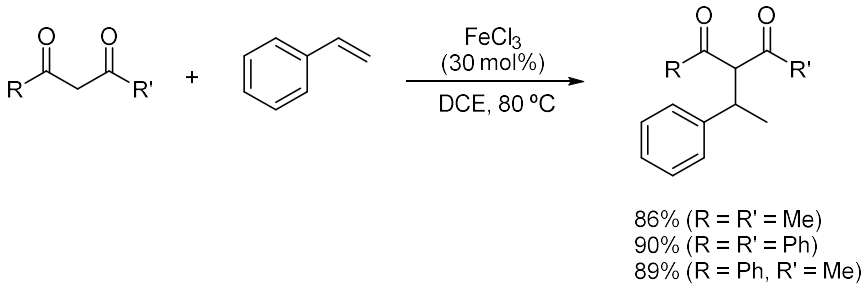

Scheme 3.3: $FeCl_3$-catalysed Michael addition of β-diketones to styrene

A similar addition of β-dicarbonyl compounds to olefins was achieved in an intramolecular manner in the presence of a silver catalyst (Scheme 3.4).[5] The resulting 6-membered products were obtained in good yields although this Michael addition reaction is limited to olefin moieties with a phenyl group at the terminal carbon atom.

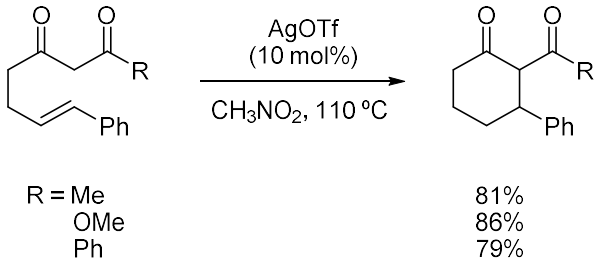

Scheme 3.4: Ag-catalysed intramolecular Michael addition of β-dicarbonyl compounds to olefins

In the following years, the advances on this field have been focused on 1,4-additions in an enantioselective fashion since this transformation offers great potential to construct stereocenters in a single step. As a result, asymmetric Michael additions became of

considerable interest for synthetic applications. The first example of enantioselective Michael addition involved coupling of β-ketoesters and methyl vinyl ketone mediated by $[Co(acac)]_2$ and a chiral diamine ligand (Scheme 3.5).[6] Although enantiomeric excess ratios were not excellent, this example became the starting point for the further development of enantioselective Michael additions.

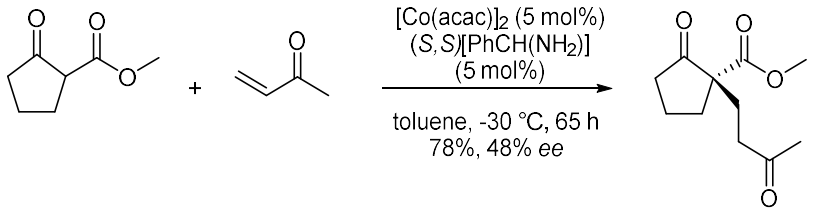

Scheme 3.5: Early example of an asymmetric Michael addition catalysed by cobalt

An improvement of enantioselectivity of Michael additions of β-ketoesters to different enones was achieved with a chiral phosphine palladium complex reported by Hamashima (Scheme 3.6).[7] The use of the novel chiral palladium complex afforded products with high yields and excellent enantioselectivities.

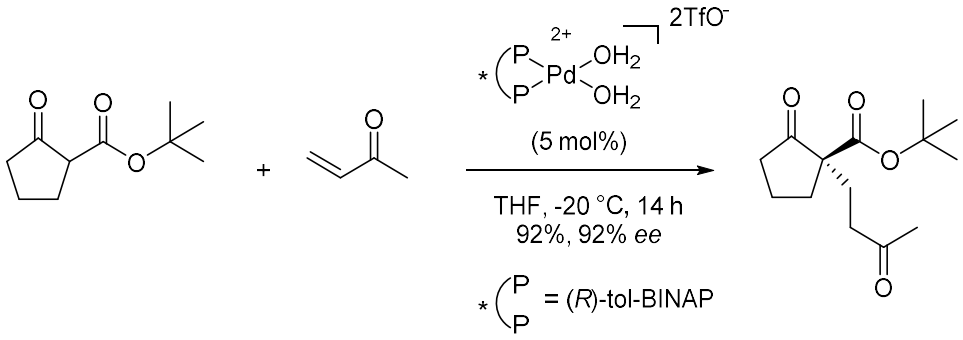

Scheme 3.6: Pd-catalysed enantioselective Michael addition of β-ketoesters to methyl vinyl ketone

On the other hand, asymmetric Michael addition of dimethyl malonate to cyclopentenone was reported to be catalysed by a chiral ruthenium amino complex (Scheme 3.7).[8] This method afforded the addition products with high yields and good enantioselectivities. Moreover, useful data on the insight of the reaction mechanism was provided through the isolation of catalyst intermediates formed from the coordination of malonates substrates to the ruthenium catalyst.

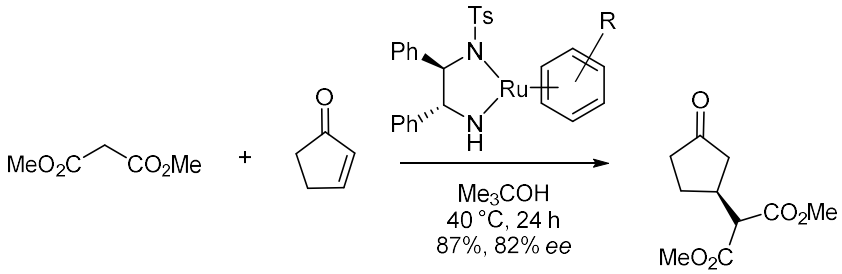

Scheme 3.7: Ru-catalysed enantioselective Michael addition of dimethyl malonate to cyclopentenone

Other transition metals such iridium complexes were also efficient catalysts for Michael addition reactions. A binuclear iridium hydride effectively mediated the addition of ethyl cyanoacetate to acrylonitrile with quantitative yield of the double addition product (Scheme 3.8).[9]

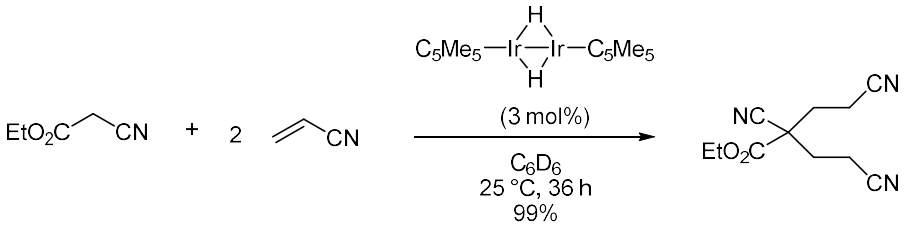

Scheme 3.8: Michael addition of cyanoesters to acrylonitrile catalysed by a binuclear iridium complex

In the last decades, numerous other catalytic systems were reported which broaden the scope of Michael donors and acceptors and explore other potential catalysts. For instance, active methylene compounds such as disulfones have been proved suitable Michael donors for the addition to α,β-unsaturated carbonyl compounds catalysed by a ruthenium hydride complex (Scheme 3.9).[10]

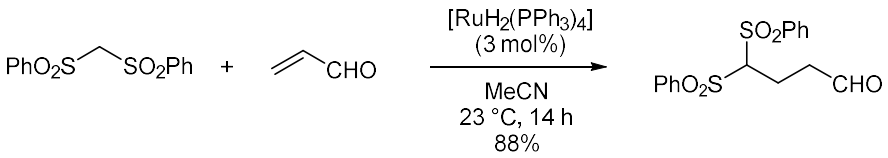

Scheme 3.9: Michael addition of disulfones as Michael donors

Michael additions were also performed with catalysts based on inexpensive metals such as copper. Thus, Mann and co-workers reported the enantioselective construction of

quaternary stereocenters by the derivatization of carbonyl Michael donors with chiral amine auxiliaries (Scheme 3.10).

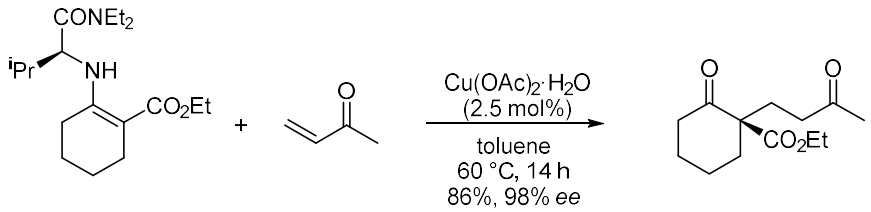

Scheme 3.10: Conjugate addition of enamines to methyl vinyl ketone catalysed by copper

Recently, lanthanide derivatives have emerged useful catalysts that also permit access to asymmetric additions. Interestingly, Michael reactions were reported in aqueous media at room temperature by using $Yb(OTf)_3$ as catalyst. This lanthanide salt gave good results in the addition of β-ketoesters with ethylacrylate; remarkably, the catalyst could be reused.[11] Complexes of other lanthanides such as europium[12] and lanthanum[13] also effectively mediate the addition of activated Michael donors to various olefins.

The described examples show that many catalysts consisting in transition metal and lanthanide complexes effectively mediate Michael additions of activated C-H nucleophiles, that is, C-H acids that contain at least two electron-withdrawing substituents at the α-carbon. However, the scope of Michael type hydroalkylations with non-activated C-H nucleophiles is narrow.

To date, the hydroalkylation using relatively weak C-H acidic substrates has been accomplished *via* directed C-H activation. N-heterocycles and carbonyls are common directing groups used in these transformations. For example, directed alkylation of α-C-H bonds in amines with various olefins in the presence of a ruthenium catalyst was reported by Murai *et al* (Scheme 3.11).[14] Pyridyl and pyrimidyl moieties served here as directing groups. The reaction, however, produced mixtures of mono- and dialkylated products in most of the cases.

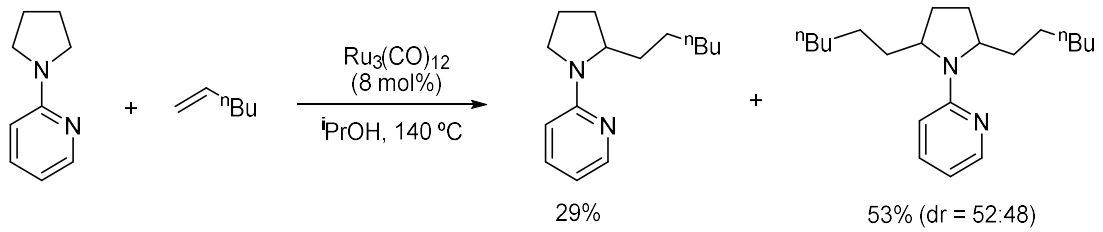

Scheme 3.11: Ru-catalysed alkylation of C-H bonds adjacent to nitrogen atoms

Similar directed alkylations of C-H bonds were later developed with substrates containing a removable benzoxazole chelating group (Scheme 3.12).[15] The reaction was catalysed by an iridium (I) complex and gave products of monoalkylation with good regioselectivity from moderate to high yields for both cyclic and linear chain amines.

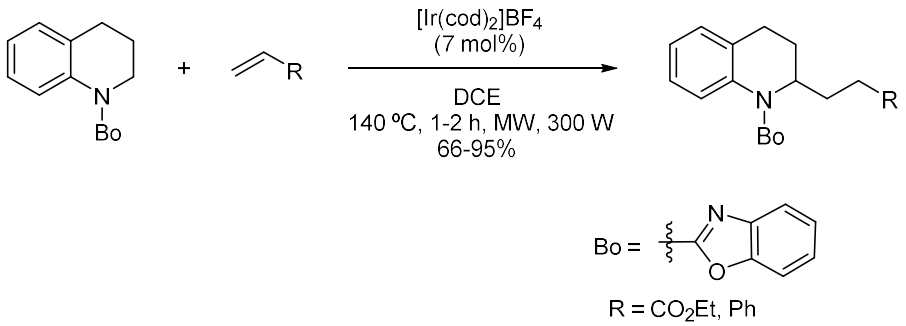

Scheme 3.12: Ir-catalysed regioselective C-H alkylation of amines using removable DG

Other example of the use of non-activated substrates is found in the enantioselective alkylation of 2-(alkylamino)pyridines with alkenes in the presence of a chiral cationic Ir(I) catalyst (Scheme 3.13).[16] This method afforded chiral amines with good yields (47-88%) and good enantiomeric excess (61-99%).

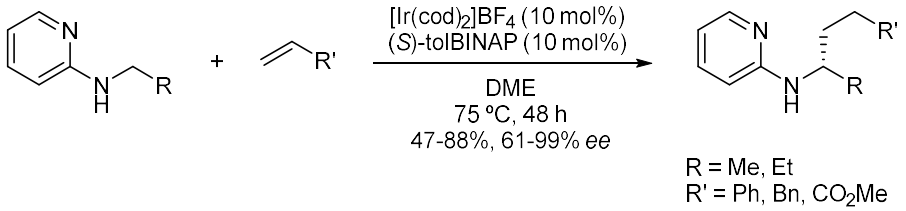

Scheme 3.13: Ir(I)-catalysed enantioselective C-H alkylation of 2-(alkylamino)pyridines with alkenes

On the other hand, the α-alkylation of aliphatic ketones was also achieved with simple olefins *via* Rh-enamine cooperative catalysis (Scheme 3.14).[17] A bifunctional ligand,

such as 1,2-dihydro-7-azaindole, was used to form enamines with ketones. This enamine serves as a cooperating ligand[18] enabling the C-H coupling with the olefin. Different 3-substituted cyclopentanones can be coupled with ethylene at the less hindered α-carbon to the carbonyl group. Various functionalities such as hydroxyls, malonates, esters, phenyls or amines were tolerated.

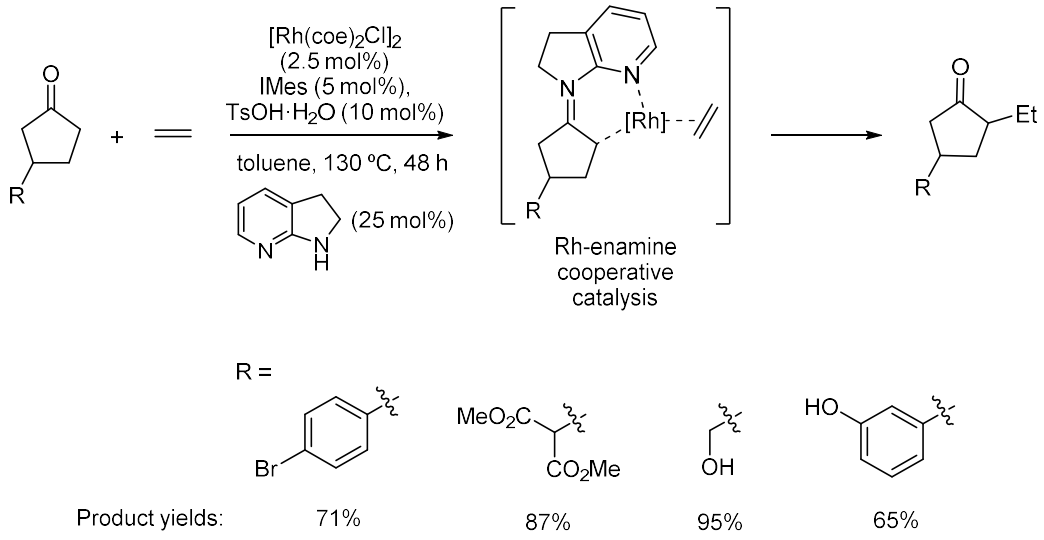

Scheme 3.14: Rh-catalysed α-alkylation of non-activated cyclopentanones with ethylene

Metal-enamine cooperative catalysis has also been employed for the intramolecular coupling of ketones with olefins using a ruthenium catalyst (Scheme 3.15).[19] This method employs 2-aminopyridine as a bifunctional ligand to promote the alkylation in a similar strategy to the previous example. Six-membered ring products were afforded from the intramolecular alkylation of cyclic ketones and olefins with good yields.

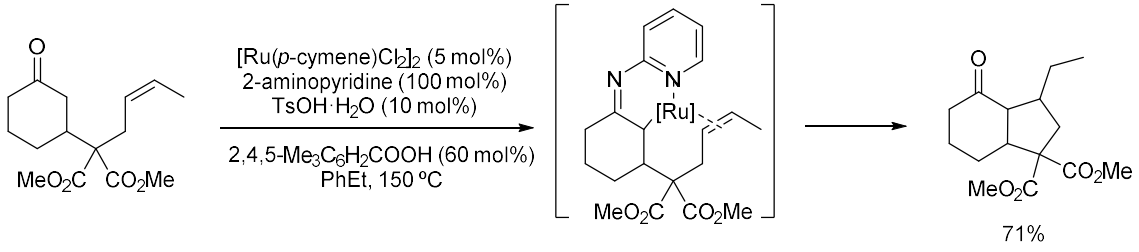

Scheme 3.15: Ru-catalysed intramolecular α-alkylation of cyclohexanones with olefins

Other functionalised non-activated substrates such as benzyl nitriles have been scarcely employed as nucleophiles since their low C-H acidity complicate their participation in metal-catalysed alkylations.[20] A progress was made for the addition of these type of

nitriles with olefins for the synthesis of glutarimides.[21] Specifically, phenylacetonitriles were added to acrylonitrile in the presence of an iridium pentahydride complex and the resulting dinitrile product underwent hydrolysis to give the corresponding glutarimide (Scheme 3.16). The scope of this method included mainly C-H acidic nitriles and only two non-activated substrates were reported (R = Me, Et). Although high catalyst loadings and temperatures were used, these substrates smoothly reacted with acrylonitrile to give glutarimides in 92-94% yields.

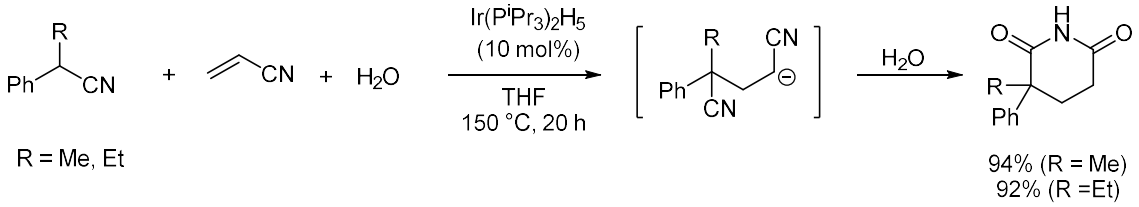

Scheme 3.16: Ir-catalysed synthesis of glutarimides *via* Michael addition benzyl nitriles to acrylonitrile

More recently, two examples of Michael-type additions of non-activated nitriles have been reported; the reactions were catalysed by exotic metal pincer-type complexes. The first of these examples described by Milstein and co-workers employed a rhenium PNP pincer complex (Scheme 3.17).[22] The use of this pincer complex was crucial for activation of benzyl cyanide *via* metal-ligand cooperation and enabling Michael addition of this compound to α,β-unsaturated esters and ketones, such as methyl acrylate, methyl vinyl ketone or 2-cyclohexen-1-one. The corresponding Michael adducts were afforded in moderate to good yields (55-93%).

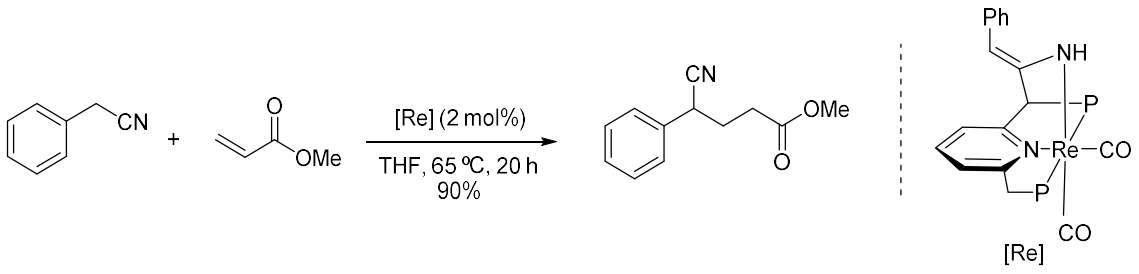

Scheme 3.17: Michael addition of non-activated benzyl cyanide to methyl acrylate catalysed by a Re PNP-pincer complex

The second example reported by the Milstein's group involved the use of a manganese PNP-pincer complex to promote the conjugate addition of non-activated nitriles to various α,β-unsaturated carbonyl compounds (Scheme 3.18).[23] Remarkably, this was the first reported example of the use of aliphatic nitriles as Michael donors. The list of nitriles included acetonitrile, propionitrile, butyronitrile and benzyl cyanide.

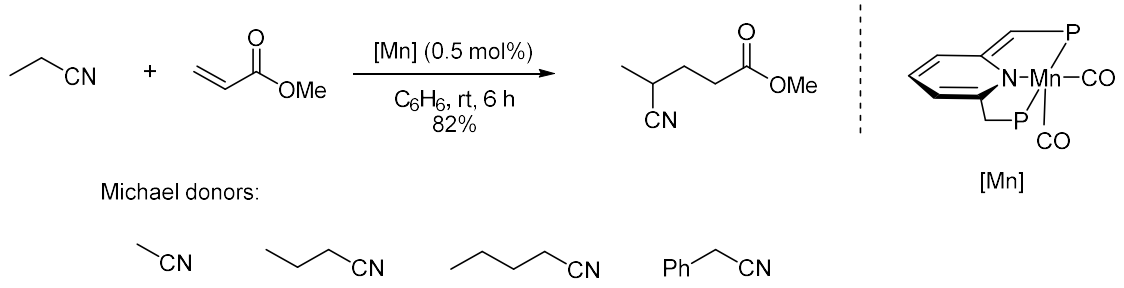

Scheme 3.18: Michael addition of non-activated aliphatic nitriles to methyl acrylate catalysed by a Mn PNP-pincer complex

In conclusion, there are only a few examples of Michel-type additions (hydroalkylations) of weakly acidic C-H nucleophiles and most of these examples involve activation of primary or secondary α-C-H bonds. To date, alkylations of non-activated tertiary C-H bonds have not yet been investigated. However, the use of this kind of substrates can provide straightforward access to products with quaternary centres of high synthetic interest.

Herein, we aim to develop a catalytic Michael-type reaction with weakly C-H acidic nucleophiles bonds, such as alkyl aryl nitriles. We are particularly interested in using substrates bearing tertiary C-H bonds that serve as convenient building blocks to create new functionlized compounds with quaternary centres. Notably, the development of this reaction would significantly extend the scope of known Michael type additions and would open new opportunities for synthesis of complex molecules with new stereocenters. In this context, we seek to further explore the synthetic utility of this Michael-type hydroalkylation by the coupling of this process with another catalytic process that will be discussed in following sections.

3.2. Development of Ir-catalysed Michael addition of aryl nitriles to 2-cyclohexen-1-one

In the present chapter, a novel Ir-catalysed Michael-type hydroalkylation reaction of non-activated nitriles with cyclic α,β-unsaturated ketones is reported (Scheme 3.19). The idea arose from our previous findings on the reversibility of the C-C bond cleavage of dinitriles where the hydroalkylation of acrylonitrile with diphenylacetonitrile was found to be promoted by $Ir(P^iPr_3)_2H_5$ (Chapter 2, section 2.2).

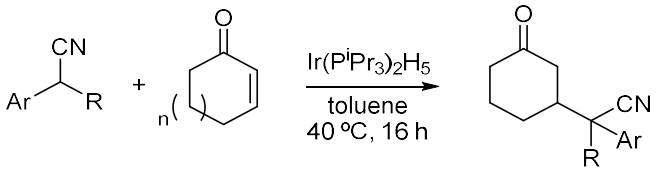

Scheme 3.19: Developed Ir-catalysed Michael-type hydroalkylation reaction of non-activated alkyl aryl nitriles

The described Michael-type hydroalkylation occurs under mild conditions and provides a straightforward access to new substituted cyclohexanones containing a quaternary centre. This method compliments existing synthetic pathways toward substituted cyclohexanones that are important building blocks for organic synthesis including production of polymers[24] and pharmaceuticals.[25,26] In addition, this method constitutes one of the few examples of conjugate additions with non-activated nitriles as Michael donors.

Finally, we illustrated the synthetic applicability of our Michael-type hydroalkylation for the synthesis of *meta*-substituted phenols *via* substituted cyclohexanones (Scheme 3.20). Phenol derivatives are valuable precursors for industrial manufacture of resins, plastics, dyes, herbicides, pigments as well as drugs.[27, 28] Standard synthetic methods to obtain substituted phenols such as aromatic substitutions are limited to *orto*- and *para*-substituted derivatives.[29] However, the preparation of *meta*-substituted phenols is more challenging and only a small number of catalytic synthesis has been reported previously. Herein, we describe the synthesis of the novel *meta*-substituted phenol **71** containing a quaternary carbon *via* a facile catalytic method.

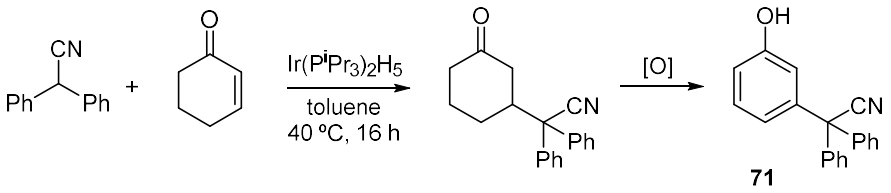

Scheme 3.20: Catalytic hydroalkylation reaction to form substituted cyclohexanones followed by subsequent dehydrogenation to form *meta*-substituted phenol **71**

3.2.1. Optimization of reaction conditions with $Ir(P^iPr_3)_2H_5$ catalyst

After our finding that the $Ir(P^iPr_3)_2H_5$ complex catalyses the Michael-type addition of diphenylacetonitrile to acrylonitrile (Chapter 2, section 2.2), we aimed to explore the scope of this reaction. As starting point, we devised the Michael addition of diphenylacetonitrile **3** to 2-cyclohexen-1-one **60a** as model reaction. With this aim, 2-cyclohexen-1-one **60a** (10 equiv) and diphenylacetonitrile **3** were allowed to react in the presence of 10 mol% of $Ir(P^iPr_3)_2H_5$ in toluene at 80 °C for 16 h (Scheme 3.21). For our delight, this reaction led to the formation of the desired 2-(3-oxocyclohexyl)-2,2-diphenylacetonitrile **61a** in 93% GC yield at full conversion of nitrile **3**.

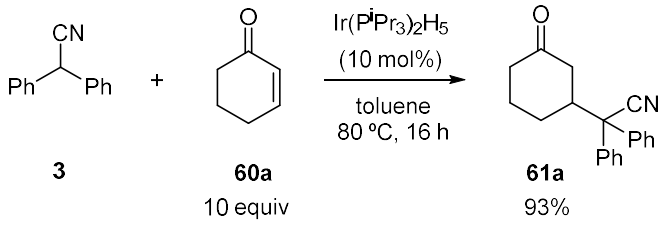

Scheme 3.21: Model Ir-catalysed Michael addition of dipheylacetonitrile to 2-cyclohexen-1-one

Encouraged by these results, we explored the optimal conditions to conduct this reaction. Firstly, optimisation of the amount of the cyclic ketone was carried out in toluene at 80 °C for 16 h (Table 5.1). The decrease in the number of equivalents of **60a** to 5 and 2 equiv did not dramatically affect the yield of product **61a**, which was obtained in 91% yield in both cases (entries 2 and 3).

We next studied whether the reaction can be conducted at milder temperature (Table 5.1). Initially, the model Michael addition was tested at 60 °C using 10 equiv of ketone **60a**

which afforded the product **61a** in 96% yield (entry 4). Decreasing of temperature to 40 °C led to excellent yield of the desired cyclohexanone, 98% (entry 5). However, conducting this reaction at room temperature led to a lower yield of 40% (entry 6).

Optimization of the amount of 2-cyclohexen-1-one at 40 °C gave similar results to the experiments conducted at 80 °C. The use of 5 and 3 equiv of ketone **60a** at 40 °C produced the desired product **61a** in 97 and 95% yield, respectively (entries 7 and 8). When the amount of ketone was decreased to 2 equiv, the desired product **61a** was obtained in 90% yield (entry 9). The decrease of amount of ketone to 1.5 equiv slightly diminished the yield of the product to 83% (entry 10).

Table 3.1: Optimization of temperature and ratio of **3** to **60a** in the model reaction.

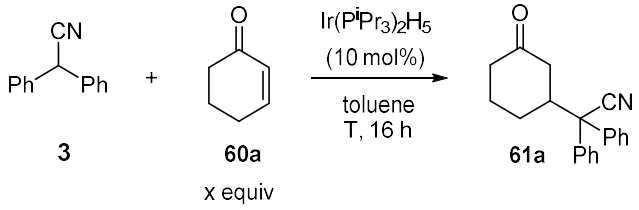

Entry	T, °C	60a, equiv	Conversion 3, %	Yield 61a, %
1	80	10	93	93
2	80	5	91	91
3	80	2	91	91
4	60	10	96	96
5	40	10	98	98
6	rt	10	40	40
7	40	5	97	97
8	40	3	95	95
9	40	2	90	90
10	40	1.5	85	83

[a]: Yields and conversions determined by GC. Reaction conditions: Substrate **3** (0.16 mmol, 0.2 M), substrate **60a** (X equiv, 0.4 M), $Ir(P^iPr_3)_2H_5$ (10 mol%), dodecane (GC standard) in toluene (0.8 ml).

During this screening, we observed formation of side products when 5 or more equivalents of ketone were used. GC and GC-MS data indicated the formation of cyclohexanone, phenol and traces of 2-cyclohexen-1-one dimer **62** which was later confirmed by NMR and MS (Scheme 3.22).

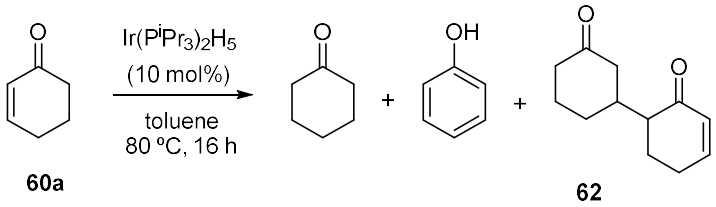

Scheme 3.22: By-products formed from 2-cyclohexen-1-one during the model hydroalkylation reaction

The formation of cyclohexanone and phenol can be explained by the Ir-catalysed transfer hydrogenation of **60a**, where one molecule of **60a** acts as a hydrogen acceptor and a second one as a hydrogen donor.[30] The hydrogenation of 2-cyclohexen-1-one **60a** to cyclohexanone occurs by the *in situ* generation of dihydrogen from the dehydrogenation of the ketone forming phenol. On the other hand, by-product **62** is formed by the dimerization of ketone **60a** *via* Michael addition.[31] This ketone **60a** can act as a Michael donor and undergo a nucleophilic attack to a second molecule of **60a** affording product **62**.[32] Hence, the minimisation of the amount of cyclohexenone **60a** is important for suppressing the side reactions and getting cleaner hydroalkylation reactions.

Once the amount of ketone was optimized, the catalyst loading was screened at 40 °C with 2 equivalents of ketone **60a** (Table 3.2). Remarkably, lowering of the catalyst loadings from 5 mol% to 0.5% did not affect the yield of the desired product **61a** significantly. When 5 or 2 mol% of $Ir(P^iPr_3)_2H_5$ were employed, **61a** was obtained in 95% yield in both cases (entries 1 and 2, respectively). Similarly, 1 and 0.5 mol% of iridium catalyst gave **61a** in 93% yields (entries 3 and 4).

Table 3.2: Optimization of catalyst loading[a]

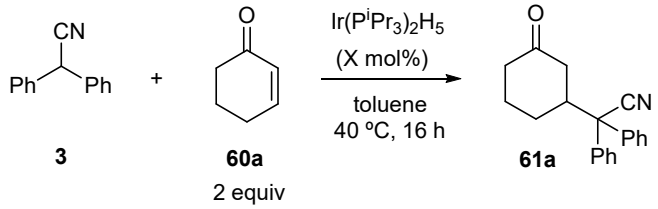

Entry	Catalyst loading, mol%	Conversion 3, %	Yield 61a, %
1	5	95	95
2	2	95	95
3	1	93	93
4	0.5	93	93

[a]: Yields and conversions determined by GC. Reaction conditions: Substrate **3** (0.16 mmol, 0.2 M), substrate **60a** (X equiv, 0.4 M), Ir(P^{i}Pr$_3$)$_2$H$_5$ (X mol%), dodecane (GC standard) in toluene (0.8 ml) at 40 °C for 16 h.

In summary, the screening of the Ir-catalysed hydroalkylation of 2-cyclohexen-1-one with diphenylacetonitrile allowed us to identify the use of 0.5 mol% of iridium catalyst at 40 °C with 2 equivalents of ketone **60a** as the optimal conditions to conduct this reaction. When this catalytic experiment was scaled up from 0.16 to 0.8 mmol of nitrile **3**, the desired cyclohexanone **61a** was obtained in 94% isolated yield under the optimised conditions.

3.2.2. Proposed catalytic cycle

A general catalytic cycle for this Michael-type hydroalkyltion is shown on Scheme 3.23. This catalytic cycle has been rationalised based on our previous mechanistic studies of the C-C cleavage of dinitriles and on the principle of microscopic reversibility.

The catalytic cycle starts with the generation of the active catalytic species "IrL$_2$H" *via* releasing of dihydrogen from the starting iridium pentahydride complex (L= P^{i}Pr$_3$) or *via* hydrogenation of cyclohexenone. Then, alkyl aryl nitrile coordinates to the iridium through the nitrogen atom to generate intermediate **63**. The N-coordinated alkyl aryl nitrile in **63** undergoes C-H activation by the iridium centre to give complex **38'**.

According to our previous mechanistic studies, we propose the formation of complex **37'** as a reaction intermediate from the coordination of a second molecule of alkyl aryl nitrile to complex **38'** (Chapter 2, Section 2.10). Subsequently, 2-cyclohexen-1-one **60a** coordinates to complex **38'** through the carbonyl oxygen atom[33,34] to give complex **64**. The next step involves the nucleophilic attack of the α-deprotonated alkyl aryl nitrile to the conjugated double bond of the ketone to form the new C-C bond and generating complex **65**. We propose that **65** exists as N- and η^1-O-bonded enolato complex. The coordination of enolato ligands through the O atom to the metal is supported by literature precedents.[35, 36] Finally, the desired product **61a** is formed after reductive elimination and the active catalytic species are regenerated.

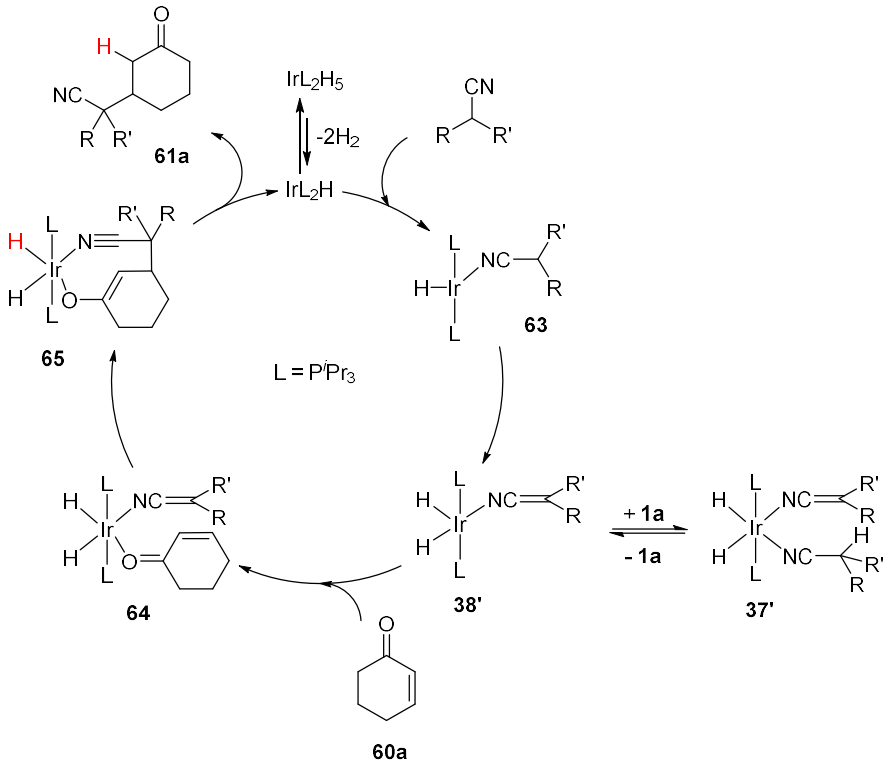

Scheme 3.23: Proposed mechanism of Ir-catalysed Michael addition of alkyl aryl nitriles to 2-cyclohexen-1-one **60a**

3.2.3. Screening of catalysts

Similar to the catalyst screening conducted for the C-C bond cleavage of unstrained dinitriles (Chapter 2, Section 2.3), we aimed to find a more stable catalytic system that could be used instead of the extremely air-sensitive $Ir(P^iPr_3)_2H_5$ complex. To achieve this, we sought an alternative catalyst that can be generated *in situ* from commercially available sources and can mediate the Michael addition of diphenylacetonitrile to 2-cyclohexen-1-one in comparable yields to the $Ir(P^iPr_3)_2H_5$ complex.

This screening was focused on iridium complexes as have been shown to effectively mediate selected Michael additions.[9,37] As discussed in the previous section, we propose that the present C-C forming reaction implicate the C-H activation of diphenylacetonitrile **3** as one of the initial steps of this transformation. Based on this, we focused our screening on catalysts potentially active to mediate C-H functionalisation such as phosphine,[38,39] phenanthroline[40,41] and N-heterocyclic carbene iridium complexes.[42,43] Similar to the screening conducted for the C-C cleavage of dinitriles, these complexes were generated *in situ* from the combination of the corresponding ligand and $[Ir(cod)Cl]_2$. Ligands with different electronic and steric properties were tested. For this screening, the Michael addition of diphenylacetonitrile **3** to ketone **60a** (2 equiv) was conducted using 2.5 mol% of $[Ir(cod)Cl]_2$ and corresponding ligand in toluene at 40 °C for 16 h.

We probed several monodentate phosphines (10 mol%) including triisopropylphosphine, di(1-adamantyl)-n-butylphosphine, tricyclohexylphosphine, and CyJohnPhos (Table 3.3, entries 1-4) as well as the bidentate phosphine (±)-BINAP (5 mol%) (Table 3.3, entry 5). Unfortunately, none of the tested phosphine ligands led to the formation of the desired product **61a**.

On the other hand, 3,4,7,8-tetramethyl-1,10-phenanthroline and $[Ir(cod)Cl]_2$ were also tested as catalytic system (Table 3.3, entry 6) but product **61a** was not afforded under these conditions. In front of this result, no other phenanthrolines were tested.

Table 3.3. Screening of catalysts[a]

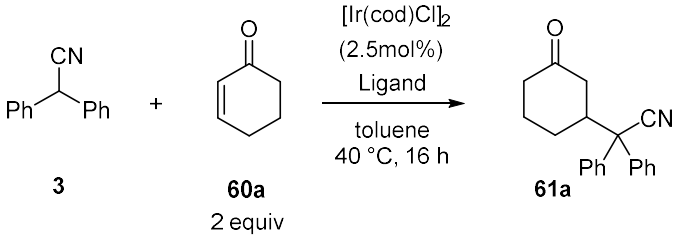

Entry	Ligand	Base	Conversion 3, %	Conversion 60a, %	Yield 61a, %
1	P^iPr_3	-	0	17	0
2	Ad_2PBu	-	0	23	0
3	PCy_3	-	0	23	0
4	CyJohnPhos	-	0	18	0
5	rac-BINAP	-	0	49	0
6	Me_4-phen	-	0	23	0
7	IBu·HBF_4	^{t}BuONa	3	100	3
8	SIMes·HCl	^{t}BuONa	36	44	36
9	IPropyl·HBF_4	^{t}BuONa	25	100	25
10	IAd·BF_4	^{t}BuONa	55	100	55
11	IPr·HCl	^{t}BuONa	81	90	81
12	SIPr·HCl	^{t}BuONa	80	71	80
13[b]	SIPr·HCl	^{t}BuONa	94	56	94
14[c]	SIPr·HCl	^{t}BuONa	89	80	89
15	SIAd·BF_4	^{t}BuONa	85	74	85
16	IMes·HCl	^{t}BuONa	92	63	92

[a]: Conversions and yields determined by GC. Reaction conditions: Substrate **3** (0.16 mmol, 0.2 M), substrate **60a** (2 equiv, 0.4 M), $[Ir(cod)Cl]_2$ (2.5 mol%), ligand (monodentate: 10 mol%, bidentate: 5 mol%), base (12 mol%, if required), dodecane (GC standard) in toluene (0.8 ml) at 40 °C for 16 h. [b]: 3 equiv of 2-cyclohexen-1-one were used. [c]: Using $[Ir(coe)_2Cl]_2$ (2.5 mol%) as a catalyst.

Thereupon, various N-heterocyclic carbene (NHC) iridium complexes were also tested combining $[Ir(cod)Cl]_2$ and free NHC generated *in situ* from NHC salts (10 mol%) with sodium *tert*-butoxide (12 mol%). Herein, several NHC (Figure 3.1) with different electronic and steric properties were tested (Table 3.3, entries 7-16). When the reaction was conducted with IBu·HBF_4 (Table 3.3, entry 7), very low yields of product **61a** were obtained. Moderate yields of the desired product were obtained with SIMes·HCl, IPropyl·HBF_4 and IAd·HBF_4: 36, 25 and 55% yield, respectively (entries 8-10). Delightfully, the use of ligands IPr·HCl and SIPr·HCl afforded cyclohexanone **61a** in 81 and 80% yield, respectively (entries 11 and 12). Promising results obtained with SIPr·HCl, encouraged us to optimise the reaction conditions with this ligand to improve the yield of the product **61a**. With this aim, the amount of ketone **60a** was increased to 3 equiv using SIPr·HCl as a ligand which afforded product **61a** in 94% yield (entry 13). In addition, an alternative iridium source such as $[Ir(coe)_2Cl]_2$ (2.5 mol%) was also tested with SIPr·HCl (10 mol%) leading to the addition product **61a** in 89% yield (entry 14). Finally, the NHC ligands SIAd·BF_4 and IMes·HCl were tested which afforded product **61a** in excellent yields: 85 and 92%, respectively (entries 15 and 16).

In summary, the screening of an alternative catalytic system allowed to identify several N-heterocyclic carbene iridium complexes as active catalyst to promote the model Michael addition. Specifically, SIPr·HCl, IPr·HCl, SIAd·BF_4 and IMes·HCl in combination with $[Ir(cod)Cl]_2$ and ^{t}BuONa generate active catalysts for the synthesis of product **61a** in excellent yields.

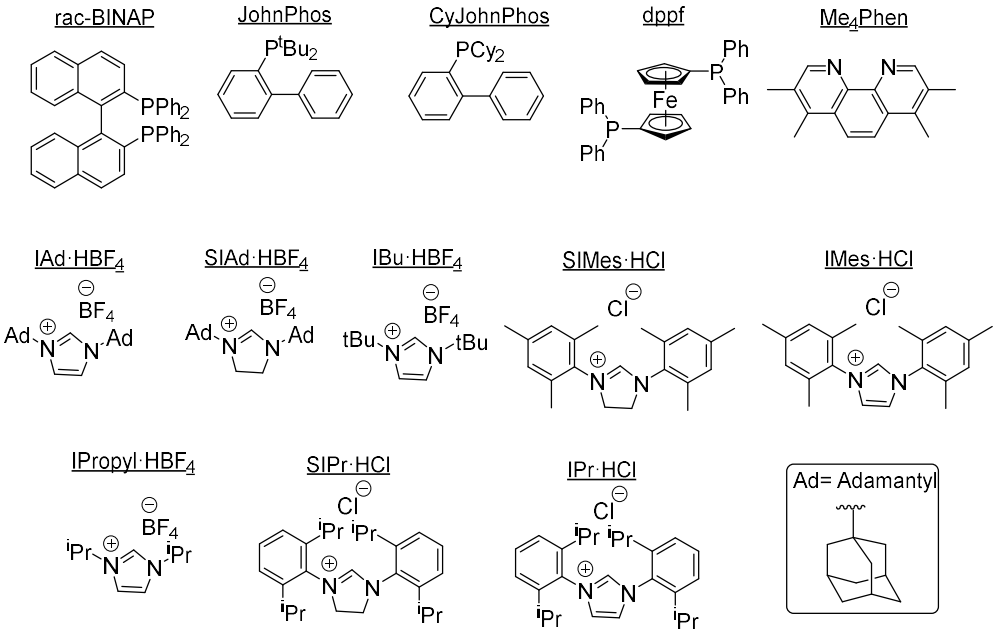

Figure 3.1: Screened ligands for the Ir-catalysed hydroalkylation of 2-cyclohexen-1-one

During our screening studies with NHC ligands, 2-cyclohexen-1-one **60a** was consumed in most of these experiments even when low yields of product **61a** were obtained (Table 3.3, entries 7, 9 and 10). These results might indicate the consumption of ketone **60a** *via* a side process under these conditions. To understand the origin of this process, we conducted some control experiments using cyclohexenone **60a** (2 equiv) in the presence of diphenylacetonitrile **3** under different reaction conditions (Table 3.4). Initially, when the model Michael addition reaction was conducted in the absence of catalyst, ligand and additive (Table 3.4, entry 1), no conversion of any of the substrates **3** and **60a** was observed. Similarly, when the model reaction was conducted in the presence of $[Ir(cod)Cl]_2$, both substrates appeared to be unreactive (entry 2). Afterwards, when the reaction was conducted in the presence of IAd·HBF_4 and ^{t}BuONa, complete consumption of the ketone was observed (entry 3). When the model reaction was conducted in the presence of catalytic amounts of ^{t}BuONa (12 mol%), ketone **60a** was fully consumed (entry 4).

Table 3.4: Control experiments[a]

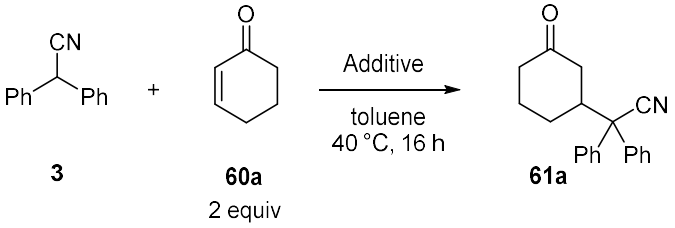

Entry	Additive, mol%	Conversion 3, %	Conversion 60a, %	Yield 61a, %
1	-	0	0	0
2	$[Ir(cod)Cl]_2$ (2.5)	0	0	0
3	IAd·HBF_4 (10), ^{t}BuONa (12)	14	100	0
4	^{t}BuONa (12)	10	100	0

[a]: Reaction conditions: Substrate **3** (0.16 mmol, 0.2 M), substrate 60**a** (2 equiv, 0.4 M), dodecane (GC standard) in toluene (0.8 ml) at 40 °C for 16 h.

These results indicated the instability of 2-cyclohexen-1-one in the presence of ^{t}BuONa. To test this idea, ketone **60a** (1 equiv) was allowed to react with ^{t}BuONa (6 mol%) in toluene at 40 °C for 16 h (Scheme 3.24). The analysis by GC and GC-MS revealed the formation of two addition products **62** and **66** in 20 and 41% GC yields, respectively at 61% conversion of the ketone. The formation of products **62** and **66** was confirmed by NMR after their isolation in 10 and 21% isolated yield, respectively. The formation of products **62** and **66** is the result of the 1,4-addition between two molecules of ketone **60a**. Base-catalysed dimerization of this ketone to form product **62** in the presence of CsF has been reported previously.[31]

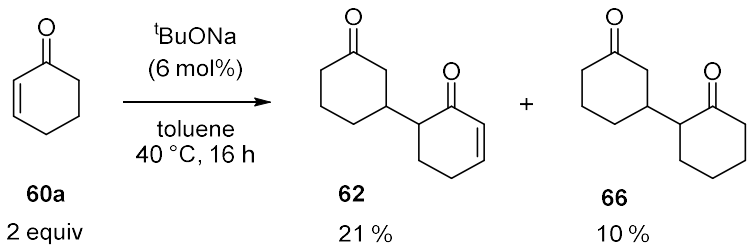

Scheme 3.24: Dimerisation of 2-cyclohexen-1-one catalysed by ^{t}BuONa

Although some of the tested N-heterocyclic carbene iridium complexes have been shown to be active catalysts, these require higher catalyst loadings (5 mol%) compared to $Ir(P^iPr_3)_2H_5$ (0.5%) and promote undesired side reactions with ketone **60a**. For this reason, $Ir(P^iPr_3)_2H_5$ was selected as catalyst for investigation of scope and limitation of the hydroalkylation of non-activated nitriles to cyclic ketones.

Before turning to further investigation of the $Ir(P^iPr_3)_2H_5$ catalysed Michael-type hydroalkylation, we explored the potential activity of organocatalysts in this transformation. A wide variety of organocatalysts have been proved to mediate Michael addition reactions.[44] Most of the reported organocatalysed Michael additions are limited to C-H activated substrates as Michael donors, such as cyanoesters, dialkyl malonates, diketones etc. and there are no described examples of organocatalytic Michael-type reactions with non-activated C-H substrates.

Recently, Belokon *et al.* studied the Michael addition reaction of cyanoester **67** to 2-cyclohexen-1-one catalysed by (*S*)-BIMBOL in combination with phenolate lithium salt which afforded product **68** in excellent yield (Scheme 3.25).[45]

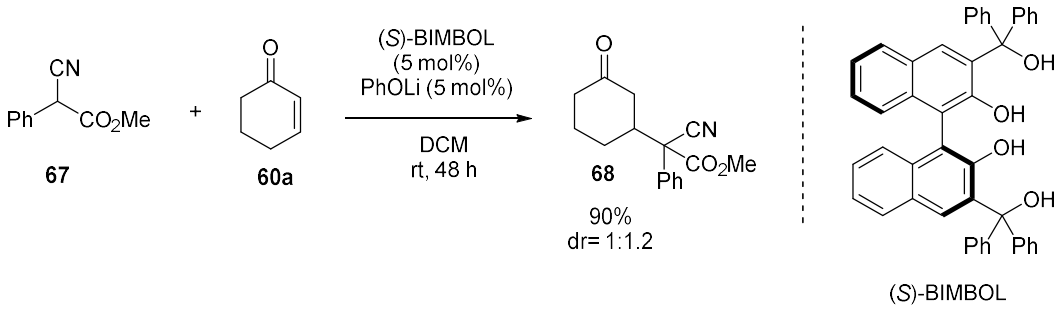

Scheme 3.25: Michael addition of 2-cyclohexen-1-one catalysed by (S)-BIMBOL and PhOLi

Based on the similarity of our method with this organocatalytic reaction to afford substituted cyclohexanones, we tested the activity of (±)-BIMBOL to mediate Michael addition of diphenylacetonitrile **3** to 2-cyclohexen-1-one **60a**. Thus, diphenylacetonitrile **3** and 2-cyclohexen-1-one **60a** (1 equiv) were allowed to react with (±)-BIMBOL (5 mol%) and PhOLi (5 mol%) in DCM at room temperature for 48 h (Scheme 3.26). This experiment showed that both substrates are completely unreactive under these conditions. The reaction was also conducted at 80 °C but no formation of expected product **61a** was observed either.

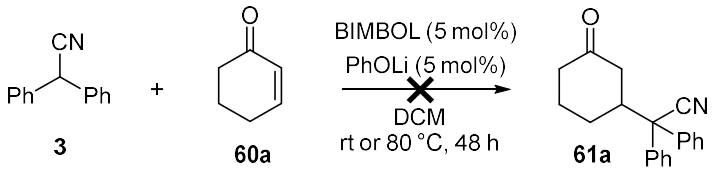

Scheme 3.26: Michael addition of nitrile **3** to ketone **60a** catalysed by BIMBOL and PhOLi

This experiment indicates that the Michael addition of a non-activated nitrile is not mediated by an organocatalyst such as BIMBOL. In contrast, our developed Ir-catalysed Michael addition activates this kind of substrate affording the addition products with excellent yield indicating the novelty of our developed catalytic method.

3.2.4. Scope of cyclic α,β-unsaturated ketones

The excellent results obtained during the optimization of the Ir-catalysed Michael addition of diphenylacetonitrile to 2-cyclohexen-1-one with $Ir(P^iPr_3)_2H_5$ (Section 5.2.1) encouraged us to examine the scope of cyclic α,β-unsaturated ketones. We sought to test a range of cyclic α,β-unsaturated ketones of different ring size and learn how the ring size affects the reactivity. With this aim, cyclic ketones of 5 and 7-membered rings were tested in the catalytic reaction. The 5-membered ketone **60b** (2 equiv) was tested as a Michael acceptor using diphenylacetonitrile **3** and 0.5 mol% of $Ir(P^iPr_3)_2H_5$ in toluene at 40 °C for 16 h (previously optimised conditions) which led to the formation of cyclopentanone **69** in 25% yield (Table 3.5, entry 1). With this initial result in hands, the reaction conditions were optimised to enhance yields of **69**. Firstly, reaction temperature was screened. The pentenone **60b** (2 equiv) was allowed to react with diphenylacetonitrile **3** in the presence of 0.5 mol% of $Ir(P^iPr_3)_2H_5$ at 80 °C which improved the product yield to 44% (entry 2). To further improve the yield, the catalyst loading was increased to 2.5 mol% at 40 °C that led to product **69** in 98% yield (entry 3).

Table 3.5: Optimization of temperature and catalyst loading of Michael addition of diphenylacetonitrile to 2-cyclopenten-1-one[a]

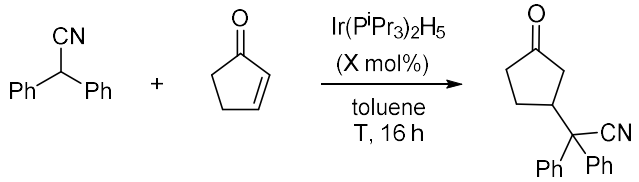

3 60b 2 equiv 69

Entry	T, °C	Catalyst loading, mol%	Conversion 3, %	Yield 69, %
1	40	0.5	28	25
2	80	0.5	46	44
3	40	2.5	99	98

[a]: Conversions and yields determined by GC. Reaction conditions: Substrate **3** (0.16 mmol, 0.2 M), substrate **60a** (2 equiv, 0.4 M), $Ir(P^iPr_3)_2H_5$ (X mol%), dodecane (GC standard) in toluene (0.8 ml) at the indicated temperature for 16 h.

Afterwards, the 7-membered ketone **60c** was tested as Michael acceptor under the optimised conditions but no desired heptanone was obtained (Table 3.6, entry 1). Also, when this reaction was conducted at 80 °C no desired heptanone was detected (entry 2).

In contrast to 5 and 6-membered ketones, heptacyclic ketone appeared to be unreactive under these conditions (Table 3.6). This result might be explained by the increased steric bulk of the seven-membered ring in **60c** as compared to the five- and six-membered ring in **60b** and **60a**, respectively. The increased steric bulk may hamper the coordination of the alkene to the iridium centre in **38'** as well as the intramolecular C-C bond forming nucleophilic attack (Scheme 3.27).

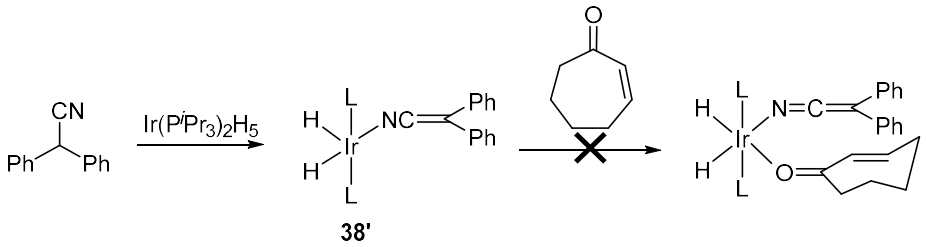

Scheme 3.27: The steric hindrance of cycloheptenone **55c** preserves the coordination to iridium complex **38'**

After investigating the effect of the ring size, we evaluated the effect of alkyl substitution in the ring. With this aim, we screened substituted 2-cyclohexen-1-ones. The methylcyclohexenone **60d** was tested with diphenylacetonitrile **3** using 0.5 mol% of $Ir(P^iPr_3)_2H_5$ at 40 °C but unfortunately, no conversion of nitrile **3** was observed and the desired cyclohexanone was not formed (entry 3). Similarly, 3-methyl-2-cyclohexen-1-one **60e** and nitrile **3** appeared unreactive under the standard conditions (entry 4).

Alkyl substituted cyclohexanones do not undergo Michael-type hydroalkylation under these conditions. Similar to the case of cycloheptenone **60c**, the steric hindrance added by the methyl group could impede the binding of ketones **60d** and **60e** to the iridium centre or slow down the intramolecular C-C bond formation. Consequently, the addition of diphenylacetonitrile to these ketones does not occur.

Table 3.6: Scope of cyclic α,β-unsaturated ketones

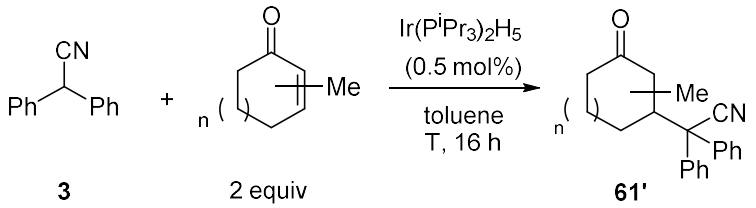

3 2 equiv 61'

Entry	Ketone	T, °C	Conversion 3, %	Yield product 61', %
1	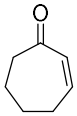 60c	40	0	0
2		80	0	0
3	 60d	40	0	0
4	 60e	40	0	0
5	 60a	40	93	93
6[b]	 60b	40	99	98

[a]: Conversions and yields determined by GC. Reaction conditions: Substrate **3** (0.16 mmol, 0.2 M), substrate **60a** (2 equiv, 0.4 M), $Ir(P^iPr_3)_2H_5$ (0.5 mol%), dodecane (GC standard) in toluene (0.8 ml) at the indicated temperature for 16 h. [b]: $Ir(P^iPr_3)_2H_5$ (2.5 mol%)

3.2.5. Scope of Michael donors

After the screening of cyclic α,β-unsaturated ketones, the scope of the Michael donors was also studied to the extension of the present Ir-catalysed Michael addition. This screening was limited to non-activated nitriles or other functionalities in which the α-C-H bond possesses low acidity. With this aim, we initially tested several aryl nitriles with

different substituents at the α-carbon atom of the nitrile. Additionally, we also screened the scope of directing groups, replacing the cyano group in nitriles for other functionalities such as ketone and pyridyl moieties to study their suitability to direct the Michael addition reaction.

Initially, we focused on benzyl nitriles with different substituents at the α-carbon. That is, either of the two phenyl groups of the model diphenylacetonitrile **3** was substituted for alkyl or aryl groups, such as methyl, benzyl, cyclohexyl, isopropyl or 2-pyridyl (Figure 3.2). The synthesis of the corresponding nitriles **3c**, **3d**, **3g** and **3h** is described in the next section.

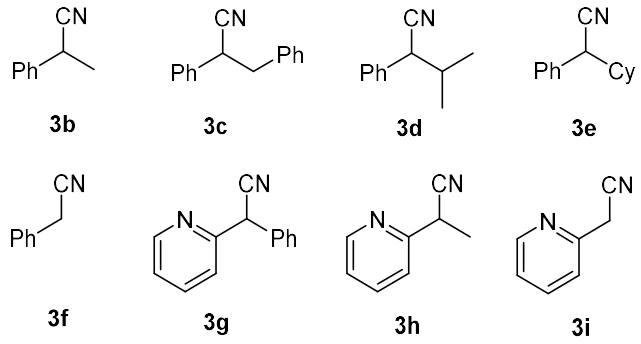

Figure 3.2: Alkyl aryl nitrile substrates for Ir-catalysed Michael-type hydroalkylation

3.2.5.1. Synthesis of aryl nitrile substrates

These substrates were synthesised *via* base-mediated nucleophilic substitution reactions. Thus, 2,3-diphenylpropanenitrile **3c** was obtained from benzyl cyanide and benzyl bromide in the presence of KOH and tetrabutylammonium bromide (TBAB) in 45% yield (Scheme 3.28).

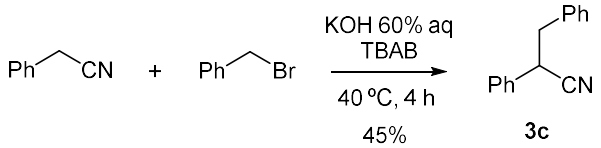

Scheme 3.28: Synthesis of 2,3-diphenylpropanenitrile

The isopropylbenzylnitrile **3d** was obtained from benzyl cyanide and isopropyl iodide with KOH and TBAB in 10% yield (Scheme 3.29).

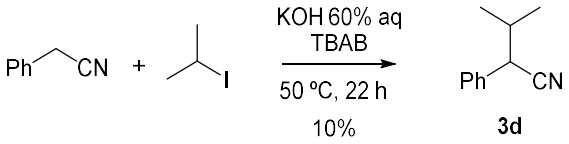

Scheme 3.29: Synthesis of 3-methyl-2-phenylbutanenitrile

Then, 2-pyridyl nitrile **3g** was prepared from benzyl cyanide and 2-bromopyridine in the presence of KOH in DMSO in 60% yield (Scheme 3.30A). Finally, 2-(2-pyridyl)propanenitrile **3h** was prepared from 2-pyridylacetonitrile and iodomethane with potassium tert-butoxide in THF in 21% yield (Scheme 3.30B).

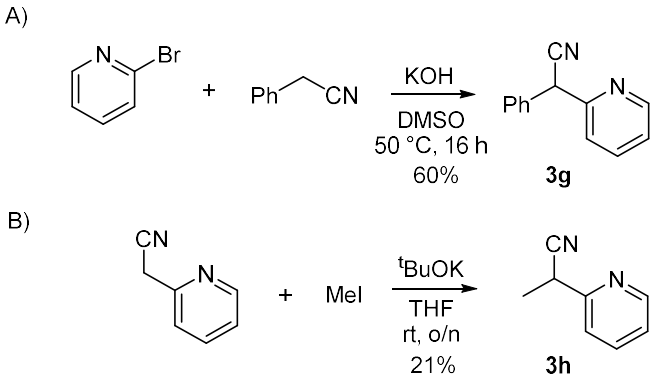

Scheme 3.30: Synthesis of A) 2-phenyl-2-(2-pyridyl)acetonitrile and B) 2-(2-pyridyl)propanenitrile

3.2.5.2. Screening of Michael donors

The aryl nitriles bearing various α-substituents of different bulkiness were screened under the optimised reaction conditions. Thus, alkyl aryl nitriles **3b-j** (Figure 3.2) were tested with 2-cyclohexen-1-one **60a** as a model substrate in the presence of 0.5 mol% of $Ir(P^iPr_3)_2H_5$ in toluene at 40 °C for 16 h (Table 3.7). The reaction of α-methyl nitrile **3b** gave the desired product **61b** in 87% isolated yield. Switching from α-methyl nitrile **3b** to a bulkier α-benzyl nitrile **3c** led to a small decrease in the yield of the cyclohexanone product from 87% (**61b**) to 80% (**61c**). The use of more sterically hindered nitriles such as α-isopropyl **3d** and α-cyclohexyl **3e** gave only low yields of corresponding products

61d (17%) and **61e** (14%) when using the standard catalyst loading of 0.5 mol% (experimental section 3.6.2.1). However, when catalyst loadings were increased to 5 mol%, good yields of 58% were obtained in both cases (Table 3.7). In the same time, the unsubstituted benzyl nitrile **3f** gave an excellent product yield of 96%, the highest of the tested nitriles. These results indicate that the $Ir(P^iPr_3)_2H_5$ is an excellent catalyst for the Michael-type addition of substituted alkyl benzyl nitriles to cyclohexenone under mild conditions. Indeed, the reaction leads to 3-substituted cyclohexanones in good to excellent yields even with relatively bulky benzyl nitriles.

Table 3.7: Scope of nitriles [a]

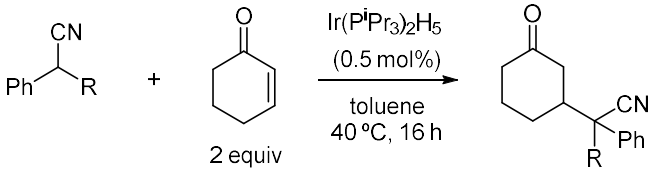

3a-j **60a** **61a-j**

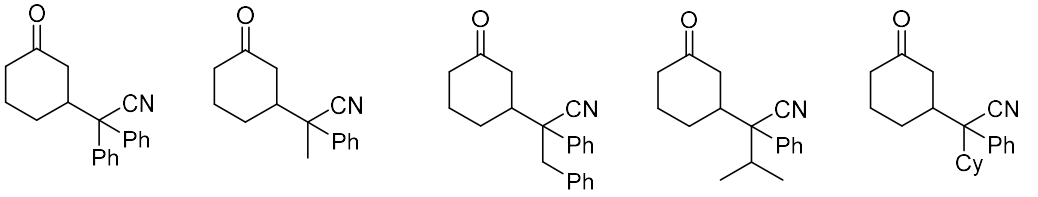

61a, 94% **61b**, 87% (1:1.7)[b] **61c**, 80% (1:1) **61d**, 58% (1:2.2)[c] **61e**, 58% (1:3.2)[c]

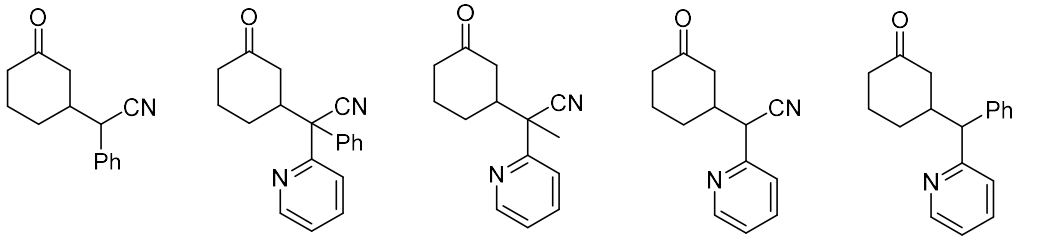

61f, 96% (1:1.1) **61g**, 95%[c] **61h**, 95% (1:1.1)[d] **61i**, 79% (1:1.02)[e] **61j**, n.d.[f]

[a] Isolated yields (dr determined by GC). Reaction conditions: Nitrile **3a-j** (0.8 mmol), 2-cyclohexen-1-one (1.60 mmol, 2 equiv), $Ir(P^iPr_3)_2H_5$ (0.004 mmol, 0.5 mol%) in toluene (4 ml) under Ar atmosphere, at 40 °C for 16 h. [b] dr determined from isolated diastereomers. [c] $Ir(P^iPr_3)_2H_5$ = 5 mol%. [d] $Ir(P^iPr_3)_2H_5$ = 2.5 mol%. [e] $Ir(P^iPr_3)_2H_5$ = 2.5 mol%, 2-cyclohexen-1-one (0.88 mmol, 1.1 equiv), [f] n.d. = not detected.

Products **61b-e** were obtained as a mixture of two diastereomers. The diastereometic ratio increase with increase in steric bulk of α-substituents in alkyl aryl nitirles: from 1:1 in

relatively unhindered **61c** to 1:3.2 in bulky **61e**. This fact may be rationalized by the steric hindrance of these substituents which complicates the addition to cyclohexenone (Table 3.7).

After testing different α-alkyl benzylic nitriles, we were also interested in screening nitriles bearing a pyridyl group in the α-position. We focused our attention in this type of functionalities because pyridine moieties are often found in compounds of pharmaceutical interest.[46] On the other hand, pyridine is also a widely used directing group for various catalytic C-H activations and its introduction into an organic molecule opens many opportunities for post-functionalisations. Specifically, pyridine directing groups enable alkylation of C-H bonds in benzylamines,[47] α-alkylation of cyclic amines[48,49] and alkylation of aromatic C-H bonds.[50] Encouraged by the importance of this functionality, we tested various pyridyl acetonitriles. As a starting point, we have chosen 2-pyridyl benzyl nitrile **3g**, which is formally obtained from the model diphenylacetonitrile **3** by replacing one of the phenyl groups for 2-pyridyl group (Table 3.7). When this substrate was used in the model Michael addition with 0.5 mol% of $Ir(P^iPr_3)_2H_5$, the product **61g** was afforded in 35% GC yield. The increase in catalyst loading to 5 mol% allowed to increase the yield to 95%. Building on these results, other pyridyl nitriles were tested. For instance, 2-pyridylpropanenitrile **3h** afforded product **61h** in 95% isolated yield in a diastereomeric ratio of 1:1.1 using 2.5 mol% of $Ir(P^iPr_3)_2H_5$. In addition, 2-pyridylacetonitrile **3i** was used as a substrate. The corresponding catalytic Michael addition with 5 mol% of Ir catalyst formed product **61i** in 48% GC yield. Under these catalytic conditions, an undesired product was detected that might correspond to cyclohexanone **70** according to GC-MS data and was formed in 52% GC yield as a mixture of diastereomers (Scheme 3.31). Product **70** can be generated from a subsequent Michael addition of product **61i** to ketone **55a**. To try to avoid the formation of this side product, the model reaction with nitrile **3i** was replicated using 2.5 mol% of catalyst which led to product **61i** in 87% GC yield and traces of undesired product **70** were still detected. After this observation, lower amount of 2-cyclohexen-1-one (1.1 equiv) with 2.5 mol% of catalyst were employed which led to product **61i** in 79% isolated yield as a mixture of diastereomers in a dr of 1:1.02 and no product **70** was detected (Table 3.7).

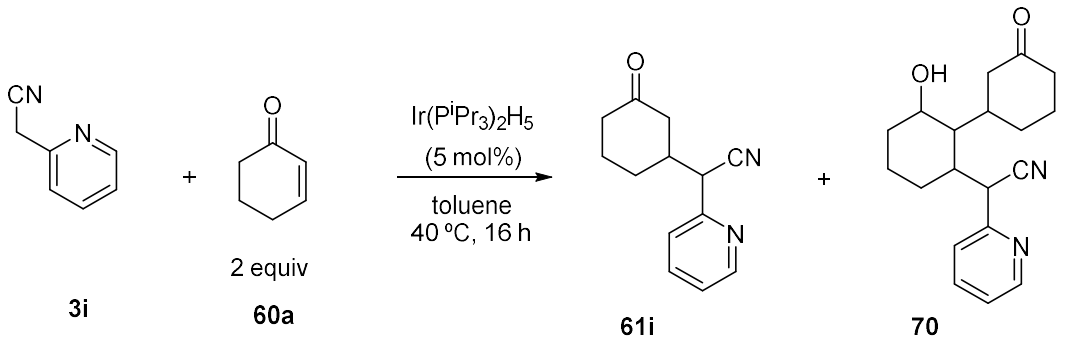

Scheme 3.31: Michael-type hydroalkylation of cyclohexenone **60a** with nitrile **3i**

Based on the excellent results with pyridyl nitrile substrates, we were interested in studying the reactivity of substrates bearing only a pyridine moiety as a directing group. To test this idea, we studied the reactivity of 2-benzylpyridine **3j** under our standard catalytic conditions. Unfortunately, this reaction did not let to formation of expected product **61j** either using 0.5 or 5 mol% of catalyst and no conversion of pyridyl **3j** was observed (Table 3.7).

We have shown that α-phenyl and α-pyridyl alkyl nitriles are excellent substrates for Ir-catalysed Michael-type hydroalkylation. We were wondering if we could expand the scope of substrates to less C-H acidic substrates such as dialkyl nitriles. With this idea in mind, cyclohexanecarbonitrile **3k** and isobutyronitrile **3l** (Figure 3.3) were tested as substrates but these nitriles remained unreacted.

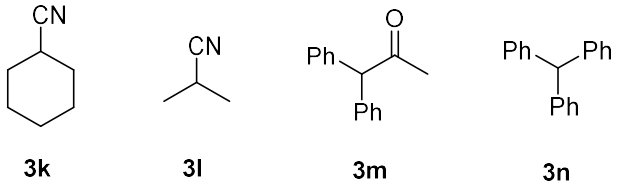

Figure 3.3: Other tested nucleophiles, non-working examples

In our efforts to expand the scope of Michael donors, we were interested in studying the reactivity of non-activated substrates with other directing functionalities than nitrile group. For example, we focused our attention on carbonyl groups as known functionalities to direct reactions involving C-H activation catalysed by iridium (as shown in Chapter 2, Section 2.4.2). With this purpose, 1,1-diphenylacetone **3m** (Figure 3.3) was tested in the catalytic reaction but the formation of the hydroalkylation product was not

observed. Finally, we tested a substrate without any directing group, but with a relative acidic benzylic C-H bond. With this aim, we selected a substrate with a α-C-H acidic bond such triphenylmethane **3n** (Figure 3.3). However, under standard reaction conditions this substrate remained unreactive, which suggests the need of a directing group such as nitrile for the Michael addition reaction of this kind.

In summary, we have developed iridium-catalyzed Michael-type hydroalkylation of α,β-unsaturated cyclic with non-activated alkyl aryl nitriles. The reaction occurs under mild conditions (40 °C) and in many cases as much as 0.5 mol% of catalyst is required. The scope of substrates encompasses benzyl nitriles bearing bulky alkyl substituents at the α-carbon, such as cyclohexyl, benzyl and isopropyl groups. In addition, 2-pyridyl analogues of benzyl nitriles also gave good yields of hydoalkylation products. It is noteworthy that for pyridyl compounds, higher catalyst loadings were needed compared to their benzyl nitrile analogous, which suggests higher reactivity of the latter.

3.3. Towards the dehydrogenation of substituted cyclohexanones to meta-substituted phenols

3.3.1. Introduction

The excellent results obtained with our developed Ir-catalysed Michael-type hydroalkylation of non-activated nitriles with cyclic α,β-unsaturated ketones encouraged us to further explore the application of this reaction. We sought to exemplify the synthetic utility of our Ir-catalysed hydroalkylation for a one pot synthesis of *meta*-alkyl phenols from cyclohexanones. This method involves the Ir-catalysed hydroalkylation as a first step with subsequent oxidation of the resulting 3-substituted cyclohexanones to phenols (Scheme 3.32).

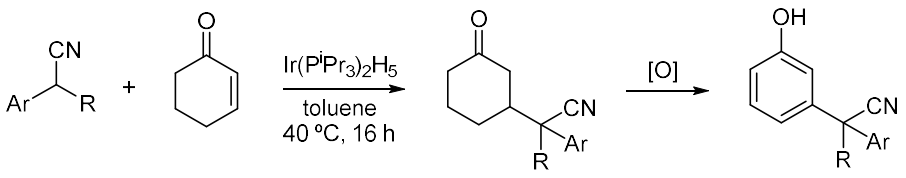

Scheme 3.32: Dehydrogenation of substituted cyclohexanones to *meta*-substituted phenols

Phenolic compounds are an extended motif of drugs and natural products that possess important pharmaceutical applications (Figure 3.4).[52] In addition, phenols are extensively used in chemical industries, such as food industry.[53,54] Hence, the development of a simple approach to substituted phenols is of important interest.

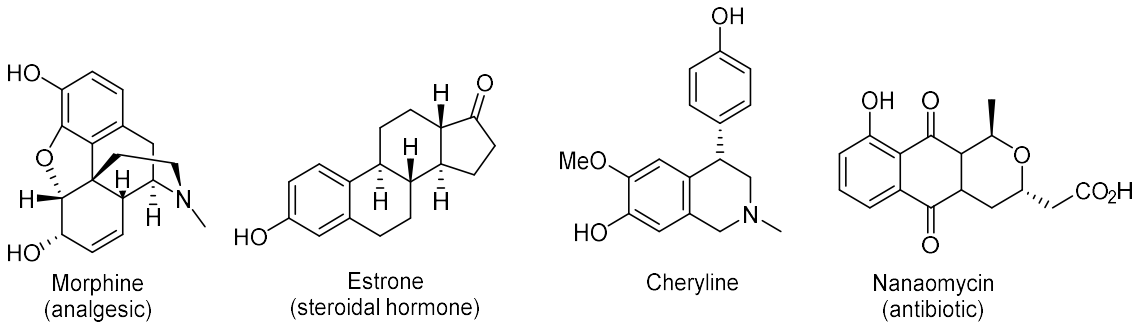

Figure 3.4: Natural products and drugs with phenol substructure

Common synthetic strategies to obtain substituted phenols rely on the functionalisation of the phenolic ring *via* electrophilic aromatic substitutions. However, the strong electronic directing effect of the OH group leads to *orto*- and *para*-substituted phenols and prevents the synthesis of *meta*-products.[29] Indeed, preparation of *meta*-substituted phenols *via* common organic synthetic methods is a challenging task that usually involves multi-step routes.[55] In the past decades, more straightforward catalytic strategies for synthesis of substituted phenols from ketones have been explored *via* dehydrogenation reactions.[56–58] For instance, Stahl *et al.* made a significant contribution in the dehydrogenation of cyclohexanones to phenols catalysed by Pd(II) in the presence of dioxygen. They discovered the use of a catalytic system based on $Pd(TFA)_2$ with 2-(N,N-dimethylamino)pyridine (^{2NMe2}py) and *p*-toluensulfonic acid (TsOH) led to high yields and conversions of this transformation (Scheme 3.33).[59]

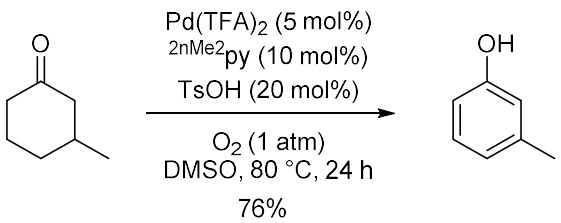

Scheme 3.33: Pd-catalysed dehydrogenation of cyclohexanones reported by Stahl

In addition, Liu *et al.* reported the palladium-catalysed dehydrogenation of cyclohexanones with different types of substituents including methyl, phenyl, furanyl or morpholinyl moieties at different positions to the carbonyl group.[60] This transformation is catalysed by Pd/C in the presence of K_2CO_3 as the additive under gas mixture atmosphere (30 vol% H_2 and 70 vol% N_2) which helps to improve the phenolic product yields (Scheme 3.34).

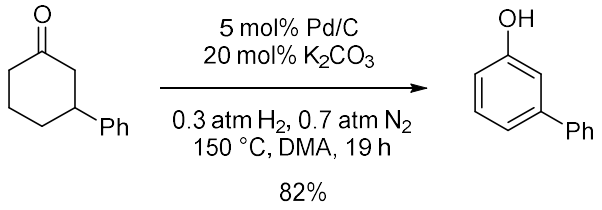

Scheme 3.34: Pd-catalysed dehydrogenation of cyclohexanones reported by Liu

The dehydrogenation of cyclohexanone to phenol was also observed by Nacci *et al.* during their studies on cyclopropanation in the presence of oxygen. Various ketones underwent cyclopropanation with styrene catalysed by $Pd(OAc)_2$ in the presence of $Cu(OAc)_2$, tetrabutylammoniumacetate (TBAA) and O_2 as oxidant.[61] When cyclopropanation of cyclohexanone was attempted, unexpected formation of phenol was observed in 50% yield (Scheme 3.35).

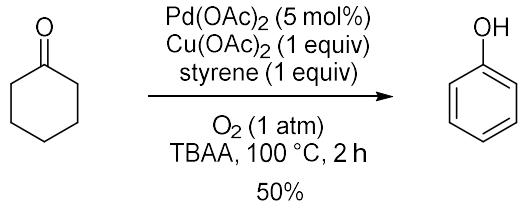

Scheme 3.35: Pd-catalysed dehydrogenation of cyclohexanone reported by Nacci

The feasibility of the facile access to *meta*-substituted phenols from cyclohexanones was also proved by a simple catalytic method with I_2 in DMSO. Liang *et al.* achieved the conversion of multisubstituted cyclohexanones to the corresponding phenol under these catalytic conditions in good yields (Scheme 3.36).[62]

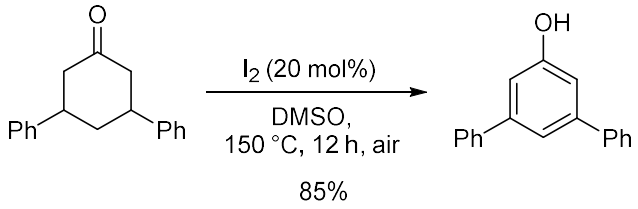

Scheme 3.36: I_2-catalysed dehydrogenation of cyclohexanone reported by Liang

However, existing examples of catalytic dehydrogenation of cyclohexanones are limited to substrates bearing aryl and simple alkyl substituents. Herein, we study a challenging dehydrogenation of a cyclohexanone bearing a quaternary carbon atom with bulky substituents. The dehydrogenation of this type of molecules is challenging because the presence of bulky substituents might hamper the coordination of the metal catalyst and slow down C-H activation required for the process. As a consequence, dehydrogenation of cyclohexanones with bulky substituents has not been investigated yet.

3.3.2. Screening of reaction conditions for the dehydrogenation of substituted cyclohexanones to meta-substituted phenols

With the aim to transform our substituted cyclohexanones to the corresponding phenols, we preliminary screened different reaction conditions based on the literature precedents.

As a model reaction, we selected the dehydrogenation of cyclohexanone **61a** which was one of the Michael addition products previously obtained (Section 3.2). Initially, the dehydrogenation of substrate **61a** was attempted following Stahl's conditions. Thus, ketone **61a** was heated with $Pd(TFA)_2$ (5 mol%), ^{2NMe2}py (10 mol%) and TsOH (20 mol%) under O_2 (1 atm) in DMSO at 80 °C. This reaction conditions led to phenol **71** in 30% yield at 70% conversion of the starting material (Scheme 3.37). To the best of our knowledge, synthesis of phenol **71** has not been described previously and therefore, herein we are reporting the formation of a novel compound. After this experiment, we also observed formation of some side products: diphenylacetonitrile **3** (11%), cyclohexenone **72** (34%), benzophenone **73** (13%) and traces of phenol **74** (Scheme 3.37).

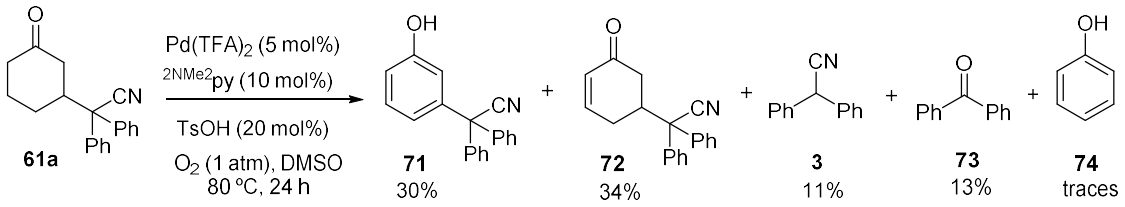

Scheme 3.37: Pd-catalysed dehydrogenation of cyclohexanone **61a**

The formation of cyclohexenone **72** can be explained by the mechanism of Pd-catalysed dehydrogenation of cyclohexanones proposed by Stahl.[63] The conversion of cyclohexanones to the corresponding phenols occurs in a double dehydrogenation step *via* a cyclohexenone intermediate after the first dehydrogenation (Scheme 3.38).

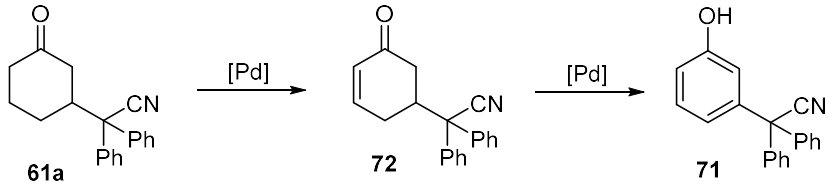

Scheme 3.38: Stepwise sequence for Pd-catalysed dehydrogenation of cyclohexanone **61a**

On the other hand, formation of diphenylacetonitrile **3** suggests that cyclohexanone **61a** undergoes retro-Michael addition *via* the cleavage of a C-C bond under these conditions (Scheme 3.39). We hypothesise that this process might occur due to the chelating abilities of the nitrile group that can coordinate to palladium. After the activation of the α-C-H bond to the ketone, the palladium centre might coordinate the cyano group[64] arranging the molecule in *syn* coplanar conformation that facilitates the β-alkyl elimination leading to formation of diphenylacetonitrile **3** and 2-cyclohexen-1-one **60a**. Subsequently, the formed diphenylacetonitrile **3** might undergo oxidative decyanation forming benzophenone **73** in the presence of O_2.[65] And on the other hand, ketone **60a** might undergo dehydrogenation affording phenol which was detected as a side product.

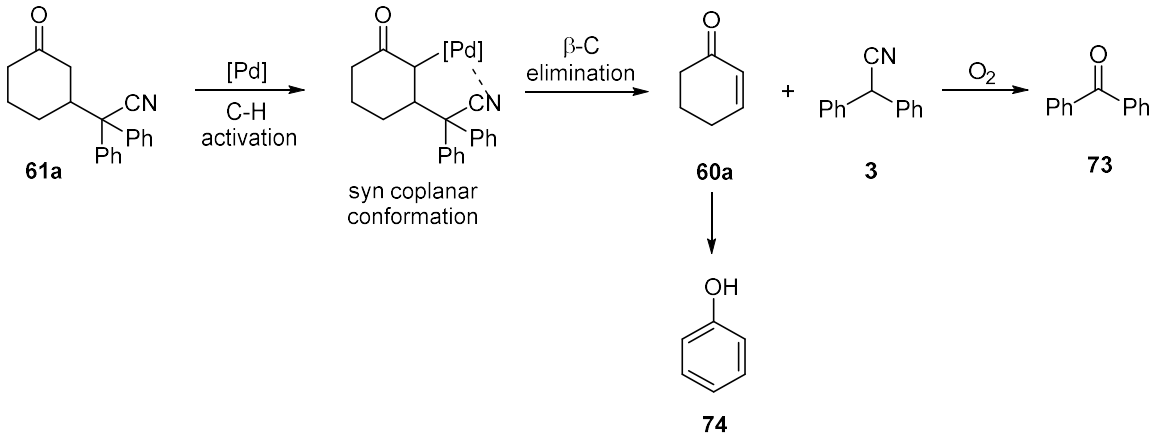

Scheme 3.39: Possible mechanism of formation of diphenylacetonitrile **3** from ketone **61a**

With these good results with Stahl´s conditions in hands, we decided to optimise catalyst loading and temperature of this reaction to try to increase the yield of phenol **71** and at the same time, reduce the formation of side products (Table 3.8). Thus, the increase of temperature to 100 °C has a favourable effect in yield ratio between phenol **71** and cyclohexenone **72** (Table 3.8, entry 4). The use of higher catalyst loadings to 10 and 20 mol% of palladium led to the highest yields of product **71** of 48 and 53% yield respectively (Table 3.8, entries 6 and 8). However, these conditions still lead to the formation of side products: diphenylacetonitrile **3**, benzophenone **73** and phenol **74** (Section 3.6.5.1.1).

We also explored whether the use of a glovebox to setup the reaction affects the product yields. Thus, we observed that this variation in the preparation of the reaction does not affect drastically the product ratio (Table 3.8, entry 2). Similarly, longer reaction times did not improve neither product **71** yields nor ratio **71**:**72** (Table 3.8, entry 3). In addition, we also decided to seek if other oxidant agents can improve the yield of **71**. The use of alternative oxidants such as Oxone or I_2 led to negligible amounts of desired phenol **71** (Table 3.8, entries 9 and 10).

Table 3.8: Optimisation of conditions for the dehydrogenation of cyclohexanone **56a** under Stahl´s conditions

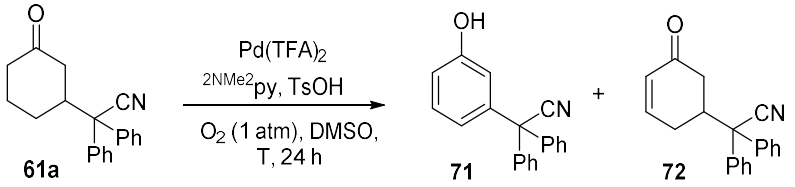

Entry	Pd: ^{2NMe2}py: TsOH, mol%	T, °C	Conversion 61a, %	Yield 71, %	Yield 72, %
1	5:10:20	80	70	30	34
2[a]	5:10:20	80	78	35	32
3[b]	5:10:20	80	73	25	22
4	5:10:20	100	73	27	13
5[c]	10:20:40	80	81	29	26
6	10:20:40	100	94	48	2
7	20:40:80	80	99	47	7
8	20:40:80	100	99	53	0
9[c]	5:10:20	80	25	3	4
10[d]	5:10:20	80	20	0	0

Reaction conditions: Cyclohexanone **61a** (0.48 mmol), $Pd(TFA)_2/^{2NMe2}$py/TsOH (mol% indicated), O_2 (1 atm), DMSO (0.8 ml), 24 h. [a]: Reaction set up in a glovebox. [b]: Reaction conducted for 48 h. [c]: Oxone (3 equiv) used as oxidant instead of O_2 [d]: I_2 (20 mol%) used as oxidant instead of O_2. All these tests led to formation of by-products diphenylacetonitrile **3**, benzophenone **73** and phenol **74**

With the aim to increase the yield of phenol **71**, we screened alternative reaction conditions for the dehydrogenation of cyclohexanone **61a**. Thus, we attempted to conduct this transformation following Liu´s conditions (Section 3.3.1). The authors indicated the effectivity of their method under both gas mixture atmosphere (30% H_2 and 70% N_2) and pure N_2 atmosphere. For convenience, we decided to test Liu's conditions under N_2 atmosphere (1 atm). Cyclohexanone **61a** was heated with Pd/C (5 mol%), K_2CO_3 (20 mol%) in N,N-dimethylacetamide (DMA) at 150 °C for 24 h under N_2 atmosphere

(Scheme 3.40). Unfortunately, this reaction did not lead to the formation of the desired phenol **71** (Table 3.9, entry 1). Instead, diphenylacetonitrile **3**, benzophenone and phenol were obtained as products in 10, 20 and 32% yield, respectively.

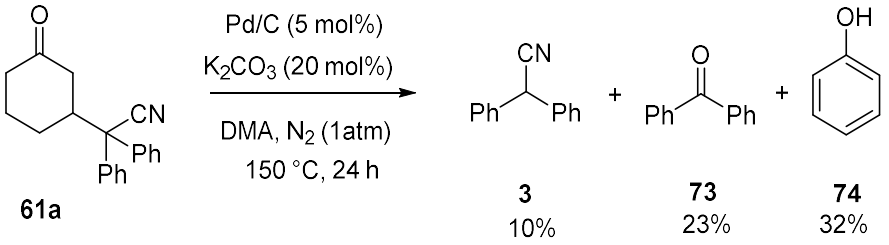

Scheme 3.40: Attempted dehydrogenation of cyclohexanone **56a** under Liu's conditions

Alternatively, dehydrogenation of cyclohexanone **61a** was attempted *via* Nacci´s conditions (Section 3.3.1). As previously mentioned, Nacci and co-workers observed the dehydrogenation of 2-cyclohexan-1-one during the study of cyclopropanation of ketones with styrene. To evaluate whether styrene participates in the dehydrogenation, we tested the oxidation of cyclohexanone **61a** under Nacci's conditions with and without styrene. By this way, ketone **61a** was mixed with $Pd(OAc)_2$ (5 mol%) in the presence of $Cu(OAc)_2$ (1 equiv), styrene (1 equiv) and TBAA at 100 °C for 4 h under O_2 (1 atm) (Table 3.9, entry 2). Unfortunately, these conditions did not lead to phenol **71**. When this experiment was replicated in the absence of styrene, formation of phenol **71** was not observed either (Table 3.9, entry 3).

The dehydrogenation of ketone **61a** was next attempted using Liang´s conditions (Section 3.3.1). When this ketone was heated with I_2 in DMSO at 80 °C for 16 h under air, diphenylacetonitrile **3** was the only product formed during the reaction (Table 3.9, entry 4).

Alternatively, we decided to test the dehydrogenation of cyclohexanone **61a** using DDQ as it have been proved to be an efficient oxidant for dehydrogenation reactions.[66, 67] Under these conditions, no desired phenol **71** was obtained (Table 3.9, entry 5).

Table 3.9: Dehydrogenation of cyclohexanone **61a**[a]

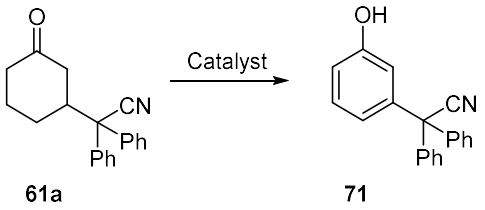

61a **71**

Entry	Catalytic conditions, mol%	Conversion 61a, %	Yield 71, %
1[b]	Pd/C (5), K_2CO_3 (20), DMA, N_2 (1 atm), 150 °C, 24 h	100	0
2	$Pd(OAc)_2$ (5), $Cu(OAc)_2$ (1 equiv), styrene (1 equiv), TBAA, O_2 (1 atm), 100 °C, 4 h	0	0
3	$Pd(OAc)_2$ (5), $Cu(OAc)_2$ (1 equiv), TBAA, O_2 (1 atm), 100 °C, 4 h	0	0
4[c]	I_2 (20), DMSO, 80 °C, 16 h	50	0
5[d]	DDQ (3 equiv), DMSO, 80 °C, 24 h	100	0

[a]: GC yields and conversions. Reaction conditions: Cyclohexanone **61a** (0.25 mmol) was allowed to react under the specified conditions. [b]: Diphenylacetonitrile **3**, benzophenone and phenol were obtained in 10, 20 and 32 % yield, respectively. [c]: Diphenylacetonitrile **3** was obtained in 50% yield. [d]: Diphenylacetonitrile **3** was obtained in 30% yield.

In conclusion, phenol **71** was synthesised as a novel compound *via* a facile catalytic dehydrogenation. The best preliminary results of the dehydrogenation of substituted cyclohexanone **61a** were obtained when $Pd(TFA)_2$ (20 mol%) in combination with ^{2NMe2}py (40 mol%) and TsOH (80 mol%) were used as catalyst in the presence of O_2 at 100 °C. Under these catalytic conditions, the partially dehydrogenated intermediate – cyclohexenone **72** – was fully converted to final phenol **71** which was obtained in 53% yield. However, formation of side products diphenylacetonitrile, benzophenone and phenol could not be avoided. In front of these preliminary results, further optimisation of the reaction, especially screening of alternative catalyst, would be required for the dehydrogenation of substituted cyclohexanones that can tolerate the presence of nitrile substituents.

3.4. Conclusions

We have developed a novel catalytic method for the Michael-type hydroalkylation of non-activated C-H nitriles to α,β-unsaturated ketones mediated by $Ir(P^iPr_3)_2H_5$. This method leads to excellent yields of substituted cyclohexanones with low catalyst loadings (0.5 mol%) and mild reaction temperatures (40 °C). It is noteworthy that no base is required in our method. In contrast to classical Michael additions, our method permits the use of weakly acidic substrates as Michael donors. The optimised reaction conditions were found to be compatible with non-activated C-H nitriles bearing different alkyl and aryl substituents, such as phenyl, methyl, benzyl and even bulky groups like cyclohexanyl and isopropyl. Interestingly, 2-pyridyl groups are also tolerated as substituents. According to the substrate screening conducted, a cyano group is required as directing group for this Michael reaction to occur. Remarkably, most of the synthesised substituted cyclohexanones have not been reported previously (compounds **61c-i**, table 3.7).

Other catalysts were found to be effective based on the combination of commercially available $[Ir(cod)Cl]_2$ and NHC ligands. Although $Ir(P^iPr_3)_2H_5$ showed the highest activity, NHC iridium complexes also gave good results at higher catalyst loadings (Ir = 5 mol%). The most effective NHC ligands found were SIPr·HCl, IPr·HCl, SIAd·HBF_4 and IMes·HCl which led to the formation of desired Michael addition product **61a** in high yields. On the other hand, we have evidenced that this Michael addition involving non-activated C-H nitriles is not mediated by an organocatalyst, such as BIMBOL, highlighting the importance of our method.

To study further applications of our hydroalkylation reaction, we conducted preliminary studies on the dehydrogenation of substituted cyclohexanones to form *meta*-substituted phenols. These studies indicated the feasibility of this reaction catalysed by $Pd(TFA)_2$ in combination with ^{2NMe2}py and TsOH. The *meta*-substituted phenol **71** containing a quaternary centre was synthesised as a novel compound.

The highest yield obtained of desired phenol **71** was 53% because of C-C cleavage side process undergone by cyclohexanone **61a** under these conditions. The presence of a nitrile group as a substituent might be the origin of the cleavage of cyclohexanone **61a**.

To try to increase the yield of the desired phenol, alternative catalysts must be tested to mediate this dehydrogenation reaction.

3.5. Future work

The development of a general method for the synthesis of *meta*-substituted alkyl phenols from cyclohexanones one pot hydroalkylation-dehydrogenation needs to be further investigated. Specially, an extensive catalyst screening for the dehydrogenation of cyclohexanones should be conducted. For this purpose, iridium complexes can be considered as alternative catalyst, as they have been described effective catalysts for alkane dehydrogenations, especially pincer iridium complexes are among the most active.[68–71] During our studies of Ir-catalysed Michael addition of diphenylacetonitrile to cyclohexenone, we observed dehydrogenation of this cyclic ketone to phenol in the presence of $Ir(P^iPr_3)_2H_5$ (Scheme 3.22). Based on this observation, this iridium pentahydride complex could be tested as catalyst for dehydrogenation of cyclohexanone **61a** in the presence of a hydrogen acceptor like *tert*-butylethylene (TBE).

Moreover, our developed two step catalytic method for the synthesis of *meta*-substituted phenols can be applied for obtaining pharmaceutically interesting scaffolds. Phenolic compounds containing quaternary ammonium moieties have been found to be biologically active compounds to treat pulmonary disorders such as compound **75** (Scheme 3.41).[72] We are interested in exploring the use of our method for the synthesis of compound **76** as a precursor to obtain phenol **75**.

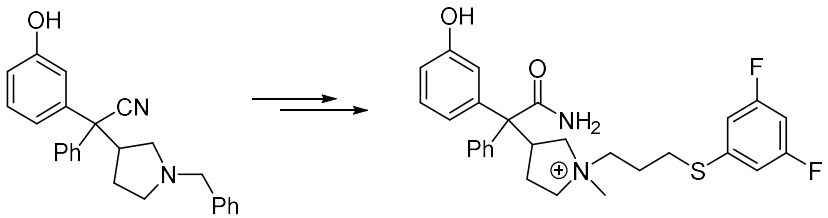

Precursor **76** **75**

Scheme 3.41: Compound **76** as a precursor to obtain the biologically active phenol **75**

Phenol **76** could be synthesised *via* the Ir-catalysed Michael addition of nitrile **3p** to cyclohexenone **60a** with the subsequent dehydrogenation of cyclohexanone **77** catalysed by Pd(II) (Scheme 3.42).

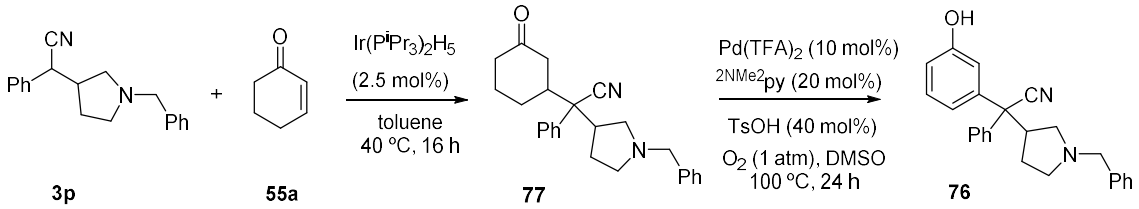

Scheme 3.42: Possible synthetic route of precursor **76** applying our developed catalytic method

The synthesis of product **76** was designed and planned to show the applicability of our developed method but remains as a near future work due to the limited time available.

3.6. Experimental section

3.6.1. General procedure for Ir-catalyzed hydroalkylation of alkyl aryl nitriles with 2-cyclohexen-1-one

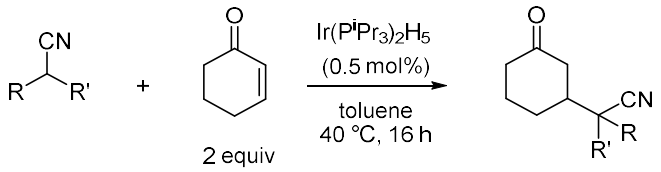

In a glovebox, $Ir(P^iPr_3)_2H_5$ complex (2.4 mg, 0.004 mmol), alkyl aryl nitrile (0.80 mmol) and dodecane (45 mg, 0.26 mmol, GC standard) were dissolved in toluene (4 ml). Then, cyclic α,β-unsaturated ketone (1.60 mmol) was added and the mixture was transferred to a 10 ml Schlenk bomb. Once outside the glovebox, the reaction was heated at 40 °C for 16 h. The reaction mixture was passed through a short silica gel column (5 ml plastic syringe filled with 4 cm of silica gel) eluted with EtOAc (15 ml). The treated reaction mixture was analysed by GC. The products were isolated by column chromatography (silica gel, eluent: EtOAc in hexane 10-50%).

3.6.2. Scope of substrates

3.6.2.1. Scope of nucleophiles

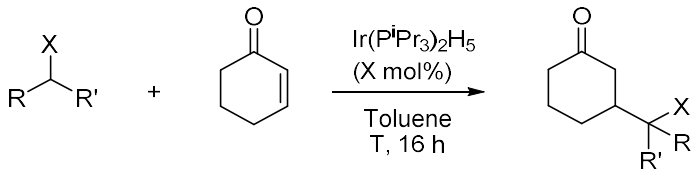

The screening of nucleophiles was conducted following the general procedure using 2-cyclohexen-1-one as a model alkene (2 equiv unless otherwise specified). Optimization of catalyst loading has been conducted in some cases, as specified for each product.

2-(3-Oxocyclohexyl)-2,2-diphenylacetonitrile (61a)

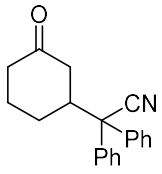

Prepared according to the general procedure using $Ir(P^iPr_3)_2H_5$ complex (2.5 mg, 0.004 mmol, 0.5 mol%), diphenylacetonitrile (154.6 mg, 0.80 mmol) and 2-cyclohexen-1-one (153.9 mg, 1.66 mmol) in toluene (4 ml) at 40 ºC for 16 h. The crude product was purified by column chromatography (silica gel, eluent: hexane:EtOAc, 10:1) to give 2-(3-oxocyclohexyl)-2,2-diphenylacetonitrile as a white solid in 94% yield. **^{1}H NMR** (400 MHz, $CDCl_3$) δ 7.56 – 7.44 (m, 4H, aromatic H), 7.43 – 7.34 (m, 4H, aromatic H), 7.34 – 7.24 (m, 1H, aromatic H), 3.03 – 2.90 (m, 1H, CH), 2.51 – 2.31 (m, 4H, CH_2), 2.20 – 2.09 (m, 1H, CH_2 + CH_2), 1.98 – 1.86 (m, 1H, CH_2), 1.84 – 1.58 (m, 2H, CH_2). **^{13}C {H} NMR** (101 MHz, $CDCl_3$) δ 209.6 (CO), 138.5 (C), 137.7 (CH), 129.2 (CH), 129.1 (CH), 128.1 (CH), 128.0 (CH), 126.5 (CH), 126.4 (CH), 120.4 (CN), 58.1 (C), 44.8 (CH), 44.3 (CH_2), 40.9 (CH_2), 27.5 (CH_2), 24.4 (CH_2). **HRMS** (CI^+) m/z 290.1549 $(M+H)^+$ (264.1539 calcd for $C_{20}H_{19}NO$ $(M+H)^+$). **IR** (FTIR) 3062, 2956, 2924, 2865, 2238, 1699, 1449 cm^{-1}.

2-(3-Oxocyclopentyl)-2,2-diphenylacetonitrile (69)

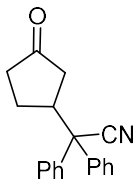

Prepared according to the general procedure using 2.5 mol% of catalyst: $Ir(P^iPr_3)_2H_5$ complex (6.9 mg, 0.013 mmol), diphenylacetonitrile (102.7 mg, 0.53 mmol) and 2-cyclopenten-1-one (84.6 mg, 1.03 mmol) in toluene (2.6 ml) at 40 ºC for 16 h. The crude product was purified by column chromatography (silica gel, eluent hexane:EtOAc, 5:1) to give 2-(3-oxocyclopentyl)-2,2-diphenylacetonitrile as a white solid in 96% yield (140 mg). **^{1}H NMR** (400 MHz, $CDCl_3$) δ 7.55 – 7.44 (m, 4H, aromatic H), 7.44 – 7.34 (m, 4H, aromatic H), 7.34 – 7.27 (m, 2H, aromatic H), 3.45 – 3.26 (m, 1H, CH), 2.56 – 2.15 (m, 4H, 2 CH_2), 2.09 – 1.87 (m, 2H, CH_2). **^{13}C {H} NMR** (101 MHz, $CDCl_3$) δ 215.5 (CO), 138.9 (C), 138.5 (C), 129.1 (CH), 128.1 (CH), 126.6 (CH), 120.5 (CN), 57.2 (C), 44.0 (CH_2), 42.5 (CH_2), 38.3 (CH), 26.3 (CH_2). **HRMS** (CI^+) m/z 276.1391 $(M+H)^+$ (276.1383 calcd for $C_{19}H_{18}NO$ $(M+H)^+$). **IR** (FTIR) 3061, 3033, 2974, 2236, 1740, 1449 cm^{-1}.

Optimisation of catalyst loading and temperature was conducted in this case. GC conversions and yields obtained were the following:

Ir catalyst loading, mol%	T (°C)	Conversion of **3**, %	Yield product **69**, %
0.5	40	28	25
0.5	80	46	44
2.5	40	99	98

2-(3-Oxocyclohexyl)-2-phenylpropanenitrile (61b)

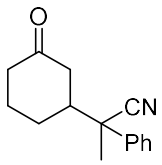

Prepared according to the general procedure using $Ir(P^iPr_3)_2H_5$ complex (2.5 mg, 0.004 mmol, 0.5 mol%), α-methylbenzyl nitrile (107.4 mg, 0.81 mmol) and 2-cyclohexen-1-one (159.9 mg, 1.66 mmol) in toluene (4 ml) at 40 ºC for 16 h. The crude product was purified by column chromatography (silica gel, eluent hexane:EtOAc, 5:1) to give two diastereomers of 2-(3-oxocyclohexyl)-2-phenylpropanenitrile as white solids in 55 and 32% yield (101.7 and 59.6 mg, respectively).

Diastereomer **61b-1** **^{1}H NMR** (400 MHz, $CDCl_3$) δ 7.36 – 7.13 (m, 5H, aromatic H), 2.65-2.54 (m, 1H, CH), 2.42 – 1.89 (m, 5H, CH+2CH_2), 1.69 (s, 3H, CH_3), 1.63 – 1.35 (m, 3H, CH_2). **^{13}C {H} NMR** (101 MHz, $CDCl_3$) δ 209.4 (CO), 138.5 (C), 129.0 (CH), 128.1 (CH), 125.6 (CH), 121.5 (CN), 47.9 (CH_2), 47.1 (CH_2), 43.9 (CH), 40.7 (C), 26.9 (CH_2), 25.4 (CH_2), 24.8 (CH_3). **IR** (FTIR) 3061, 2950, 2867, 2235, 1709, 1446 cm^{-1}.

Diastereomer **61b-2** **^{1}H NMR** (400 MHz, $CDCl_3$) δ 7.40 – 7.23 (m, 5H, ArH), 2.61 (ddt, *J* = 13.7, 4.0, 1.8 Hz, 1H, CH), 2.42 – 2.28 (m, 2H, CH_2), 2.27 – 2.17 (m, 1H, CH_2), 2.15 – 2.02 (m, *J* = 13.1, 3.7 Hz, 1H, CH_2), 2.02 – 1.88 (m, 1H, CH_2), 1.63 (s, 3H, CH_3), 1.58 – 1.31 (m, 3H, CH_2). **^{13}C {H} NMR** (101 MHz, $CDCl_3$) δ 209.5 (CO), 139.2 (C), 129.0 (CH), 128.1 (CH), 125.6 (CH), 121.5 (CN), 48.0 (CH_2), 47.2 (CH_2), 43.7 (CH), 40.8 (C), 27.2 (CH_2), 24.8 (CH_2), 24.3 (CH_3).

2-(3-Oxocyclohexyl)-2,3-diphenylpropanenitrile (61c)

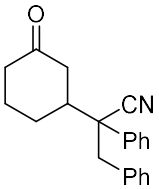

Prepared according to the general procedure using $Ir(P^iPr_3)_2H_5$ complex (2.1 mg, 0.004 mmol, 0.5 mol%), 2,3-diphenylpropanenitrile (166.3 mg, 0.80 mmol), dodecane (46.8 mg) and 2-cyclohexen-1-one (159.8 mg, 1.66 mmol) in toluene (4 ml) at 40 ºC for 16 h. The crude product was purified by column chromatography (silica gel, eluent hexane:EtOAc, 10:1) to give 2-(3-oxocyclohexyl)-2,3-diphenylpropanenitrile as a mixture of two diastereomers as white solid in 80% yield (194.7 mg), dr = 1:1 (determined by NMR). **^{1}H NMR** (500 MHz, $CDCl_3$) δ 7.35 – 7.23 (m, 3H, aromatic H), 7.22 – 7.17 (m, 2H, aromatic H), 7.17 – 7.05 (m, 3H, aromatic H), 6.90 – 6.83 (m, 2H, aromatic H), 3.53 (d, *J* = 13.4 Hz, 1H, benzyl-CH_2), 3.07 (d, *J* = 13.4 Hz, 1H, benzyl-CH_2), 2.45 (ddt, *J* = 22.8, 13.2, 7.5 Hz, 3H), 2.38 – 2.23 (m, 2H), 2.16 (t, *J* = 13.7 Hz, 1H), 2.07 (ddt, *J* = 14.3, 4.1, 2.1 Hz, 1H), 1.90 (qd, *J* = 13.2, 3.3 Hz, 1H), 1.82 – 1.64 (m, 1H). **^{13}C {H} NMR** (101 MHz, $CDCl_3$) δ 209.5 (CO), 135.5 (C), 134.6 (C), 130.2 (CH), 128.9 (CH), 128.1 (CH), 127.9 (CH), 127.1 (CH), 126.7 (CH), 120.2 (CN), 54.7 (CH_2), 46.4 (C), 44.0 (CH), 43.9 (CH_2), 40.9 (CH_2), 27.3 (CH_2), 24.5 (CH_2). **HRMS** (CI^+) m/z 304.1706 $(M+H)^+$ (304.1696 calcd for $C_{21}H_{22}NO$ $(M+H)^+$). **Elemental Analysis** Calcd for ($C_{21}H_{21}NO$): C, 83.13; H 6.98; N 4.62; Found C, 82.56; H, 6.81; N, 4.55. **IR** (FTIR) 3059, 3027, 2960, 2940, 2234, 1706, 1599, 1413cm^{-1}.

3-Methyl-2-(3-oxocyclohexyl)-2-phenylbutanenitrile (61d)

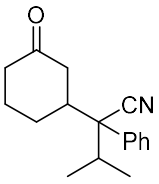

Prepared according to the general procedure using $Ir(P^iPr_3)_2H_5$ complex (17.1 mg, 0.03 mmol, 5 mol%), 3-methyl-2-phenylbutanenitrile (104.6 mg, 0.66 mmol), dodecane (36.1 mg) and 2-cyclohexen-1-one (126.0 mg, 1.30 mmol) in toluene (3.1 ml) at 40 ºC for 16 h. The crude product was purified by column chromatography (silica gel, eluent hexane:EtOAc, 10:1) to give 3-methyl-2-(3-oxocyclohexyl)-2-phenylbutanenitrile as a mixture of two diastereomers as white solid in 58% yield (97.1 mg), dr = 2.2:1 (determined by GC). The starting nitrile was recovered as a white solid in a conversion of 61% (39 mg). **^{1}H NMR** (400 MHz, $CDCl_3$) δ 7.51 – 7.30 (m, 5H, aromatic H), 2.69 – 1.93 (m, 6H, CH_2 + CH_2 + CH_2), 1.87 – 1.18 (m, 3H, CH_2 + CH), 1.06 (d, *J* = 6.6 Hz, 1H, CH_3), 1.00 (d, *J* = 6.6 Hz, 1H, CH_3), 0.90 (d, *J* = 6.8

Hz, 2H, CH_3). **^{13}C {H} NMR** (101 MHz, $CDCl_3$) δ 209.7 (CO), 209.7 (CO), 133.7 (C), 133.3 (C), 128.5 (CH), 128.5 (CH), 128.2 (CH), 128.1 (CH), 127.8 (CH), 121.3 (CN), 121.0 (CN), 57.2 (C), 44.2 (CH_2), 43.0 (CH_2), 42.7 (CH_2), 42.6 (CH_2), 41.0 (CH), 40.9 (CH), 32.3 (CH), 31.8 (CH), 27.5 (CH_2), 26.4 (CH_2), 24.5 (CH_2), 18.8 (CH_3), 18.6 (CH_3), 17.7 (CH_3), 17.2 (CH_3). **HRMS** (CI^+) m/z 256.1698 $(M+H)^+$ (256.1696 calcd for $C_{17}H_{22}NO$ $(M+H)^+$). **Elemental Analysis** Calcd for ($C_{17}H_{21}NO$): C, 79.96; H 8.29; N 5.49; Found C, 79.61; H, 8.26; N, 5.33. **IR** (FTIR) 3030, 2971, 2913, 2862, 2232, 1703, 1447 cm^{-1}.

Optimisation of catalyst loading was conducted in this case. GC conversions and yields obtained were the following:

Ir catalyst loading, mol%	Conversion **3d**, %	Yield **61d**, % (dr)
0.5	20	17 (8.5:1)
5	79	66 (2.3:1)

2-Cyclohexyl-2-(3-oxocyclohexyl)-2-phenylacetonitrile (61e)

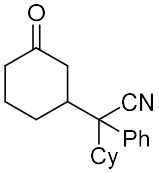

Prepared according to the general procedure using $Ir(P^iPr_3)_2H_5$ complex (12.6 mg, 0.02 mmol, 5 mol%), cyclohexylphenylacetonitrile **3e** (100 mg, 0.50 mmol), dodecane (42.0 mg) and 2-cyclohexen-1-one (103.5 mg, 1.07 mmol) in toluene (2.5 ml) at 40 ºC for 16 h. The crude product was purified by column chromatography (silica gel, eluent hexane:EtOAc, 10:1) to give 2-cyclohexyl-2-(3-oxocyclohexyl)-2-phenylacetonitrile as a mixture of two diastereomers as white solid in 58% yield (84.9 mg), dr = 3.2:1 (determined by GC). The starting nitrile was recovered as a white solid in a 39% yield (39 mg). **^{1}H NMR** (400 MHz, $CDCl_3$) δ 7.41-7.32 (m, 5H, aromatic H), 2.67 – 2.54 (m, 1H, CH), 2.38 (t, J = 12.8 Hz, 1H, CH), 2.32 – 1.86 (m, 6H, CH_2 + CH_2 + CH_2), 1.86 – 1.41 (m, 6H, CH_2 + CH_2 + CH_2), 1.40 – 0.71 (m, 6H, CH_2 + CH_2 + CH_2). **^{13}C {H} NMR** (101 MHz, $CDCl_3$) δ 209.8 (CO), 134.2 (C), 133.70 (C), 128.5 (CH), 128.4 (CH), 128.1 (CH), 128.0 (CH), 121.6 (CN), 121.3 (CN),

57.1 (C), 56.9 (C), 44.1 (CH_2), 43.0 (CH_2), 42.3 (CH_2), 41.9 (CH_2), 41.8 (CH), 41.7 (CH), 41.1 (CH), 41.0 (CH), 29.2 (CH_2), 28.9 (CH_2), 27.6 (CH_2), 27.4 (CH_2), 27.1 (CH_2), 26.5 (CH_2), 26.3 (CH_2), 25.9 (CH_2), 24.5 (CH_2), 24.5 (CH_2). **HRMS** (CI^+) m/z 296.2019 $(M+H)^+$ (296.2009 calcd for $C_{20}H_{26}NO$ $(M+H)^+$). **Elemental Analysis** Calcd for ($C_{20}H_{25}NO$): C, 81.33; H 8.53; N 4.74; Found C, 80.58; H, 8.51; N, 4.61. **IR** (FTIR) 3059, 3028, 2928, 2854, 2233, 1713, 1446 cm^{-1}.

Optimisation of catalyst loading was conducted in this case. GC conversions and yields obtained were the following:

Ir catalyst loading, mol%	Conversion **3e**, %	Yield **61e**, % (dr)
0.5	14	14 (6:1)
5	60	59 (3.3:1)
10	60	58 (3.2:1)

2-(3-Oxocyclohexyl)-2-phenylacetonitrile (61f)

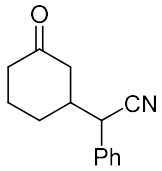

Prepared according to the general procedure using $Ir(P^iPr_3)_2H_5$ complex (4.7 mg, 0.009 mmol, 0.5 mol%), benzyl cyanide (201.7 mg, 1.72 mmol) and 2-cyclohexen-1-one (332.4 mg, 3.46 mmol) in toluene (8.5 ml) at 40 ºC for 16 h. The crude product was purified by column chromatography (silica gel, eluent hexane:EtOAc, 4:1) to give 2-(3-oxocyclohexyl)-2-phenylacetonitrile as a mixture of two diastereomers as white solid in 96% yield, dr = 1.5:1 (determined by GC). **^{1}H NMR** (400 MHz, $CDCl_3$) δ 7.46 – 7.32 (m, 6H, Ar H), 7.32 – 7.19 (m, 5H, Ar H), 3.91 (d, *J* = 4.4 Hz, 1H, CH), 3.75 (d, *J* = 5.7 Hz, 1H, CH), 2.51 – 2.35 (m, 4H, $2CH_2$), 2.35 – 2.17 (m, 6H, 2CH + $2CH_2$), 2.17 – 2.06 (m, 2H, CH_2), 1.99 (m, 2H, CH_2), 1.76 – 1.46 (m, 4H, $2CH_2$). **^{13}C {H} NMR** (101 MHz, $CDCl_3$) δ 209.05 (CO), 209.0 (CO), 133.2 (C), 132.9 (C), 129.1 (CH), 129.1 (CH), 128.5 (CH), 128.5 (CH), 127.8 (CH), 127.7 (CH), 118.9 (CN), 118.7 (CN), 45.9 (CH_2), 43.8 (CH_2), 43.4 (CH_2), 43.4 (CH), 43.2 (CH), 40.9 (CH), 40.8 (CH), 29.5 (CH_2), 27.5 (CH_2), 24.4 (CH_2), 24.3 (CH_2). **HRMS** (CI^+) m/z 214.1234 $(M+H)^+$ (214.1226 calcd for $C_{14}H_{16}NO$ $(M+H)^+$). **Elemental Analysis** Calcd

for ($C_{14}H_{15}NO$): C, 78.84; H 7.09; N 6.57; Found C, 78.70; H, 7.01; N, 6.54. **IR** (FTIR) 2947, 2887, 2854, 2239, 1704, 1451 cm^{-1}.

2-(3-Oxocyclohexyl)-2-phenyl-2-(pyridin-2-yl)acetonitrile (61g)

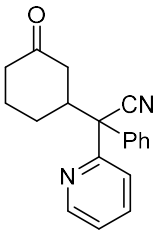

Prepared according to the general procedure using $Ir(P^iPr_3)_2H_5$ complex (13.0 mg, 0.025 mmol, 5 mol%), 2-phenyl-2-(pyridin-2-yl)acetonitrile (101.5 mg, 0.52 mmol) and 2-cyclohexen-1-one (103.2 mg, 1.07 mmol) in toluene (2.6 ml) at 40 ºC for 16 h. The crude product was purified by column chromatography (silica gel, eluting with 4:1, hexane:EtOAc) to give 2-(3-oxocyclohexyl)-2-phenyl-2-(pyridin-2-yl)acetonitrile as a mixture of two diastereomers as white solid in 95% yield (144.7 mg), dr = 4:1 (determined by ^{13}C NMR). **^{1}H NMR** (400 MHz, $CDCl_3$) δ 8.64 (t, *J* = 4.6 Hz, 1H, aromatic H), 7.80 – 7.54 (m, 4H, aromatic H), 7.45 – 7.11 (m, 4H, aromatic H), 3.52 (dtd, *J* = 14.5, 7.3, 3.7 Hz, 1H, CH), 2.58 – 2.23 (m, 3H, CH_2), 2.21 – 1.99 (m, 2H, CH_2), 1.98 – 1.52 (m, 3H, CH_2). **^{13}C {H} NMR** (101 MHz, $CDCl_3$) δ 209.9 (CO), 209.7 (CO), 156.8 (C), 156.1 (C), 149.6 (CH), 149.5 (CH), 137.4 (C), 137.4 (CH), 137.3 (CH), 136.7 (C), 129.0 (CH), 128.9 (CH), 128.2 (CH), 128.1 (CH), 126.5 (CH), 126.3 (CH), 122.8 (CH), 122.8 (CH), 122.6 (CH), 122.4 (CH), 120.1 (CN), 120.1 (CN), 59.8 (C), 59.8 (C), 45.1 (CH_2), 44.9 (CH_2), 44.5 (CH_2), 43.5 (CH_2), 41.1 (CH), 40.9 (CH), 27.8 (CH_2), 26.6 (CH_2), 24.3 (CH_2), 24.3 (CH_2). **HRMS** (ES^+) m/z 313.1323 $(M+Na)^+$ (313.1317 calcd for $C_{19}H_{18}N_2ONa$ $(M+Na)^+$). **IR** (FTIR) 3054, 2961, 2916, 2860, 2238, 1707, 1495 cm^{-1}.

Optimisation of catalyst loading was conducted in this case. GC conversions and yields obtained were the following:

Ir catalyst loading, mol%	Conversion **3g**, %	Yield **61g**, %
0.5	38	35
2.5	76	76
5	97	97

2-(3-Oxocyclohexyl)-2-(pyridin-2-yl)propanenitrile (61h)

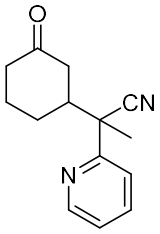

Prepared according to the general procedure using $Ir(P^iPr_3)_2H_5$ complex (9.9 mg, 0.02 mmol, 2.5 mol%), 2-(pyridine-2-yl)propanenitrile (109.2 mg, 0.83 mmol), dodecane (20.6 mg) and 2-cyclohexen-1-one (159.9 mg, 1.66 mmol) in toluene (3.8 ml) at 40 ºC for 16 h. The crude product was purified by column chromatography (silica gel, eluent hexane:EtOAc, 2:1) to give 2-(3-oxocyclohexyl)-2-(pyridin-2-yl)propanenitrile as a mixture of two diastereomers as white solid in 95% yield (178.8 mg), dr =1.1:1 (determined by NMR). **^{1}H NMR** (400 MHz, $CDCl_3$) δ 8.53 (t, *J* = 5.3 Hz, 1H, aromatic H), 7.74 – 7.60 (m, 1H, aromatic H), 7.53 (dd, *J* = 16.8, 7.9 Hz, 1H, aromatic H), 7.25 – 7.12 (m, 1H, aromatic H), 2.67 – 2.56 (m, 1H, C**H**$_2$), 2.55 – 2.42 (m, 1H, C**H**$_2$), 2.41 – 2.05 (m, 4H, 2CH_2), 2.04 – 1.78 (m, 1H, CH_2), 1.72 – 1.57 (m, 4H, CH + CH_3), 1.55 – 1.32 (m, 1H, CH). **^{13}C {H} NMR** (101 MHz, $CDCl_3$) δ 209.5 (CO), 209.4 (CO), 157.9 (C), 157.4 (C), 149.9 (CH), 149.8 (CH), 137.1 (CH), 137.1 (CH), 122.9 (CH), 122.9 (CH), 121.4 (CN), 121.4 (CN), 121.1 (CH), 121.1 (CH), 49.1 (CH_2), 49.1 (CH_2), 46.1 (CH_2), 46.0 (CH_2), 44.0 (CH), 43.3 (CH), 40.9 (C), 40.7 (C), 27.3 (CH_2), 26.5 (CH_2), 24.71 (CH_2), 24.3 (CH_2), 24.3 (CH_3), 23.9 (CH_3). **HRMS** (CI^+) m/z 229.1339 $(M+H)^+$ (229.1335 calcd for $C_{14}H_{17}N_2O$ $(M+H)^+$). **Elemental Analysis** Calcd for ($C_{14}H_{16}N_2O$): C, 73.66; H 7.06; N 12.27; Found C, 73.82; H, 7.13; N, 12.10. **IR** (FTIR) 3053, 2946, 2868, 2237, 1709, 1586, 1572, 1469 cm^{-1}.

2-(3-Oxocyclohexyl)-2-(pyridin-2-yl)acetonitrile (61i)

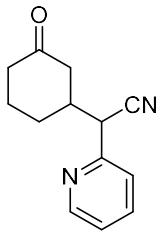

The general procedure has been slightly modified for the synthesis of this product: 1.1 equiv of 2-cyclohexen-1-one **60a** were used to avoid formation of side products. Following the modified general procedure, using $Ir(P^iPr_3)_2H_5$ complex (11.1 mg, 0.021 mmol, 2.5 mol%), 2-(pyridin-2-yl)acetonitrile (107.7 mg, 0.91 mmol), dodecane (40.9 mg) and 2-cyclohexen-1-one (91.7 mg, 0.95 mmol) in toluene (2.5 ml) at 40 ºC for 16 h. The crude product was purified by column chromatography (silica gel, eluent hexane:EtOAc, 2:1) to give 2-(3-oxocyclohexyl)-2-(pyridin-2-yl)acetonitrile as a mixture of two diastereomers as white solid in 79% yield (154.3 mg), dr = 1.02:1 (determined by NMR). **^{1}H NMR** (400 MHz, $CDCl_3$) δ 8.60 (t, *J* = 4.8 Hz, 1H, aromatic H), 7.83 – 7.68 (m, 1H,

aromatic H), 7.43 (d, J = 7.8 Hz, 1H, aromatic H), 7.33 – 7.19 (m, 1H, aromatic H), 4.14 (d, J = 4.6 Hz, 0.5H, CH), 3.93 (d, J = 6.2 Hz, 0.5H, CH), 2.69 – 2.49 (m, 1H, CH), 2.46–1.87 (m, 6H, CH_2 + CH_2 + CH_2), 1.86 – 1.48 (m, 2H, CH_2). **^{13}C NMR** (101 MHz, $CDCl_3$) δ 209.1 (CO), 208.9 (CO), 153.1 (C), 152.8 (C), 150.1 (CH), 137.3 (CH), 123.3 (CH), 123.2 (CH), 122.4 (CH), 122.1 (CH), 118.3 (CN), 118.0 (CN), 45.9 (CH_2), 45.6 (CH_2), 43.3 (CH), 41.8 (CH_2), 41.7 (CH_2), 40.9 (CH_2), 40.8 (CH_2), 29.9 (CH), 27.5 (CH), 24.4 (CH_2), 24.3 (CH_2). **HRMS** (CI^+) m/z 215.1184 $(M+H)^+$ (215.1179 calcd for $C_{13}H_{15}N_2O$ $(M+H)^+$). **Elemental Analysis** Calcd for ($C_{14}H_{14}N_2O$): C, 72.87; H 6.59; N 13.07; Found C, 72.87; H, 6.78; N, 12.40. **IR** (FTIR) 3053, 2941, 2869, 2242, 1706, 1589, 1448 cm^{-1}.

Optimisation of catalyst loading was conducted in this case. GC conversions and yields obtained were the following:

Ir catalyst loading, mol%	**60a**, equiv	Conversion **3i**, %	Yield **61i**, % (dr)	Yield of **70**, % (dr)
0.5	2	47	47 (3.7:1)	0
2.5	2	100	87 (1.2:1)	10 (2:1.1:1)
2.5	1.1	100	80 (1:1)	0
5	2	99	48 (1.2:1)	51 (2.3:1.3:1)

Poor material between **3i** and **56i** encountered is due to formation of a side product:

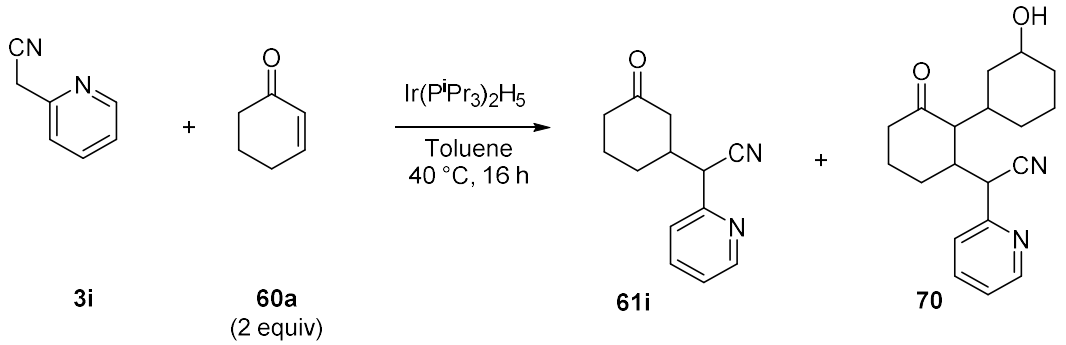

The side product was suggested to be compound **70** according to GC-MS (m/z 311.1 $(M-H)^+$, 311.4 calcd for $C_{19}H_{23}N_2O_2$ $(M-H)^+$) and obtained as a mixture of three diastereomers.

3.6.2.2. Scope of cyclic α,β-unsaturated ketones

The screening of nucleophiles was conducted following the general procedure using diphenylacetonitrile **3** as a model Michael donor (ratio diphenylacetonitrile:alkene = 1:2).

3.6.3. Syntheses of substrates

2,3-Diphenylpropanenitrile (3c)

Prepared according to literature procedure.[73]

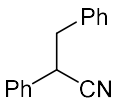

Benzyl nitrile (4.01 g, 34.26 mmol), benzyl bromide (6.18 g, 36.13 mmol) and tetrabutylammonium bromide (0.55 g, 1.70 mmol) were introduced into a 50 ml round bottom flask. While continuous stirring of the reaction mixture, 22 ml 60% aqueous solution of KOH was added dropwise. The reaction mixture was heated at 60 °C for 4 h with vigorous stirring. The reaction mixture was treated with water (15 ml), extracted with ethyl acetate (2 x 8 ml) and the combined organic layers were washed with brine (10 ml) and dried over magnesium sulphate. The crude product was purified by column chromatography (silica gel, eluent hexane:EtOAc, 30:1) and followed by recrystallization from addition of hexane to DCM (DCM:Hexane, 1:3, v/v) yielding to the product **3c** as a white solid in 45% yield (3.17 g). **^{1}H NMR** (400 MHz, $CDCl_3$) δ 7.42 – 7.22 (m, 8H, aromatic H), 7.17 – 7.12 (m, 2H, aromatic H), 4.00 (dd, *J* = 8.1, 6.6 Hz, 1H, CH), 3.17 (qd, *J* = 13.6, 7.4 Hz, 2H, CH_2). **^{13}C {H} NMR** (101 MHz, $CDCl_3$) δ 136.2 (C), 135.2 (C), 129.2 (CH), 129.0 (CH), 128.6 (CH), 128.2 (CH), 127.5 (CH), 127.4 (CH), 120.3 (CN), 42.2 (CH_2), 39.8 (CH). **IR** (FTIR) 3062, 3029, 2923, 2853, 2242, 1495, 1454.

NMR data are in accordance to the literature.[74]

3-Methyl-2-phenylbutanenitrile (3d)

Prepared according to literature procedure.[73]

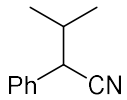

Benzyl nitrile (4.13 g, 35.28 mmol), iodopropane (6.41 g, 37.71 mmol) and tetrabutylammonium bromide (0.12 g, 0.37 mmol) were introduced into a 50 ml round bottom flask. Then, 16 ml 60% aqueous solution of KOH were added dropwise. The reaction mixture was heated at 50 °C for 22 h with vigorous stirring. The reaction mixture was treated with water (15 ml), extracted with ethyl acetate (2 x 8 ml) and the combined organic layers were washed with brine (10 ml) and dried over magnesium sulphate. The product **3d** was obtained after purification by column chromatography (silica gel, eluent hexane:EtOAc, 20:1) drying it at 85 °C under vacuum overnight as a colourless oil (0.51 g, 3.2 mmol) in 10% yield. **^{1}H NMR** (400 MHz, $CDCl_3$) δ 7.39-7.29 (m, 5H, aromatic H), 3.66 (d, J = 6.29 Hz, 1H, CH), 2.13 (sept, 1H, CH), 1.04 (dd, *J* = 6.29, 11.38 Hz, 6H, CH_3). **^{13}C {H} NMR** (101 MHz, $CDCl_3$) δ 134.9 (C), 128.8 (CH), 127.9 (CH), 127.8 (CH), 119.8 (CN), 45.1 (CH), 33.8 (CH), 20.8 (CH_3), 18.82 (CH_3). **IR** (FTIR) 3032, 2965, 2931, 2236, 1492, 1465 cm^{-1}.

2-phenyl-2-(pyridine-2-yl)acetonitrile (3g)

Prepared according to literature procedure.[75]

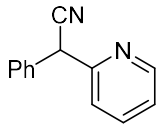

In a 25 ml round bottom flask, to a mixture of potassium hydroxide (3.58 g, 63.81 mmol) in DMSO (6.4 ml), benzyl cyanide (2.2 g, 18.80 mmol) was added dropwise and the mixture was stirred at room temperature for 30 min. Then, 2-bromopyridine (1.96 g, 12.40 mmol) was added and the reaction mixture was heated at 50 °C for 16 h. The reaction mixture was treated with cold water (15 ml), extracted with chloroform (3 x 10 ml) and dried over magnesium sulphate. The crude product was purified by column chromatography (silica gel, eluent: hexane:EtOAc, 5:1) and followed by recrystallization from addition of hexane to a solution of the product in DCM (DCM:Hexane, 1:3, v/v) yielding to the product as a white solid in 60% yield (1.46 g). **^{1}H NMR** (400 MHz, $CDCl_3$) δ 8.60 (dd, *J* = 4.8, 0.8 Hz, 1H, aromatic H), 7.70 (td, *J* = 7.7, 1.8 Hz, 1H, aromatic H), 7.48 – 7.42 (m, 2H, aromatic H), 7.42 – 7.30 (m, 4H,

aromatic H), 7.28 – 7.21 (m, 1H, aromatic H), 5.32 (s, 1H, CH). **^{13}C {H} NMR** (101 MHz, $CDCl_3$) δ 155.5 (C), 149.9 (C), 137.5 (CH), 134.7 (CH), 129.2 (CH), 128.4 (CH), 127.7 (CH), 123.1 (CH), 121.9 (CH), 119.0 (CN), 45.4 (CH). **IR** (FTIR) 3080, 3057, 3029, 2939, 2242, 1587, 1492, 1454 cm^{-1}.

2-(Pyridine-2-yl)propanenitrile (3h)

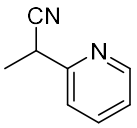

In a 100 ml Schlenk flask under argon atmosphere, 2-(pyridin-2-yl)acetonitrile (2.57 g, 21.7 mmol) was dissolved in anhydrous THF (25 ml) and cooled with an ice bath. Then, sodium tert-butoxide (2.46 g, 21.9 mmol) was added as a solid and the mixture was allowed to stir for 1 h at 0 °C. Iodomethane (3.10 g, 21.7 mmol) in anhydrous THF (10 ml) was added to the previous mixture at 0 °C. The reaction mixture was allowed to warm up to room temperature and was stirred overnight. The solvent was removed under vacuum and the crude product was dissolved in ethyl acetate (50 ml) and water (25 ml) was added. The aqueous layer was extracted with ethyl acetate (3 x 40 ml) and the combined organic layers were washed with water (30 ml), brine (30 ml) and dried over magnesium sulphate. After purification by column chromatography (silica gel, eluent: hexane:EtOAc, 4:1), the product was obtained as a white solid (0.61 g) in 21% yield. **^{1}H NMR** (400 MHz, $CDCl_3$) δ 8.58 (d, J = 4.2 Hz, 1H, aromatic H), 7.72 (td, J = 7.7, 1.7 Hz, 1H, aromatic H), 7.44 (d, J = 7.8 Hz, 1H, aromatic H), 7.31 – 7.19 (m, 1H, aromatic H), 4.05 (q, J = 7.3 Hz, 1H, CH), 1.70 (d, J = 7.3 Hz, 1H, CH_3). **^{13}C {H} NMR** (101 MHz, $CDCl_3$) δ 156.1 (C), 149.9 (CH), 137.4 (CH), 122.9 (CH), 121.0 (CH), 120.9 (CN), 33.7 (CH), 19.6 (CH_3). **IR** (FTIR) 3053, 2989, 2941, 2244, 1588, 1572, 1473, 1434, 748 cm^{-1}.

3.6.4. Screening of catalysts

3.6.4.1. General procedure

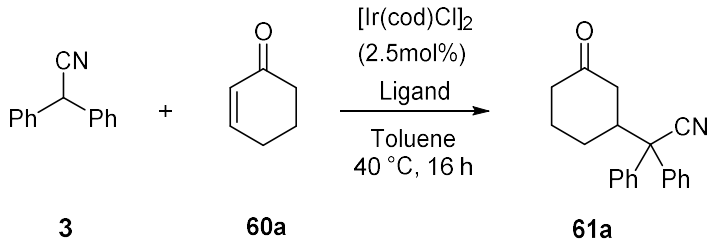

3 **60a** **61a**

In a glovebox, $[Ir(cod)Cl]_2$ (3.7 mg, 0.005 mmol, 2.5 mol%), ligand (0.1 eq), ^tBuONa (2.3 mg, 0.02 mmol, only added when using carbene ligands) were introduced to a 4 ml *via*l. Then, diphenylacetonitrile (38.6 mg, 0.2 mmol) and dodecane (20 mg, GC standard) dissolved in toluene (0.8 ml) were added. Finally, 2-cyclohexen-1-one (38.4 mg,0.4 mmol) was added and the *via*l was closed with a Teflon lined screw cap. The mixture was stirred at 40 °C for 16 h outside the glovebox. The reaction mixture was passed through a short silica gel column (5 ml plastic syringe filled with 4 cm of silica gel) eluted with EtOAc (15 ml) and was analyzed by GC.

Table 6.1: Screening of catalytic system for hydroalkylation of diphenylacetonitrile with 2-cyclohexen-1-one[a]

Entry	Ligand (mol%)	Base (mol%)	Ir catalyst (mol%)	T, °C	Conversion of **3**, %	Conversion of **60a**, %	Yield of **61a**, %
1	$PiPr_3$ (10)	-	$[Ir(cod)Cl]_2$ (2.5)	40	0	17	0
2	Ad_2PBu (10)	-	$[Ir(cod)Cl]_2$ (2.5)	40	0	23	0
3	PCy_3 (10)	-	$[Ir(cod)Cl]_2$ (2.5)	40	0	23	0
4	Rac-BINAP (5)	-	$[Ir(cod)Cl]_2$ (2.5)	40	1	18	0
5	CyJohnPhos	-	$[Ir(cod)Cl]_2$ (2.5)	40	0	49	0

6	Me_4-phen	-	$[Ir(cod)Cl]_2$ (2.5)	40	0	23	0
7	IBu ·HBF_4 (10)	^{t}BuONa (12)	$[Ir(cod)Cl]_2$ (2.5)	40	3	100	3
8	SIMes·HCl (10)	^{t}BuONa (12)	$[Ir(cod)Cl]_2$ (2.5)	40	36	44	36
9	IPropyl·HBF_4 (10)	^{t}BuONa (12)	$[Ir(cod)Cl]_2$ (2.5)	40	25	100	25
10	IAd·HBF_4 (10)	^{t}BuONa (12)	$[Ir(cod)Cl]_2$ (2.5)	40	55	100	55
11	SIPr·HCl (10)	^{t}BuONa (12)	$[Ir(cod)Cl]_2$ (2.5)	40	80	71	80
12	IPr·HCl (10)	^{t}BuONa (12)	$[Ir(cod)Cl]_2$ (2.5)	40	81	90	81
13[b]	SIPr·HCl (10)	^{t}BuONa (12)	$[Ir(cod)Cl]_2$ (2.5)	40	94	56	94
14	SIPr·HCl(10)	^{t}BuONa (12)	$[Ir(coe)_2Cl]_2$ (2.5)	40	89	80	89
15	SIAd·HBF_4 (20)	^{t}BuONa (22)	$[Ir(cod)Cl]_2$ (5)	40	85	74	85
16[b]	SIAd·HBF_4 (10)	^{t}BuONa (12)	$[Ir(cod)Cl]_2$ (2.5)	40	45	100	45
17	SIAd·HBF_4 (10)	^{t}BuONa (12)	$[Ir(cod)Cl]_2$ (2.5)	60	35	100	35
18	IMes·HCl (10)	^{t}BuONa (12)	$[Ir(cod)Cl]_2$ (2.5)	40	92	63	92

[a]: Conversions and yields determined by GC. Reaction conditions: Substrate **3** (0.16 mmol, 0.2 M), substrate **55a** (2 equiv, 0.4 M), $[Ir(cod)Cl]_2$ (2.5 mol%), ligand (monodentate: 10 mol%, bidentate: 5 mol%), base (12 mol%, if required), dodecane (GC standard) in toluene (0.8 ml) at 40 °C for 16 h. [b]: 3 equiv of 2-cyclohexen-1-one were used. [b]: 3 equiv of 2-cyclohexen-1-one were used.

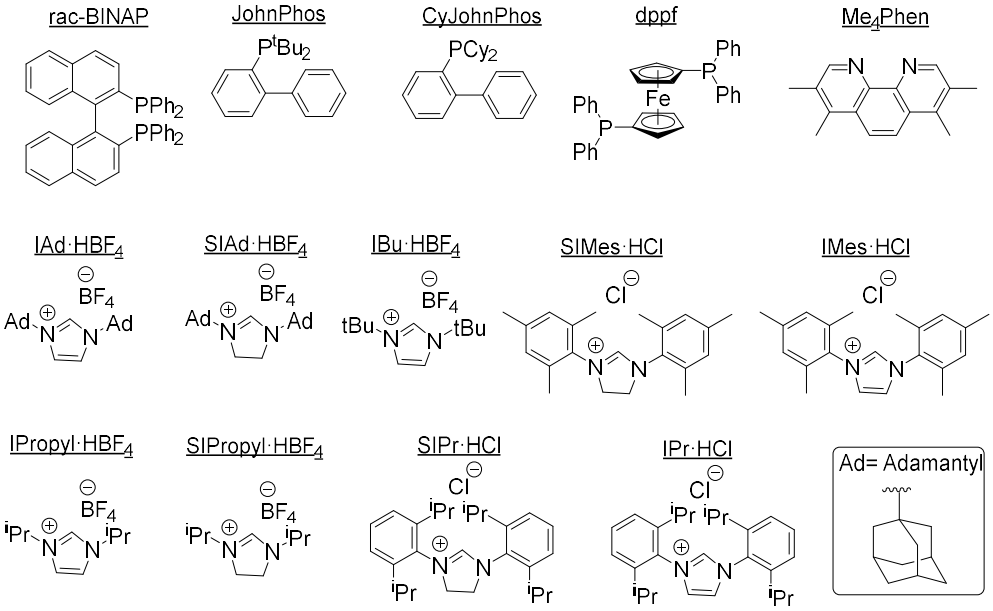

3.6.4.2. Control experiments for Ir-catalysed Michael addition of alkyl aryl nitriles with 2-cyclohexen-1-one 60a

3.6.4.2.1. Control experiments with 2-cyclohexen-1-one 60a and ^{t}BuONa

In a glovebox, 2- cyclohexen-1-one (200 mg, 2.08 mmol) and ^{t}BuONa (12 mg, 0.12 mmol) were dissolved in toluene (5.2 ml) in a 10 ml Schlenk flask. The reaction mixture was heated at 40 °C for 16 h, cooled to room temperature and filtered using a syringe filter. The solvent was evaporated under vacuum and the crude product was purified by column chromatography (silica gel, eluent: Hexane: EtOAc, 2 : 1). Two products were isolated:

[1,1'-Bi(cyclohexan)]-3-ene-2,3'-dione (62)

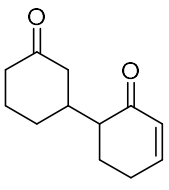

Yellowish oil. Isolated yield = 21%. **^{1}H NMR** (400 MHz, $CDCl_3$) δ 6.69 (s, *J* = 4.17 Hz, 1H, CH), 2.99 (m, 1H, CH), 2.51-1.52 (m, 14 H, $6CH_2$+2CH). **^{13}C {H} NMR** (101 MHz, $CDCl_3$) δ 211.2 (CO), 198.4 (CO), 144.2 (CH), 141.8 (CH), 46.3 (CH_2), 41.2 (CH_2), 38.7 (CH_2), 37.6 (CH_2), 30.6 (CH_2), 26.0 (CH_2), 25.0 (CH_2), 22.7 (CH_2). **HR-MS** (CI+) m/z 193.1230 $(M+H)^+$ (193.1223 calcd for $C_{12}H_{16}O_2$ $(M+H)^+$).

NMR data are in accordance to the literature.[31]

[1,1'-Bi(cyclohexane)]-2,3'-dione (66)

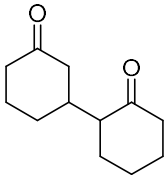

Yellowish oil. Isolated yield = 10% as mixture of isomers. **^{1}H NMR** (400 MHz, $CDCl_3$) δ 2.38-1.12 (m, 18 H, 8 CH_2 + 2 CH). **^{13}C {H} NMR** (101 MHz, $CDCl_3$) δ 211.5 (CO), 211.4 (CO), 54.4 (CH), 45.6 (CH_2), 44.5 (CH_2), 41.3 (CH_2), 37.5 (CH), 37.2 (CH_2), 29.6 (CH_2), 28.8 (CH_2), 28.0 (CH_2), 25.2 (CH_2). **MS** (CI+) m/z 195.1 $(M+H)^+$ (194.2 calcd for $C_{12}H_{19}O_2$ $(M+H)^+$).

NMR data are in accordance to the literature.[76]

3.6.4.3. General procedure for BIMBOL-catalyzed Michael addition of diphenylacetonitrile 3 to 2-cyclohexen-1-one 55a

Experiment conducted following described procedure.[45]

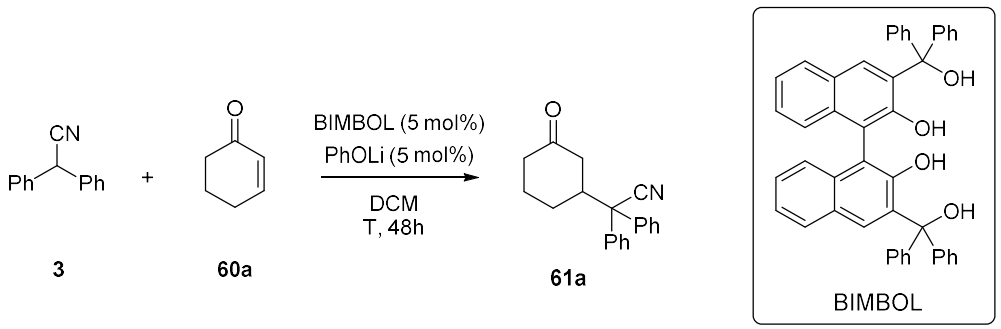

3 60a 61a

In a glovebox, (±)-BIMBOL (16.3 mg, 0.025 mmol, 5 mol%) and PhOLi (2.6 mg, 0.025 mmol) were added to a 4 ml *via*l equipped with a sealable screw cap and 2-cyclohexen-1-one (52.9 mg, 0.55 mmol) dissolved in dry DCM (1 ml) was added. The mixture was stirred for 5 min and then, diphenylacetonitrile (99.1 mg, 0.52 mmol) and dodecane (25.9 mg, GC standard) were added. The reaction mixture was stirred at room temperature for 48 h and the reaction was analysed by GC without further treatment.

Results on (±)-BIMBOL-catalyzed Michael addition of diphenylacetonitrile **3** to 2-cyclohexen-1-one **60a**:

Catalyst loading, mol%	T, °C	Conversion of 3, %	Conversion of 60a, %	Yield of 61a, %
BIMBOL (5), PhOLi (5)	rt	0	0	0
BIMBOL (5), PhOLi (5)	80	0	0	0

3.6.4.3.1. Synthesis of (±)-3,3'-Bis(diphenylhydroxymethyl)-2,2'-dihydroxy[1,1']-binaphtalenyl ((±)-BIMBOL)

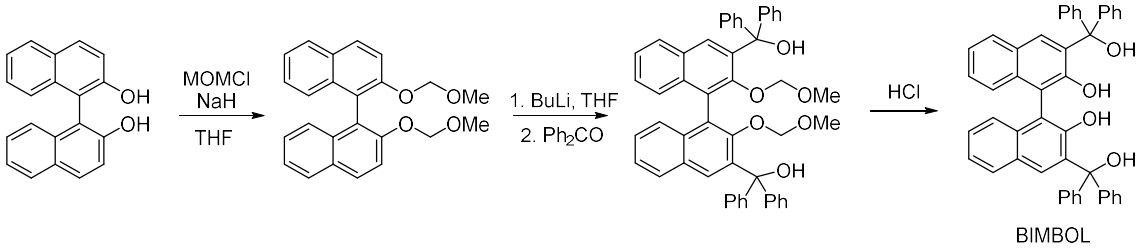

Synthesis of (±)-2,2'-Bis(methoxymethoxy)-1,1'-binaphtyl

Prepared according to literature procedure.[77]

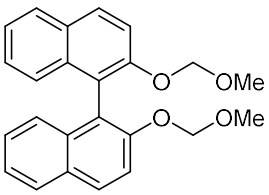

To a 3-neck 250 ml round bottom flask equipped with a stir bar and a dropping funnel, NaH (0.76 g, 31.6 mmol) was mixed in dry THF (63 ml) under argon atmosphere and the mixture was cooled down to 0 °C. A solution of (±)-2,2'-dihydroxy-1,1'-binaphtyl (3.99 g, 13.9 mmol) in dry THF (21 ml) was added *via* the dropping funnel at 0 °C. Then, chloromethyl methyl ether (2.3 ml, 31.2 mmol) was added dropwise at 0 °C and the reaction mixture was allowed to stir at room temperature for 4.5 h. Saturated aqueous NH_4Cl (30 ml) was added to the flask and the reaction mixture was extracted with DCM (3 x 20 ml). The combined organic layers were washed with brine (25 ml) and dried over Na_2SO_4. The solvent was evaporated under vacuum and the product was obtained after the recrystallization from addition of hexane to DCM (DCM:Hexane, 1:3, v/v) yielding

to the expected product as a white solid in 66% yield (3.42 g). **^{1}H NMR** (400 MHz, $CDCl_3$) δ 8.10 – 7.79 (m, 4H, Ar H), 7.74 – 7.51 (m, 2H, aromatic H), 7.38 (s, 2H, aromatic H), 7.34 – 7.12 (m, 4H, aromatic H), 5.20 – 4.95 (m, 4H, CH_2), 3.18 (s, 6H, CH_3). **^{13}C {H} NMR** (101 MHz, $CDCl_3$) δ 152.7 (C), 134.0 (C), 129.9 (C), 129.4 (CH), 127.9 (CH), 126.3 (CH), 125.6 (CH), 124.1 (CH), 121.3 (C), 117.3 (CH), 95.2 (CH_2), 55.8 (CH_3).

Synthesis of (±)-3,3'-Bis(diphenylhydroxymethyl)-2,2'-dihydroxy (MOM protected) [1,1']-binaphtalenyl

Prepared according to literature procedure.[78]

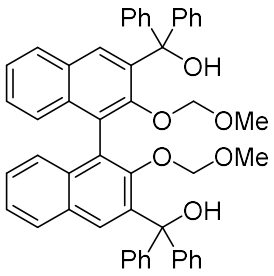

(±)-2,2'-Bis(methoxymethoxy)-1,1'-binaphtyl (3.40 g, 9.09 mmol) was dissolved in dry THF (40 ml) under argon atmosphere and the mixture was cooled down to 0 °C. nBuLi (24 ml, 45.5 mmol, 1.6 M in hexanes) was added dropwise over a period of 10 min and the dark brown mixture was stirred at 0 °C for 3 h. Then, benzophenone (4.91 g, 27.0 mmol) was added as a solid at 0 °C and the green reaction mixture was warmed to room temperature and stirred overnight. The reaction was quenched with saturated aqueous NH_4Cl (40 ml) and the reaction mixture was extracted with DCM (3 x 20 ml). The combined organic layers were washed with brine (60 ml), dried over $MgSO_4$ and evaporated to dryness. The residue was purified by column chromatography (silica gel, Hexane:EtOAc, 10:1) and recrystallized from DCM/Hexane to give the product as a white solid in 22% yield (1.62 g). **^{1}H NMR** (400 MHz, $CDCl_3$) δ 7.62 (d, J = 7.9 Hz, 2H, aromatic H), 7.47 – 7.41 (m, 4H, aromatic H), 7.39 – 7.27 (m, 20H, aromatic H), 7.22 – 7.11 (m, 4H, aromatic H), 5.80 (s, 2H, OH), 3.82 (d, J = 4.8 Hz, 2H, CH_2), 3.77 (d, J = 4.8 Hz, 2H, CH_2), 2.82 (s, 6H, $2CH_3$). **^{13}C {H} NMR** (101 MHz, $CDCl_3$) δ 152.9 (C), 146.8 (C), 146.4 (C), 140.4 (C), 133.7 (C), 130.7 (CH), 129.6 (CH), 128.7 (CH), 127.9 (CH), 127.8 (CH), 127.7 (CH), 127.2 (CH), 127.1 (CH), 125.4 (CH), 125.3 (CH), 98.9 (CH_2), 82.0 (C), 57.0 (CH_3).

Synthesis of (±)-3,3'-Bis(diphenylhydroxymethyl)-2,2'-dihydroxy[1,1']-binaphtalenyl (BIMBOL)

Prepared according to literature procedure.[78]

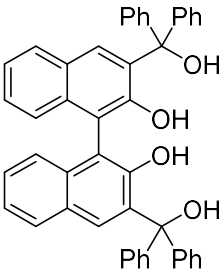

To a two-neck 100 ml round bottom flask equipped with a condenser under argon atmosphere, (±)-3,3'-Bis(diphenylhydroxymethyl)-2,2'-dihydroxy (MOM protected) [1,1']-binaphtalenyl (1.6 g, 2.17 mmol) was dissolved in THF (32 ml) and then, 3M HCl (6 ml) was added and the reaction mixture was heated to reflux for 6 h. The reaction quenched with 10% aqueous $NaHCO_3$ (30 ml) and the reaction was extracted with EtOAc (3x 25 ml). The combined organic phases were washed with water (20 ml), brine (10 ml) and were dried over $MgSO_4$. The product was obtained after recrystallization from addition of hexane to DCM (DCM:Hexane, 1:3, v/v) yielding to BIMBOL as a white solid in 52% yield (0.72 g). **^{1}H NMR** (400 MHz, $CDCl_3$) δ 7.62 (d, *J* = 6.8 Hz, 2H, aromatic H), 7.42 – 7.27 (m, 24H, aromatic H), 7.20 – 7.05 (m, 4H, aromatic H), 6.51 (s, 2H, 2 OH), 4.61 (s, 2H, 2 OH). **^{13}C {H} NMR** (101 MHz, $CDCl_3$) δ 151.1 (C), 145.5 (C), 145.2 (C), 133.8 (C), 133.1 (C), 131.0 (C), 128.9 (CH), 128.23 (CH), 128.1 (CH), 128.0 (CH), 127.8 (C), 127.6 (C), 127.6 (CH), 127.4 (CH), 124.2 (CH), 124.0 (CH), 114.0 (CH), 83.0 (C). **HRMS** (CI+) m/z 615.2322 $(M+H-2H_2O)^+$ (615.2319 calcd for $C_{46}H_{30}O_2$ $(M+H-2H_2O)^+$) **IR** (FTIR) 3498, 3265, 3057, 3028, 1804, 1622, 1594 cm^{-1}.

3.6.4.3.2. Synthesis of lithium phenoxide

Prepared according to the literature procedure.[79]

To a 50ml Schlenk flask under argon atmosphere, phenol (3.16 g, 33.6 mmol) was mixed with dry hexane (10 ml) and then, ^{n}BuLi (21 ml, 33.6 mmol, 1.6 M in hexanes) was added at room temperature while continuous stirring of the reaction mixture. A white precipitate was formed immediately. The reaction mixture was allowed to stir for 30 min. Then, the white precipitate was washed with hexane (4 x 5 ml) and was dried under vacuum. The product was obtained as a white solid in 76% yield. **^{1}H NMR** (400 MHz, D_2O) δ 7.09 (t,

J = 6.8 Hz, 2H, aromatic H), 6.65 – 6.45 (m, 3H, aromatic H). **^{13}C {H} NMR** (101 MHz, D_2O) δ 167.32 (C), 129.83 (CH), 118.78 (CH), 114.71 (CH).

3.6.5. Dehydrogenation of 2-(3-oxocyclohexyl)-2,2-diphenylacetonitrile to the corresponding meta-substituted phenols

3.6.5.1. General procedure for Pd-catalyzed aerobic oxidative dehydrogenation of cyclohexanone 61a to *meta*-substituted phenol 66 (Stahl´s conditions)

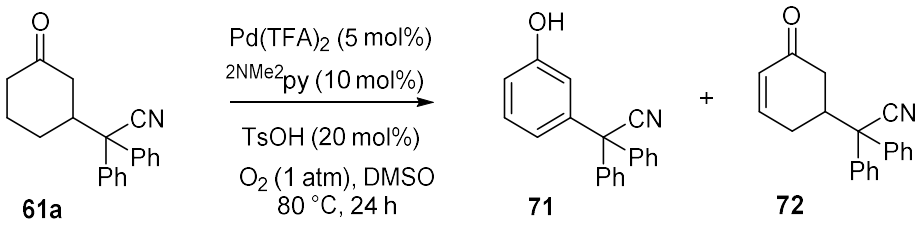

Experiment conducted following described procedure.[63]

To a 4 ml *via*l, $Pd(TFA)_2$ (5.1 mg, 0.015 mmol), 2-(N,N-dimethylamino)pyridine (3.8 mg, 0.03 mmol), p-toluensulfonic acid (11.5 mg, 0.06 mmol), 2-(3-oxocyclohexyl)-2,2-diphenylacetonitrile **61a** (88.1 mg, 0.30 mmol) were dissolved in DMSO (0.5 ml) and the mixture was bubbled with O_2 for 10 min. Then, the mixture was heated at 80 °C for 24 h under O_2 atmosphere. After cooling down the reaction mixture, EtOAc (3 ml) was added to the mixture, followed by saturated solution of aqueous NH_4Cl (5 ml) and the crude product was extracted with EtOAc (3 x 5 ml). 1 ml of the combined organic layers was added to a GC *via*l and dodecane (2.5 mg) was introduced, and the mixture was analysed by GC to calculate conversion and yields. The organic layer was dried under magnesium sulphate and the solvent was removed under vacuum. The crude product was purified by column chromatography (silica gel, eluent: Hexane:AcOEt 4:1). Two products were isolated that corresponded to phenol **71** and cyclohexenone **72**:

2-(3-Hydroxyphenyl)-2,2-diphenylacetonitrile (71)

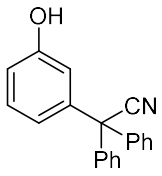

White solid. 22% isolated yield. **^{1}H NMR (400 MHz, $CDCl_3$)** δ 7.48 – 7.29 (m, 6H, aromatic H), 7.28 – 7.12 (m, 5H, aromatic H), 6.89 – 6.78 (m, 1H, aromatic H), 6.78 – 6.65 (m, 2H, aromatic H), 5.32 (bs, 1H, OH). **^{13}C {H} NMR** (101 MHz, $CDCl_3$) δ 155.9 (C), 141.7 (C), 139.9 (2C), 129.9 (CH), 128.8 (CH), 128.7 (CH), 128.2 (CH), 123.3 (CH), 121.2 (CN), 116.0 (CH), 115.3 (CH), 57.2 (C). **HRMS** (CI^+) m/z 286.1223 $(M+H)^+$ (286.1226 calcd for $C_{20}H_{16}NO$ $(M+H)^+$). **IR** (FTIR) 3418, 3070, 3025, 2958, 2244, 1769, 1489 cm^{-1}.

2-(5-Oxocyclohex-3-en-1-yl)-2,2-diphenylacetonitrile (72)

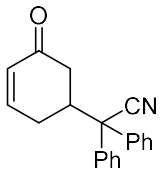

White solid. 27% isolated yield. **^{1}H NMR** (500 MHz, $CDCl_3$) δ 7.49 (dd, *J* = 13.7, 7.6 Hz, 4H, aromatic H), 7.38 (q, *J* = 7.9 Hz, 4H, aromatic H), 7.30 (q, *J* = 7.2 Hz, 2H, aromatic H), 7.00 – 6.91 (m, 1H, CH), 6.10 (dd, *J* = 10.0, 2.7 Hz, 1H, CH), 3.39 – 3.20 (m, 1H, CH), 2.60 – 2.42 (m, 3H, CH_2+CH), 2.37 – 2.26 (m, 1H, CH). **^{13}C {H} NMR** (126 MHz, $CDCl_3$) δ 197.6 (CO), 148.7 (CH), 137.8 (C), 137.3 (C), 129.7 (CH), 129.3 (CH), 129.3 (CH), 128.3 (CH), 128.2 (CH), 126.5 (CH), 126.4 (CH), 120.2 (CN), 57.5 (C), 41.3 (CH_2), 40.7 (CH), 28.9 (CH_2). **HRMS** (CI^+) m/z 288.1390 $(M+H)^+$ (288.1383 calcd for $C_{20}H_{18}NO$ $(M+H)^+$).

3.6.5.1.1. Optimisation of reaction conditions (Stahl´s conditions)

Optimisation of reaction conditions was conducted following the general procedure by changing ratio of components of the catalytic system and temperature as indicated in the table.

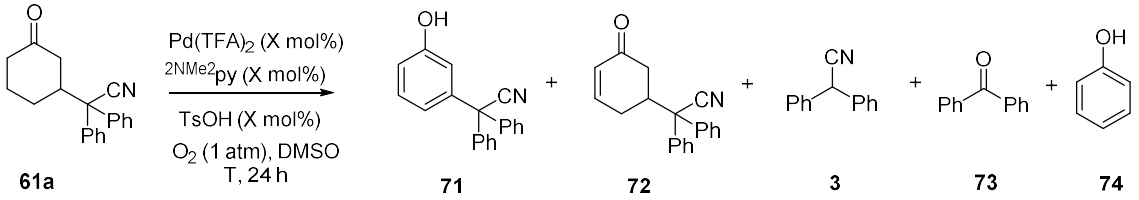

Entry	Ratio Pd: ^{2NMe2}py:TsOH, mol%	T, °C	Conversion of **61a**, %	Yield of **71**, %	Yield of **72**, %	Yield of **3**, %	Yield of **73**, %	Yield of **74**, %
1	5:10:20	80	70	30	34	6	5	1
2	5:10:20[a]	80	78	35	32	8	9	2
3	5:10:20[b]	80	73	25	22	6	5	5
4	5:10:20	100	73	27	13	9	11	7
5	10:20:40	80	81	29	26	8	9	5
6	10:20:40	100	94	48	2	11	19	19
7	20:40:80	80	99	47	7	12	16	20
8	20:40:80	100	99	53	0	10	15	19

Reaction conditions: Cyclohexanone **61a** (0.48 mmol), $Pd(TFA)_2$:^{2NMe2}py:TsOH (mol% indicated), O_2 (1 atm), DMSO (0.8 ml), 24 h. [a]: Reaction set up in a glovebox. [b]: Reaction conducted for 48 h.

3.6.5.1.2. Screening of oxidants

Optimisation of reaction conditions was conducted following the general procedure by changing the oxidant agent as indicated in the table.

Ratio Pd: ^{2NMe2}py:TsOH, mol%	Oxidant, equiv	T, °C	Conversion of **61a**, %	Yield of **71**, %	Yield of **72**, %	Yield of **3**, %	Yield of **73**, %	Yield of **74**, %
5:10:20	Oxone (3)	80	29	3	4	11	0	0
5:10:20	I_2 (0.2)	80	20	0	0	20	0	0

3.6.5.2. Screening of alternative methods for dehydrogenation of cyclohexanone 56a

3.6.5.2.1. Pd/C-catalyzed dehydrogenation of cyclohexanone 61a to phenol 66

Experiment conducted following described procedure.[60]

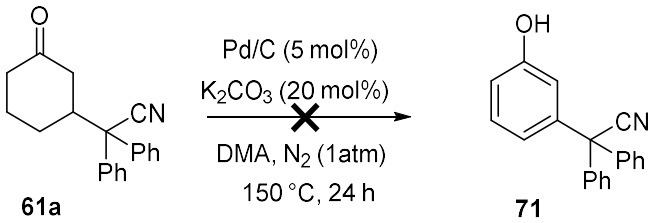

Cyclohexanone **61a** (73.2 mg, 0.25 mmol), Pd/C 10%wt (13.6 mg, 5 mol%) and K_2CO_3 (7.6 mg, 0.05 mmol) were introduced to a 5 ml Schlenk flask. Then, N,N-dimethylacetamide (0.5 ml) was added and the mixture was bubbled with N_2 for 10 min. The reaction was heated at 150 °C for 24 h under N_2 atmosphere. Then the reaction mixture was cooled down, dodecane (23.6 mg) and EtOAc (6 ml) were added to the reaction mixture. The Pd/C was filtered and the reaction mixture was treated with water (2 ml), 2M HCl (2 ml) and extracted with EtOAc (3 x 3 ml). The reaction mixture was analysed by GC. No phenol **71** was detected but, diphenylacetonitrile **3**, benzophenone and phenol were formed in 10, 20 and 32% yield, respectively.

3.6.5.2.2. $Pd(AcO)_2$-catalyzed dehydrogenation of cyclohexanone 61a to phenol 66

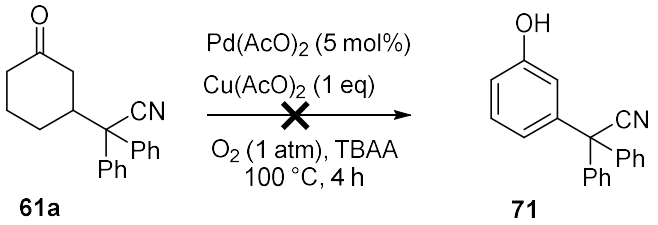

Method A

Experiment conducted following described procedure.[61]

$Pd(OAc)_2$ (2.6 mg, 0.01 mmol), $Cu(OAc)_2$ (45.4 mg, 0.25 mmol), 2-(3-oxocyclohexyl)-2,2-diphenylacetonitrile **61a** (71.5 mg, 0.25 mmol), styrene (69.9 mg, 0.25 mmol), dodecane (30 mg) and tetrabutylammonium acetate (0.2 ml) were added to a 10ml Schlenk bomb and the reaction vessel was purged with O_2 for 10 min. The reaction mixture was heated at 100 °C for 4 h under O_2 atmosphere using a balloon. Then, the mixture was treated with aq HCl 2M (2 ml). The crude product was extracted with EtOAc (5 x 2 ml) and the combined organic layers were passed through Celite path. Then, the combined organic extracts were analysed by GC. No phenol **71** was detected.

Method B

Same procedure as Method A but in the absence of styrene:

$Pd(OAc)_2$ (2.4 mg, 0.01 mmol), $Cu(OAc)_2$ (44.9 mg, 0.25 mmol), 2-(3-oxocyclohexyl)-2,2-diphenylacetonitrile **61a** (71.1 mg, 0.25 mmol), dodecane (30 mg) and tetrabutylammonium acetate (0.2 ml) were added to a 10 ml Schlenk bomb and the reaction vessel was purged with O_2 for 10 min. The reaction mixture was heated at 100 °C for 4 h under O_2 atmosphere using a balloon. Then, the mixture was treated with aqueous HCl 2M (2 ml). The crude product was extracted with EtOAc (5 x 2 ml) and the combined organic layers were passed through Celite path. Then, the combined organic extracts were analysed by GC. No phenol **71** was detected.

3.6.5.2.3. I_2-catalyzed dehydrogenation of cyclohexanone 61a to phenol 66

Experiment conducted following described procedure.[62]

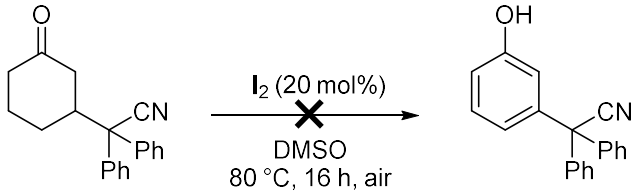

61a **71**

2-(3-oxocyclohexyl)-2,2-diphenylacetonitrile **61a** (74.1 mg, 0.25 mmol), iodine (14.9 mg, 0.05 mmol), dodecane (24.2 mg) and DMSO (0.5 ml) were added to a 4 ml *via*l in air. The *via*l was closed with an open top Teflon lined screw cap with a needle pierced in it and the reaction was heated at 80 °C for 16 h. Once the reaction mixture was cooled down to room temperature, aqueous $Na_2S_2O_3$ (3 ml) was added and the crude product was extracted with EtOAc (3 x 2ml). Then, the combined organic layers were analysed by GC to calculate yields and conversions. No phenol **71** was detected.

3.6.5.2.4. Dehydrogenation of cyclohexanone 61a to phenol 67 with DDQ

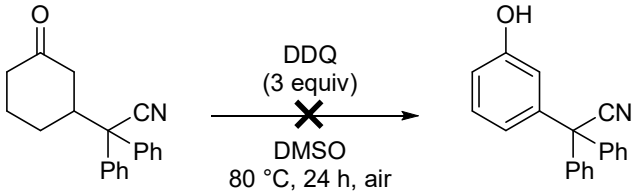

56a **71**

In a 4 ml *via*l, 2-(3-oxocyclohexyl)-2,2-diphenylacetonitrile **61a** (71.0 mg, 0.25 mmol), DDQ (165.6 mg, 0.72 mmol), dodecane (24.2 mg) and DMSO (0.5 ml) were weighted in air. The reaction was heated at 80 ºC for 16 h. Then, dodecane (21.6 mg) was added. Water (1 ml) was added to the reaction mixture and the crude product was extracted with EtOAc (3 x 3 ml). The combined organic layers were analysed by GC. Unfortunately, no phenol **71** was detected.

3.7. References

(1) Perlmutter, P. *Conjugate addition reactions in organic synthesis*; 2013.

(2) Comelles, J.; Moreno-Mañas, M.; Vallribera, A. *Arkivoc* **2005**, *2005* (ix), 207–238.

(3) Nelson, J. H.; Howells, P. N.; DeLullo, G. C.; Landen, G. L. *J . Org. Chem* **1980**, *45* (7), 1246–1249.

(4) Duan, Z.; Xuan, X.; Wu, Y. *Tetrahedron Lett.* **2007**, *48* (29), 5157–5159.

(5) Yao, X.; Li, C.-J. *J. Org. Chem.* **2005**, *70* (14), 5752–5755.

(6) Brunner, H.; Hammer, B. *Angew. Chemie Int. Ed. English* **1984**, *23* (4), 312–313.

(7) Hamashima, Y.; Hotta, D.; Sodeoka, M. *J. Am. Chem. Soc.* **2002**, *124* (38), 11240–11241.

(8) Watanabe, M.; Murata, K.; Ikariya, T. *J. Am. Chem. Soc.* **2003**, *125*, 7508–7509.

(9) Hou, Z.; Koizumi, T.; Fujita, A.; Yamazaki, H.; Wakatsuki, Y. *J. Am. Chem. Soc.* **2001**, *123* (24), 5812–5813.

(10) Gómez-Bengoa, E.; Cuerva, J. M.; Mateo, C.; Echavarren, A. M. *J. Am. Chem. Soc.* **1996**, *118* (36), 8553–8565.

(11) Keller, E.; Feringa, B. L. *Tetrahedron Lett.* **1996**, *37* (11), 1879–1882.

(12) Bonadies, F.; Lattanzi, A.; Orelli, L. R.; Pesci, S.; Scettri, A. *Tetrahedron Lett.* **1993**, *34* (47), 7649–7650.

(13) Kim, Y. S.; Matsunaga, S.; Das, J.; Sekine, A.; Ohshima, T.; Shibasaki, M. *J. Am. Chem. Soc.* **2000**, *122* (27), 6506–6507.

(14) Chatani, N.; Asaumi, T.; Yorimitsu, S.; Ikeda, T.; Kakiuchi, F.; Murai, S. *J. Am. Chem. Soc.* **2001**, *123* (44), 10935.

(15) Lahm, G.; Opatz, T. *Org. Lett.* **2014**, *16* (16), 4201–4203.

(16) Pan, S.; Matsuo, Y.; Endo, K.; Shibata, T. *Tetrahedron* **2012**, *68* (44), 9009–9015.

(17) Mo, F.; Dong, G. *Science (80-.).* **2014**, *345* (6192), 68–72.

(18) Grützmacher, H. *Angew. Chemie Int. Ed.* **2008**, *47* (10), 1814–1818.

(19) Lim, H. N.; Dong, G. *Angew. Chemie Int. Ed.* **2015**, *54* (50), 15294–15298.

(20) Do, J.; Kim, S.-G. *Tetrahedron Lett.* **2011**, *52* (18), 2353–2355.

(21) Takaya, H.; Yoshida, K.; Isozaki, K.; Terai, H.; Murahashi, S.-I. *Angew. Chemie Int. Ed.* **2003**, *42* (28), 3302–3304.

(22) Vogt, M.; Nerush, A.; Iron, M. A.; Leitus, G.; Diskin-Posner, Y.; Shimon, L. J. W.; Ben-David, Y.; Milstein, D. *J. Am. Chem. Soc.* **2013**, *135* (45), 17004–17018.

(23) Nerush, A.; Vogt, M.; Gellrich, U.; Leitus, G.; Ben-David, Y.; Milstein, D. *J. Am. Chem. Soc.* **2016**, *138* (22), 6985–6997.

(24) Lin, C.-J.; Huang, S.-H.; Lai, N.-C.; Yang, C.-M. *ACS Catal.* **2015**, *5* (7), 4121–4129.

(25) Badham, N. F.; Chen, J. H.; Cummings, P. G.; Dell'Orco, P. C.; Diederich, A. M.; Eldridge, A. M.; Mendelson, W. L.; Mills, R. J.; Novack, V. J.; Olsen, M. A.; Rustum, A. M.; Webb, K. S.; Yang, S. *Org. Process Res. Dev.* **2003**, *7* (1), 101–108.

(26) Di Bussolo, V.; Catelani, G.; Mastrorilli, E.; Di Bugno, C.; Giorgi, R. *Tetrahedron Asymmetry* **1996**, *7* (12), 3585–3592.

(27) Tyman, J. H. P. *Synthetic and natural phenols*; Elsevier, 1996.

(28) Rappoport, Z. *The chemistry of phenols*; Wiley, 2003.

(29) Tyman, J. H. P. In *Synthetic and Natural Phenols*; Elsevier, 1996; pp 23–45.

(30) Sakaguchi, S.; Yamaga, T.; Ishii, Y. *J. Org. Chem.* **2001**, *66* (33), 4710–4712.

(31) Linderman, R. J.; Ghannam, A.; Badejo, I. *J. Org. Chem.* **1991**, *56* (17), 5213–5216.

(32) Ru Hwu, J.; Hakimelahi, G. H.; Chou, C.-T. *Tetrahedron Lett.* **1992**, *33* (43), 6469–6472.

(33) Lin, Y.; Ma, D.; Lu, X. *Tetrahedron Lett.* **1987**, *28* (27), 3115–3118.

(34) Mestroni, G.; Zassinovich, G.; Camus, A.; Martinelli, F. *J. Organomet. Chem.* **1980**, *198* (1), 87–96.

(35) Alvarez, S. G.; Hasegawa, S.; Hirano, M.; Komiya, S. *Tetrahedron Lett.* **1998**, *39* (29), 5209–5212.

(36) Hasegawa, Y.; Gridnev, I. D.; Ikariya, T. *Bull. Chem. Soc. Jpn.* **2012**, *85* (3), 316–334.

(37) Carmona, D.; Ferrer, J.; Lorenzo, M.; Lahoz, F. J.; Dobrinovitch, I. T.; Oro, L. A. *Eur. J. Inorg. Chem.* **2005**, *2005* (9), 1657–1664.

(38) Arndtsen, B. A.; Bergman, R. G. *Science (80-.).* **1995**, *270*, 1970.

(39) Kunin, A. J.; Eisenberg, R. *J. Am. Chem. Soc* **1986**, *108*, 535–536.

(40) Liskey, C. W.; Hartwig, J. F. *J. Am. Chem. Soc.* **2013**, *135* (9), 3375–3378.

(41) Simmons, E. M.; Hartwig, J. F. *Nature* **2012**, *483* (7387), 70–73.

(42) Corberán, R.; Sanaú, M.; Peris, E. *J. Am. Chem. Soc* **2006**, *128*, 3974–3979.

(43) Mas-Marzá, E.; Poyatos, M.; Sanaú, M.; Peris, E. *Inorg. Chem.* **2004**, *43*, 2213–2219.

(44) Zhang, Y.; Wang, W. *Catal. Sci. Technol.* **2012**, *2* (1), 42–53.

(45) Belokon, Y. N.; Gugkaeva, Z. T.; Maleev, V. I.; Moskalenko, M. A.; Tsaloev, A. T.; Khrustalev, V. N.; Hakobyan, K. V. *Tetrahedron: Asymmetry* **2011**, *22* (2),

167–172.

(46) Baumann, M.; Baxendale, I. R. *Beilstein J. Org. Chem* **2013**, *9*, 2265–2319.

(47) Jun, C.-H.; Garza, D. G.; Baxter, J. C.; Hoff, C. D.; Kamatani, A.; Sonoda, M.; Chatani, N. *Chem. Commun.* **1998**, *9* (13), 1405–1406.

(48) Bergman, S. D.; Storr, T. E.; Prokopcová, H.; Aelvoet, K.; Diels, G.; Meerpoel, L.; Maes, B. U. W. *Chem. - A Eur. J.* **2012**, *18* (33), 10393–10398.

(49) Kulago, A. A.; Van Steijvoort, B. F.; Mitchell, E. A.; Meerpoel, L.; Maes, B. U. W. *Adv. Synth. Catal.* **2014**, *356* (7), 1610–1618.

(50) Chen, X.; Goodhue, C. E.; Yu, J.-Q. *J. Am. Chem. Soc.* **2006**, *128* (39), 12634–12635.

(51) Bordwell, F. G. *Acc. Chem. Res.* **1988**, *21* (12), 456–463.

(52) Tyman, J. H. P. In *Synthetic and Natural Phenols*; Elsevier, 1996; pp 558–661.

(53) Solymosi, K.; Latruffe, N.; Morant-Manceau, A.; Schoefs, B. In *Colour Additives for Foods and Beverages*; 2015; pp 3–34.

(54) Nirmal, N. P.; Rajput, M. S.; Prasad, R. G. S. V.; Ahmad, M. *Asian Pac. J. Trop. Med.* **2015**, *8* (6), 421–430.

(55) Maertens, G.; L ’homme, C.; Canesi, S.; Zhang, C. *Front. Chem.* **2015**, *2*, 115.

(56) Moriuchi, T.; Kikushima, K.; Kajikawa, T.; Hirao, T. *Tetrahedron Lett.* **2009**, *50* (52), 7385–7387.

(57) Yi, C. S.; Lee, D. W. *Organometallics* **2009**, *28* (4), 947–949.

(58) Wenzel, T. T. *J. Chem. Soc., Chem. Commun.* **1989**, *0* (14), 932–933.

(59) Izawa, Y.; Pun, D.; Stahl, S. S. *Science (80-.).* **2011**, *333* (6039), 209–213.

(60) Zhang, J.; Jiang, Q.; Yang, D.; Zhao, X.; Dong, Y.; Liu, R. *Chem. Sci.* **2015**, *6*, 4674.

(61) Cotugno, P.; Monopoli, A.; Ciminale, F.; Milella, A.; Nacci, A. *Angew. Chemie* **2014**, *126* (49), 13781–13785.

(62) Liang, Y.-F.; Li, X.; Wang, X.; Zou, M.; Tang, C.; Liang, Y.; Song, S.; Jiao, N. *J. Am. Chem. Soc.* **2016**, *138* (37), 12271–12277.

(63) Pun, D.; Diao, T.; Stahl, S. S. *J. Am. Chem. Soc.* **2013**, *135* (22), 8213–8221.

(64) Zhou, C.; Larock, R. C. *J. Am. Chem. Soc.* **2004**, *126* (8), 2302–2303.

(65) Kulp, S. S.; McGee, M. J. *J. Org. Chem.* **1983**, *48* (22), 4097–4098.

(66) Reetz, M. T.; Stephan, W. *Liebigs Ann. der Chemie* **1980**, *1980* (4), 533–541.

(67) Braude, E. A.; Brook, A. G.; Linstead, R. P. *J. Chem. Soc.* **1954**, *0* (0), 3569.

(68) Crabtree, R. H.; Mellea, M. F.; Mihelcic, J. M.; Quirk, J. M. *J. Am. Chem. Soc.* **1982**, *104* (1), 107–113.

(69) Gupta, M.; Hagen, C.; Kaska, W. C.; Cramer, R. E.; Jensen, C. M. *J. Am. Chem. Soc.* **1997**, *119* (4), 840–841.

(70) Choi, J.; MacArthur, A. H. R.; Brookhart, M.; Goldman, A. S. *Chem. Rev.* **2011**, *111* (3), 1761–1779.

(71) Zhang, Y.; Yao, W.; Fang, H.; Hu, A.; Huang, Z. *Sci. Bull.* **2015**, *60* (15), 1316–1331.

(72) Ji, Y.-H.; Husfeld, C.; Lange, C.; Lee, R.; Mu, Y. Quaternary ammonium diphenylmethyl compounds useful as muscarinic receptor antagonists. WO2008103426 (A1), 2008.

(73) Barbasiewicz, M.; Marciniak, K.; Fedoryński, M. *Tetrahedron Lett.* **2006**, *47* (23), 3871–3874.

(74) Löfberg, C.; Grigg, R.; Whittaker, M. A.; Keep, A.; Andrew, D. *J. Org. Chem.* **2006**, *71* (21), 8023–8027.

(75) Herold, F.; Kleps, J.; Szczęsna, B.; Anulewicz-Ostrowska, R. *J. Heterocycl.*

Chem. **2002**, *39* (4), 773–782.

(76) Sankararaman, S.; Sudha, R. *J. Org. Chem.* **1999**, *64* (6), 2155–2157.

(77) Wu, T. R.; Shen, L.; Chong, J. M. *Org. Lett.* **2004**, *6* (16), 2701–2704.

(78) Wang, Q.; Chen, X.; Tao, L.; Wang, L.; Xiao, D.; Yu, X.-Q.; Pu, L. *J. Org. Chem.* **2007**, *72* (1), 97–101.

(79) den Besten, R.; Harder, S.; Brandsma, L. *J. Organomet. Chem.* **1990**, *385* (2), 153–159.

Chapter 4

Conclusions

This thesis has been focused on the study of the cleavage and the formation of unstrained aliphatic carbon-carbon bonds mediated by homogeneous iridium catalysts. The main project of this thesis consisted of mechanistic studies of Ir-catalysed selective, reductive cleavage of unstrained C-C single bonds in dinitriles. Based on our experimental and computational studies, this process has been proposed to occur *via* directed C-H activation by alkene deinsertion through a retro-Michael type reaction as the key C-C breaking steps. The proposed catalytic cycle involves the formation of a C-H activated N,N-coordinated dinitrile complex that after the C-C bond cleavage leads to the formation of N-coordinated deprotonated diphenylacetonitrile and N-bound acrylonitrile. The proposed mechanism illustrates the requirement of two directing groups to promote the C-C bond cleavage, according to DFT calculations and experimental results.

Remarkably, our investigations show that the alkene deinsertion is a reversible process that is driven by the subsequent irreversible hydrogenation and polymerisation of the formed alkene. This irreversible consumption of the alkene explains the feasibility of the thermodynamically unfavourable alkene deinsertion.

On the other hand, exhaustive NMR monitoring experiments allowed the detection and the isolation of a relevant catalytically active intermediate complex **37**. This complex was found to catalyse both the C-C cleavage in the dinitrile substrate and its microscopic reverse C-C forming hydroalkylation with comparable yields to the original pentahydride iridium complex.

Furthermore, the feasibility of the selective, catalytic reductive cleavage of non-strained aliphatic C-C bonds using hydrogen or alcohols as reductants was investigated. Remarkably, these studies allowed us to report the first example of selective transfer hydrogenolysis of unstrained C-C bonds with excellent product yields using cyclohexanol as transfer hydrogenation agent.

As future work, the use of an heterogenized version of the catalyst can be envisioned. It would be relevant to study the deposition of the catalyst on a suitable inert surface, such as a polymer, to investigate the possibility of catalyst recovery and reuse.

The first part of this PhD project allowed us to explain the mechanism of not only the C-C cleavage of dinitriles but also the corresponding microscopic reverse C-C bond forming hydroalkylation process. These results led us to envision a second project focused on the development of a novel methodology for the iridium-catalysed Michael-type hydroalkylation of cyclic α,β-unsaturated ketones with alkyl aryl nitriles. This base-free methodology allowed us to synthesise a range of novel 3-substituted cyclohexanones in excellent yields using low catalyst loadings (0.5 mol%) and mild conditions (40 ºC). Remarkably, this catalytic methodology is compatible with non-activated C-H nitriles containing different alkyl and aryl substituents, including bulky groups such as isopropyl or cyclohexyl.

To explore further applications of the designed catalytic hydroalkylation, preliminary investigations for the synthesis of *meta*-substituted phenols *via* the dehydrogenation of substituted cyclohexanones were conducted. These studies showed the feasibility of the envisioned dehydrogenation catalysed by $Pd(TFA)_2$, ^{2NMe2}py and TsOH leading to the *meta*-substituted phenol **71** in good yields (53%). Further studies are currently on progress to improve the yields of the desired *meta*-substituted phenol and to avoid observed C-C cleavage side processes of the starting cyclohexanone **61a**.